SOLVENT FREE TECHNOLOGIES FOR POLYMER BASED CRYSTAL ENGINEERING AND DRUG DELIVERY

S. A. KORDE

Ph.D

UNIVERSITY OF BRADFORD

2015

SOLVENT FREE TECHNOLOGIES FOR POLYMER BASED CRYSTAL ENGINEERING AND DRUG DELIVERY

Sachin Abasaheb KORDE

Submitted for the degree of

Doctor of Philosophy

School of Life Sciences

University of Bradford

2015

Abstract

Sachin Abasaheb Korde

Solvent Free Technologies for Polymer based Crystal Engineering and Drug Delivery

Keywords: Crystal Engineering, Polymer, Drug Delivery

Current research focuses on the effect of different continuous solid state shear based processing for the production of pharmaceutical amorphous system and cocrystals for poorly water soluble APIs. The S3M technology is getting first time reported for its application in pharmaceutical field and it is considered as technology with good potential for development of pharmaceutical dosage forms. The main objectives of this study include the effect of two solid state shear processes on the product properties in case of solid dispersions and cocrystals. Hot melt extrusion technology has been widely explored for the production of pharmaceutical solid dispersions and cocrystals, it would be helpful to compare how the new invented S3M technology will differ from the existing solid state shear process. The S3M has been also explored for the advantages over HME process in terms of residence time, plasticiser free dispersions, effect of process on degradation of drugs during processing. For this purpose, the process and material modifications during operation of these two technologies was important aspects of this study. The pharmaceutical drugs chosen for the solid dispersion purpose were carbamazepine, ibuprofen, glibenclamide which are BCS class II drugs and paracetamol from BCS class III drug was selected as model drug for solid dispersion manufacturing with PVP

VA64, HPMCP HP55, HPMCAS, Ethyl cellulose as polymers. In case of cocrystals selected drugs were carabamazepine, caffeine, paracetamol and ibuprofen with co-formers nicotinamide, saccharin, salicylic acid, glutaric acid, oxalic acid, maleic acid. The selections of co-formers were done on the basis of functional group complementarity between drug and co-former. All the details about the pairs for cocrystals and for solid dispersions are given in experimental section. Carbamazepine has been explored in depth for solid dispersions with different polymers and with different co-formers in case of cocrystals. The effect of process variables and amount of shear applied during processing was deciding factor in product output and quality. The end product in case of both the solid dispersions and cocrystals varied in their physicochemical, morphological and drug release properties HME process needed addition of plasticisers during preparation of solid dispersions whereas S3M was plasticiser free process which gave good insight on how this will affect the product performance during evaluation studies. The solid dispersions in case of HME were had smooth surfaces and which are non-porous in nature whereas in case of S3M the solid dispersions were highly porous in nature. The differences in the structural and morphological features of solid dispersions somehow did not affect the drug release of drug during in-vitro dissolution studies and both the solid dispersions did not show much difference in drug release. In case of cocrystals processing on S3M it was observed that the S3M process is dependent on the use of polymer as process aid. For this purpose PEO, PVP VA64 and HPMCP HP55 were selected as model polymer as process aid during processing of cocrystals, out of which PEO has been explored widely as processing aid due to its process suitability, low melting and ability to withstand high shear during processing. PVP VA64 was used only in case of

carbamazepine cocrystals with salicylic acid and HPMCP HP55 in case of caffeine cocrystals with maleic acid. The effect of concentration of PEO in case of carbamazepine cocrystals as processing aid was studied (concentration range 5%, 10%, 15%, 25% w/w). The concentration of PEO in case of HME cocrystals had direct effect on the drug release of drug dissolution studies which was reduced in case of higher concentration of PEO (25% w/w), which was not observed in case of S3M processes carbamazepine cocrystals. The product in case of cocrystals by S3M was thread like structures whereas in case of HME cocrystals were in form of screw shaped compact mass. The difference in morphological and structural properties of cocrystals did not had major effect on drug release in case of S3M process but in case of HME processed cocrystals the higher amount of polymer slowed the drug release.

The degradation studies in case of drugs carbamazepine, paracetamol were carried out whereas in case of polymer for HPMCP HP55 were carried out. It was found that HME processed samples showed higher degradation as compared to S3M processed one in both the cases solid dispersions and cocrystals. This can be attributed to high residence time in case of HME as compared to S3M process.

The effect of two high shear processes HME and S3M had significant effect on the morphological and structural properties of the solid dispersions and cocrystals. The variation in the structural and morphological properties did not have direct effect on the drug release of drug during dissolution studies. HME and S3M both the processes had some positive and some negative aspects within them for processing of pharmaceutical dispersions and cocrystals.

In case of HME the use of plasticiser is mandatory to maintain low torque levels during processing and to avoid blockage of extruder barrel, whereas in case of S3M the process is plasticiser independent and processing of solid dispersion is very easy as compared to HME with low residence time. Processing of plain drug or co-former was easy in case of HME whereas in case of S3M processing it was mandatory to use polymer as processing aid specially during processing of cocrystals.

In case of process controls HME has excellent control over the process parameters which can be controlled and manipulated as per requirement, whereas S3M technology needs to have technical modifications to have better control over its processing parameters. The S3M can be a revolutionary technology for pharmaceutical industry once it is upgraded with better control and optimised process parameters.

I do not know what I appear to the world; but to myself I seem to have been only like a boy playing on a sea-shore, and diverting myself in now and then finding a smoother pebble or a prettier shell than ordinary, whilst the great ocean of truth lay all undiscovered before me.

Sir Issac Newton

DEDICATED TO MY BELOVED

FAMILY MEMBERS

ACKNOWLEDGEMENT

It is indeed a privilege to express a deep sense of gratitude towards Professor Anant Paradkar for his wise guidance & strong support throughout my thesis work. Besides his serenity, patience and cheerful nature, his positive attitude, constructive criticism and constant encouragement helped me build inner strength required to accomplish my work. Apart from being an efficient supervisor, I found him as a caring guardian as well.

I wish to express my sincere and respectful thanks to my co-supervisor Dr. Adrian Kelly for his constant inspiration and motivation throughout my dissertation work. I would also like to thank Professor Phil Coates for giving me the opportunity to participate in UK China Science Bridges Program and visit China.

I would like to acknowledge and express my obligations to Centre for Pharmaceutical Engineering Sciences and IRC, University of Bradford for providing the necessary infrastructure and all the facilities required for carrying out my research work. I am also thankful to all the technicians especially in IRC who have helped me whenever needed.

I would like to thank my Dr. Ravindra Dhumal who kept an eye on the progress of my work and always available when I needed advises. I can't thank enough to my brother Dr. Rohit Mulik who has been inspiration to achieve this milestone in my life, thanks for all your kind suggestions and never ending support.

I would like to thank RCUK Science Bridges China/EPSRC Global Engagements Research Workshop, co-hosted with Sichuan University and the Chengdu Science & Technology Bureau, 2013 held in Sichuan University, Chengdu, China through which S3M was found and explored in this current study.

I acknowledge the support extended by Analytical Centre, University of Bradford for offering me characterisation facility. I am also thankful to UKIERI for offering

me an opportunity to do collaborative research with Professor Ashwini Nangia's group at University of Hyderabad, India and Professor Rajsuryanarayanan's group at University of Minnesota, USA.

I express my heartfelt thanks to all my friends Sudhir, Niten, Dr. Suyog, Ratnadeep, Amit, Hrushikesh for their help and support during my research work and also for all kinds of discussions and pleasant company.

Words are inadequate enough to put across my feelings for my lifetime friends Sumit, Ashish, Achyut, Viraj, Deepak, Harshal, Ravi for their trust and support whenever needed during my tough times.

This acknowledgement would be incomplete without the mention of lovely wife Supriya for her love and support. I feel a deep sense of gratitude towards my family for their never ending support and trust in me which helped me part of my vision and taught me the good things that really matter in life.

Above all, I thank God almighty for showering his infinite bounties, graces and mercies upon me. Any attempt to acknowledge by name, the help received by me during completing the project runs the risk of omitting someone. Therefore following must be preceded by sincere thanks to all who rendered their valuable assistance and concerned guidelines to me.

TABLE OF CONTENTS

List of Figures

List of Tables

Abbreviations

API		Active pharmaceutical ingredient
BCS	:	Biopharmaceutical classification system
EMA	:	European Medicines Agency
GRAS	:	Generally regarded as safe
HME	:	Hot melt extrusion
S3M	:	Solid state shear mill
Tg	:	Glass transition temperature
API	:	Active pharmaceutical ingredients
CMC	:	Critical micellar concentration
PVP	:	Polyvinylpyrrolidone
CD	:	Cyclodextrin
GI	:	Gastrointestinal
PEG	:	Polyethylene glycol
HPMCAS	:	Hydroxypropylmethylcellulose acetate succinate
HPMCP HP55	:	Hydroxypropylmethylcellulose phthalate
PEO	:	Polyethylene oxide
USFDA	:	United States Food and Drug Administration
NDA	:	New drug application
ANDA	:	Abbreviated new drug application
SCF	:	Supercritical fluid technology
SFCC	:	Solvent free continuous cocrystallisation
PXRD	:	Powder X-ray diffraction
DSC	:	Differential scanning calorimetry
NIR	:	Near infrared
SEM	:	Scanning electron microscopy
SS	:	Stainless steel
rpm	:	Revolution per minute
PLC	:	Programmable logic controller
DVS	:	Dynamic vapour sorption
*i*GC	:	Inverse gas chromatography
FID	:	Flame ionisation detector
IBU	:	Ibuprofen
PARA	:	Paracetamol
GLIB	:	Glibenclamide

CBZ	:	Carbamazepine
SAL	:	Salicylic acid
CAF	:	Caffeine
MAL	:	Maleic acid
SACC	:	Saccharin
NIC	:	Nicotinamide
GLUT	:	Glutaric acid
OXAL	:	Oxalic acid
HPLC	:	High performance liquid chromatography
UPLC	:	Ultra performance liquid chromatography
TEC	:	Triethyl citrate
UV	:	Ultraviolet
HCl	:	Hydrochloric acid
PDA	:	Photodiode array
CC	:	Cocrystal

Chapter 1. Introduction

Many of the new drug entities have solubility issues associated which hampers their bioavailability, leading to a low therapeutic effect. Low solubility has created a major challenge to modify and transform existing dosage forms into more suitable dosage forms with improved performance (Leuner, 2000). Drug has to be in solution form at the site of absorption to achieve a pharmacological effect, which increases dose size of these low solubility drugs.

Biopharmaceutical classification system (BCS) for pharmaceutical drugs has classified drugs into four categories owing to their solubility and permeability. Most pharmaceutical drugs and new chemical entities belong to the BCS class II category. There are many techniques evolving and reported in the literature to improve the solubility of BCS class II drugs, which have low solubility and high permeability. Among many approaches, use of different components and additives such as adsorbents, surfactants (Vasconcelos *et al*., 2007) and co-solvents (Majerik, *et al.* 2007) are some of the preliminary attempts reported for solubility enhancement. Micronisation is one of the most widely investigated techniques for solubility enhancement by reducing the particle size; many researchers have reported increasing therapeutic efficacy of the drug by decreasing its dose by micronisation (Rasenack and Muller, 2004). Micronisation helps to increase the surface area of the drug particle and wettability which in turn increases the drug dissolution. Chemical modification of drugs has also been investigated for solubility improvement of poorly water soluble drugs; prodrugs are the bio-reversible form of the original

drug which can be obtained by derivatisation of the parent drug. Prodrugs include complex and salt formation of the parent drug which has higher solubility. In prodrugs, important attempts have been made by introducing ionisable components in the parent drug entity based on its ionisation capacity. This method has limitations due to poor ionisation ability of the parent drug. Salt formation of the parent drug depends on the acidic and basic ability of the drug, only ionisable drug molecules can be converted into highly soluble salts. This technique is limited to the weak acidic and basic nature of pharmaceutical drugs which may not be suitable for neutral drugs for example griseofulvin.

Crystal engineering for solubility improvement is emerging as an excellent approach and has proven its potential for many BCS class II drugs. Two among various crystal engineering approaches which are adopted for solubility improvement are cocrystallisation (cocrystals) and amorphisation (solid dispersion). Current European Medicines Agency (EMA) guidelines have given a classification for types of solids and its subdivision into cocrystal and amorphous system (

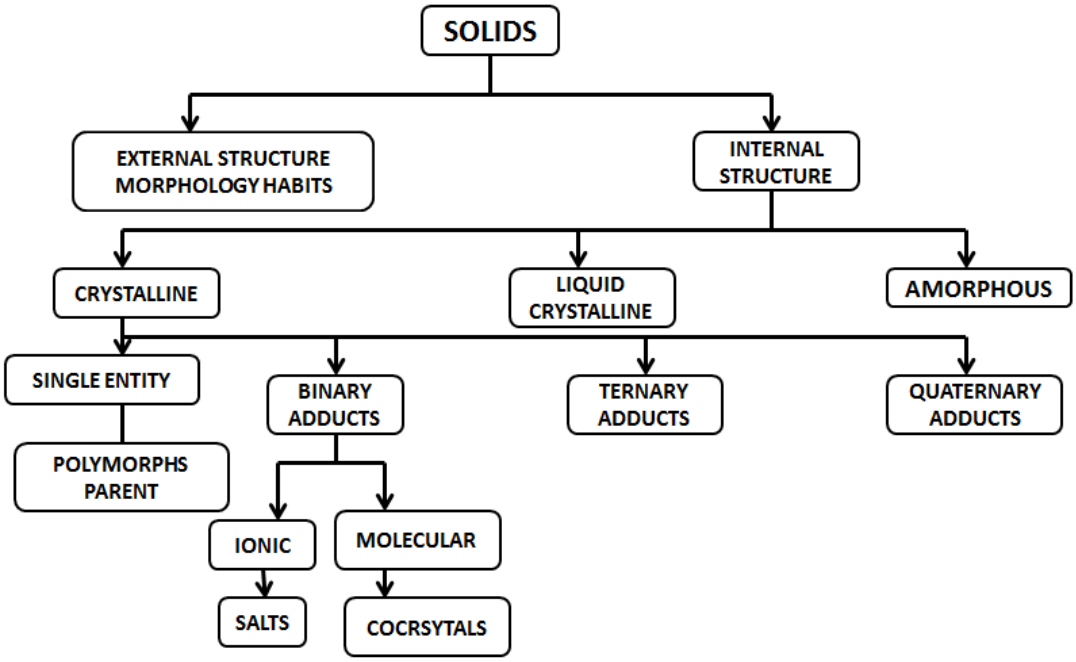

Figure 1.1).

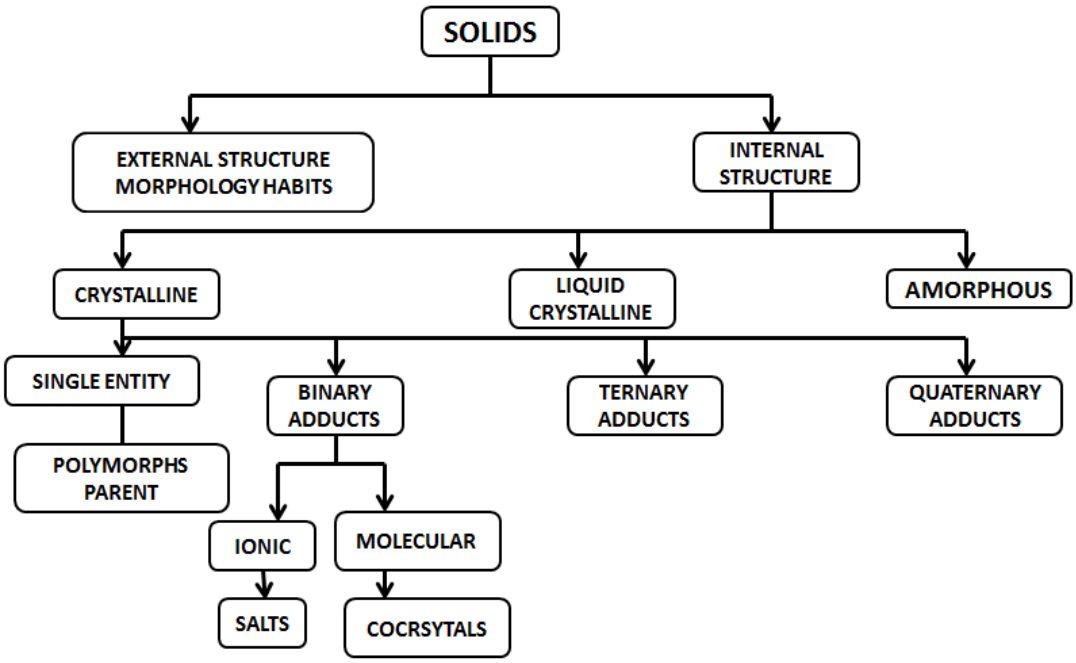

Figure 1.1: Subdivision of solid state material of an active moiety (European Medicine Agency, 2014)

Cocrystals are generally modified chemical entities which involve hydrogen bonding between a low water soluble active pharmaceutical drug and GRAS (generally regarded as safe) molecules (Schultheiss and Newman, 2009). Generally GRAS molecule can vary from dicarboxylic weak acids to highly soluble entities. Several techniques have been reported for cocrystallisation of pharmaceutical drugs using various GRAS molecules. Solution based cocrystallisation is a common technique to obtain pure cocrystals of the parent drug using generally an organic solvent alone or their mixture in specified ratios. Grinding/ co-grinding and liquid assisted grinding are some of the common methods of cocrystallisation (Sladkova, *et al.* 2014). Many milling technologies have also been investigated for cocrystallisation such as ball mill, vibratory mill or kneading (Balaz, 2008). Many advanced techniques have emerged in crystal engineering for cocrystal formation such as hot melt extrusion (HME), ultrasound techniques, microwaves, spherical cocrystallisation and rotary controlled vaporization from a solvent mixture (Pagire, *et al*., 2013, Aher, *et al*., 2010). All the solvent assisted techniques for cocrystal formation have a major drawback of stability; the solvent assisted processes show destabilisation over time. Solvent free techniques provide an advantage over solvent assisted techniques because of better stability which are more stable for long periods of time. Details of these techniques and processes are reviewed in the next chapter.

Solid dispersions are the most widely investigated crystal engineering based approach for solubility improvement of poorly water soluble drugs. Solid dispersions include the amorphisation of the active pharmaceutical ingredient into a suitable water soluble polymer matrix (Leuner, 2000). Active

pharmaceutical ingredients can be completely soluble in the polymer matrix or dispersed in particulate form. As stated earlier, reduction in particle size of drug to sufficient lower level can amorphise the drug with improved solubility (Khadka, *et al.* 2014). Homogenous mixing of two components in solid dispersion systems is important owing to their eutectic melting; uneven mixing may cause failure in achieving an amorphous system. Solid dispersion techniques have evolved with time based solvent based techniques and in recent years solvent free processing. Solvent free techniques include various milling technologies such as ball mill, planetary mill, vibratory mill etc. (Sareen, *et al.* 2012; Yang, *et al.* 2014). Other than milling technologies freeze drying has also been successfully used for solid dispersion preparation for a long period of time (Bandarkar and Khattab, 2011). Solvent based techniques for drug amorphisation include spray drying which is an excellent technique for preparation of solid dispersions but has stability issues due to the traces of the residual solvent present (Lakshman, *et al*., 2008). Solvent free processing techniques such as HME and various solvent free milling technologies can overcome this issue. Current study involves the use of HME and Solid State Shear Mill (S3M) for developing cocrystals and solid dispersions for selected pharmaceutical drugs.

Hot melt extrusion technology has been adapted from the polymer extrusion industry and has found applications in the pharmaceutical industry in solid state processing of pharmaceutical drugs and polymers (Lakshman, *et al.,* 2008). Hot melt extrusion is a melt shear based technology which ensures homogenous mixing of the drug and polymer above the softening (glass transition (T_g)) temperature of the polymer (Kim, *et al.,* 2011). Not all polymer

and drug combinations have ideal properties for the HME process. To enable them to be used for this process, often different additives have to be used such as plasticisers and Tg lowering components. Being a high temperature and shear process, many of the pharmaceutical polymers and low Tg drugs face the degradation problems in HME (Liu, *et al*., 2013). Use of suitable plasticisers which help to reduce the processing temperature, torque during process will help to reduce degradation. Recrystallisation from melt extruded products can be stimulated by the plasticiser present during stability. Plasticiser free processing of the drug polymer mixture may not be always possible in melt extrusion process for a chosen drug polymer combination.

S3M process is another solvent free technology investigated for preparation of cocrystal and solid dispersion. S3M is very high shear based milling technology without external heating. Unlike HME, plasticiser free processing is possible with S3M with considerably lower residence time and high throughput. Through its three dimensional scissoring mechanical stress mechanism each part of polymer or molecule faces a high and equal shear during the process. This research is the first report of S3M technology for pharmaceutical applications.

The current study involves the use of hot melt extrusion and high shear milling processes for the formation of cocrystals and amorphous systems for developing amorphous dosage forms for various pharmaceutical drugs and assessment of their pharmaceutical performance in terms of drug release, crystallinity and microscopic studies.

<u>Aims and objectives of current study can be summarised as,</u>

Current research focuses on comparative studies between two solid state shear processing technologies HME and S3M for production of solid dispersions and cocrystals and their comparative pharmaceutical assessment studies in sense of physicochemical properties and there performance in terms of drug release.

Objectives of current study are

- To formulate pharmaceutical cocrystal and amorphous systems using hot melt extrusion and solid state shear mill
- To investigate the use of different polymers and additives during processing on HME and S3M and their effect on product.
- To study how variables of S3M and hot melt extrusion affect product performance in terms of drug release
- To study the effect of polymer additives on cocrystal formation using S3M and hot melt extrusion
- To compare the performance behaviour of plasticised amorphous systems (HME processed) and non-plasticised amorphous system (S3M processed) in terms of drug release.

Chapter 2. Background

It is necessary that a drug should be in the solution form before it is absorbed through the membrane (Bikiaris, 2011). Around 40 % of new active pharmaceutical ingredients (APIs) and many of the APIs which are already on the market have poor water solubility. Solubility enhancement to improve bioavailability of poor water soluble APIs has remained a major challenge over recent years. As a result of low solubility a higher dose of API is required to achieve the same therapeutic effect (Serajuddin, *et al*. 2000). Nainar *et al*., (2012) explained the biopharmaceutical classification system (BCS) which divided APIs into four different classes based on their solubility and permeability (Table 2.1).

Table 2.1: BCS classification for pharmaceutical APIs

CLASS I High Soluble, High Permeable	CLASS II Low Soluble, High Permeable
CLASS III High Soluble, Low Permeable	CLASS IV Low Soluble, Low Permeable

As oral dosage forms such as tablets and capsules enjoy wide popularity, the BCS Class II APIs, which show dissolution limited absorption, have attracted maximum attention of pharmaceutical scientists over the last two decades.

2.1 Solubility improvement approaches

In the last two decades various formulation, particle and crystal engineering strategies have been developed to address the issue of poor water solubility of APIs. Surfactant based systems, inclusion complexes, particle size

reduction and crystal engineering approaches such as development of salts, polymorphs, stabilised amorphous form and recently cocrystals are commonly used approaches (Hanpin, 2012).

Surfactants improve bioavailability of the API through enhanced solubilisation, wettability, dissolution and reduction in in-vivo precipitation (Serajjudin, 1998). Surfactant based improvement is useful in liquid as well as solid oral delivery systems. One of the major challenges in the use of surfactant is significant variation in Critical Miceller Concentration (CMC) depending on the sources which may affect product performance. Cyclodextrin (CD) complexes of APIs especially with substituted β-cyclodextrins having very high water solubility such as hydroxypropyl β-cyclodextrin and sulfo-butyl ether β-cyclodextrin are commonly used. The API molecule is accommodated in the hydrophobic core of the cyclodextrin and is released under physiological conditions. It has been recently reported that inclusion of a small amount of water-soluble polymers such as polyvinylpyrrolidone (PVP) can improve complexation efficiency (Shah *et al*., 2011). It is important that the API CD binding constant should not be too high, otherwise the complex will not readily dissociate. The high molecular weight of cyclodextrins is a major challenge especially for high dose APIs.

Particle size reduction to the submicron size is carried out to improve API solubility. Size reduction technologies include top-down approaches such as milling, high pressure homogenisation (Romanski *et al*., 2011) and various bottom-up approaches include ultrasound assisted crystallisation (Aher, et al. 2010) and supercritical fluid crystallisation (Majerik, *et al*., 2007). Bead milling technologies like Elan's Nanocrystal® have demonstrated significant

commercial success in the area of nanosuspensions. Stabilisation of nanoparticulate systems is a major challenge.

As a focus of this research is comparative evaluation of two technologies to obtain stabilised amorphous forms and cocrystals, a detailed account of these solid forms and related technologies will be discussed here.

The API in solid form can exist in various crystal or amorphous states depending on the components of the system and order of arrangement as shown in Figure 2.1.

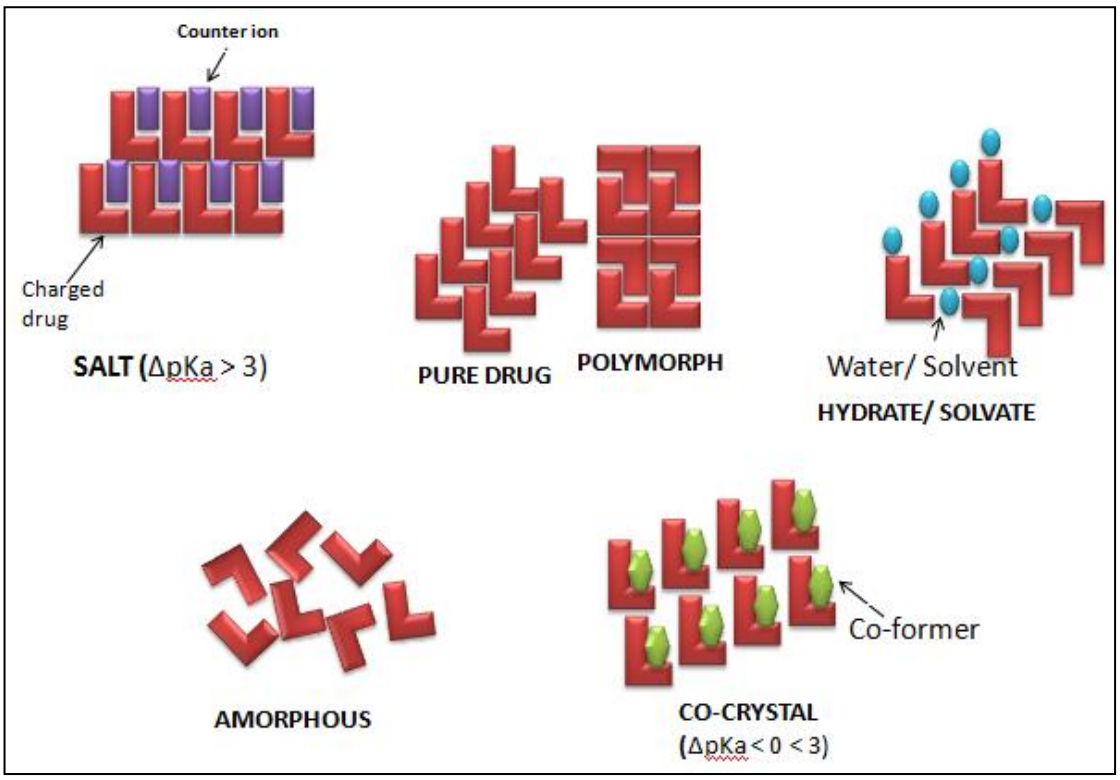

Figure 2.1: Solid state forms of APIs

A salt contains an ionisable drug molecule combined with a counter ion to form a neutral complex. Salts exhibit higher solubility than that of parent compounds having weak acidic or basic characteristics. There are reports of lipophilic salts of drug such as propranolol oleate (Crowly *et al*, 2007) which

have lower water solubility compared to the parent API. Salt formation of the parent API has shown tremendous improvement in API dissolution, which has increased the number of improved bioavailability APIs in the pharmaceutical industry. In some cases, a salt after dissolution transforms into respective acid and base, which may precipitate depending on solubility. It may also cause high alkalinity or acidity at the site of absorption leading to patient compliance issues. Salt formation is not possible for neutral or weakly ionisable APIs.

Solvates can be defined as crystal structures containing stoichiometric or non-stoichiometric proportions of the solvent; if the solvent is water then it is termed a hydrate. The solubility of the anhydrous form of an API is higher compared to the hydrate, which can be attributed to the thermodynamic stability of the hydrate due to hydrogen bonds between the parent compound and water (Bartolomei, *et al*., 2000). Hydrates can be converted into the anhydrous form of API by application of heat, temperature and stress.

A polymorph is a solid crystalline phase, which exhibits the possibility of at least two different molecular arrangements of the compound in the solid state (Kulkarni, *et al*. 2013). Polymorphs show differences in properties such as solubility, melting point, dissolution rate, lattice energy, density, optical and electrical properties, vapour pressure, hardness etc. Generally, the most stable polymorph of the drug is commercially used. The transformation of crystal from one form to another can occur under various conditions. Development and stabilisation of metastable polymorphs has been explored to achieve higher dissolution rates. For example, Kulkarni *et al*., (2013) produced a stabilised metastable triclinic form of artemesinin through a hot

extrusion technique, which showed about three times faster dissolution compared to the stable commercially available orthorhombic form.

2.2 Stabilised amorphous form/Solid dispersion

The amorphous state of solid exhibits a short range molecular order but has no long range order of packing molecule like in crystalline forms. In other words, the molecules are arranged in an ordered form in relation to the neighbouring molecule but such order does not exist all over the solid and the molecular confirmation is also flexible. Occurrence of amorphous forms is common in proteins, peptides, polymers and some sugars. Though amorphous solids show high solubility and dissolution rate their physical and chemical stability is lower than the crystalline form. The amorphous form exhibits a glass transition temperature (Tg) where due to molecular mobility it is transformed into a rubbery state. The amorphous form has a tendency to transform into a more stable crystalline form. If a stable crystalline form exists, an amorphous form will transform into the crystalline form upon if sufficient molecular mobility is allowed. The API can be maintained in the amorphous form by dispersing it in a high Tg substance and storing it at least 50 °C below the Tg of the mixture. Materials such as citric acid, urea, mannitol and polymers having high Tg and tendency to form hydrogen bonds are used to stabilise the amorphous form of a drug. The dispersion of an API into the matrix of these small molecules or polymers is termed solid dispersion and depending on the state of the dispersion these can be further defined as eutectic mixtures, solid solutions or solid suspensions (Table 2.2).

Table 2.2: Types of solid dispersion (Adapted from Singh *et al*. 2011)

Sr No.	Type	Comment	No. of phases	API	Matrix
				*	**
1	Eutectic	Very first type of solid dispersion reported	2	C	C
2	Crystalline matrix precipitation	Less explored	2	A	C
3	Solid solution				
	Continuous solid solution	High miscibility at all ratios	1	M	C
	Discontinuous solid solution	Molecular dispersion of API with partial miscibility	2	M	C
	Substitutional solution	API is molecularly dispersed with difference in molecular diameter between two phases. In this the API and matrix are subsititutional which can be continuous or discontinuous.	1 or 2	M	C
	Interstitial solid solutions	Less miscible, discontinuous with molecular diameter of API 59% of that of matrix	2	M	C
4	Glass suspension	Cooling rate decides the size of dispersed API in matrix after	2	C	A

		crystallisation of drug in amorphous matrix.			
5	Glass suspension	Cooling rate decides the size of dispersed API in matrix after crystallisation of API in amorphous matrix.	2	A	A
6	Glass solution	API and matrix should possess good miscibility or solid solubility or complex formation upon fast cooling or evaporation during preparation	1	M	A

*A: matrix in amorphous state, C: matrix in crystalline state

**A: Molecular dispersion of API cluster in amorphous form in matrix, C: crystalline API dispersed in the matrix, M: Molecular dispersion of the API throughout the matrix

Another classification based on types of carrier used categorises solid dispersion into three generations (Figure 2.2)

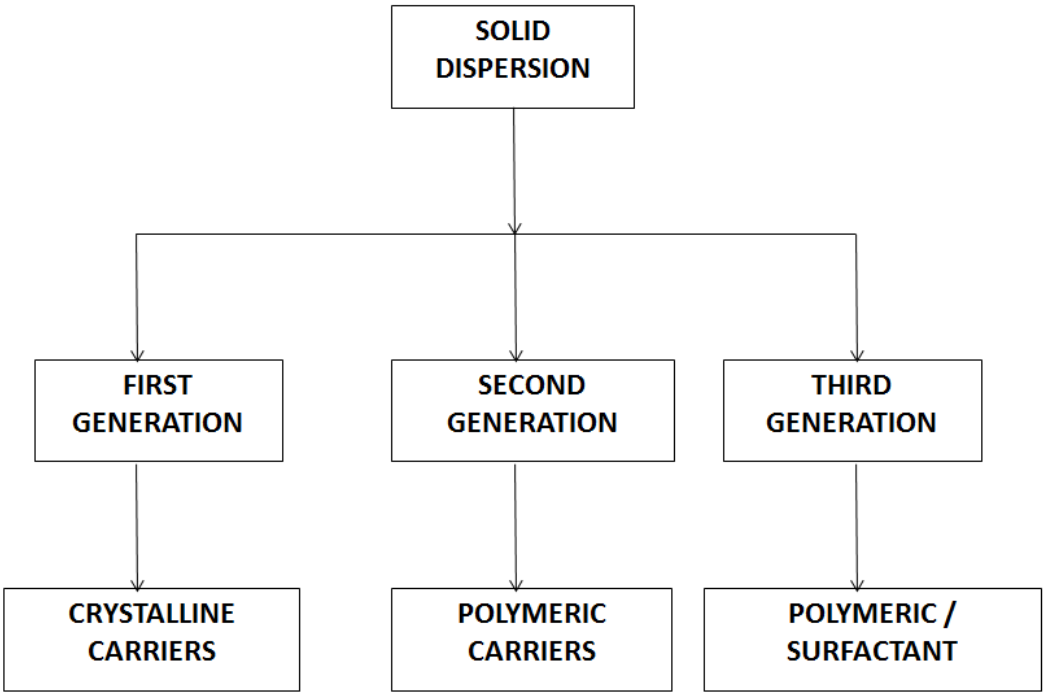

Figure 2.2: Classification of solid dispersion

The eutectic mixtures and the solid dispersions where the polymeric matrix is crystalline such as solid solutions are considered first generation solid dispersions (polyethylene glycols, urea and polyoxyethylene-polyoxypropylene (Pluronic®) Leunar, 2000). Systems containing amorphous matrix states such as glass solutions and glass suspensions are considered as second generation solid dispersion. Examples of amorphous polymers include PVP (Simonelli, *et al*., 1969), Polyethylene glycols (Guyot, *et al*., 1995), polymethacrylates (Ceballos, *et al*., 2005) and natural polymers such as hydroxypropylmethylcellulose (HPMC), ethyl cellulose (Ohara, *et al*., 2005), hydroxypropylcellulose (Tanaka, *et al*., 2005) which are cellulose derivatives and starch derivates, like cyclodextrins (Rodier, *et al*., 2005)). Recently there are some reports where a surfactant has been added in addition to the polymer and these are classified as third generation solid

dispersions for example gelucire 44/14 (Chauhan, *et al*., 2005) and poloxamer 407 (Majerik, *et al*., 2007).

2.2.1 Dissolution from solid dispersions

Solid dispersions being one of the major focus areas in solubility enhancement involve making APIs miscible in a suitable polymer matrix in desired ratio (Leuner, 2000).

The steps in the dissolution of a typical oral dosage form are shown in Figure 2.3. The modified Noyes and Whitney equation (Hattori, *et al*., 2013) explains the relationship between rate of dissolution and various factors.

$$\frac{dC}{dt} = \frac{AD(Cs - C)}{h} \qquad \text{..... (1)}$$

where, *dC/dt* is rate of dissolution, *A* is the surface area available for dissolution, *D* is the diffusion coefficient, *Cs* is the solubility of the compound in the dissolution medium, C is the concentration of API at time *t* and *h* is the thickness of boundary layer near to the surface of the dissolving material.

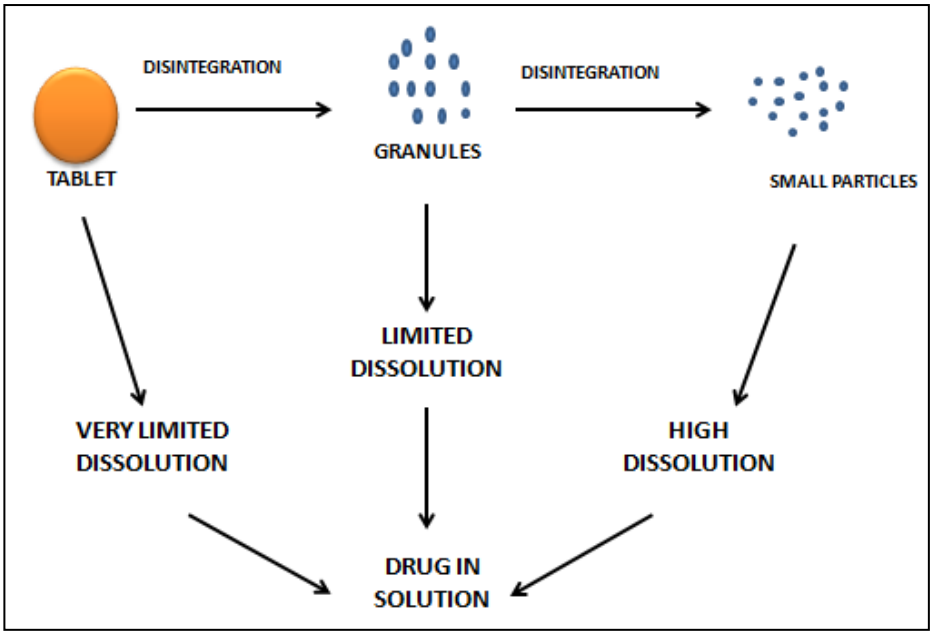

Figure 2.3: Steps in the dissolution of solid dosage forms (adopted from Gibaldi, 1977)

In conventional tablet and capsule dosage forms generally the particle size of the API is more than 5 μm whereas; in solid dispersions the effect of surface area is not important as the API is molecularly dispersed within the matrix (Serajuddin 1999).

The rate of API absorption is dependent on the concentration of API present in solution form at the site of absorption. High apparent solubility leads to achievement of higher API concentration in the solution and in turn faster absorption. If the rate of API dissolution is too high it causes supersaturation of the API in the GI fluids. In such cases a spring effect is observed due to precipitation of the API, as shown in Figure 2.4.

In solid dispersions the polymer matrix maintains the API in a dissolved or dispersed state throughout its shelf life. If the dispersion matrix is hydrophilic it enhances apparent solubility of the API and accelerates its dissolution, which provides higher concentration at the site of absorption leading to an improvement in bioavailability. Sometimes the bioavailability enhancement is not achieved because high API concentration is not maintained long enough as the API precipitates out, which is the “spring effect”. Polymers help to maintain the solution concentration by inhibiting nucleation that is the “parachute effect”. Hence in solid dispersions polymers enhance apparent solubility and also help in avoiding the spring effect.

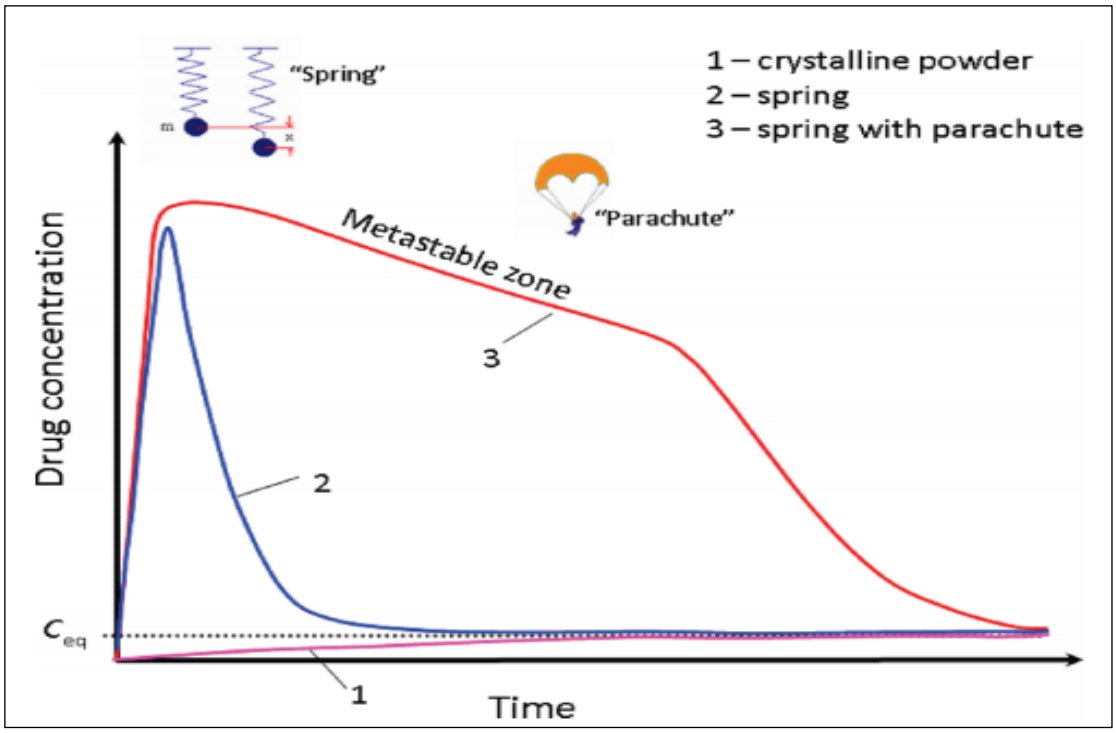

Figure 2.4:Representation of spring-parachute effect. (Babu and Nangia, 2011)

Li *et al.,* (2013) compared the ability of different cellulose ester derivatives in solubility enhancement and stability of an ellagic acid solid dispersion. PVP shows high solubility enhancement in 0.1 N HCl but the high supersaturation levels caused precipitation of ellagic acid. Cellulose esters showed incomplete release at pH 6.8 but avoided any precipitation; therefore cellulose esters were concluded to be more useful compared to PVP.

Mogal *et al.,* (2012) studied the role of porosity in solid dispersions in faster API release, compared to other formulations. It was suggested that the reticular polymer which forms a web like structure (Figure 2.5) which shows a slower dissolution rate compared to solid dispersions prepared using linear polymers.

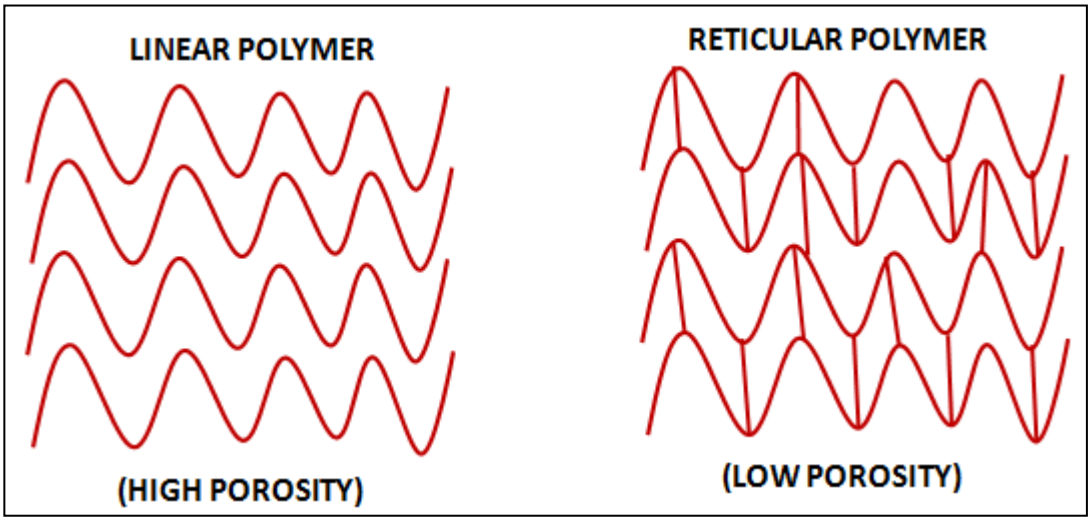

Figure 2.5: Porosity variation according to the type of polymer (Kim *et al*., 2011)

2.2.2 Methods of preparation of solid dispersion

Though Sekiguchi and Obi reported the concept of solid dispersions in 1961, commercial exploitation of this concept was very limited until recently. A review of the status of solid dispersions by Serajuddin published in 1999 (Serajuddin, 1999) suggested that slow progress towards commercialisation in almost 40 years due to a need for scalable manufacturing technologies and stability issues associated with the amorphous state. Solvent evaporation and melt fusion techniques were explored in depth.

In solvent evaporation the API and polymer are dissolved in a solvent and the solvent is evaporated to achieve a uniform dispersion of API in the polymer matrix. Chiou and Riegelman (1971) first reported use of this technique griseofulvin - PEG 6000 pair. The main challenge is selection of a solvent which has the ability to dissolve a hydrophobic API and hydrophilic polymer in the desired ratio. For example, for preparation of a solid dispersion containing 10% griseofulvin in PEG 6000 the solid: ethanol ratio was 1:100. The

requirement of high amounts of solvent makes the process expensive and environment of unfriendly. Attempts were made to reduce the solvent amount using solvent mixtures, surfactants, pH optimisation which could bring down the solid: solvent ratio in the range of 1:25 to 1:60 but still issues like residual solvent and long duration of evaporation remained the major limiting factors (Serajuddin, 1999).

Spray drying has proved to be a scalable and commercially viable technology for solid dispersion. Though spray dried solid dispersions have been successfully launched it still suffers from the challenges associated with use of solvent (Paradkar *et al*., 2004).

2.2.2.1 Melting method

Sekiguchi prepared solid dispersion by melting using urea as a carrier (Sekiguchi, 1961). The melting method consists of melting of the API and carrier in a desired ratio to form a homogenous molten mixture and its subsequent cooling using a suitable cooling method. Later this solid form is pulverised and formulated into a suitable dosage form (Owusu-Ababio, 1998).

Several drawbacks are associated with melting methods, when the API polymer mixture is subjected to high temperature; there are chances of degradation attributed to the thermal properties of either of the components or interaction between the two components at high temperature (Serajuddin, 1999). The molten mass during cooling may crystallise or entrap moisture (Venkitachalam, 1992). Miscibility of the molten components is essential to achieve homogeneity in the final product (Lordi, 1984). Depending on the

process the nature of the end product and its physicochemical properties will change and in turn affect API release.

Recently, Taylor's group reported the role of polymers in inhibition of nucleation and growth of paracetamol crystals from the melt. Polyacrylic acid enhanced nucleation rate whereas HPMCAS inhibited nucleation (Ilevbare *et al*., 2012). Polyacrylic acid and PVP were found to be good inhibitors of crystal growth while HPMCAS had no effect. This investigation provides an approach for understanding and selection of polymers for solid dispersions to be prepared by melt method.

Melt extrusion has proved to be a solvent free, scalable approach for manufacturing of solid dispersions and Kaletra (Zolidex) was the first product introduced by Abbott using this technology (Breitenbach, 2002). Further details of melt extrusion technology are provided in the later parts of this section.

Although melting methods have several disadvantages, hot melt extrusion can be used as the best tool for effective melt solid dispersion manufacturing (Breitenbach, 2002). Hot melt extrusion is a modified melt and shear based manufacturing process which can assure effective mixing of two components irrespective of their individual melting differences by applying simultaneous stress and temperature. Hot melt extrusion has proven to be a viable option for development of oral delivery systems for various APIs.

There are many reports on solid dispersions by hot melt extrusion which are summarised below,

Lakshman, (2008) studied the effect and applications of HME in development of physic-chemically stable sold dispersions for low water soluble drugs. The solid dispersions were prepared by solvent evaporation and HME. The drug loading achieved was 20% with low or no degradation. The use of surfactant improved dissolution. Sarode, (2013) studied the effect of drug polymer interactions on the supersaturation levels in solid dispersions. Indomethacin, Itraconazole and griseofulvin with hydrophilic polymers such as Eudragit EPO, Eudragit L-100-55, Eudragit L-100, HPMCAS-LF, HPMCAS-MF, Pharmacoat 603, and Kollidon VA-64 were used. The improved dissolution profiles of resulting solid dispersions were contributed to drug polymer interaction during extrusion.

In case of thermally unstable drugs polymer combination approaches were used to avoid any degradation during extrusion. Liu *et al.,* (2013) studied the use of polymer combination using carbamazepine as model drug with Kollidon® VA64, Soluplus® and Eudragit® EPO. The drug polymer miscibility at temperatures below melting point of carbamazepine was achieved. Solid dispersions with soluplus and EPO combination were most stable. HME processed solid dispersions have been compared with other processes, Dong *et al*., (2008) studied the effect of different processes on the solid state characteristics of the solid dispersions. HME process yielded more stable solid dispersion when compared against co-precipitation. The suitability of HME process for various drugs have been examined in combination with suitable polymers, Chokshi *et al*., (2005) studied the suitability of HME process for indomethacin solid dispersions using PVP and poloxomer polymers, Indomethacin poloxomer combination showed poor solubility.

Zhang and McGinity, (1999) have studied the use of HME for manufacturing sustained release tablets, Chlorpheniramine maleate was used as model drug and polyethylene oxide (PEO) as polymer, the resultant tablets were stable and dissolution of these tablets were controlled by swelling phenomena by PEO.

Recently, McGinity's group reported a novel continuous technology KinetiSol® (Hughey *et al.,* 2010) (Little and Rice *et al*. (2004) US6709146) based on thermokinetic mixing. Thermokinetic mixing involves application of very high mechanochemical stress through friction for a very short period of time, which helps avoid resultant degradation due to the high stress environment (Figure 2.6). The mechanism is described as fusion owing to the shear and fiction, which help to process and transform APIs in amorphous state in a very short residence time with minimum thermal exposure. This process has been utilised for manufacturing solid dispersions of many APIs such as itraconazole, meloxicam etc. Formulation of low melting APIs is also possible using this technique due low thermal exposure to avoid resultant degradation. Plasticiser free processing is claimed to be one of the major advantages of this technology.

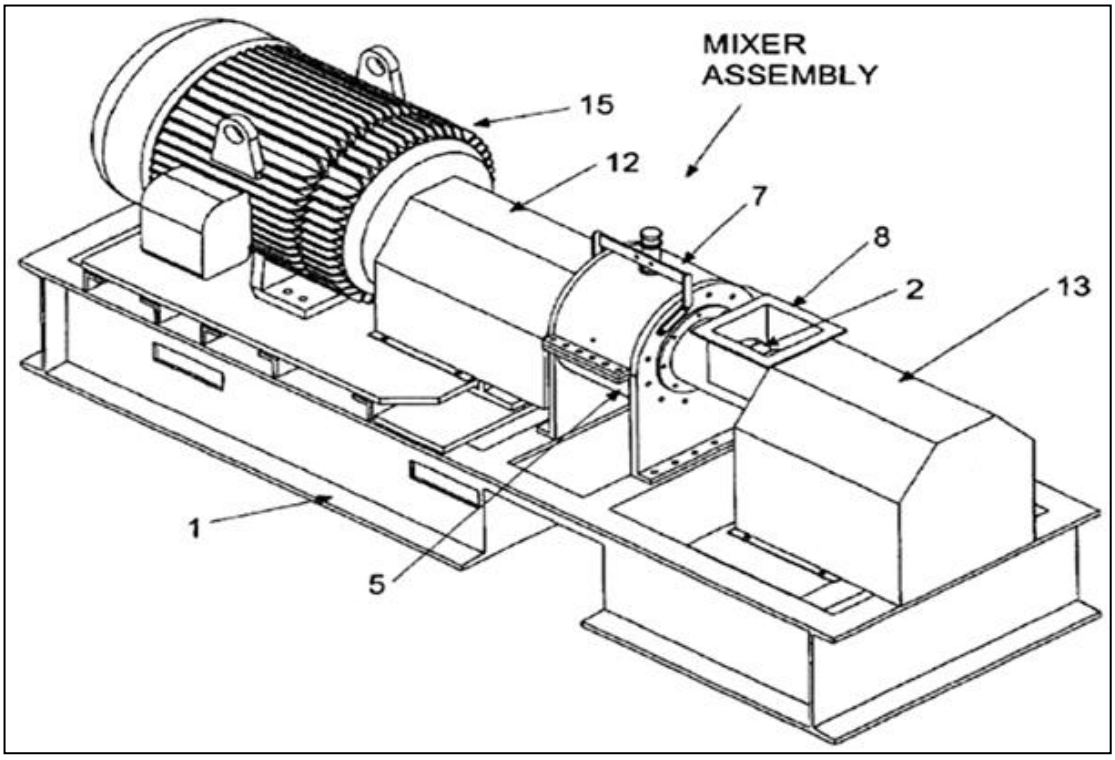

Figure 2.6: Thermokinetic Mixer (Little and Rice, US6709146)

2.2.2.2 Milling

Milling technologies have been used in the pharmaceutical industry for size reduction purpose for many years. Extensive size reduction during milling can lead to a breakdown of crystalline structures of API to very fine powder in the amorphous state. There are a few reports of use of different types of mills to obtain solid dispersions.

Zhao *et al.,* (2011) used laboratory planetary scale ball mill with Tanshinone IIA as model drug, poloxomer 188 was used as surfactant. The resultant ball milled solid dispersion showed improved dissolution rate with improved stability for 60 days. Shin *et al*., (1998) used ceramic ball mill to prepare furosemide solid dispersion with crosspovidone, the resultant was stable over one year at room temperature, it was concluded that drug dissolution was improved due to improved drug polymer interaction.

Nokhodchi *et al*., (2007) used vibratory ball mill for preparation of solid dispersion for chlordiazepoxide. The solid dispersion by ball mill was compared with solvent evaporated dispersion which showed higher drug release. Al-obaidia *et al*., (2013) studied solid dispersion for griseofulvin with hydroxypropyl methyl cellulose acetate succinate. Retsch MM20 95 vibratory ball mill was able to form a good hydrogen bonding between drug and polymer.

High energy ball mill is also a better process for converting drug polymer into amorphous state, Branham *et al*., (2012) prepared a saquinavirmesylate solid dispersion using high energy ball mill. They could achieve unique non-porous particles with unique structural features, there was no metal contamination observed upon 15 hours of milling.

Ball milling is mainly a batch process which requires long milling times of at least a few hours to achieve the amorphous state and the control on product quality is difficult.

The major focus of this research is evaluation of a continuous solid state shear milling (S3M) technology developed at Sichuan University, for processing of solid dispersions. The details of S3M technology are discussed in later parts of this Chapter.

Table 2.3: FDA approved marketed solid dispersions (Huang and Dai, 2014)

Product name	Drug	Polymer	Dose (mg)	Drug melting point (°C)	Technology	Approval year
Cesamet	Nabilone	PVP	1	160	---	1985
Sporanox	Itraconazole	HPMC	100	166	Spray drying on sugar beads	1992
Prograf	Tacrolimus	HPMC	5	128	Spray drying	1994
Kaletra	Lopinavir/ ritonavir	PVP/VA	200/50	125/122	Melt extrusion	2005
Intelence	Etravirine	HPMC	200	265	Spray drying	2008
Zotress	Everolimus	HPMC	0.75	115	Spray drying	2010
Novir	Ritonavir	PVP/VA	100	122	Melt extrusion	2010
Onmel	Itraconazole	HPMC	200	166	Melt extrusion	2010
Incivek	Telaprevir	HPMCAS	375	246	Spray drying	2011
Zelboraf	Vemurafenib	HPMCAS	240	272	Co-precipitation	2011
Kalydeco	Ivacaftor	HPMCAS	150	291	Spray drying	2012

2.3 Cocrystallisation

In recent year's cocrystals have been widely explored for the dissolution rate enhancement of the poorly water soluble drugs. Cocrystals are multicomponent crystals containing components in a stoichiometric ratio. The components forming cocrystals are solid at ambient temperature and may be atoms, ions or molecules held by non-covalent bonding such as hydrogen or halogen bonds. (Jones *et al*.,2006).

Desiraju (1995) was the first to report cocrystals as molecular complexes which include multicomponent systems bonded by intermolecular non-covalent interactions. After much discussion a generally considered definition of a cocrystal as defined by Shan and Zaworotko (2008) is a *cocrystal is a multiple component crystal in which all components are solid under ambient conditions when in their pure form. These components co-exist as a stoichiometric ratio of a target molecule or ion and a neutral molecular cocrystal former(s)"* (Shan and Zaworotko, 2008).

Cocrystals are "s*olids that are crystalline materials composed of two or more molecules in the same crystal lattice"*, as per USFDA. An API and a co-former are the two components in pharmaceutical cocrystals. Cocrystals show significantly different physicochemical properties compared to that of the API.

US FDA in its Novel drug applications (NDAs) or abbreviated new drug applications (ANDAs) approval claims of cocrystals requires 1. Need to investigate when the API and co-former interact and which kind of interaction

exists between them, unlike ionic interaction in salts, neutral or non-ionic interactions should exist. Generally the difference between pKa (ΔpKa) values of the API and co-former is less than zero, the proton transfer will be negligible which tends to form a cocrystal. If the ΔpKa difference is more than 3 there will be a complete proton transfer and it will form a salt. When the ΔpKa value is between 0-3 then the ionization behaviour and extent of proton transfer is unpredictable.

According to USFDA guidelines the API should dissociate from its co-former/ excipients before reaching to the site action. In case of a cocrystal the 'API-co-former' complex should be treated as an intermediate product. Cocrystal containing pharmaceutical products is not considered to contain a new API but a specifically designed drug product intermediate which will contribute to its improved performance.

2.3.1 Co-former selection

As the co-former is an important part of successful cocrystal formation, co-former selection has become a very crucial step, mainly based on "synthon" approaches (Desiraju, 1995). The co-former molecule should possess specific molecular fragments to form "supramolecular synthons". The synthon approach basically suggests that one particular group on the parent API and the co-former play an important role in successful cocrystallisation. Because of these co-formers with complementary functional groups should be selected. Some of the major molecular synthons used are carboxylic acid-acid, amide-amide, acid-pyridine and the acid amide (Thakuria, *et al*., 2013). The synthon approach has some disadvantages that formation of supramolecules is not quantitative in the sense that even after formation a

supramolecule might not fit well into the ordered crystalline space. A computational approach has been reported for selection of co-formers, based on the polarity and shape complementarity for cocrystallisation (Qiao, *et al*., 2011). Abramov *et al*., (2012) considered the influence of fluid phase thermodynamics for co-former selection, based on the comparative study of excess enthalpy of the API and co-former (Abramov *et al*., 2012).

2.3.2 Methods of cocrystal formation

To date, many methods have been reported for cocrystal formation. Among the reported techniques, solution cocrystallisation and grinding are the most commonly used and have been widely explored. Solution based methods include evaporation, reactive crystallisation and cooling crystallisation (Figure 2.7). Grinding method generally includes solvent assisted grinding and neat grinding.

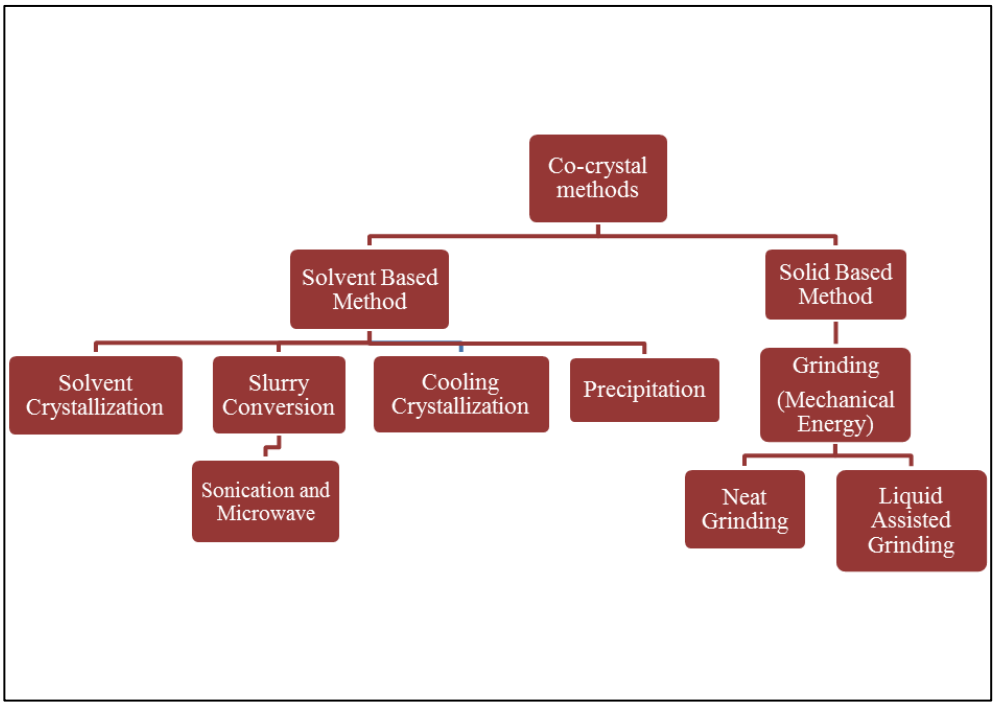

Figure 2.7: Classification of cocrystal preparation methods

There has been an emergence of new techniques for cocrystal formation such as supercritical fluid cocrystallisation (Padrela *et al*. 2009), hot-stage microscopy (Berry *et al*. 2008), ultrasound assisted cocrystallisation (Aher *et al*. 2010), microwave assisted cocrystallisation (Pagire *et al*. 2013) and spherical cocrystallisation (Pagire *et al*. 2013).

2.3.2.1 Solution crystallisation

In solution crystallisation the two components are dissolved in a suitable solvent system and supersaturation is achieved to obtain a cocrystal phase. Supersaturation may be achieved by any conventional technique such as evaporation or cooling.

The solution process is complex as it depends on solubility of the two components and rate of supersaturating the solution. Selection of suitable solvent or solvent mixture becomes more challenging in the case of non-congruently soluble drug co-former pair for example caffeine: maleic acid (Aher *et al*., 2010) compared to congruently soluble pairs such as carbamazepine: saccharin (Pagire *et al*., 2013). Generally, a ternary phase diagram is used to select suitable compositions for cocrystallisation (Blagden *et al*., 2007). The major disadvantages of solution cocrystallisation include low yield, chances of unreacted components present as impurities, generation of polymorphs and solvates, degradation of API or co-former due to solvent based reactions such as hydrolysis.

2.3.2.2 Grinding method

Grinding methods are categorised as neat grinding and solvent assisted grinding. Neat grinding or dry grinding is a solvent free technique and involves a stoichiometric concentration of both the components subjected to grinding manually using a mortar and pestle or any mechanical mixing device such as a ball mill or a vibratory mill. Dry grinding needs one or both components to have a higher vapour pressure in the solid state (Friscic and Jones, 2009). Many cocrystal pairs have been reported to form cocrystals by dry grinding (Karki *et al*., 2009). The mechanism for dry grinding is reported by many researchers to include different types of intermediate phases, molecular level diffusion, eutectic formation or amorphous state in which one of the distinctive phase (gas, liquid or a amorphous solid) should exhibit higher mobility than the parent components (Friscic and Jones, 2009).

Solvent assisted grinding or kneading is a wet grinding technique where mixing of the two components is assisted by use of a small amount of a suitable solvent (Shan *et al*., 2002). The improved mixing causes effective orientation and conformation with improved interfaces exposure and collision of the two components in the presence of solvent (Trask *et al*., 2004). The formation of cocrystal nuclei in solvent may enhance the overall cocrystallisation rate of the system and provide control of polymorphic transformation of the cocrystal. The solvent assisted grinding technique has been widely used for formation of new cocrystals as well in improvement of existing cocrystals (Weyna *et al*., 2009).

There has been an emergence of new techniques for cocrystallisation in the last few years some of which are described below.

2.3.2.3 Supercritical fluid technology (SCF)

SCF based crystal engineering has seen a large growth in the past decade in various applications for processing of materials and as a substitute to many solvent based processes. The SCF as a solvent provides advantages such as high solubility for many molecules, miscibility with other organic solvents which can be used as an anti-solvent. The SCF technique uses lower amount of organic solvent compared to other conventional solution based processes hence can be utilised with thermally sensitive and structurally unstable APIs (Qiao *et al*., 2011). Padrela *et al*., (2009) studied the three important aspects of the supercritical fluid in terms of power of solvent, atomization improvement and anti-solvent effect for indomethacin - saccharin cocrystals with different sizes.

2.3.2.4 Ultrasound assisted cocrystallisation

Ultrasound waves can be used for the formation of cocrystal from solution or slurry. The Cavitation energy of ultrasound waves form cocrystal nuclei in solutions or slurries. Aher *et al*., (2013) reported ultrasound assisted solution crystallisation of a non-congruently soluble pair of caffeine - maleic acid. The process generated 2:1 cocrystals compared to a 1: 1 stoichiometry, which was attributed to high levels of supersaturation resulting from the application of ultrasound energy.

2.3.2.5 Microwave assisted cocry*stallisation*

Microwaves can be an effective energy source in cocrystal formation. It is believed that microwaves can excite the molecular dipole moment and excite the dipolar rotation, which helps to increase the molecular mobility of the

system (Pagire *et al*., 2013). This increased molecular mobility converts energy through dielectric heating. Pagire *et al*., has reported that caffeine maleic acid cocrystal 1:1 can be obtained using microwave heating which is attributed to controlled saturation at the interface of components and dielectric properties of the solvents used.

Solvent based techniques have several disadvantages with regard to the stability of the cocrystal formed. Solvent free techniques other than grinding are emerging as alternative green techniques for cocrystal formation. HME and S3M or pan mill have been explored for formation of various cocrystals in the current study.

2.3.2.6 Cocrystallisation by hot melt extrusion

Solvent Free Continuous Cocrystallisation (SFCC) using hot melt extrusion is a continuous, green technique for cocrystal formation reported by Paradkar *et al.,* (WO2010013035). SFCC involves cocrystallisation by application of shear and heat in a twin screw extruder (Figure 2.8). The shear is controlled using a suitable screw geometry, screw speed and residence time. The temperature inducing processing is maintained at the melting point of the lower melting component or eutectic point of the mixture. Melt extrusion involves efficient mixing and increased surface area of contact between the components which accelerates the non-covalent bonding between the API and co-former.

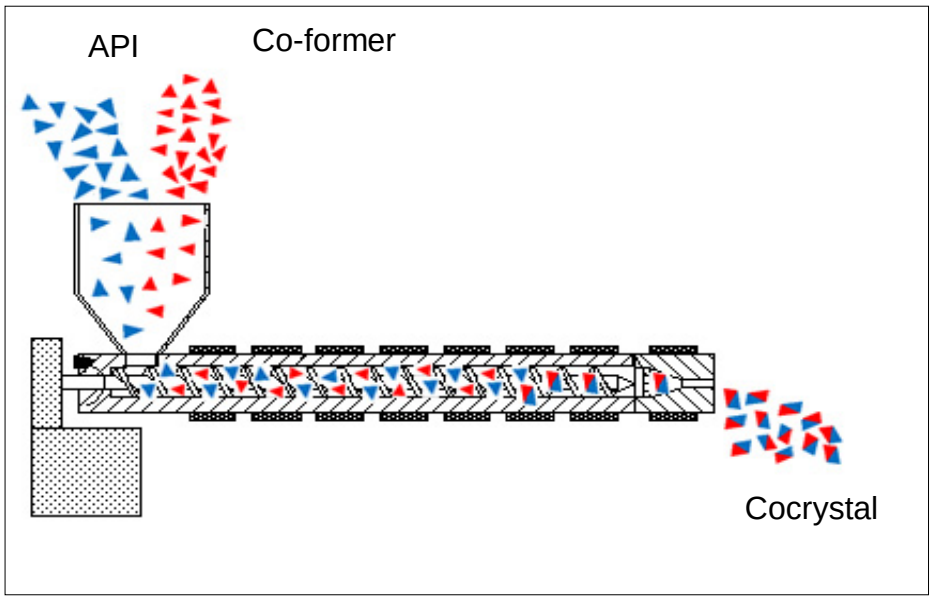

Figure 2.8: Schematics of cocrystallisation by HME

Application of SFCC has been demonstrated for successful cocrystallisation of many pairs such as ibuprofen - nicotinamide (1:1), carbamazepine - saccharin (1:1), carbamazepine - nicotinamide (1:1), caffeine - maleic acid (1:1 and 2:1), theophylline: maleic acid (1:1) etc. Dhumal *et al.* (2010) successfully prepared ibuprofen: nicotinamide (1:1) cocrystals in the form of agglomerates by hot melt extrusion (Dhumal *et al*., 2010). The additional advantage of the melt extrusion process is that it can form agglomerates of the cocrystals which is advantageous in downstream processing. The hot melt extrusion process is explained in detail in the later parts of this chapter.

2.3.3 Characterisation of cocrystals

Pharmaceutical cocrystals are generally characterised based on their chemical structure and physical properties. Cocrystal structural determination can be carried out by powder X-ray diffraction, single crystal X-ray crysatllography, Raman spectroscopy and Infrared spectroscopy (IR spectroscopy). Each cocrystal formed has a different crystallinity than the

starting components, which can be differentiated by X-ray scattering (Schultheiss and Newman, 2009). The change in crystallinity pattern occurs due to the non-covalent hydrogen bond formation between the API and co-former. Raman and IR spectroscopy are mainly used for structural analysis and detecting hydrogen bonding between API and co-former. IR spectroscopy has proved to be an excellent technique for differentiating hydrogen bond formation in cocrystal entities (Jaysankar *et al*., 2006), whereas Raman spectroscopy is a unique technique to find out polymorphism in cocrystals and starting crystal component.

Carbamazepine: saccharin (CBZ:SACC) 1:1 cocrystal exists in two polymorphic forms. FT-IR analysis helps understand and differentiate between two polymorphs of CBZ: SACC 1:1 cocrystal polymorphs. Polymorph I shows -N-H functional bond streching at 3500-3300 cm^{-1}, whereas in case of polymorph II the -N-H stretching can be seen at 3430 cm^{-1} and 3350 cm^{-1} (Portar *et al*. 2008). Differential scanning calorimetry (DSC) and hot stage microscopy are used as tools for screening as well as characterisation of cocrystal including detection of polymorphs and unreacted components.

To study crystal shape and size properties, microscopic studies like scanning electron microscopy (SEM) can be used. Surface energy measurement is one of the most important aspects of cocrystal characterisation processed by different shear based processes HME and S3M. The change in crystal habits and surface properties of cocrystals by different methods will show differences in surface energies which will affect the overall pharmaceutical performance. Surface heterogeneity measurement will provide an idea about the change in surface energy of the respective material. Differential vapour

sorption analysis is another important tool to study the behaviour of the water vapour sorption by different cocrystals and the amount of vapour sorbed can be correlated to the total crystalline content of system.

Both the approaches can be the solution for low water solubility issues of selected BCS class II drugs. Solid dispersions mainly deals with the making drug amorphous by solubilising or dispersing it in polymer matrix whereas in case of cocrystal the conversion of drug into a cocrystalline complex by bonding with co-former. The characterisation method and processes used for solid dispersions and cocrystals can be used for each other, for example HME, S3M like solid state high shear processes can be used for manufacturing solid dispersions as well as cocrystals. Characterisation method will include same all basic technologies such as thermogravemetric analysis (DSC), X-ray diffraction analysis, FT-IR, NIR and dissolution studies. DSC analysis will focus on the absence of melting endotherm for drug in solid dispersion whereas in case of cocrystal it will focus on typical endotherm generated by newly formed cocrystal which will be different from drug and co-former. In case of X-ray diffraction analysis due to the absence of any crystalline entity in solid dispersion will confirm its amorphous nature whereas in case of cocrystal there will be unique crystalline pattern will be observed which will be different from both drug and co-former.

Advantages of solid dispersion over cocrystals will be more based on the nature and structure of drug molecule. If drug molecule does not have hydrogen bond forming ability with co-former or if it does not have complementary functional group to form hydrogen bond with the co-former, in such case forming solid dispersion for that particular drug will be more

advisable. Disadvantage of solid dispersion cab be focussed on the stability issues of the system, amorphous systems are generally high energy systems which usually tend to convert into crystalline form and hence disturbing or breaking the amorphous nature. Disadvantage of cocrystal formulation can be owed to nature of process, unlike solution crystallisation one has to optimised any other process to higher precision to get phase pure cocrystal.

It will be more convenient to choose one approach among solid dispersion and cocrystal depending upon nature of drug, its functional group, its ability to form amorphous system, its ability to form cocrystals etc. In terms of scale up it will very challenging to confirm which approach will be better than other as both the approaches solves the low solubility issues related with drug and its other physicochemical properties. Performance of both the system will be based more on the need of drug release pattern, stability of the system. It will not be wise to choose one over other in terms of their performance because performance will vary according to the need of the formulation. In term of sustained, controlled release of drug solid dispersion will be better option than cocrystal whereas in terms of rapid release vice versa. In terms of scalability and economic point of view it will be difficult to compare directly which will be more feasible and cost effective. It will be wiser to say the nature of starting material will decide the total cost and scalability challenge for solid dispersion and cocrystals. It will change with type of drug, polymer and co-former respectively.

The current study has also explored formulation of solid dispersion system using different polymer and processes.

2.4 Processing technologies

Cocrystal and solid dispersion technologies have proved their potential in solubility enhancement and have been widely accepted by the industry. The current study includes the solid state processing of pharmaceutical drugs, co-formers and different polymers for continuous manufacturing of cocrystals and solid dispersion dosage forms. The two solid state processing techniques adopted are,

1. Hot melt extrusion and

2. Solid state shear milling (S3M/ Pan Mill)

2.4.1 Hot melt extrusion

Since its introduction into the pharmaceutical industry hot melt extrusion has proven to be a useful complementary technique compared to routine pharmaceutical processes.

2.4.1.1 Hot Melt Extrusion overview

Hot melt extrusion technology is a very commonly used technique in the plastics industry for the extrusion of different plastics and polymers to achieve mixing and to tailor the properties of the polymer composites (Kaufman and Falcetta,1977).

The plastics industry extruder has been modified for application in the pharmaceutical industry. Pharmaceutical grade extruders use stainless steel (SS 316) contact parts, have improved temperature control and are designed to achieve easy cleaning.

Extruders can be divided into two types (Crowley *et al*., 2007), namely ram extruders and screw extruders. A broad classification of extruders is given in Figure 2.9,

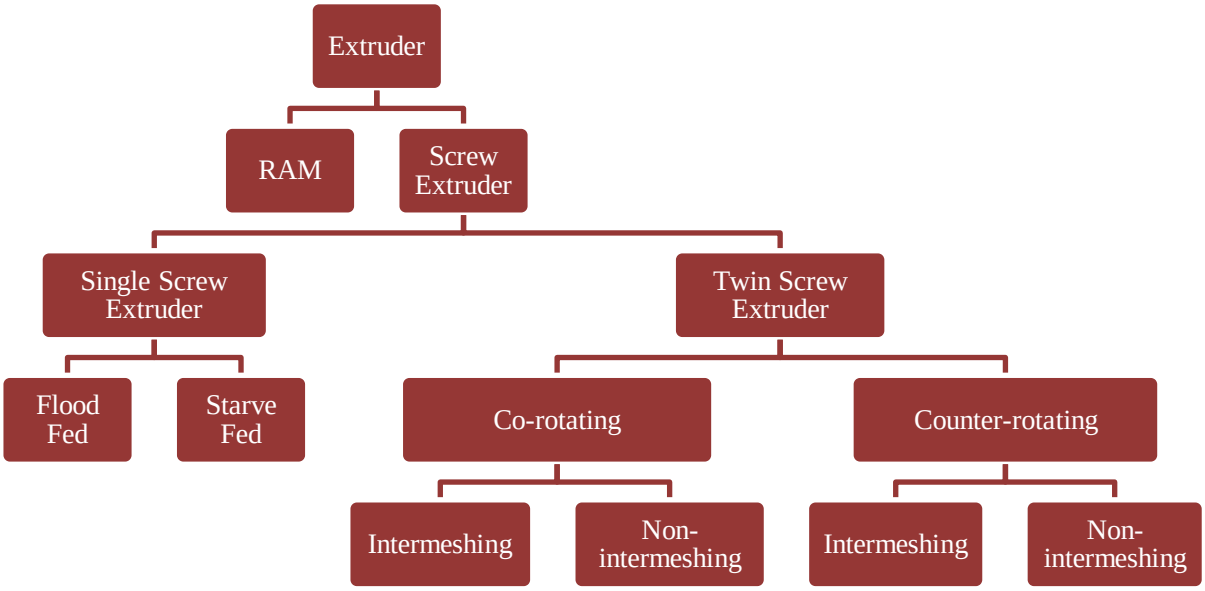

Figure 2.9: Various types of hot melt extruder

Ram extrusion is also called vertical extrusion, which involves the use of a piston to force a molten polymer through a die of desired shape. There are no specific mixing mechanisms in the ram extruder, the cylindrical conveying compartment in which premixed polymer blend is kept at a required temperature profile, once the polymer blend softens it is then forced through the desired die with the use of ram piston to achieve a required shape. It is difficult to achieve homogenous extrudates using ram extrusion because of a lack of an effective mixing mechanism which can be overcome by screw extrusion.

A typical HME process involves three important steps, a) upstream processing which involves feeding of the material (polymer and API) b) compounding or extrusion step which involves melting, mixing and discharge of the homogenise molten mass, c) downstream steps which involve cooling and shaping of the extrudates also called pelletizing. The steps are shown in Figure 2.10.

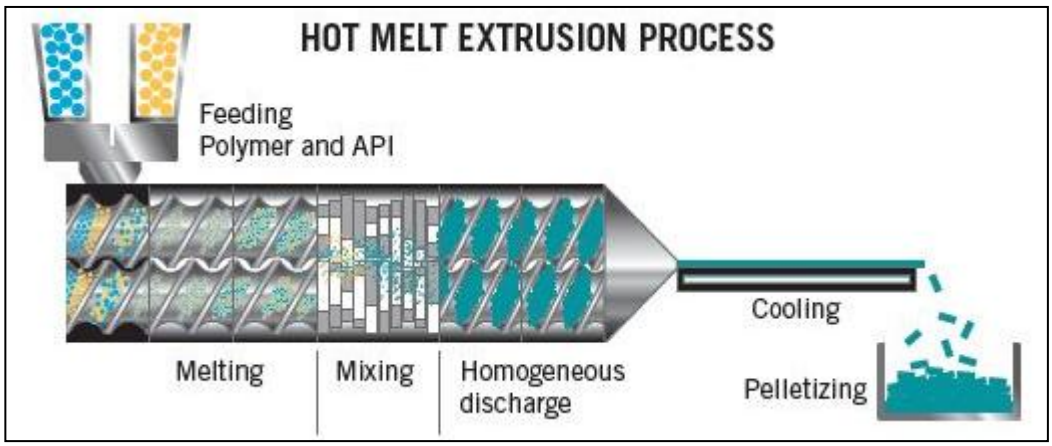

Figure 2.10: Hot melt extrusion steps (Courtesy Particle science, 2011)

Screw extruders are again divided into two types, single screw and twin screw extruders (Figure 2.11). A single screw extruder is generally used for melt conveying purposes and does not provide significant mixing. A twin screw extruder is composed of two screws placed side by side with range of configurations and different zones. The molten mass is transported and sheared until the end zone where the extruded product is collected. Twin screw extrusion is used where there is need for effective homogeneity in the end product.

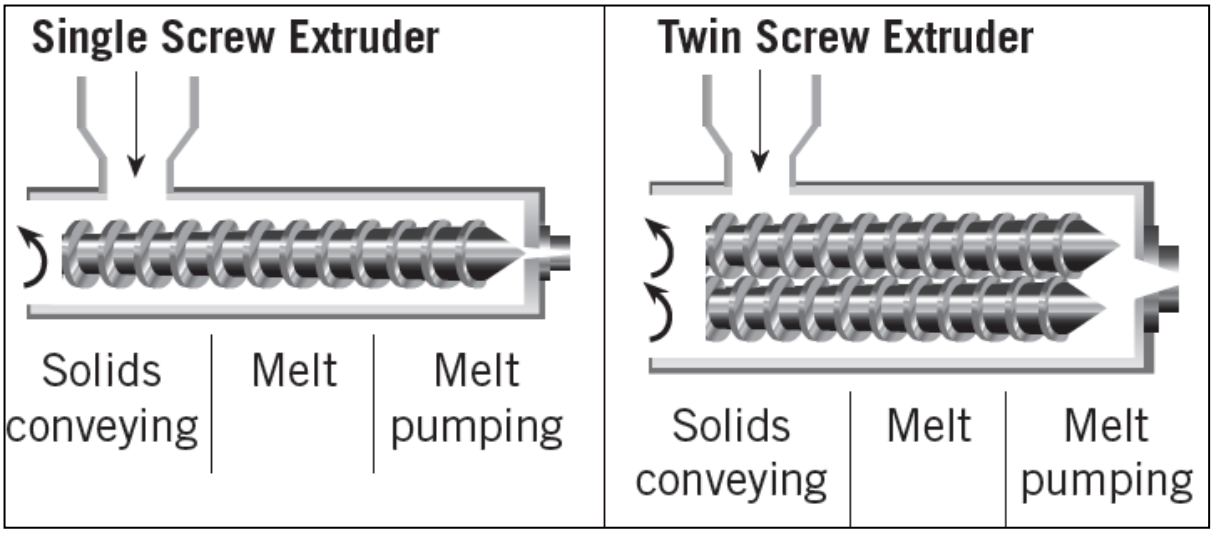

Figure 2.11: Representative images for single and twin screw extruder (Courtesy Particle science 2011).

The movement of the two screws in a twin screw extruder can be co-rotating or counter-rotating (Figure 2.12). Counter rotating screws involve high shear compared to co rotating screws, so whenever there is a need for high stress to deform and process material, counter rotating screws are preferred over co-rotating where conveying of material is required at a given temperature with optimum mixing, co-rotating screws are preferred. The high stress involved in the extrusion process with counter rotating screws may cause material entrapment, high pressure and lower output whereas co-rotating screws are easier to operate (Breitenbach, 2002).

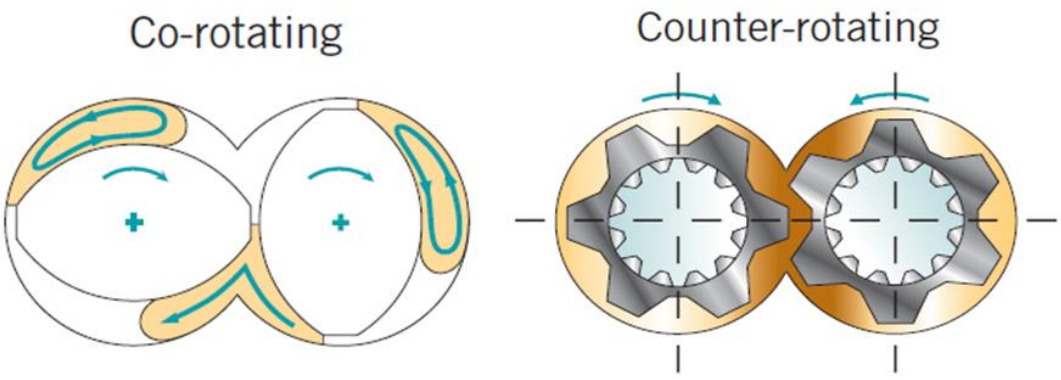

Figure 2.12: Counter rotating and co-rotating screws (Courtesy Particle science 2011)

The operation of a pharmaceutical extruder involves the following steps. a) The extruder preheated to get the optimum temperature profile before adding the drug polymer mixture, the different zones are adjusted to different set temperatures according to the ease of extrusion process and according to the melting temperature profile of the carrier polymer and drug mixture. Preheating helps to melt the polymer effectively and avoids the barrel jamming and creating the high torque which may start accumulating unmelted drug polymer mixture (Doetsch, 2003). b) The polymer drug mixture melts in the melting zone where temperature is maintained based on the melting or eutectic point and rheological properties of the mixture. The forward movement of the material is caused by the shear applied between the screw and barrel wall and by forward movement of the conveying screws which help to deliver the mixture to the die. Material is subjected to higher friction along the wall of the barrel and less friction between the screws (Luker, 2003).

The current hot melt extrusion studies have done using a Thermo Scientific Pharmalab 16mm twin screw extruder (Figure 2.13)

Figure 2.13: Thermo Fisher Pharmalab 16mm extruder (Thermoscientific, 2012)

Many low Tg drugs cannot be processed through hot melt extrusion due to potential degradation (Crowely *et al*., 2007). Residence time is relatively high in the case of melt extrusion which may result in degradation of some APIs (Crowely *et al*., 2007). Die blocking is another problem in the case of melt extrusion, in many cases temperature of extrusion process kept at Tg of the carrier polymer, but it cannot assure effective mixing of the drug in polymer matrix as this unmolten mass creates huge pressure in the system and causes die blocking. Use of plasticizers due to these problems has become common in extrusion processes for many polymer drug combinations. Plasticisation affects the physicochemical properties, stability and downstream processability of the extrudates (Bounartzi *et al*., 2014).

The energy consumption in hot melt extrusion processing is generally governed by torque levels and temperature during processing. The energy

consumption during melt extrusion can be reduced by use of a suitable plasticiser.

Downstream operations involve milling of melt extruded products to formulate them into suitable dosage forms such as tablets and capsules. The reduction in energy consumption during downstream processing of the extrudates is important as it will have direct effect on stability of the milled materials.

2.4.2 Solid state shear mill (S3M)

A solid state shear mill (Xu *et al*., 1996) based on the pan mill design has been developed at Sichuan University, China. S3M is a continuous milling technology and differs from other milling technology in its mechanochemical behaviour (Balaz, 2008). S3M is a pan mill designed in such a way that it will subject material to ultra-high shear and stress conditions by three principle processes namely pulverisation, high shear mixing and stress reaction caused due to high shear. The stress created during processing plays an important role in mechanochemistry. This mill has been used successfully for mechanochemical applications ranging from pulverisation, depolymerisation, and composite formation and grafting which are summarised in the next section.

A schematic diagram showing the design of pan mill is shown in Figure 2.14.

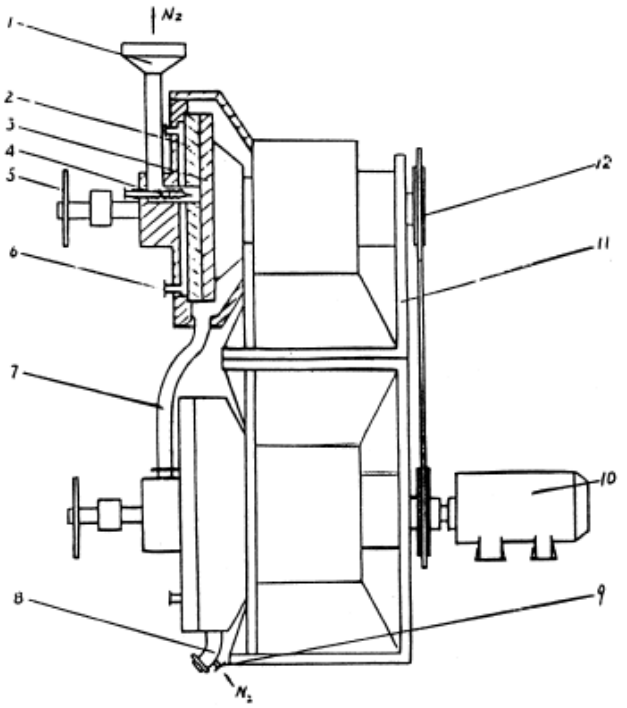

1. inlet, 2. stationary pan, 3. moving pan, 4. feeding screw, 5.helve, 6. medium entrance, 7. flexible tube, 8. outlet, 9. entrance for inert gas, 10. motor, 11. stand, 12. drive system

Figure 2.14: Pan mill equipment design (Xu *et al*., 1996)

The S3M consists of two in-laid pans, a rotar and a stator made up of wear resistant materials with specially treated surfaces. The pans have specifically engineered diametrical lines equally engraved into the surface (Figure 2.15) which create high shear during milling, an ideal feature for particle size reduction.

Figure 2.15: Typical pan surface

The stator is fixed on the equipment case and a rotor pan is mounted on the axis attached with motor. The motor power varies between 2-20 kW, depending upon mode of equipment. The pressure exerted on the pan can be adjusted with the handle which can be varied in the range 800-10000 N. Pan mill speed can be adjusted in the range of 10-200 rpm. The system is sealed and in the advanced version there is provision for circulation of gas or water in the jacket of the moving pan for temperature control. S3M is designed with different modes horizontal, vertical or series (two or three system one below other) for a more efficient milling process.

Both the surfaces of the stationary and moving pans are equally divided into a series of diametrical lines. On each region there are several bevels and the ridges of the bevels are parallel to dividing lines. The pair of pans are placed facing each other such that the bevels and ridges of both pans creating many unit cells. The shape and volume of these unit cells changes during movement of the moving pan on the stationary pan, resulting reduction in particle size. It forms a three dimensional schemes because of these bevels

and ridges during movement of the moving pan. Theoretical analysis and optimization of these ingenious structures has led to the formation of pan mill equipment a schematic of the pans is shown in Figure 2.16,

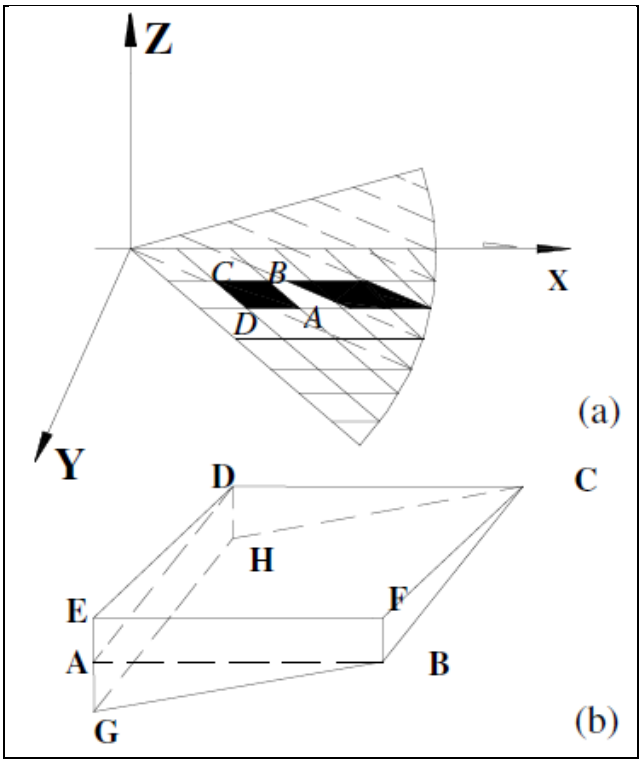

Figure 2.16: a) Pattern of moving pan on stationary pan, b) Three dimensional scheme for unit cell CDEF-CHGB (Xu *et al*., 1996)

The characteristic shear mechanism in S3M involves three steps, stress activation, stress degradation and stress synthesis. Simultaneous application of very high shear and stress on the material during the S3M process causes generation of new surfaces and may also rupture of bonds and formation of new bonds which initiates the formation of new structures (Xu *et al*., 1996). These high stresses may enhance elongation of the bonds between polymers and additive material and breaking bonds to form new surfaces which help to generate free radicals, cross-linking and branching.

Various polymers have been processed on S3M mostly higher molecular weight plastic polymers have been processed on the solid state shear mill such as polypropylene, polystyrene, poly (vinyl chloride), polyethylene with respect to size reduction, nanocomposite preparation and solid state grafting. S3M technology has been applied for processing of plastic materials and higher molecular weight polymers.

Zhang *et al*., (2007) has studied morphological and structural development of hardwood cellulose during mechanochemical pre-treatment using S3M. The mechanochemical properties were changed drastically in case of cellulose wood. The characteristic properties including particle size, molecular structure, and crystal structure were analysed by particle size analyser SEM, FT-IR and wide angle X-ray analysis. The thermal stability of S3M processed cellulose wood showed good thermal stability and higher solubility in aqueous alkali. S3M application in case of rubber polymer has been investigated widely, Zhu *et al*., (2010) has studied the effect of S3M for better processability and foamability of ground tire rubber. The resultant composite properties were improved upon S3M processing. The composite properties showed excellent foamability when compared against conventional melt method.

S3M has been explored for pulverisation ability on different polymers. Wang *et al*., (2002) showed that the S3M processing parameters can be optimised for better pulverisation of the polymers. Effect of different processing parameters of S3M on pulverisation showed it can be improved as per requirement. The most effective S3M way to pulverise given polymers was found at low rotational speed and high load. Another S3M application includes

delamination of layered minerals. Shao *et al*., (2005) studied the intercalation and exfoliation of talc using S3M. It was observed that intercalation can be achieved using S3M without use of any liquid additive.

Reduction in size of carbon nanotubes using S3M was achieved in case of polyamide 6 (Shao *et al*., 2006). The cutting of multi-walled carbon nanotubes gave significant reduction in size with straighter open ends; SEM studies revealed that there is homogenous dispersion of carbon nanotubes throughout polyamide 6. Size reduction being the major application for S3M, Lua and Wang, (2004) studied the formation of polypropylene/iron composite powders using S3M. It was observed that size reduction was scale down to nanometre level and the crystalline structure of polypropylene was completely disappeared. The size reduction to nanometre level is attributed to compression, stretching and fracture of cracks during S3M. Similar way Liu and Wang, studied the composite formation for high dielectric constant PP/BaTiO_3 using S3M.

Xia *et al*., (2004) studied the preparation of polypropylene/carbon nanotubes composite powder by mechanochemical pulverisation using S3M. Liu *et al*., (2007) studied the preparation of high flame retardant polypropylene by loading it with magnesium hydroxide using S3M, it was observed that there was high degree of blending and dispersion with improved chemical interaction and compatibility. The melt flow ability and processability was also improved.

S3M has been widely explored for solid state grafting of the higher molecular weight plastic polymers. Liu *et al*., (2008) studied the solid phase grafting of

hydroxymethyl acrylamide onto polypropylene using S3M. High shear and stress forced bonding in grafting was observed with macromolecular radical generation. The surface area was significantly improved due to size reduction.

To improve mechanical properties of different composites S3M process can be modified as per the need of end product. Shao *et al*., (2006) studied the effect of S3M on polymer blends of polyamide and polypropylene. It was observed that there was excellent control on morphology of resultant blend with improved mechanical properties. This resultant blend showed improved melt processing when subjected to melt extrusion and injection moulding.

S3M has three dimensional unique shear forces which act on the processing material. As compared to other mills all type of materials can be processed on pan mill hard, brittle, ductile etc.

It has been reported that high shear milling can induce amorphisation in the processing material by breaking down its crystalline structure to very fine size and convert it into amorphous form. Milling technology has great potential for manufacturing and processing materials to its amorphous form.

Chapter 3. Experimental

This chapter will provide details about materials used, drug profiles, processing methodologies used for generation of solid dispersions and cocrystals and characterisation techniques.

3.1 Materials

Drugs: Carbamazepine (TAJ pharmaceuticals lot no. TPL/CARB/002), Ibuprofen (TAJ pharmaceuticals), Caffeine (Sigma-Aldrich), Paracetamol (Medex), Glibenclamide (Medex)

Co-formers: Salicylic acid, Nicotinamide, Oxalic acid, Saccharin, Glutaric acid, Maleic acid. All the co-formers were obtained from Sigma-Aldrich Ltd. UK.

Polymers: HPMCP HP55 (ShinEtsu), HPMCAS (ShinEtsu), PVP VA64 (BASF), Ethyl Cellulose (BASF), Polyethylene oxide (PEO N80) (Colorcon)

3.2 Material profiles

3.2.1 Drugs

Four poorly water soluble drugs having different physicochemical properties and challenges were selected as model molecules for preparation of solid dispersions and cocrystals using HME and S3M. The rationale for selection of drug was based on the challenges related to them for formulating into solid dispersions and cocrystals for improving solubility was the main aspect, other

related challenges are enlisted in Table 3.1 and 3.2. All the selected drugs were BCS class 2 drugs except paracetamol which is BCS class 3 drug which has fair solubility in water but there many problems associated with formulation of paracetamol, one of which is its bitter taste and other is compressibility problem during tabletting of paracetamol (Karki, *et al.* 2009). The physicochemical data and related information about these drugs is summarised in Table 3.1.

Table 3.1: Drug profiles

Property	Ibuprofen	Paracetamol	Glibenclamide	Carbamazepine
Chemical structure	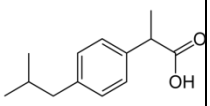	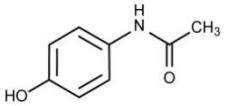	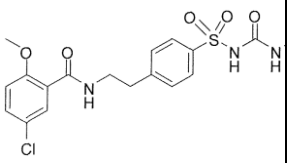	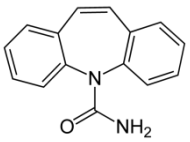
Molecular weight (g/mol)	206.29	151.169	494	236.26
Solubility (mg/L)	21	20	4	17.7
BCS class	II	III	II	III
Dose (mg)	400	500	5	200
Melting point (°C)	76	169	170	190
Glass transition temperature (°C)	-50	23	60	50
Solid	√	√	√	√

dispersion				
Cocrystals	√	√	X	√
Challenges	Low Tg	Low Tg, degradation, high dose	Low dose, erratic absorption	Degradation, polymorphism
References	Brabender C, *et al*. 2002	Sibik *et al*. 2014, Nainar *et al*. 2012	Babu and pandit, 1999, Chauhan *et al*. 2005	Sethia and Squillante, 2004, Patterson *et al*. 2008

3.2.2 Polymers

Polymers were selected on the basis of variable physicochemical properties and nature. The details of polymers are given in Table 3.2

Table 3.2: Polymer profiles

Properties	PEO	PVP VA64	HPMCP HP55	HPMCAS	Ethyl cellulose
Description	Synthetic polyether, hydrophilic, suitable for solid dispersion and as plasticiser	Vinylpyrrolidone-vinyl acetate copolymer, hydrophilic, suitable for solid dispersion	Cellulose ester with pH dependent solubility, soluble at pH 6.8, used for enteric coating	Cellulose ester with pH dependent solubility, soluble at pH 6.8, nucleation and crystal growth inhibitor, used for enteric coating	Cellulose ether, hydrophobic, suitable for controlled release

				and solid dispersion	
Class	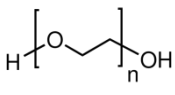	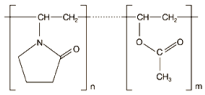	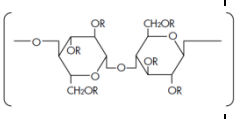	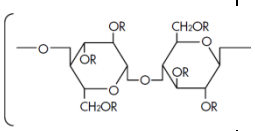	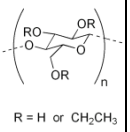
Amorphous /crystalline	Crystalline	Amorphous	Amorphous	Amorphous	Amorphous
Tm/Tg (°C)	75	110	145	123	140
Challenges	Low melting point, depolymerisation, hygroscopic	Medium Tg, hygroscopic	Breaking of ester linkage due to temperature and shear, destabilisation of drug, phthalate impurities, high Tg	Breaking of ester linkage due to temperature and shear, destabilisation of drug, high Tg	High Tg
References	DOW, 2002	BASF, 2011	Ghosh, *et al*. 2011, ShinEtsu, 2009	Ghosh, *et al*. 2011, ShinEtsu, 2009	Hercules, 2011

3.3 Methods

This section will explain in details the general experimentation on S3M and HME technologies followed by general characterisation techniques used. A separate section on solid dispersions and cocrystals will provide details about specific batches prepared by these two techniques and specific evaluation methods. At the end of this chapter a section has been included about the preliminary studies on energy consumption during milling.

3.3.1 S3M technology

The solid state shear mill which is used in this research was fabricated at Sichuan University. The experiments were conducted in Professor Qi Wang's laboratory at State Key Lab of Polymer Materials Engineering, Polymer Research Institute, Sichuan University. The principle and theory of S3M are described in detail in Section 2.4.2. A typical S3M is shown in Figure 3.1.

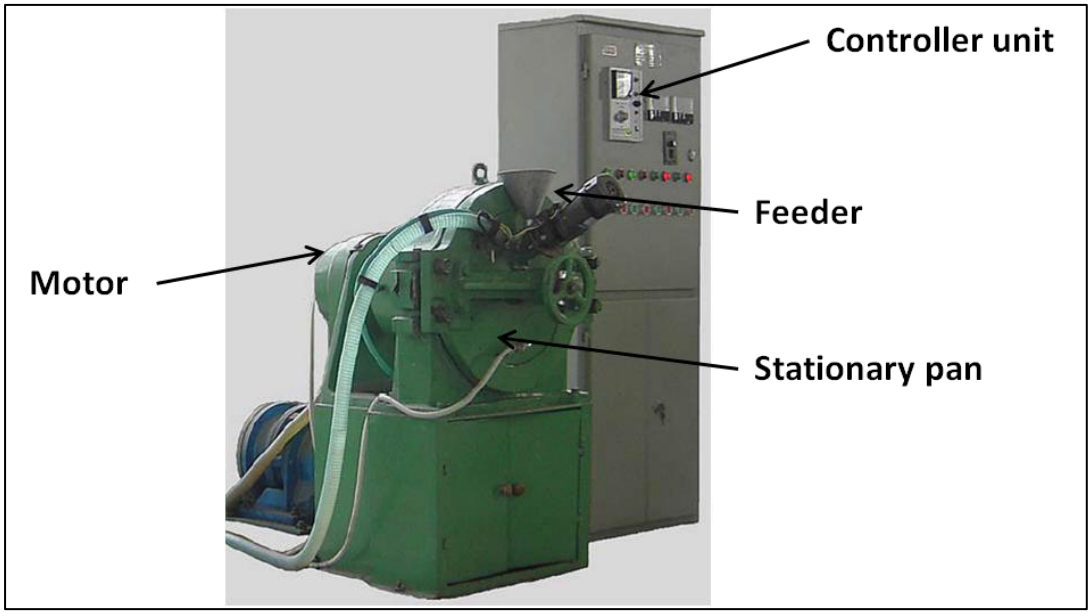

Figure 3.1: A typical S3M equipment

3.3.1.1 Preliminary trials

Three S3M mills S3M1, S3M2 and S3M3 with different configurations were used for preliminary trials. The parameters of the three mills are summarised in Table 3.3 and explained using Figure 3.2. The photographs of the three mills are shown in Figure 3.3.

Table 3.3: Different S3M mills with different parameters

S3M type/Parameters	Radius (R) (cm)	Division number (n)	Slot number (m)	Slot top width (δ)	Bevel angle (α)
S3M 1	10	8	14	Low	Small
S3M 2	30	8	14	Medium	High
S3M 3	30	8	14	High	Medium

The parameters R, η, m, d and bevel angle η are explained using Figure 18

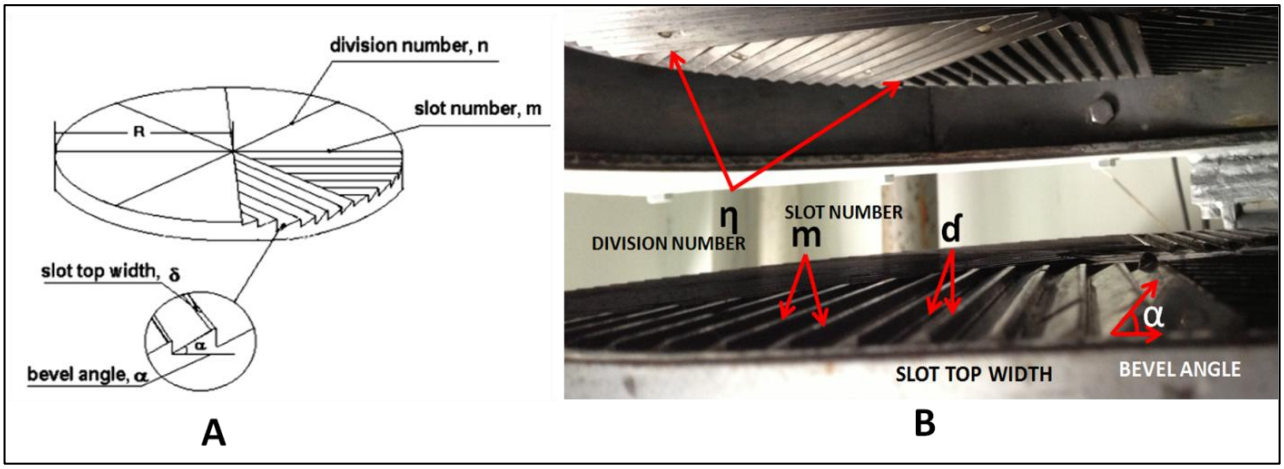

Figure 3.2: S3M in-laid pans A) Schematic B) Original

Preliminary trials for solid dispersions were conducted using salicylic acid and VA64 as model drug and polymer respectively. Salicylic acid was sieved through an 80 mesh to break any agglomerates. For each batch 300 gm of drug: polymer mixture containing the two components in a 1:1 weight ratio was prepared by mixing the two components in a turbula mixer. The mixture was fed separately to S3M1, S3M2 and S3M3. The gap between the pans was adjusted to ensure a residence time of each mixture in the mill for at least 30 secs. A retention time of only 10 secs could be achieved in S3M2

even at lowest clearance between the pans. The speed of rotation was set between 20 to 50 rpm (available range 20-200 rpm). The product was collected and characterised using PXRD as described in section 3.4.2. The drug: polymer mixture showed good flowability in all mills with a retention time of 30-40 secs achieved in S3M1 and S3M3. The PXRD data showed that the drug was partially converted into the amorphous form at the end of the first cycle in S3M3, whereas S3M1 and S3M2 did not show any amorphous conversion. Therefore, product obtained at the end of cycle 1 from S3M3 was again subjected to additional cycles. The product samples were collected at the end of each cycle and subjected to PXRD analysis. The amorphous solid dispersion was formed at the end of cycle 3. Therefore S3M3 was used for preparation of solid dispersions in the next phase of study.

Feasibility for cocrystal formulation using S3M was carried out using salicylic acid: nicotinamide 1:1 as a model cocrystal pair. Both the components were sieved through an 80 mesh separately and a 300 gm mixture containing a 1:1 molar ratio of the 2 components was mixed in a turbula mixer for 10 min. The binary mixture was fed to S3M1, S3M2 and S3M3 separately. The powder could not flow through the gaps between the pans and clogged all the mills. The batches when processed at higher pan clearance could not retain the mixture for more than 10 sec providing no shearing action. Therefore next batches were processed with the addition of 10% PEO N80 by weight to the binary mixture; pan clearance was maintained at minimum with rotation speed between 20-50 rpm.

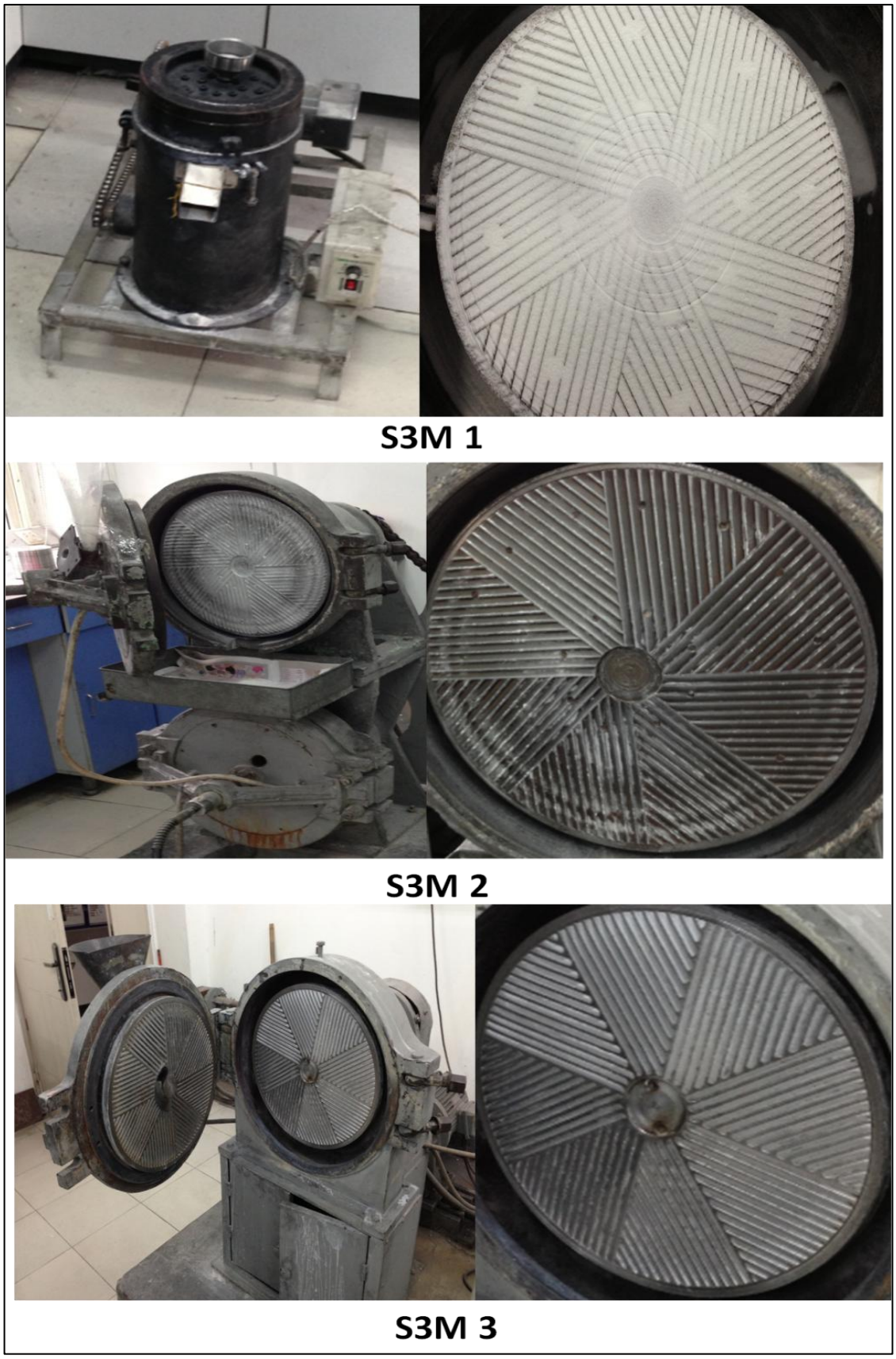

Figure 3.3: Three S3M mills used S3M1, S3M2 and S3M3

The material showed good flowability with residence time between 30-40 sec in S3M1 and S3M3, whereas it was 10 sec for S3M2. The product obtained was subjected to PXRD evaluation. The PXRD studied revealed that product obtained from S3M3 was only subjected to complete amorphisation and formation of phase pure cocrystals. Therefore S3M3 mill was used for all cocrystal trials in the next part of the study.

3.3.2 Hot melt extrusion process

Hot melt extrusion trials were conducted using a Pharmalab 16 (Thermo Fisher Scientific, Karlsruhe Germany) co-rotating twin screw extruder with 16 mm screw diameter and screw length to diameter ratio of 40:1 (Figure 3.4). Details about the principles of hot melt extrusion were explained in section 2.4.1.

Figure 3.4: Pharmalab 16 co-rotating twin screw extruder

The screws are made up of different screw elements. Conveying elements help to carry material along the length of the extruder and mixing elements apply high shear to ensure homogenous mixing under a given temperature profile. Typical screw elements are shown in Figure 3.5.

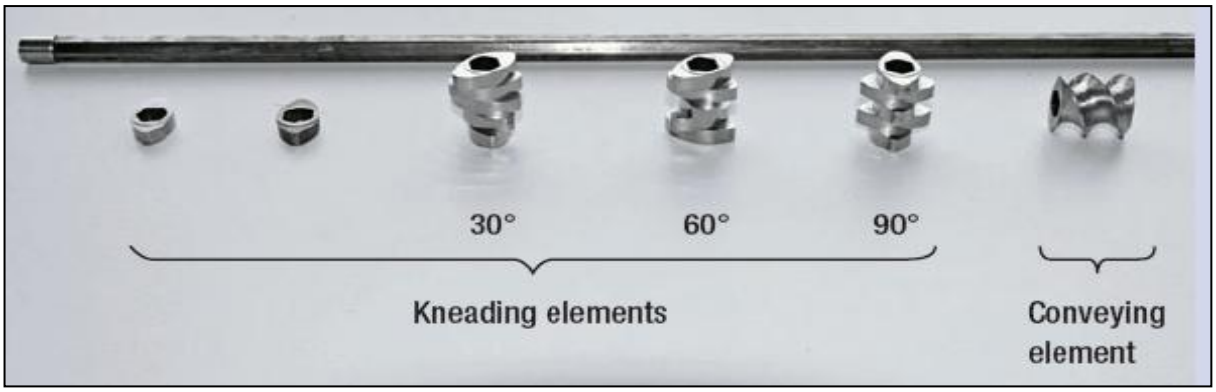

Figure 3.5: Typical screw elements with different geometry

The screw configuration was comprised of three identical mixing zones separated by three conveying elements. In the mixing zone the screw elements were arranged in the order 30°, 30° and 90° in a direction from the hopper to discharge end. This configuration provides high shear to the material in the mixing zone. The typical conveying zone and mixing zone geometries are shown in Figure 3.6 and their distribution over the screw length are summarised in Table 3.4.

The screw rotation speed was set at 100 rpm for all batches, and the temperatures of the nine heated barrel and die zones were set according to the requirements of the respective solid dispersion and cocrystal batches.

Pressure and temperature sensors were provided near the discharge zone as shown in Figure 3.7. The temperature, pressure and torque are monitored using a Programmable logic controller (PLC) display.

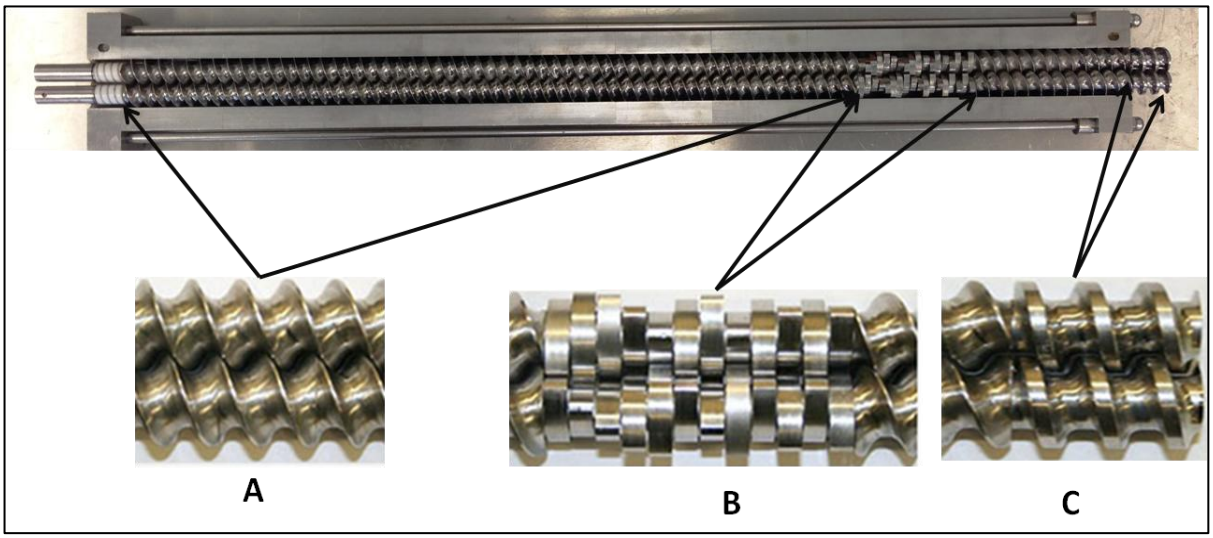

Figure 3.6: Twin screw with different zone A. Conveying, B. Dispersive mixing, C. Discharge

Table 3.4: Screw configuration used for extrusion trials on Pharma lab 16

Length (mm)	Element type
22	Forward conveying
0.5	30 forward mixing
0.5	60 forward mixing
0.5	90 mixing
3	Forward conveying
0.5	30 forward mixing
0.5	60 forward mixing
0.5	90 mixing
3	Forward conveying

0.5	30 forward mixing
0.5	60 forward mixing
0.5	90 mixing
6	Forward conveying
1.5	Discharge

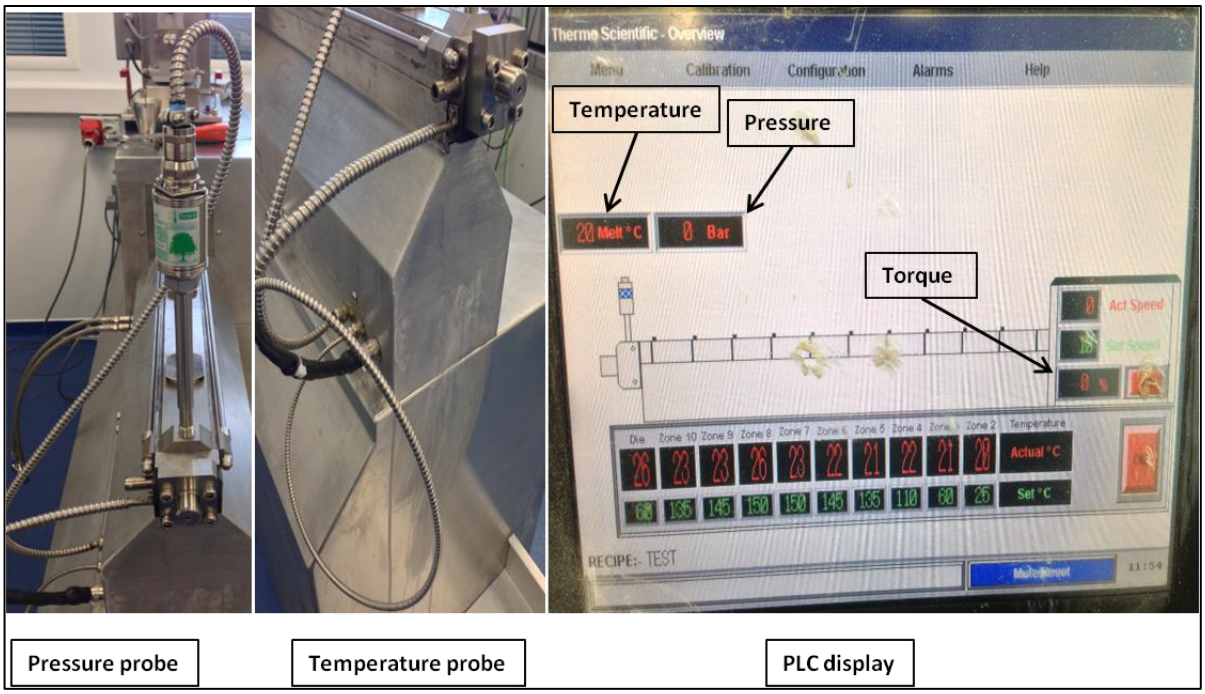

Figure 3.7: Temperature and pressure sensors and PLC display

Pharmalab 16 provides nine temperature controlled zones across the barrel. The HME preliminary trials were performed using salicylic acid – PVP VA 64 pairs for solid dispersions and salicylic acid – nicotinamide for cocrystals. The temperature profiles used for the solid dispersion and cocrystal batches are provided in Table 3.7 and Table 3.9 respectively.

The batch size was kept constant at 300 gm for all batches. Feed rate was kept the same for all the batches at 0.3 kg/h using a gravimetric twin screw feeder (Congrav OP1T, Brabender, Germany, Figure 3.8). An extruder die

was used in case of all solid dispersion batches, whereas all cocrystal batches were carried out without an extruder die.

Figure 3.8: Gravimetric feeder (Congrav OP1T, Brabender, Germany)

3.4 Characterisation techniques

3.4.1 Differential Scanning Calorimetry (DSC)

A TA Instruments Q2000 differential scanning calorimeter (Crawley, UK) was used for recording thermograms of pure and processed cocrystal and solid dispersion batches which is equipped with an RSC90 cooling unit. This was used to analyse and comprehend heat flow in the starting crystalline components as well as the resulting products. Indium metal was used for the calibration of instrument. Around 1.5-3 mg of each sample was loaded into the aluminium pan. An accurately weighed blank aluminium pan was used as

reference. All samples were recorded using suitable temperature profile according to the melting behaviour of the API. A heating rate of 10°C/ min or 20°C/ min was used and a nitrogen flow rate was kept at 50 mL/min to maintain inert environment.

3.4.2 Powder X-ray Diffraction (PXRD)

All the cocrystal and solid dispersion samples were crushed to reduce their particle size by milling or grinding in mortar and pestle and then subjected to powder X-ray diffraction analysis. A Bruker D8 diffractometer (Coventry, UK) was used, having X-ray wavelength 0.154 nm and a 40 KV Cu source with filament emission 40 mA. Scanning range for all the samples was kept between 2 to 30° (2θ) using a 0.01° step width and 1 s time count, while the scatter slit and receiving slit were 0.2° and 1° respectively. A silica sample holder was used in cases where the available sample size was limited.

3.4.3 Fourier Transform Infrared Spectroscopy (FT-IR)

All the samples were analysed by FT-IR analysis using a Perkin Elmer Spectrum 100 FT-IR spectrometer. A small amount of powder or extrudate sample was kept on the diamond crystal in such a way that it should cover the area of diamond crystal and with the help of rotating vertical shaft. Powdered material or extrudate was pressed against the diamond crystal to a predetermined pressure which was confirmed by generation of signal sound. Once the sample was placed properly, measurements were recorded. For all the samples the scanning scale was kept in the range of 600 to 4000 cm^{-1} with 16 scans per sample.

The assembly involves an electronically stabilised source and detector for accurate results with high repeatability. The obtained spectrum was processed using GRAMS/AI software. All the solid dispersion samples were analysed by FT-IR and compared with the spectrum of the pure drug and the polymer.

3.4.4 Near Infrared Spectroscopy (NIR)

All the cocrystal and solid dispersion samples were subjected to NIR analysis. An FT-NIR analyser (Antaris II, Thermo Scientific, UK) with the halogen lamp assembly made up of quartz with a fibre-optic probe assisted with detector (InGaAs). Powdered samples were kept in glass vials with a clear and transparent bottom and placed on the NIR integrating sphere covering the exposed sample area of the vial bottom. A spectra measurement was performed every 30 seconds in the wave number range of 4500-9000 cm^{-1}, an average of 32 scans and resolution of 16 cm^{-1}. Samples of pure components of drug and polymer were also analysed by NIR analysis. Data processing was performed using Thermo Scientific, version 3.0 , TQ Analyst Operation software.

3.4.5 Scanning Electron Microscopy (SEM)

SEM was used to study morphology and structural features of solid dispersion and cocrystals batches. Self-adhesive carbon mounts were used to mount samples on aluminium pin stubs (Agar Scientific, Stansted, UK). SEM images of the mounted samples were collected using an FEI Quanta

400 scanning electron microscope (Cambridge UK) under vacuum and XTM microscope control software V 2.3.

3.4.6 Dynamic Vapour Sorption analysis (DVS)

Dynamic vapour sorption study was conducted for selected sold dispersion and cocrystal samples to evaluate water sorption at different humidity conditions at a constant temperature. A DVS Advantage (Surface Measurement Systems, UK) instrument was used for all DVS studies. A schematic representation of the instrument is shown in Figure 3.9. Isotherms were recorded at a constant temperature of 25 ºC. The % RH change for the sorption and desorption steps was kept at 20% RH at each step and the equilibration time was 60 min. Distilled water was used as a solvent for all the DVS analyse. Nitrogen (N_2) was used as inert gas for constant pressure (2.5 N/m^2)

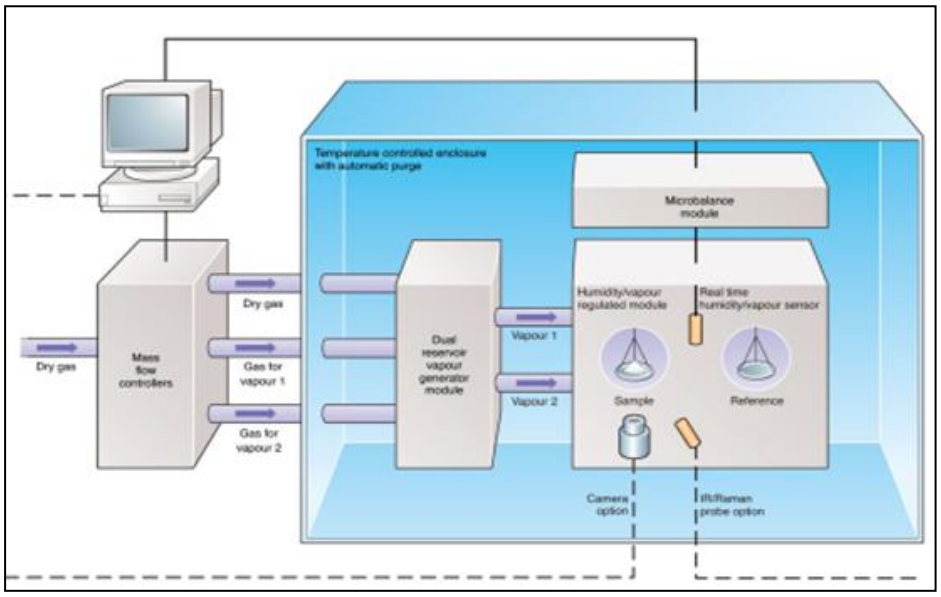

Figure 3.9: Schematic for DVS instrument (SMS, UK, 2014)

Selected solid dispersion samples were analysed for water sorption, desorption, % weight gain and % weight loss at defined %RH were calculated.

3.4.7 Surface energy analysis

Solid dispersion and cocrystal samples which were subjected for DVS analysis were also subjected to surface energy analysis using inverse gas chromatography. The instrument used for surface energy analysis was a Surface Measurement Systems (SMS, UK) iGC surface energy analyser, which is 2nd generation equipment for chromatographic sorption. It has 12 reservoirs for different solvent vapour application and holds two columns. The column temperature was maintained at 30 ºC and flame ionisation detector (FID) was used for estimation of the probe molecule. The experimental parameters are given in Table 3.5.

Table 3.5: Experimental parameters for surface energy measurement

Probe Solvent	% coverage	Column temperature	Flow (sccm)	Flow time (minutes)	FID gain
Octane	0.06	30 °C	5	20	1 X
Octane	0.065	30 °C	5	20	1 X
Octane	0.07	30 °C	5	20	1 X
Octane	0.08	30 °C	5	20	1 X
Octane	0.09	30 °C	5	20	1 X
Octane	0.095	30 °C	5	20	1 X

Octane	0.1	30 °C	5	20	1 X
Nonane	0.06	30 °C	5	20	1 X
Nonane	0.065	30 °C	5	20	1 X
Nonane	0.07	30 °C	5	20	1 X
Nonane	0.08	30 °C	5	20	1 X
Nonane	0.09	30 °C	5	20	1 X
Nonane	0.095	30 °C	5	20	1 X
Nonane	0.1	30 °C	5	20	1 X
Decane	0.06	30 °C	5	20	1 X
Decane	0.065	30 °C	5	20	1 X
Decane	0.07	30 °C	5	20	1 X
Decane	0.08	30 °C	5	20	1 X
Decane	0.09	30 °C	5	20	1 X
Decane	0.095	30 °C	5	20	1 X
Decane	0.1	30 °C	5	20	1 X

The columns used for the current study were Silane treated columns made up of glass with size length 30 cm and 3 mm internal diameter. Sample loading used for all the cocrystal and solid dispersion was in the range of 200-300 mg. The average surface area exposed for surface energy measurement was around 0.5 m^2. The column was conditioned at 30 °C at 0% RH. The surface energy data was analysed by SMS Cirrus software.

3.5 Solid dispersion

Solid dispersions were prepared by S3M and HME techniques. This section provides details about composition the of solid dispersion batches,

processing variables and performance and degradation testing carried out for different batches.

3.5.1 Solid dispersions using S3M technology

Four drugs, ibuprofen (IBU), paracetamol (PARA), glibenclamide (GLB) and carbamazepine (CBZ) and four polymers PVP VA64 (VA), ethylcellulose (EC), HPMCP (HP) and HPMCAS (AS) were selected for preparation of solid dispersions.

The selection of drug was based on the various challenges associated with them as described in Table 3.1. Being BCS class II drugs Ibuprofen, glibenclamide and carbamazepine were selected majorly due to their low solubility issues. Paracetamol was selected enhance its physicochemical properties in terms of tabletting and compression. Similar way polymers were selected as per challenges associated with them as mentioned in Table 3.2. The use of PVP VA64 as carrier polymer in solid dispersion system has been widely explored, whereas HPMCP HP 55 and HPMCAS being coating polymer and majorly used in coating of tablets are been explored for their potential to form a solid dispersion with considering their degradation challenge. Similar way ethyl cellulose has been explored coating and controlled release coating purposes; here it has been tried for carrier in solid dispersion system for slower drug release over the time period.

The ratio of drug to polymer was kept 1:2 w/w based on the trials previously carried out on hot melt extrusion prior commencing the actual work. Loading of 33% drug of drug into polymer was observed to give amorphous system

using hot melt extrusion process, the 50% loading of drug (CBZ) was tried in case of PVP VA64 and HPMCP HP55 polymers to check the potential of those polymers to load higher amount of drugs and to form solid dispersion of CBZ. The higher drug loading in solid dispersion will help to increase the drug dose where it is needed in case of some drugs with low water solubility.

A total of 11 batches were processed using different drug polymer combinations and ratios. Details of these batches are summarised in Table 3.6. The batch code includes drug code, polymer code and ratio followed by the letter S in parentheses indicating S3M technology. The basis of selection of the drugs and polymers is explained in the results and discussion section (Chapter 5).

All batches were processed using S3M3 mill and batch size was maintained at 300 g. Process parameters were maintained as explained in the preliminary trials in section 3.3.1.1. The residence time of the material was between 30 -40 sec for each cycle but it could not be measured accurately as the mill did not have a rate measurement system and has very high throughput. The number of cycles was kept constant at three for all batches except for batch IBUVA12(S). IBUVA12(S) showed low Tg values and yielded a product in first cycle. All other solid dispersion batches were subjected to three S3M cycles respectively.

Table 3.6: Solid dispersion batches prepared by S3M technology

Sr	Batch code	Drug	Polymer	Drug:polymer	No.of

No				ratio by weight	cycles
1	IBUVA12(S)	Ibuprofen	PVP VA64	1:2	2
2	IBUHP12(S)	Ibuprofen	HPMCP HP55	1:2	3
3	PARAHP12(S)	Paracetamol	HPMCP HP55	1:2	3
4	GLBVA12(S)	Glibenclamide	PVP VA64	1:2	3
5	GLBEC12(S)	Glibenclamide	Ethylcellulose	1:2	3
6	CBZVA12(S)	Carbamazepine	PVP VA64	1:2	3
7	CBZVA11(S)	Carbamazepine	PVP VA64	1:1	3
8	CBZHP12(S)	Carbamazepine	HPMCP HP55	1:2	3
9	CBZHP11(S)	Carbamazepine	HPMCP HP55	1:1	3
10	CBZAS12 (S)	Carbamazepine	HPMCAS	1:2	3
11	CBZEC12(S)	Carbamazepine	Ethylcellulose	1:2	3

Products obtained from all batches were subjected to characterisation using PXRD, DSC, SEM, FTIR and NIR techniques as described in section 3.4. Selected batches were subjected to DVS and surface energy analysis as per the procedures elaborated in section 3.4. The release of drug from all batches was studied using the method described in section 3.5.3.1, while process induced degradation of paracetamol and carbamazepine was evaluated using the HPLC technique described in section 3.5.3.2.

3.5.2 Solid dispersion using HME

All drug polymer combinations processed for solid dispersions using S3M were also subjected to HME. Processing of some of the drug polymer

combinations using melt extrusion was difficult due to very high torque; therefore a suitable plasticiser was used to aid processing of these batches.

Selection of plasticisers were based on trial and error approach, both the plasticisers were tried for all the combination of drug and polymers in 25 gram batches and accordingly the most process suitable plasticiser for respective drug: polymer combination were chosen. Triethyl citrate (TEC) and Polyethylene glycol 2000 (PEG) in concentration 10 – 15 % w/w were used as plasticisers to achieve processability of the solid dispersion. All other parameters were kept constant for all solid dispersion batches.

HME and S3M process were carried out as described in section 3.5 of this chapter. The temperature profile and plasticiser concentration used during HME processing with Batch codes are described in Table 3.7.

Table 3.7: Solid dispersion hot melt extrusion batches

Sr no.	Batch details								
1	IBUVA12(H)								
Extruder barrel zone	10	9	8	7	6	5	4	3	2
Temp.(°C)	80	80	80	80	80	50	40	35	25
2	IBUHP12(H)								
Extruder barrel zone	10	9	8	7	6	5	4	3	2
Temp.(°C)	130	130	130	130	110	100	75	50	25
3	PARAHP12(H)+ 10% TEC								

Extruder barrel zone	10	9	8	7	6	5	4	3	2
Temp.(°C)	150	150	150	150	130	110	75	50	25
4	GLBVA12(H)+ 10% PEG								
Extruder barrel zone	10	9	8	7	6	5	4	3	2
Temp.(°C)	120	120	120	120	110	100	75	50	25
5	GLBEC12(H)+ 10% PEG								
Extruder barrel zone	10	9	8	7	6	5	4	3	2
Temp.(°C)	160	160	160	160	140	100	75	50	25
6	CBZVA12(H) + 10% PEG								
Extruder barrel zone	10	9	8	7	6	5	4	3	2
Temp.(°C)	110	110	110	110	90	80	60	40	25
7	CBZVA11(H) + 15% PEG								
Extruder barrel zone	10	9	8	7	6	5	4	3	2
Temp.(°C)	100	100	100	100	90	80	60	40	25
8	CBZHP12(H) + 10% TEC								
Extruder barrel zone	10	9	8	7	6	5	4	3	2
Temp.(°C)	160	160	160	160	140	120	80	60	35
9	CBZHP11(H) + 15% TEC								
Extruder barrel zone	10	9	8	7	6	5	4	3	2
Temp.(°C)	150	150	150	150	135	110	80	60	35
10	CBZAS12 (H) + 10% PEG								

Extruder barrel zone	10	9	8	7	6	5	4	3	2
Temp.(°C)	150	150	150	150	135	110	80	60	35
11	CBZEC12(H) + 10% TEC								
Extruder barrel zone	10	9	8	7	6	5	4	3	2
Temp.(°C)	140	140	140	140	125	100	80	60	35

All solid dispersion batches were analysed for DSC, XRD, FT-IR, NIR, DVS and surface energy analysis as described in section 3.4.

3.5.3 Product performance testing

The solid dispersion batches obtained were subjected to evaluation of drug release and investigation of potential process induced degradation. This section will provide details of the methodology for this testing.

3.5.3.1 Drug release

Drug release from the solid dispersion batches was studied using USP 2 dissolution test apparatus (Copley Scientific, Type NE4-COP, Serial No. 14355). Samples were analysed using a suitable UV spectrophotometric method. The dissolution medium volume used during testing was 900 ml at 37°C, other details about dissolution testing parameter such as dissolution medium and speed of rotation are summarised in Table 3.8.

Selection of dissolution medium was done using USP reference dissolution medium for respective drugs. In case of HPMCP HP55 and HPMCAS the selection of dissolution medium was done according to the nature of polymer

and not according to drug. As HPMCP HP55 and HPMCAS are pH dependent polymers dissolution medium selected was buffer pH 6.8 to dissolve the entire drug present in dissolution samples over the period of dissolution time. All other dissolution medium was selected according to USP standards for respective drugs (Table 3.8).

All solid dispersion batches dissolution samples were analysed using a JASCO V-630 spectrophotometer. The spectral measurements were carried out using Spectra Manager 2.0 software. Calibration curves for the APIs were obtained using the respective dissolution medium in the range of 1-10 microgram/ml strength of the drug solution. Calibration curve equations and R^2 values were obtained by regression analysis. Timely samples were withdrawn during dissolution and UV absorbance was recorded at wavelengths reported in Table 3.8.

Table 3.8: Dissolution parameters for solid dispersion batches

Sr. No.	Batch	Dissolution Media	Wavelength (nm)	RPM
1	IBUVA	Phosphate Buffer pH 7.2	221	50
2	IBUHP	Phosphate Buffer pH 7.2	221	50
3	CBZVA	Water 1% SLS	288	75
4	CBZHP	Phosphate Buffer pH 7.2	288	75
5	CBZAS	Phosphate Buffer pH 7.2	288	75
6	CBZEC	Water	288	100

7	PARAHP	Phosphate buffer pH 6.8	243	75
8	GLIBVA	Phosphate buffer 7.4	240	50
9	GLIBEC	0.1 M HCl (pH 1.2)	240	75

3.5.3.2 Drug and polymer degradation

S3M and HME are shear based technologies which may cause degradation of the temperature or shear sensitive APIs and polymers during processing. Degradation of carbamazepine, paracetamol and HPMCP were investigated using suitable HPLC method.

HPLC analyses were performed using a Waters HPLC system comprising a separation module (Waters e-2695) integrated with a degasser and a photodiode array detector (PDA-2998). The HPLC chromatograms collected at suitable wavelengths were analysed using Empower 3 software.

3.5.3.2.1 Carbamazepine

Iminostilbene is a thermal degradation product of carbamazepine (Naima *et al*., 2001). A reported gradient HPLC method was used for the simultaneous detection of carbamazepine and Iminostilbene. The HPLC conditions used were as follows:

Column: C18 Waters Symmetry, dimensions of 4.6× 250 mm with 5 um particles size.

Solvent system: Solvent A: acetonitrile acidified with 0.1 % v/v formic acid

Solvent B: deionised water acidified with 0.1 % v/v formic acid.

Injection volume: 10 µL;

Flow rate: 1.2 mL/min.

Wavelengths: 285 nm, 253 nm, 219 nm

Linearity range: 10 -60 µg/mL

3.5.3.2.2 Paracetamol

The degradation product of paracetamol is 4-amino phenol (Bhimavarapu *et al*. 2011). A reported gradient HPLC method was used for analysis details are as follows,

Column: C18 Waters Symmetry, dimensions of 4.6× 250 mm with 5 um particle size.

Solvent system: Solvent A: Acetonitrile

Solvent B: phosphate buffer pH 3

Injection volume: 10 µL;

Flow rate: 0.5 mL/min.

Wavelengths: 227 nm

Linearity range: 20 -160 µg/mL

3.5.3.2.3 HPMCP

The degradation products of HPMCP are phthalic acid and phthalic anhydride (Karandikar, *et al*. 2015). A reported gradient HPLC method was used for analysis of phthalic acid and phthalic anhydride (Karandikar, *et al*. 2015). The HPLC conditions are as follows,

Column: Waters spherisorb ODS 2 column with the dimension of 3 µm particle size, 4.6 internal diameter and 60 mm length

Solvent system: Solvent A: 0.5 M potassium dihydrogen phosphate (KH_2PO_4)

Solvent B: Methanol

Injection volume: 50 µL;

Flow rate: 1 mL/min.

Wavelengths: 215 nm

Linearity range: 10 -50 µg/mL

3.6 Cocrystals

Cocrystals of ibuprofen, caffeine, paracetamol and carbamazepine with different co-formers were attempted using solution crystallisaton, HME and S3M. Solution crystallisation was carried out to obtain pure cocrystals and to investigate difference in the properties as per the method of preparation. The coformers used include nicotinamide (NIC), maleic acid (MAL), oxalic

acid (OXA), salicylic acid (SAL), saccharin (SAC) and glutaric acid (GLU). The different batches and method used are summarised in Table 3.9. Processing of cocrystals was carried out as per the S3M and HME methods described earlier in Sections 3.3.1 and 3.3.2.

Table 3.9: Cocrystal batch details

Sr. No.	Cocrystal	Solution	HME	S3M
1	IBU:NIC 1:1	√	---	√
2	IBU:NIC 1:1 10% PEO	---	√	√
3	IBU:NIC 1:1 10% VA64	---	√	√
4	CAF:MAL 1:1	√	√	---
5	CAF:MAL 1:1 15% HP55	---	√	√
6	PARA:OXA 1:1	√	√	---
7	PARA:OXA 1:1 15% PEO	---	√	√
8	CBZ:SAL 1:1	√	√	---
9	CBZ:SAL 1:1 5% PEO	---	√	√
10	CBZ:SAL 1:1 10% PEO	---	√	√
11	CBZ:SAL 1:1 15% PEO	---	√	√
12	CBZ:SAL 1:1 25% PEO	---	√	√
13	CBZ:SAL 1:1 15% PVP VA64	---	√	√
14	CBZ:SAL 1:1 25% PVP VA64	---	√	√
15	CBZ:SAC 1:1	√	√	---
16	CBZ:SAC 1:1 15% PEO	---	√	√
17	CBZ:NIC 1:1	√	√	---

18	CBZ:NIC 1:1 15% PEO	---	√	√
19	CBZ:GLUT 1:1	√	√	---
20	CBZ:GLUT 1:1 15% PEO	---	√	√

For all S3M processing of crocrystals the processing conditions were maintained constant as described for preliminary trials using S3M3 mill.

The temperature profiles used for HME processing of different cocrystals are summarised in Table 3.10.

Table 3.10: Cocrystal batch and process details for hot melt extrusion

Sr. no.	Batch details								
1.	Ibuprofen: Nicotinamide 1:1								
Extruder barrel zone	10	9	8	7	6	5	4	3	2
Temp.(°C)	25	70	70	70	60	50	40	30	25
2.	Ibuprofen: Nicotinamide 1:1 + 10% PEO								
Extruder barrel zone	10	9	8	7	6	5	4	3	2
Temp.(°C)	25	70	70	70	60	50	40	30	25
3.	Ibuprofen: Nicotinamide 1:1 + 10% VA64								
Extruder barrel zone	10	9	8	7	6	5	4	3	2
Temp.(°C)	25	70	70	70	60	50	40	30	25
4.	Caffeine: Maleic acid 1:1								
Extruder barrel zone	10	9	8	7	6	5	4	3	2

Temp.(°C)	25	110	110	110	90	70	50	40	25
5.	Caffeine: Maleic acid 1:1 + 15% HPMCP HP55								
Extruder barrel zone	10	9	8	7	6	5	4	3	2
Temp.(°C)	25	100	100	100	80	60	40	30	20
6.	Paracetamol: Oxalic acid 1:1								
Extruder barrel zone	10	9	8	7	6	5	4	3	2
Temp.(°C)	25	100	100	100	80	60	40	30	20
7.	Paracetamol: Oxalic acid 1:1 + 15% PEO								
Extruder barrel zone	10	9	8	7	6	5	4	3	2
Temp.(°C)	25	100	100	100	80	60	40	30	20
8.	Carbamazepine: Salicylic acid 1:1								
Extruder barrel zone	10	9	8	7	6	5	4	3	2
Temp.(°C)	25	150	150	150	135	110	80	50	25
9.	Carbamazepine : Salicylic acid 1:1 + 5% PEO								
10.	Carbamazepine : Salicylic acid 1:1 + 10% PEO								
11.	Carbamazepine : Salicylic acid 1:1 + 15% PEO								
12.	Carbamazepine : Salicylic acid 1:1 + 25% PEO								
13.	Carbamazepine : Salicylic acid 1:1 + 15% PVP VA64								
14.	Carbamazepine : Salicylic acid 1:1 + 25% PVP VA64								
Extruder barrel zone	10	9	8	7	6	5	4	3	2
Temp.(°C)	25	110	110	110	100	80	60	40	25
15.	Carbamazepine: Saccharin 1:1								

Extruder barrel zone	10	9	8	7	6	5	4	3	2
Temp.(°C)	25	145	145	145	130	100	70	50	25
16.	Carbamazepine : Saccharin 1:1 + 15% PEO								
Extruder barrel zone	10	9	8	7	6	5	4	3	2
Temp.(°C)	25	110	110	110	100	80	60	40	25
17.	Carbamazepine: Nicotinamide 1:1								
Extruder barrel zone	10	9	8	7	6	5	4	3	2
Temp.(°C)	25	140	140	140	120	100	70	50	25
18.	Carbamazepine :Nicotinamide 1:1 + 15% PEO								
Extruder barrel zone	10	9	8	7	6	5	4	3	2
Temp.(°C)	25	110	110	110	100	80	60	40	25
19.	Carbamazepine: Glutaric acid 1:1								
Extruder barrel zone	10	9	8	7	6	5	4	3	2
Temp.(°C)	25	110	110	110	100	80	60	40	25
20.	Carbamazepine :Glutaric acid 1:1+ 15% PEO								
Extruder barrel zone	10	9	8	7	6	5	4	3	2
Temp.(°C)	25	110	110	110	100	80	60	40	25

3.6.1 Solution crystallisation

3.6.1.1 CBZ: SAL 1:1 cocry*stal*

CBZ:SAL 1:1 pure cocrystal were prepared by a solution crystallisation method. 11.8075 gm of CBZ and 6.91 gm of SAL were weighed accurately

and dissolved in 180 ml of HPLC grade acetonitrile with simultaneous stirring and heating. The resultant solution was allowed to cool and stand at room temperature for 24 hours. The resultant mixture was filtered and dried. The cocrystal yield was 87.6%.The material obtained was characterised for crystal form using powder X-ray diffraction (PXRD).

3.6.1.2 CBZ:SACC 1:1 cocry*stal*

CBZ:SACC 1:1 pure cocrystals were prepared by a solution method. For this purpose anhydrous CBZ (21 gms, 0.089M) and SACC (16.3 gms, 0.089M) were weighed accurately and dissolved in 280 ml of a mixture of ethanol: methanol (62.5:37.5 V/V) at 70 °C and heating continued till one hour under reflux. The temperature of the system was decreased by 10 °C increments until the solution precipitated. Precipitates were observed around in 60-50 °C, finally temperature was decreased to 30 °C. The resultant mixture was filtered, separated and washed with cold ethanol. The resultant cocrystals were dried at room temperature. Yield for CBZ:SACC 1:1 CC was 86.5%. The material obtained was characterised for crystal form using PXRD.

3.6.1.3 CBZ:NIC 1:1 cocry*stal*

CBZ:NIC 1:1 pure cocrystals were prepared by solution method. For this purpose anhydrous CBZ 10.635 gms (0.045M) and NIC 5.497 gms (0.045M) were weighed accurately and dissolved in a 200 ml solvent mixture of 70:30 V/V ethanol: methanol mixture. Solids were dissolved by heating a mixture at 65 °C and refluxed for one hour under stirring. After required stirring the resultant mixture was cooled to room temperature, separated by filtration and

washed with 20 ml ethanol. The resultant cocrystals was dried at 30 °C for 48 hours. Yield for CBZ:NIC 1:1 CC was 85.4%. The material obtained was characterised for crystal form using PXRD.

3.6.1.4 CBZ: GLUT 1:1 cocry*stal*

CBZ: GLUT 1:1 CC were prepared by solution method. For this purpose CBZ 14.157 gms and GLUT 7.9245 gms were weighed accurately and dissolved in 150 ml of HPLC grade acetonitrile with heating and stirring. The solution was concentrated until all the solvent is evaporated and allowed to cool at room temperature for 24 hours. The resultant mixture was filtered, separated and air dried. Yield for CBZ:GLUT 1:1 CC was 80.4%. The material obtained was characterised for crystal form using PXRD.

3.6.1.5 CAF:MAL 1:1 cocry*stal*

CAF:MAL 1:1 CC were prepared by microwave assisted cocrystallisation. Cocrystallisation was performed using a microwave reactor (Monowave 300, Anton Paar GmbH, Austria). A 1:1 molar mixture of CAF and MAL (2.5 g) were weighed accurately and to this 100 uL water was added. Experiments were carried out in a 30 mL capacity glass tube under stirring at 600 rpm. The temperature for cocrystallisation was kept at 80 °C with holding period of 90 secs. The material obtained was characterised for crystal form using PXRD.

3.6.1.6 PARA:OXA 1:1 cocry*stal*

PARA: OXAL 1:1 CC were prepared by solution method. For this purpose PARA and OXAL were weighed accurately according to their molar ratio with 1:1 stoichiometry. Solids were dissolved in 200 ml of solvent mixture of 1:1 chloroform: methanol. The solution was evaporated slowly with gentle heating and cooled down to room temperature. The resultant solution was kept for 24 hours then filtered and separated. The material obtained was characterised for crystal form using PXRD. PARA:OXAL 1:1 CC yield was 87%.

All cocrystal batches were analysed for DSC, XRD, FT-IR, NIR analysis by using procedures described in previous sections respectively.

3.6.2 Cocrystal dissolution

The UV spectra of the drug and coformer were recorded and interference of the components was checked by overlaying the spectra of both components. For the pairs which did not show any significant interference a UV method was used whereas an HPLC method was developed for the pairs which showed overlap. The overlay spectra for different cocrystal pairs are shown in figures from Figure 3.10 to Figure 3.15.

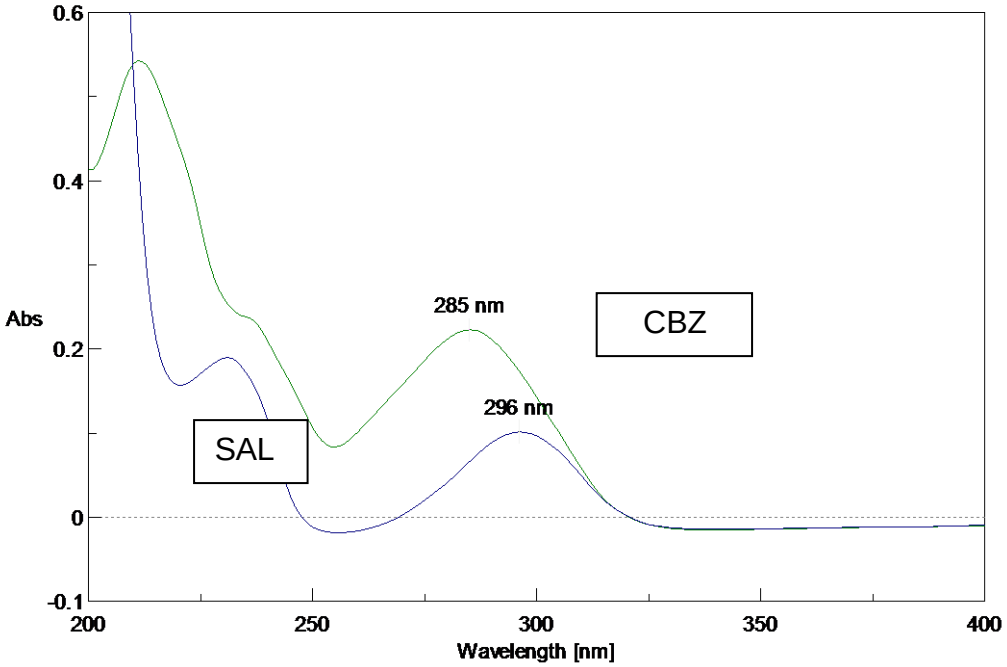

Figure 3.10: Overlay of UV spectra of carbamazepine and salicylic acid

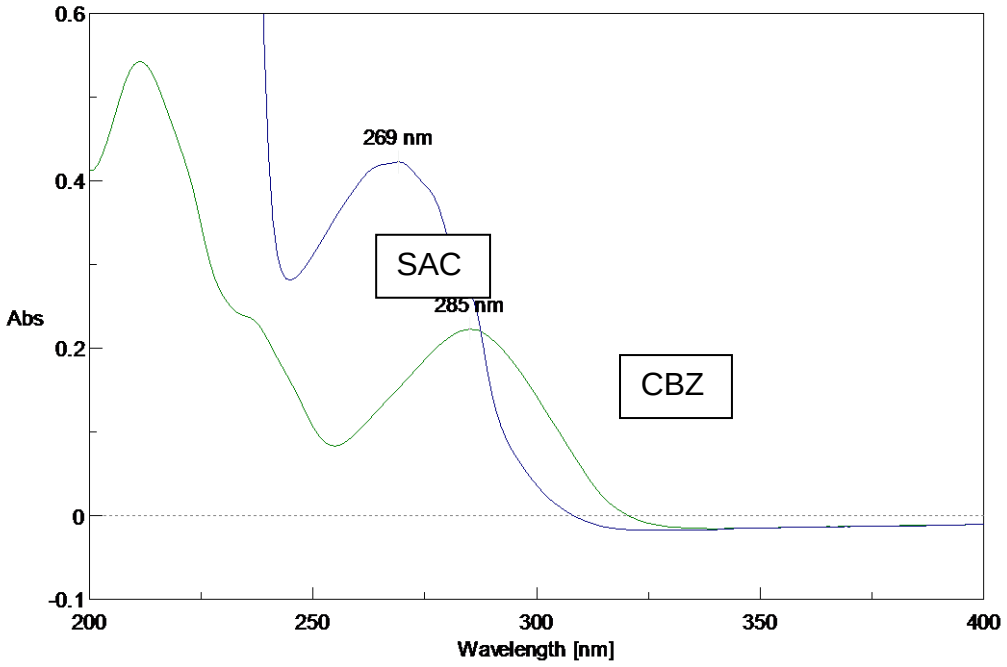

Figure 3.11: Overlay of UV spectra of carbamazepine and saccharin

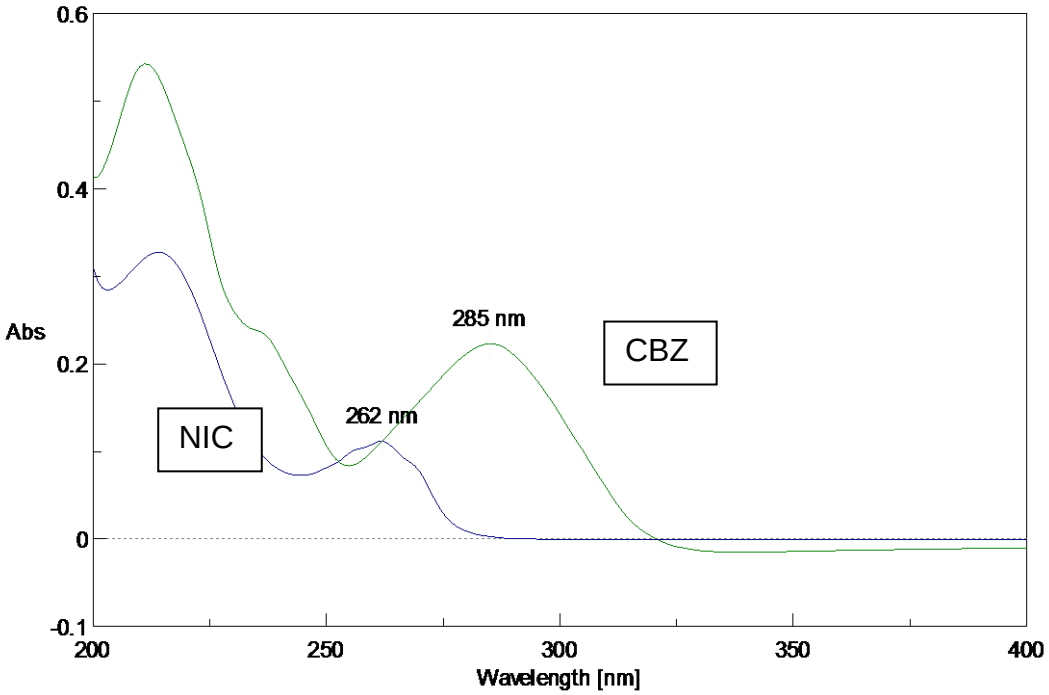

Figure 3.12: Overlay of UV spectra of carbamazepine and nicotinamide

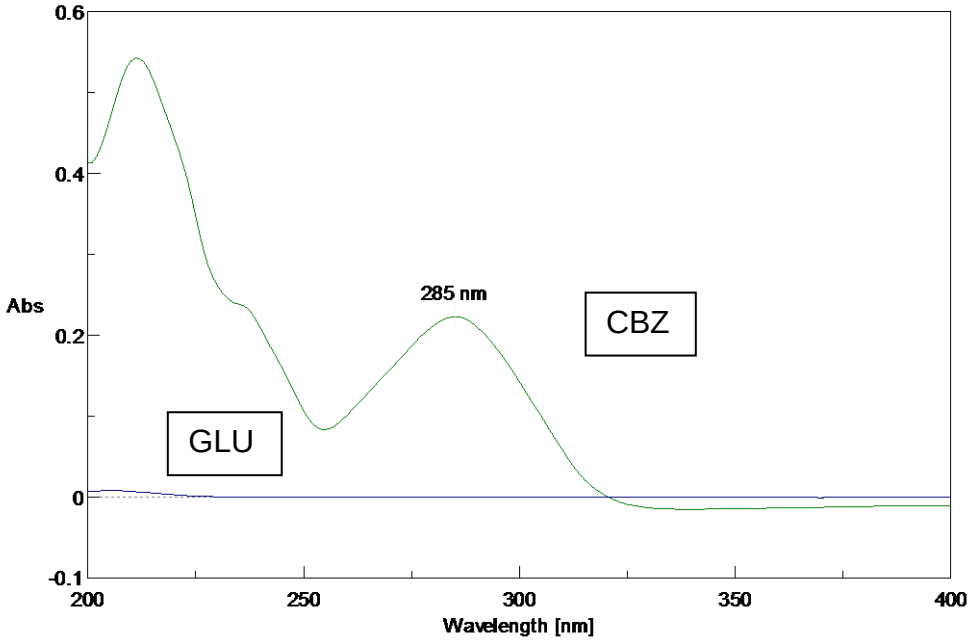

Figure 3.13: Overlay of UV spectra of carbamazepine and glutaric acid

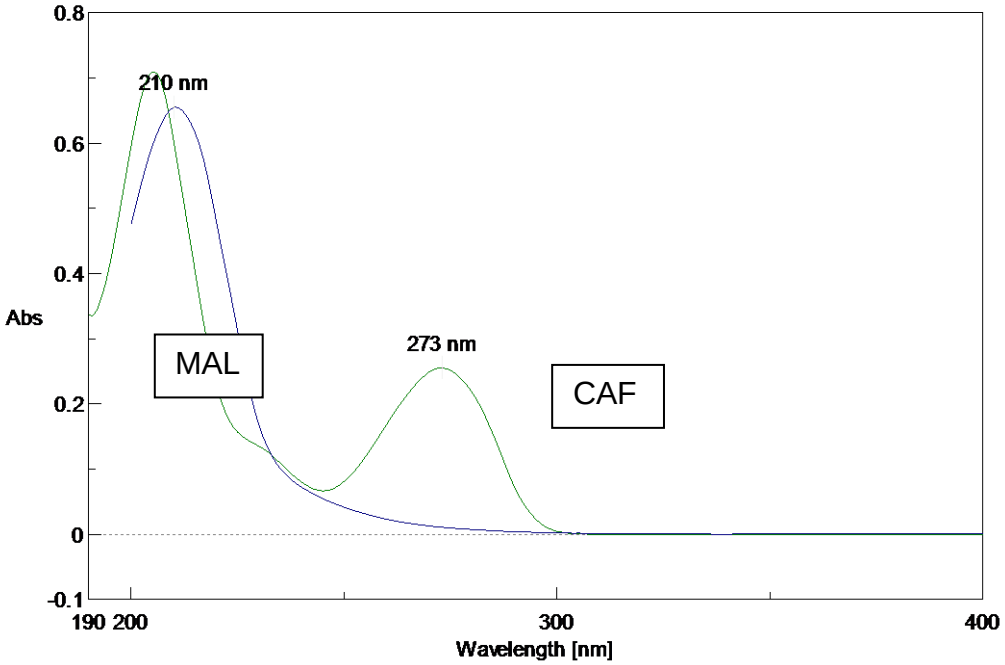

Figure 3.14: Overlay of UV spectra of caffeine and maleic acid

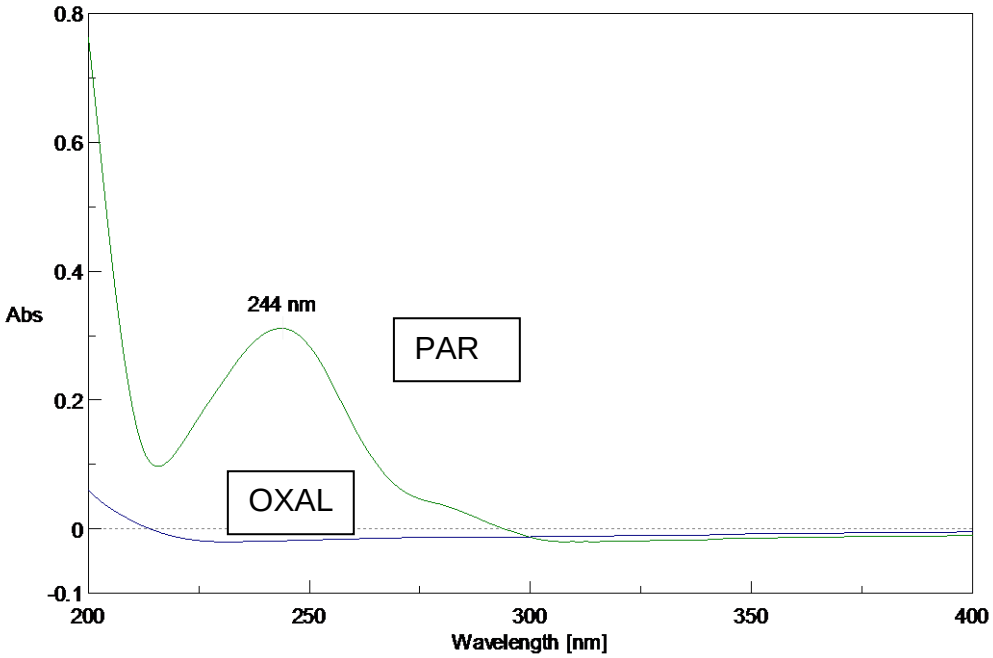

Figure 3.15: Overlay of UV spectra of paracetamol and oxalic acid

Except PARA: OXA all cocrystal pairs required HPLC or Ultra-HPLC separation. Paracetamol was estimated at 244 nm. Although glutaric acid did not interfere with CBZ estimation a UPLC method used for other CBZ pairs was used for estimation of dissolution of CBZ from this pair. HPLC method was used for caffeine – maleic acid and all CBZ containing cocrystals were evaluated using a UPLC method. Iminostibene was also estimated in all CBZ containing batches using the HPLC method.

The major difference between HPLC and UPLC was higher precision for the simultaneous determination of drug and co-former in given mobile phase. Simultaneous elution was easily obtained in UPLC and after many attempts it was not possible in HPLC, which was possible due to the detectors could use very small amount of injection volume and flow rate in case of UPLC to differentiate between drug and co-former and elute them separately in single mobile phase and injection sample.

3.6.2.1 HPLC method for caffeine and maleic acid

HPLC analysis for CAF and MAL was used for dissolution analysis. The HPLC conditions used were as follows:

Column: C18 Waters Symmetry, dimensions of 4.6× 250 mm with 5 um particles size.

Solvent system: Solvent A: Methanol

Solvent B: deionised water acidified with 0.1 % v/v orthophosphoric acid.

Injection volume: 50 µL;

Flow rate: 1.2 mL/min.

Wavelengths: 209 nm

Linearity range: 2-32 µg/mL

3.6.2.2 CBZ cocrystal dissolution study

All CBZ cocrystal dissolution studies were analysed by ultra-performance liquid chromatography (UPLC). UPLC gradient method details are as follows,

Column: Waters Acquity column with dimensions of 130Å, 5 um particle size, 4.6 mm internal diameter and 50 mm length

Solvent system: Solvent A: Acetonitrile

Solvent B: deionised water acidified with 0.1% orthophosphoric acid

Injection volume: 50 µL;

Flow rate: 0.6 mL/min.

Wavelengths: CBZ- 285 nm, SAL- 296 nm, SAC- 269 nm, NIC- 262 nm

Linearity range: 10-100 µg/mL

Chapter 4. Results and Discussion

The results and discussion has been divided in four chapters.

Chapter 4 will provide details about the basis for selection of drugs and polymers, selection of equipment and general processing conditions especially in case of S3M.

Chapter 5 provides results and discussion concerning the application of S3M and HME technology for processing of solid dispersions. The major emphasis will be on understanding the differences in formulation requirements to achieve processability. It also provides comparative evaluation of drug release, morphology, physical and chemical stability of the solid dispersions processed using these two processing techniques.

Chapter 6 deals with results and discussion concerning the application of S3M and HME techniques for manufacture of cocrystals. The properties of the cocrystals have been compared with cocrystals prepared by conventional solution crystallisation process.

Chapter 7 this chapter provides an overall discussion about the challenges and opportunities in the shear based development enabling technologies for solid dispersion and cocrystal manufacture.

This research is focussed on exploring an innovative technology in the area of polymer processing to address challenges of pharmaceutical product development. S3M is a proprietary technology developed at Sichuan University, access to which was enabled through the EPSRC funded Science Bridges China collaboration.

One of the major objectives of this research is to explore applications of S3M technology for manufacture of solid dispersions and cocrystals. To provide confidence in the enabling technology it is essential to demonstrate and study its application for drugs and polymers with the wide range of physicochemical properties.

4.1 Selection of drugs and polymers

The criteria for selection of drugs included water solubility, thermal stability, melting point and glass transition temperature. Safety and availability of the drugs were also important factors as the facility in China was in an engineering laboratory without any air handling facilities. Similarly, considering the scale of the operation required quantities of each drug in the order of 3- 4 Kg.

DSC thermograms and PXRD patterns of the drugs are shown in Figure 4.1 and Figure 4.2 respectively,

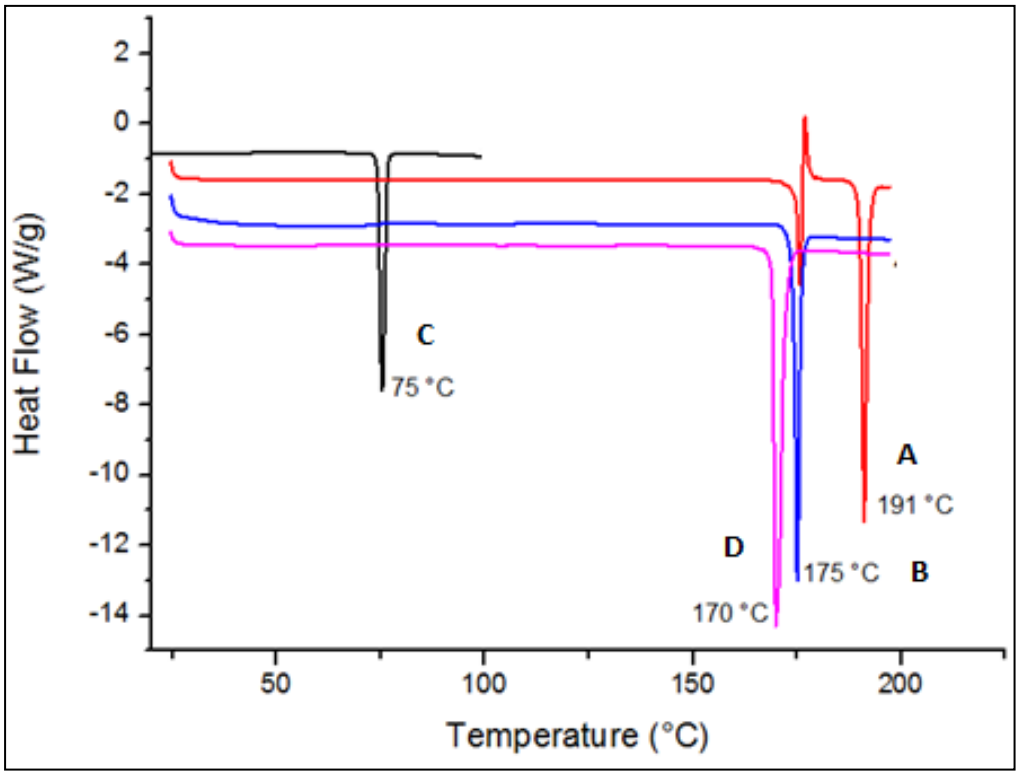

[A- Carbamazepine, B- Glibenclamide, C- Ibuprofen, D- Paracetamol]

Figure 4.1 DSC thermograms of carbamazepine, glibenclamide, ibuprofen and paracetamol

The melting endotherms were observed at 75 °C for Ibuprofen, 170 °C for paracetamol, 175 °C for glibenclamide and 191 °C for carbamazepine (Figure 4.1).

Crystalline CBZ shows two melting endotherms, the first one at 175 ºC and the second one at 191 ºC due to the polymorphic change. The polymorphic transformation from CBZ form III to CBZ form I gives two melting endotherms (Grzesiak *et al*., 2002).

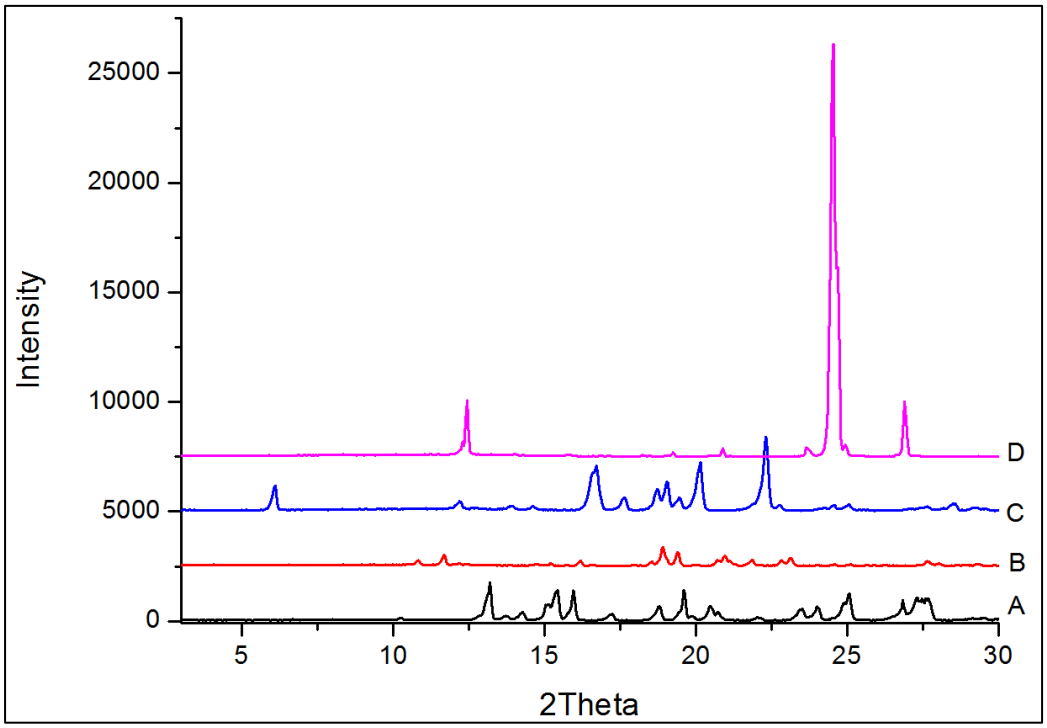

[A-Carbamazepine, B-Glibenclamide, C- Ibuprofen, D- Paracetamol]

Figure 4.2 PXRD of the carbamazepine, glibenclamide, ibuprofen and paracetamol

PXRD patterns of the drugs shows respective characteristic peaks at defined 2θ values with respective peak intensities (Figure 4.2). The 2θ values from respective PXRD are given in Table 4.1

Table 4.1 2θ values for selected drugs

Drug	2θ values from PXRD
Ibuprofen	6.12, 12.2, 16.72, 17.64, 19.04, 20.16, 22.32
Glibenclamide	10.84, 11.68, 16.2, 18.92, 19.4, 20.96, 21.84, 23.16
Paracetamol	12.45, 24.55, 26.9
Carbamazepine	13.2, 13.72, 14.28, 15.44, 15.96, 17.24, 18.8, 19.6, 20.48, 23.52, 24.66, 25.08, 26.84, 27.32

DSC thermograms and PXRD patterns of the polymers are shown in Figure 4.3 and Figure 4.4 which confirm the amorphous nature of the polymers.

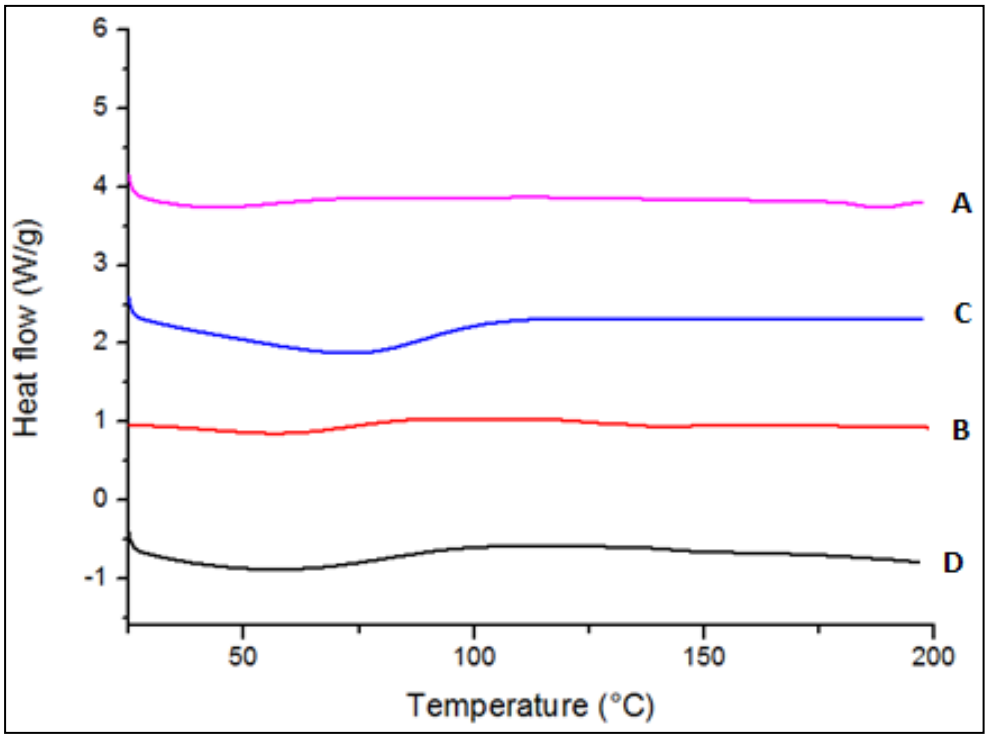

[A- Ethyl cellulose, B- HPMCAS, C- PVP VA64, D- HPMCP HP55]

Figure 4.3 DSC thermograms for Ethyl cellulose, HPMCAS, PVP VA64 and HPMCP HP55

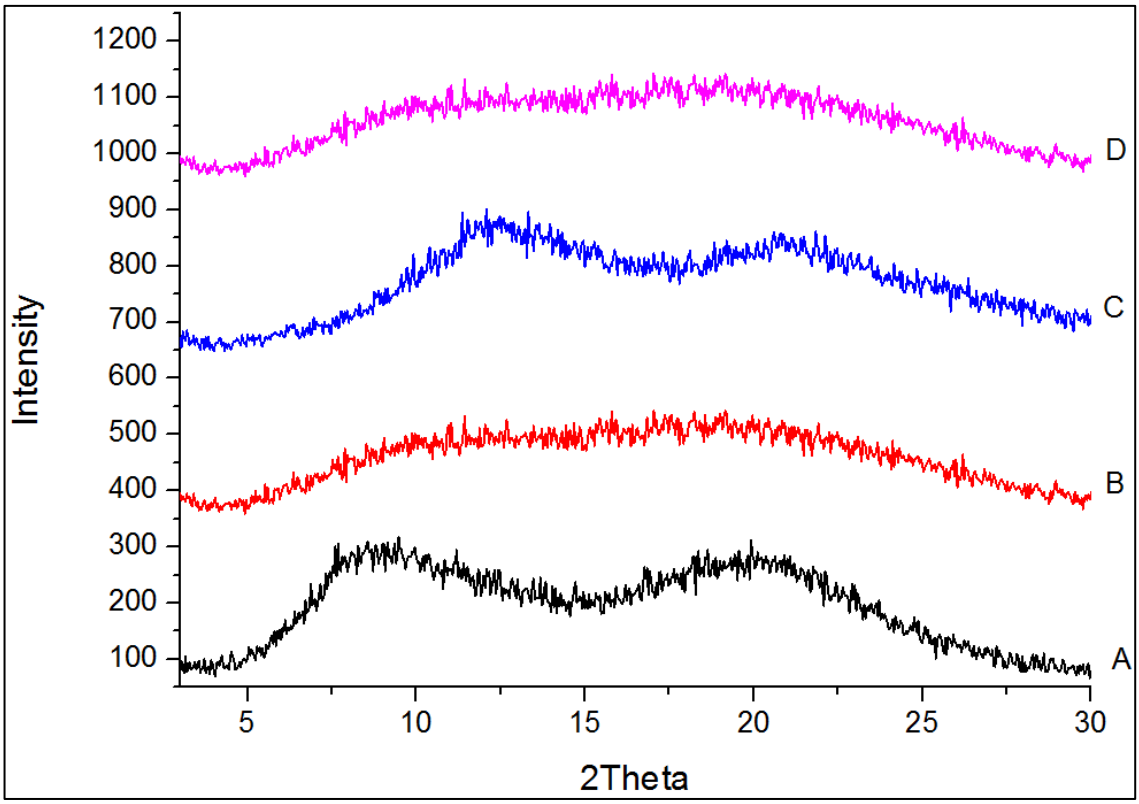

[A-Ethyl Cellulose, B- HPMC AS, C- PVP VA64, D- HPMCP HP55]

Figure 4.4 PXRD for ethyl cellulose, HPMCAS, PVP VA64 and HPMCP HP55

PXRD patterns of polymers show that there was no crystalline peak which confirms that all polymers are amorphous in nature (Figure 4.4).

During processing using S3M and HME, temperature increases due to friction in S3M or a combination of external heating and shear in HME. Therefore glass transition temperature of the drugs is an important selection criterion. Processing of low Tg drugs becomes challenging due to plasticisation of polymers which limits the drug polymer ratio. High temperature and shear also raises concerns about degradation of drugs and polymers during processing therefore molecules such as carbamazepine and

paracetamol which are susceptible to degradation were included. Degradation of polymers during HME is also well reported (Karandikar, *et al*. 2015) therefore HPMCP, a cellulose ester, was selected as a polymer with potential for degradation. Another important criteria considered in the selection of these drugs was the potential to form cocrystals. Therefore drugs with known coformers were used for cocrystal experiments to prove the application of the technology.

Drugs were selected based on the above discussed criteria include ibuprofen, paracetamol, carbamazepine and glibenclamide (Table 4.2). Glibenclamide was used only for the solid dispersion experiments due to constraints on availability whereas the rest of the molecules were used for preparation of solid dispersion as well as cocrystals.

Table 4.2 Physico-chemical properties of the drugs

Drug	**Solubility (mg/L)**	**Tg (°C)**	**Challenges**	**Reference**
Ibuprofen	21	-50	Low Tg drug	Brabender C, *et al*. 2002
Paracetamol	20	23	Formation of 4-amino phenol and quinone-imine due to hydrolysis at high temperature (US006028222)	Sibik *et al*. 2014, Nainar *et al*. 2012
Carbamazepine	17.7	50	Formation of Iminostilbene at 150°C	Sethia and Squillante, 2004, Patterson *et al*. 2008
Glibenclamide	4	60	Low dose	Babu and pandit, 1999, Chauhan *et al*. 2005

Pharmaceutical polymers with Tgs in the range of 110 – 145 °C were selected including a cellulose ester which is susceptible to thermal

degradation. The polymers used in this study include PEO N80 (Tg- -45°C) (DOW, 2002), PVP VA64 (Tg- 110°C) (BASF, 2011), HPMCP HP55 (Tg- 145°C) (Ghosh, *et al*. 2011, ShinEtsu, 2009), HPMCAS (Tg- 123°C) and ethyl cellulose (Tg- 140°C) (Hercules, 2011).

4.2 Preliminary trials

There are several reports about the application of S3M for preparation of polymer composites which were discussed in details in Section 2.4.2, but the objectives of these experiments were different to the current research and there is little opportunity for extrapolation of that understanding to pharmaceutical systems and the objectives set in this research. Therefore preliminary experiments were essential to develop some understanding, develop skills and set up the experimental field.

4.2.1 S3M trials

S3M trials were conducted for salicylic acid as a model API, PVP VA 64 as a polymer for solid dispersion and nicotinamide as a coformer for cocrystallisation. The batches trial batches were processed on S3M1, S3M2 and S3M3.

Table 4.3 Preliminary trials on S3M and selection of S3M

Batch details	S3M1	S3M2	S3M3
SAL:VA64 1:2	End product did not show formation of amorphous phase at the end of the cycles. No. Of cycles- 20 Amount of shear was very less.	The residence time was fraction of seconds and material flew through the gap between two pans with minimum or no shear. No amorphous end	At the end of 3rd cycle there was complete conversion of drug and polymer mixture into amorphous end product. Relatively very high shear

		product No. Of cycles- 5	and rise in temperature of the product.
SAL:NIC 1:1 10% PEO	End product did not show partial or full conversion into cocrystals. No. Of cycles- 20 Very less shear.	End product did not show formation of cocrystals. Minimum or no shear during milling with least residence time. No. Of cycles- 5	Complete conversion of drug and co-former into phase pure cocrystalline end product. Residence time was 5-10 secs with relatively very high shear during 1^{st} cycle.

The observations were previously reported in section 3.3.1.1 and are summarised in Table 4.3

In S3M n>2 and 0>α>π/2, the dihedral angle θ is the angle between the moving pan and the stationary pan δ slots. Consider that the pan is moving on the stationary pan when k^{th} slot of the moving pan interacts with l^{th} slot of the stationary pan the slot distances L and S are shown in Figure 4.5. The lower bevel and upper bevel are denoted by λ and μ respectively. Another term commonly used in the cutting devices is turning angle which is the angle through which the moving pan turns on the stationary pan.

The value of Ø is between 0 to 2π/n. At the beginning of the cycle Ø=0 when Ø changes from 0 to 2π/n at that instant θ becomes zero. This action is similar to the scissor action. Therefore S3M can be imagined as three dimensional scissors. This continuous pressure and cutting action provides extremely high shear in S3M.

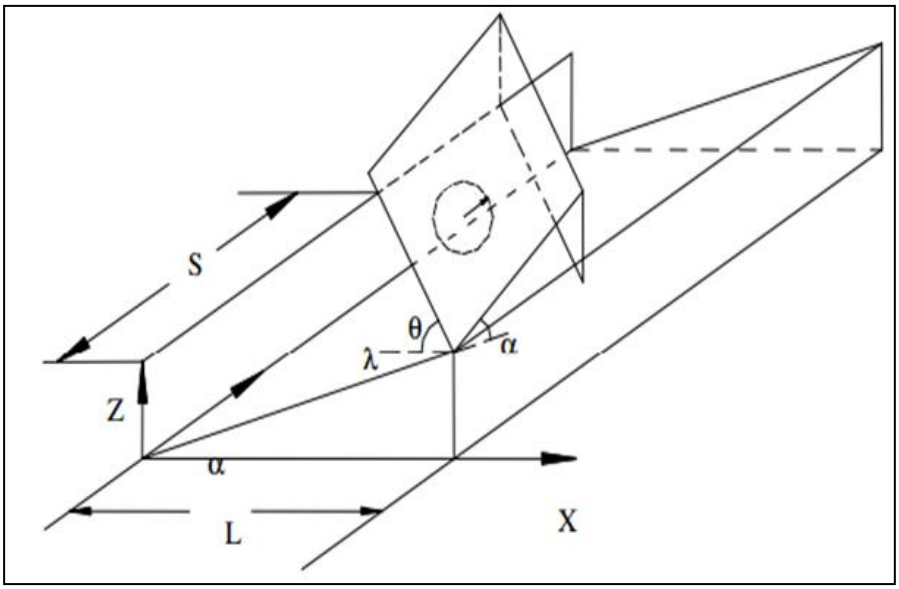

Figure 4.5 Schematics of moving and stationary bevels of mill pan

The preliminary trials of solid dispersion and cocrystal batches showed that S3M1 and S3M2 were not effective in causing transformation. In S3M1 the diameter of the pan is low, whereas in S3M2 the bevel angle α is high. The failure of S3M1 could be explained by understanding the relationship between radius R of the pan and the shear applied, Xu *et al*., derived an equation to explain the trajectory of the particles in the mill. It was observed that particle movement in the mill follow a spiral path. This suggested that the actual distance travelled by the particle is far greater than the radius of the pan. During the travel of the path across the spiral trajectory the particle is subjected to significant shear causing transformation to occur. The spiral path and angular velocity attained by the particles are a function of radius R and speed of rotation of the moving pan. In small mill the spiral path length is not enough to provide the ultimate stress required to rupture the crystal

lattice. Similarly, as the objective is to disturb the crystal lattice and not particle size reduction the multiple cycle approach alone was not effective as reported by other authors for generation of nanomaterials (Xia *et al*., 2004). The failure of S3M2 to generate solid dispersion can be attributed to high bevel angle. The relatively large space between two slots did not allow material residence and was unable to subject it to shearing action.

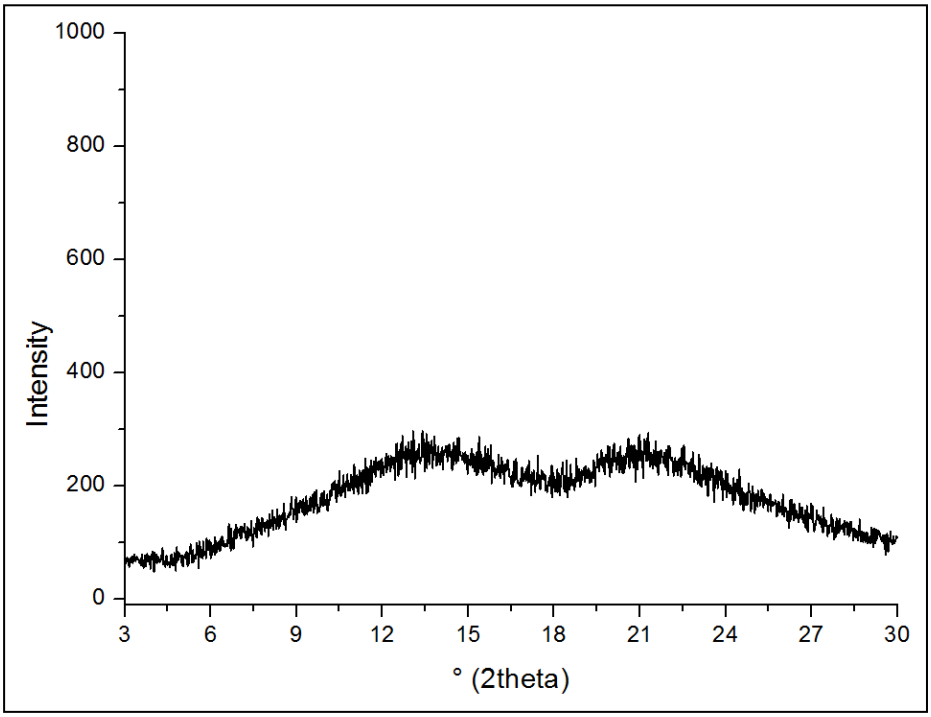

Figure 4.6 PXRD for Salicylic acid: PVP VA64 1:2 solid dispersion at the end of cycle 3 processed by S3M

In the case of S3M3 which has a medium bevel angle and a radius of 30 cm, it could hold the material long enough such that the polymeric system could be sheared easily. Although there was partial conversion it was not completely amorphous at the end of cycle 1. The material after recycling for two additional consecutive cycles converted into the amorphous form (Figure 4.6), in other words the process of achieving molecular dispersion could not

be completed in one cycle. It was not possible to estimate the exact shear provided per cycle because of the number of variables. The clearance between the pans was maintained minimum so ɗ of two pans meet each other so that shear applied would be high.

The salicylic acid - nicotinamide cocrystal batches also worked only with S3M3. The challenge during processing of cocrystal batches was flow of the material.

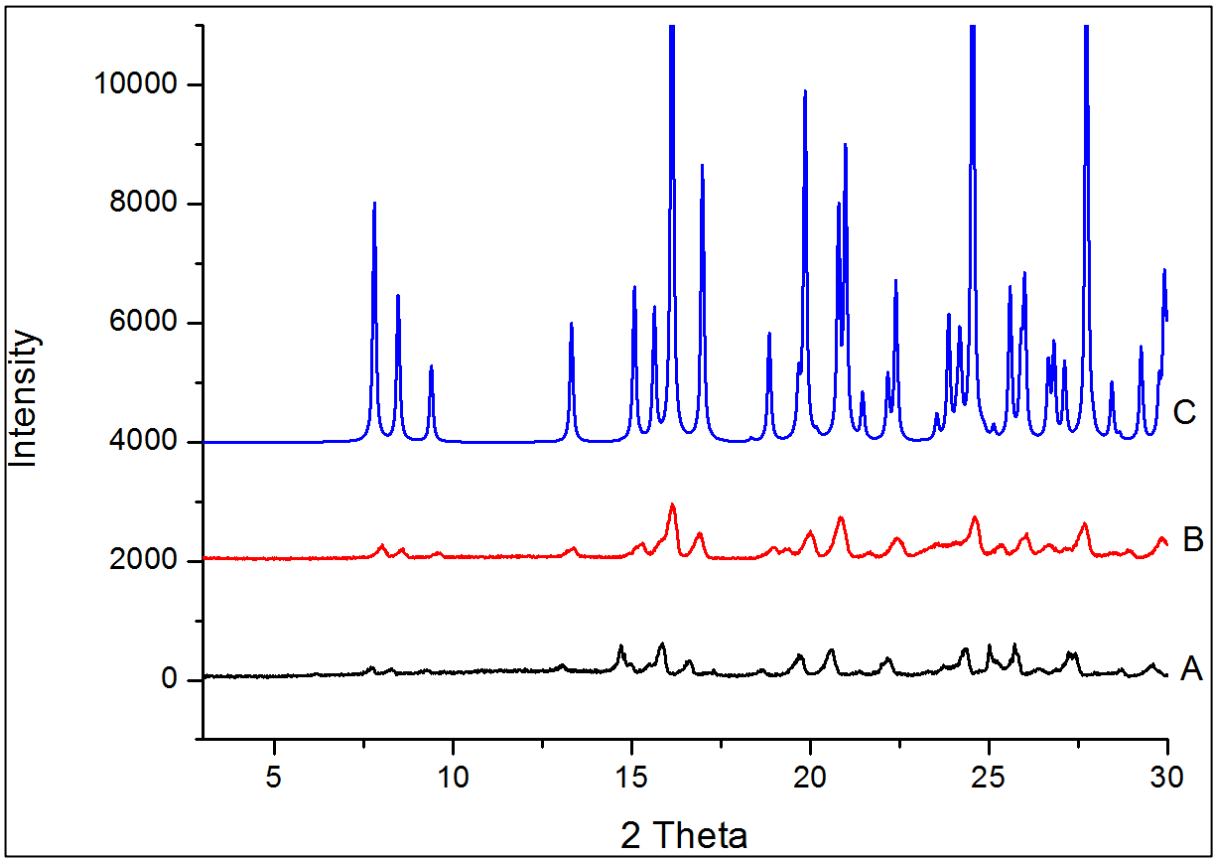

[A- S3M SAL:NIC 1:1 10% PEO, B-HME SAL:NIC 1:1 10% PEO]

Figure 4.7 PXRD for Salicylic acid: nicotinamide 1:1 cocrystal with 10% PEO processed by A: HME, B: S3M and C: Reference PXRD pattern from CSD

The mill was blocked and the powder was compacted in the spaces between consecutive slots. Addition of PEO enabled flow of material, avoided

compaction and application of shear. The generation of shear stress by the scissor action require a material which can be stretched and stressed. The stress fields could not be generated for the powder material of small organic molecules such as salicylic acid and nicotinamide but the presence of PEO helped to process the fine powder material through S3M (Figure 4.7).

The use and selection of PEO was based on the actual trial and outcomes during the S3M processing. The way PEO behaved under high shear and stress environment of S3M with excellent stretch ability of its chains and at its melting point covering both drug and co-former into it. PEO being crystalline in nature was able to form phase pure cocrystals when added as processing aid during S3M processing, the crystalline nature of PEO in the cocrystalline matrix might have lost and it was difficult to find out due to the amount of PEO present in the total mixture of cocrystal matrix.

The role of PEO could not be explained completely with the available data but it worked as an aid to improve flowability (SAL:NIC 1:1 showed an angle of repose of 19.65° whereas SAL:NIC 1:1 10% PEO showed 21.80°), lowering of eutectic point or melting point of either component (Table 4.4). The lowering of melting point onset and enthalpy of melting indicates that a small portion of the material has become miscible with the polymer. The polymer might have worked as a medium for the two components to interact in the molecular state. This hypothesis could not be proved at this stage but a similar hypothesis was proposed for slurry crystallisation process where the rate of cocrystallisation has been enhanced through application of shear

using ultrasound energy (Apshingekar, 2014) or accelerated solution process through use of microwaves (Pagire, *et al*. 2013).

Table 4.4 Effect of PEO thermogram of processed 1:1 SAL:NIC pair

% PEO	Salicylic acid			Nicotinamide		
	Onset (°C)	End (°C)	Enthalpy (J/g)	Onset (°C)	End (°C)	Enthalpy (J/g)
0	157	166	173	124	135	190
5	151	168	130	122	133	178
10	138	167	121	119	135	167
15	127	165	89	118	134	144

At 5 % w/w PEO addition flow was found to be unsatisfactory whereas at 20 % w/w of PEO the product showed reduced crystallinity. Therefore concentration of PEO was restricted to 10 % and 15% for the trial.

4.2.2 HME trials

Application of HME for manufacture of solid dispersions has been well established therefore feasibility trials were not conducted using HME. A comparative evaluation has been carried out using other pairs which are reported in Chapter 5.

The application of HME for preparation of cocrystals has been well reported (Dhumal *et al*, 2010; Kelly *et al*, 2012). The advantages of this technology for cocrystallisation have been discussed in Section 2. A feasibility trial was conducted to explore the effect of addition of polymer, though recently Boksa *et al* reported development of carbamazepine – nicotinamide cocrystals in the presence of 21 % w/w Soluplus (its polyvinyl caprolactam-polyvinyl acetate-polyethylene glycol graft copolymer with an amphiphilic chemical structure) and the process is termed as matrix assisted cocrystallisation

using HME (Boksa *et al*., 2014). SAL – NIC cocrystals were produced successfully in the presence of 10 % PEO without loss of crystallinity or generation of amorphous phase. The amount of PEO to be present during the processing of cocrystals on S3M was based on trial and error approach. 5-25% w/w PEO was added and tried for the formation of the phase pure cocrystals. The higher amount of PEO i.e. 25% w/w formed more like amorphous structure in the end product with very low crystalline nature of cocrystal and more of amorphous nature with reduced crystalline characteristic peaks in X-ray diffraction analysis, turning cocrystalline material into amorphous system will majorly affect the rapid release of drug through cocrystals and will slow it down due to the amorphous nature of the system, whereas in case of 10 and 15% w/w concentration of PEO it was possible to get phase pure cocrystals without losing its crystallinity. The presence of cocrystals was confirmed using PXRD (Figure 4.3). The screw configuration and other processing parameters were used as described in the literature to maintain high shear.

Chapter 5. Results and discussions of solid dispersion

This chapter will provide a detailed account of the development of solid dispersions using S3M3 and HME technology. The main objective is to exemplify the data using drugs and polymers with different physicochemical properties processed by these two technologies. The four drugs which have been selected as model molecules are ibuprofen, paracetamol, glibenclamide and carbamazepine. The chapter has been divided into four sections devoting a section for each drug.

5.1 Ibuprofen

Ibuprofen is a model molecule with low Tg, low melting point drug with high dose posing challenges in shear based processing. Ibuprofen solid dispersions were prepared with PVP VA64 and HPMCP HP55.

5.1.1 Glass Transition Temperature

Considering the challenge due to low Tg of ibuprofen, Tg of the ibuprofen-PVP VA64 system was first estimated using DSC as well as the Fox and Taylor equation. The 1:2 IBU: PVP VA64 physical mixture was heated to 100 °C and subsequently cooled to -50° C after 10min hold at 100° C. It showed Tg of the mixture at 33.52 °C (Figure 5.1).

The Tg of each drug-polymer mixture was predicted theoretically using the Fox equation (Fox and Flory, 1950)

$$\frac{1}{T_g} = \frac{W_{drug}}{T_g,drug} + \frac{1-W_{drug}}{T_g,polymer} \qquad \text{..... Equation 1}$$

Where, W_{drug} is the weight fraction of the drug, and 1- W_{drug} is the weight fraction of the polymer, *Tg,drug* is the glass transition temperature of the drug, *Tg,polymer* is the glass transition temperature of the polymer. The weight fraction of drug will have a direct effect on the glass transition temperature of the drug polymer mixture, as drug concentration will increase the composition and respective weight fractions will change. The predicted Tg using the Fox equation was found to be 39.51 °C. There seems to be confirmation between the experimentally determined and predicted Tg values of ibuprofen and PVP VA64 mixture, variation in the values can be attributed to variation in the ratio due to sampling error (sample may not contain exactly a 1:2 ratio of the drug :polymer) while carrying out DSC. Similarly the observed and predicted Tg for IBU: HP55 1:2 mixture was 41.75 °C and 54.46 °C respectively.

5.1.2 Calibration curve

The calibration curve for IBU was linear over the concentration range of 1-10 ug/ml. Linearity was calculated using the calibration curve, slope of the equation is 0.0526, constant -0.0022 with R^2 of 0.9993 (Figure 5.1). From the calibration equation it can be confirmed that linearity follows Beer's law and shows good linearity in the selected range.

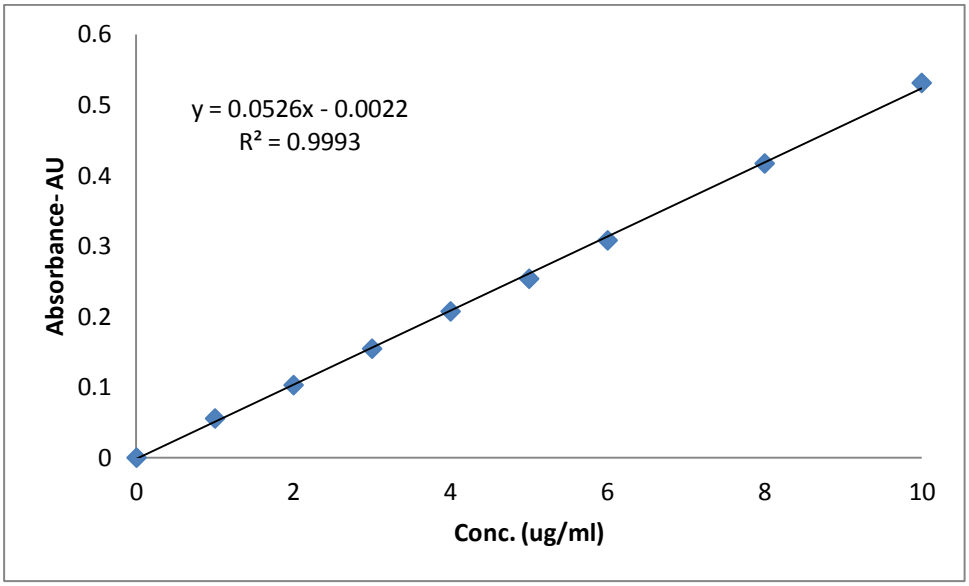

Figure 5.1 Ibuprofen calibration curve by UV spectrophotometer at 221nm

5.1.3 Processing of solid dispersion

Accurately weighed 300 gm mixture of IBU: PVP VA64 in 1:2 ratios was blended using a turbula mixer. The resultant blend was then subjected to milling on S3M3. The material flow was good during the first cycle and at the end of first cycle slight lumps and agglomerates were observed. The end product of first cycle was again fed into the S3M3 for a second milling cycle, during which there was a rise in mill temperature which caused complete melting of the drug: polymer mixture inside the mill. The molten mass was so sticky and caused adhesion of the rotary and stationary pans together. The S3M3 was blocked at the end of the second cycle which caused a difficulty for end product collection and cleaning of the mill. The sticky product was then collected and subjected to PXRD analysis to ensure the formation of a solid dispersion. In the case of IBU: HP55 1:2 experiments the flow of the mixture was excellent, at the end of the first cycle the material was powdery in nature and there was no formation of any agglomerated mass or lumps, at

the end of second cycle the small agglomerates started forming which were again fed back for the third cycle and at the end of the third cycle there was formation of agglomerates and solidified mass. The HME for IBU solid dispersion batches were carried out using the temperature profiles as mentioned in Section 3.5.2. During HME processing of IBU: VA64 1:2 very viscous extrudate strands were formed which were sticky in nature and when kept together strands formed a homogenous mass. In the case of HME processing of IBU: HP55 1:2 extrudates formed a good strand.

The problems in processing due to formation of sticky molten mass with PVP VA64 is mainly due to the low Tg of the mixture which is about 39 °C whereas the processing issues were not encountered with HPMCP – Ibuprofen batches due to high Tg.

5.1.4 Characterisation of solid dispersion

End products from S3M3 and HME were subjected to characterisation to confirm their amorphous nature and assess pharmaceutical performance.

5.1.4.1 PXRD

PXRD was carried out as described in Section 3.4.2. [**A**-Ibuprofen, **B**-HME Ibuprofen:HP55 1:2, **C**-HME Ibuprofen:VA64 1:2, **D**-S3M Ibuprofen:HP55 1:2, **E**-S3M Ibuprofen:VA64 1:2]

Figure 5.2 shows PXRD pattern for ibuprofen and its solid dispersions with PVP VA64 and HPMCP HP55 processed by HME and S3M3, The PXRD pattern for ibuprofen shows characteristic peaks at various intensities whereas it clearly showed complete absence of characteristic peaks for

ibuprofen in solid dispersions with PVP VA64 and HPMCP HP55 in both the cases (HME and S3M3).

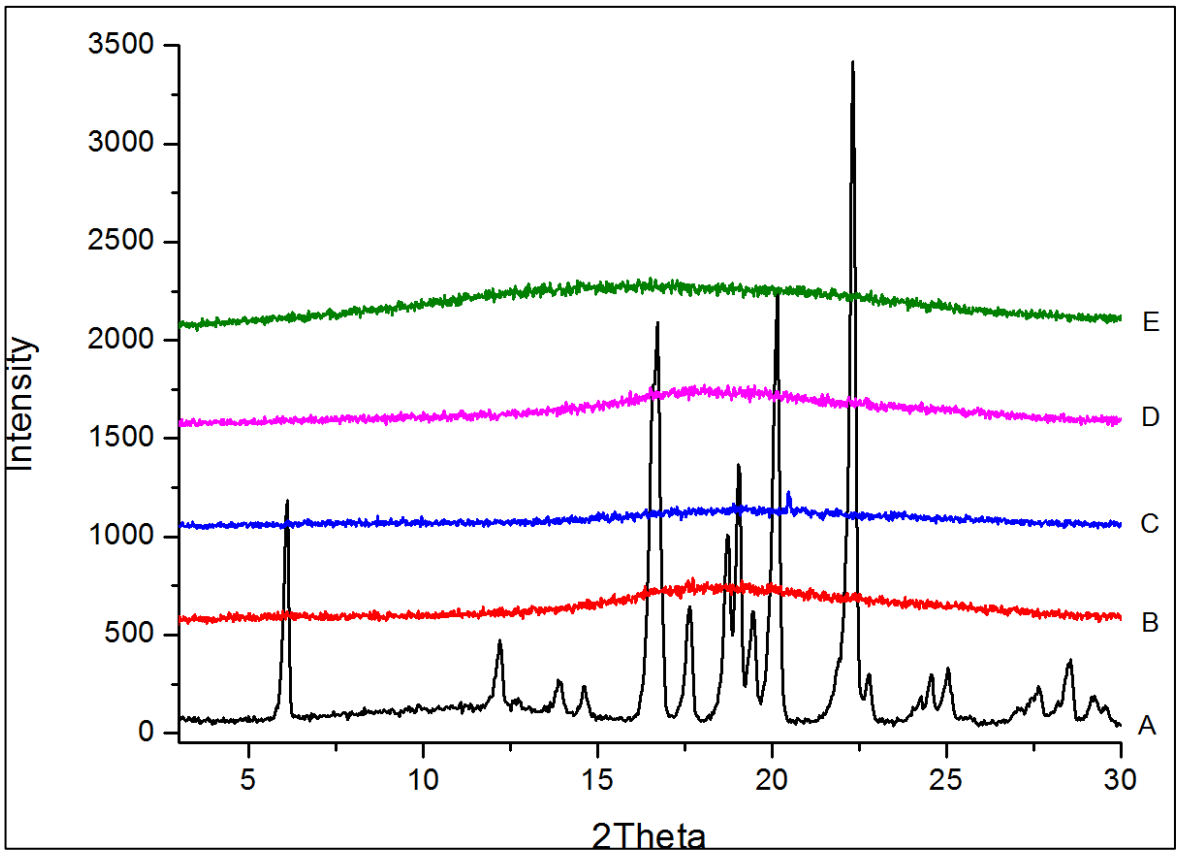

[**A**-Ibuprofen, **B**-HME Ibuprofen:HP55 1:2, **C**-HME Ibuprofen:VA64 1:2, **D**-S3M Ibuprofen:HP55 1:2, **E**-S3M Ibuprofen:VA64 1:2]

Figure 5.2 PXRD for Ibuprofen solid dispersions with HPMCP HP55 and PVP VA64 processed by HME and S3M3

5.1.4.2 DSC

DSC was carried out as mentioned in Section 3.4.1. The DSC thermogram for ibuprofen showed a sharp melting endotherm at 75 °C (Figure 5.3), whereas B and C are physical mixtures of ibuprofen with respective polymers which show a melting endotherm for ibuprofen at 75 °C. Thermograms D and E are for HME processed solid dispersions for IBU: VA64 1:2 and IBU:HP55

1:2 respectively, which did not show any melting endotherm similar to S3M3 processed IBU:VA64 1:2 (F) IBU:HP55 1:2 (G) solid dispersions which also showed an absence of crystalline endotherm for ibuprofen.

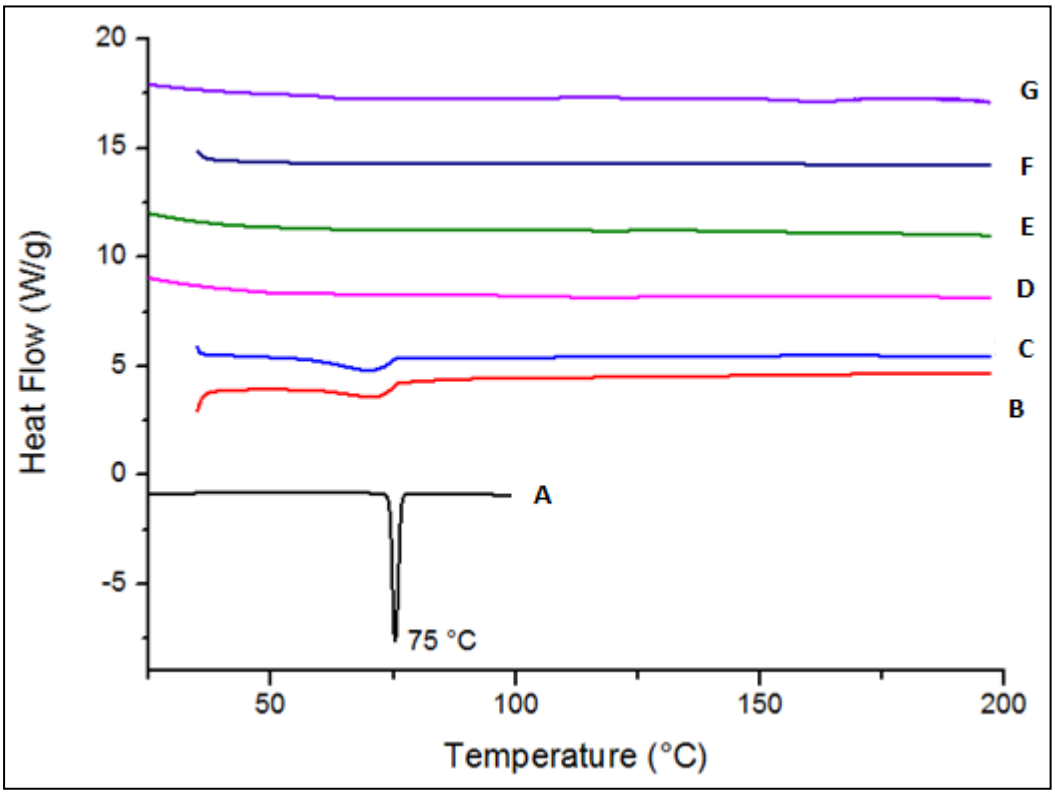

[**A**- Ibuprofen, **B**- Ibuprofen:VA64 1:2 physical mixture, **C**- Ibuprofen:HP55 1:2 physical mixture, **D**- HME Ibuprofen:VA64 1:2, **E**- HME Ibuprofen:HP55 1:2, **F**- S3M Ibuprofen:VA64 1:2, **G**- S3M Ibuprofen:HP55 1:2]

Figure 5.3 DSC thermograms for ibuprofen solid dispersions processed by HME and S3M3

5.1.4.3 SEM

SEM was carried out as mentioned in Section 3.4.5. Surface features from SEM analysis for ibuprofen solid dispersions show that in the case of HME extrudates, the end product is completely non-porous and has smooth surface features whereas in case of S3M3, processed dispersions are highly porous, fractured and irregular surface (Figure 5.4).

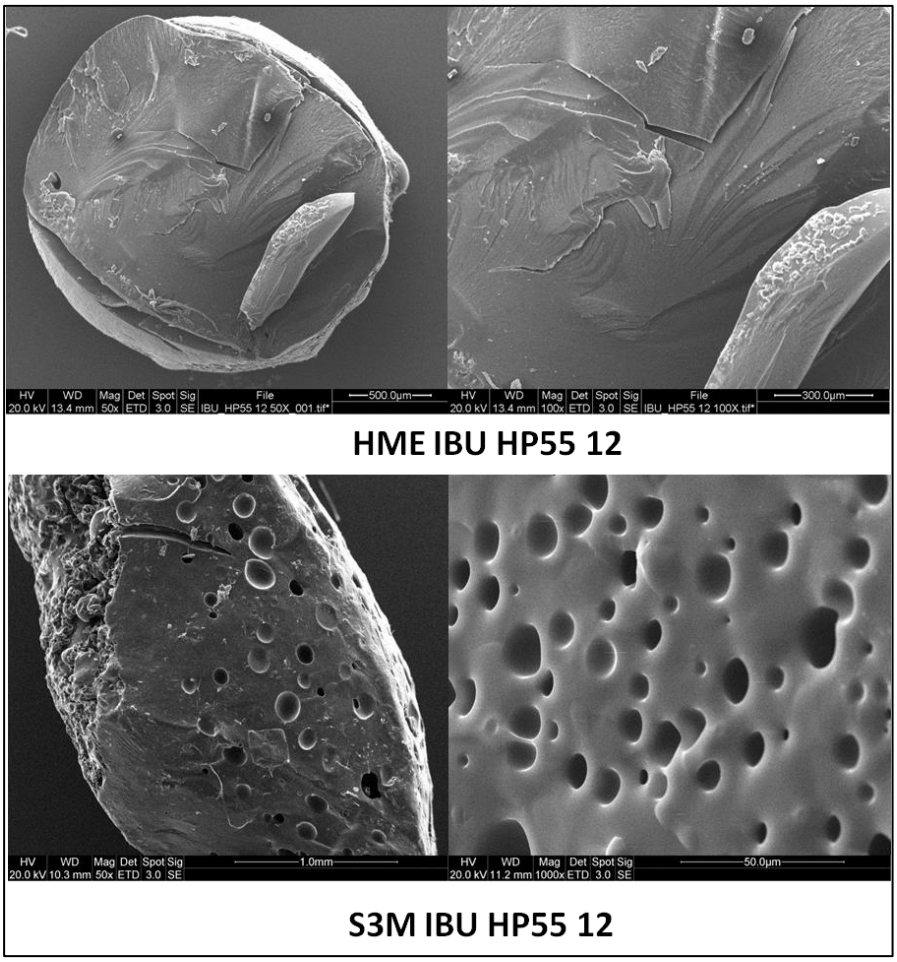

Figure 5.4 Surface morphology by SEM of ibuprofen solid dispersions processed by HME and S3M

The high porous nature of solid dispersions in case of S3M3 can be contributed to three dimensional scissoring actions which exerts very high shear on the material. This very high shear causes distortion of the polymer structure during S3M processing. Upon discussion with the S3M expertise at Sichuan University, China, it was revealed that in milling of higher molecular weight polymers, gases could be generated due to bond ruptures upon melting of polymers. These gases released from compact molten polymer mass may have caused generation of the porous structure. In case of IBU:

HP55 solid dispersions generation of highly porous structure during S3M3 processing might be due to the presence of slight moisture in the mixture which released upon high shear application. In case of HME processed solid dispersions the highly compact and non-porous structure might have formed due to the molten and high pressure nature of flow in the extruder barrel and die.

5.1.4.4 FTIR

FT-IR was carried out as mentioned in Section 3.4.3. FT-IR spectral vibration for ibuprofen showed characteristic stretching at 1714 cm^{-1} which can be attributed to –COOH stretching (Xu, *et al*. 2007). Both processes showed exactly similar stretching in solid dispersion. The finger print stretching spectra for ibuprofen at 777cm^{-1} remained the same in IBU: HP55 1:2 solid dispersions and did not show any shift or broadening (Chen, *et al*. 2012) (Figure 5.7). Hydrogen bonds can formed in IBU:PVP VA64 and IBU:HP55 in respective functional groups as shown in Figure 5.5 and Figure 5.6.

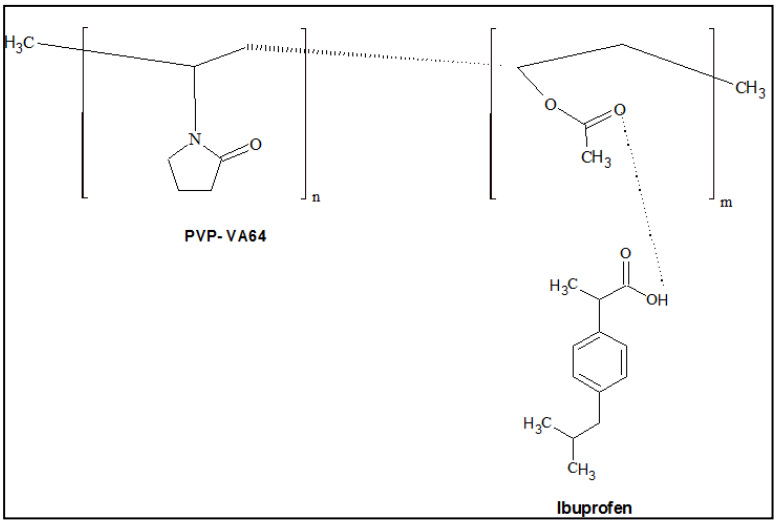

Figure 5.5 Hydrogen bonding between Ibuprofen and PVP VA64

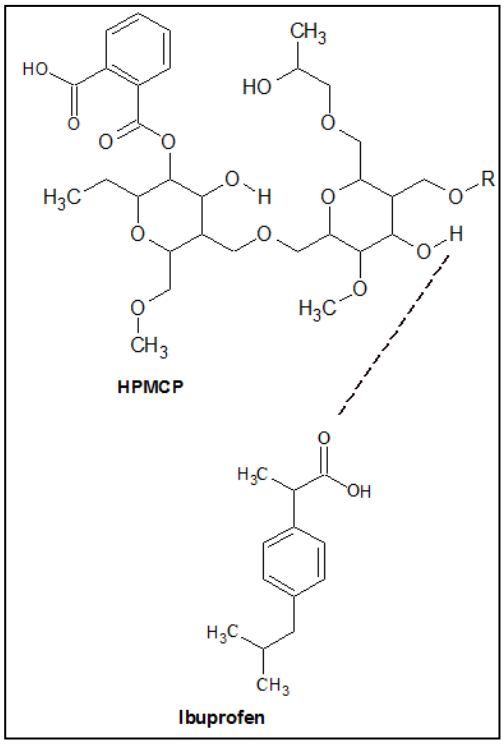

Figure 5.6 Hydrogen bonding between Ibuprofen and HPMCP HP55

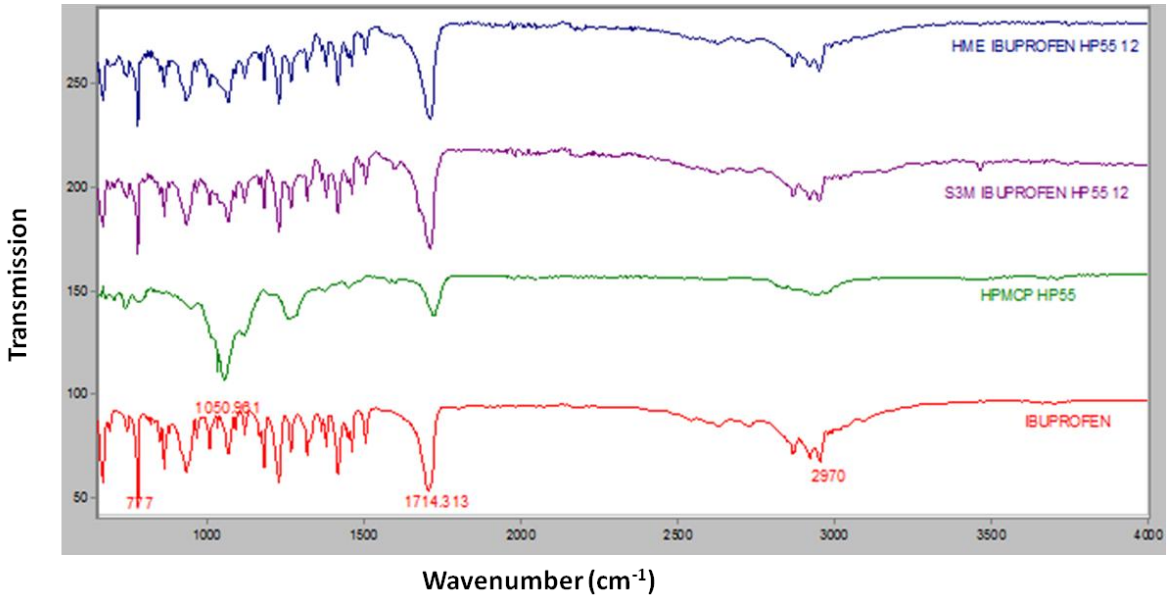

Figure 5.7 FT-IR spectra for Ibuprofen:HP55 1:2 solid dispersions processed by HME and S3M

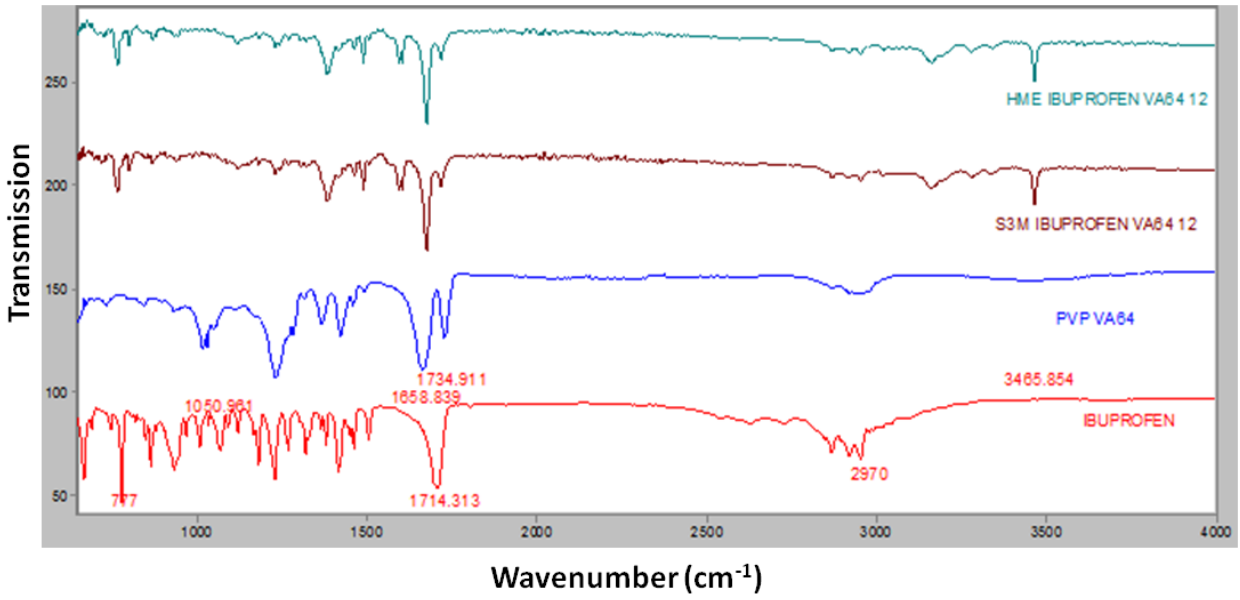

Figure 5.8 FT-IR spectra for Ibuprofen: PVP VA64 1:2 solid dispersions processed by HME and S3M

In the case of Ibuprofen VA64 solid dispersions the finger print stretching for ibuprofen at 942 cm^{-1} completely disappeared (Figure 5.7). A new stretching vibration appeared at wave number 3465 cm^{-1} which may be a contribution of the hydrogen bond formation between –COOH of ibuprofen with carbonyl bonds of PVP VA64 (Xu *et al*. 2007). The –OH stretching of –COOH of ibuprofen was broadened in case of both the solid dispersion samples. Therefore it can be concluded that ibuprofen forms good intermolecular hydrogen bonding with PVP VA64 (Figure 5.8).

5.1.4.5 NIR

NIR analysis was carried out as described in Section 3.4.4. NIR spectra for ibuprofen show highest absorbance at 1676 and 1692 nm in the first overtone region of characteristic NIR absorption spectra (Figure 5.8) (Burns and Ciurczak, 2009), whereas for PVP VA64 at 1685 nm and for HP55 at 1662 nm.

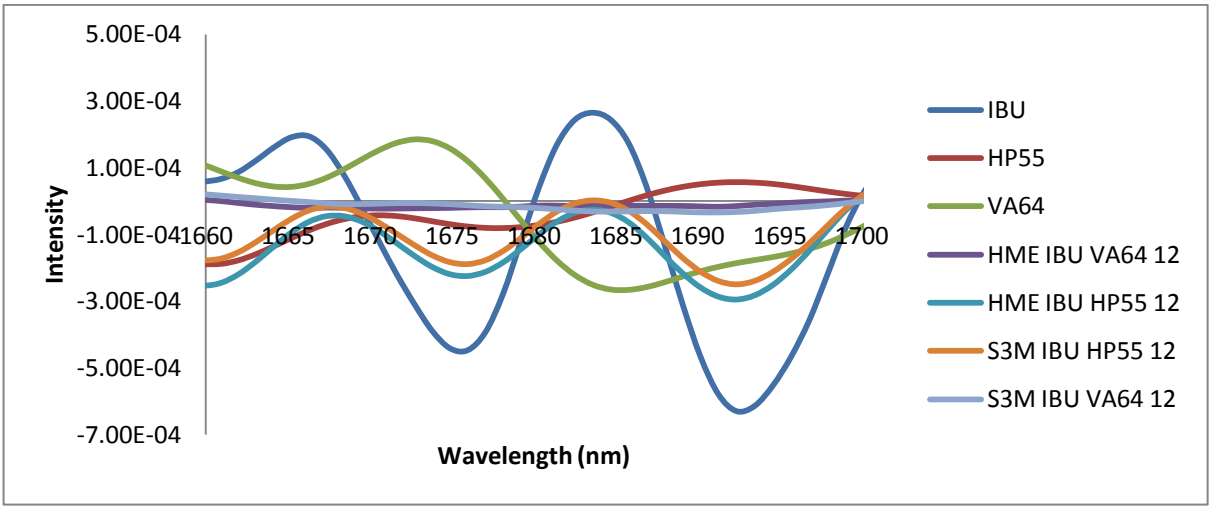

Figure 5.9 NIR spectra for Ibuprofen solid dispersions processed by HME and S3M

Ibuprofen solid dispersions with PVP VA64 did not show any significant or no absorption at the characteristic wavelength of ibuprofen and PVP VA64 in both the cases HME and S3M. The presence of hydrogen bonding between ibuprofen and PVP VA64 could not be confirmed by NIR spectra. In the case of HP55 solid dispersions the characteristic wavelengths of absorption were observed at 1676 and 1692 nm respectively in both the HME and S3M processed solid dispersions. Out of which HME processed solid dispersions showed higher absorption than S3M processed which might due to contribution of the higher extent of hydrogen bond formation between –COOH group of ibuprofen and –COOR group of HP55 (Figure 5.6).

5.1.4.6 Dissolution

The content of IBU in both solid dispersions processed by HME and S3M3 was assayed by UV spectroscopy. In the case of IBU: VA64 1:2 the assay for HME were 99.5±2.12% and S3M 98±1.41%, in the case of IBU: HP55 1:2 the assay for HME 100.5±0.7% and S3M 99±1.4%.

Dissolution studies were carried out as mentioned in 3.5.3.1. and dissolution parameters were as described in Table 3.8. Dissolution profile for IBU solid dispersions shows a faster release in the case of PVP VA64 solid dispersions processed by HME and S3M whereas in the case of solid dispersions with HP55, HME processed dispersions show slightly higher release than S3M processed (Figure 5.9). In the case of IBU: VA64 1:2 dispersion all the drug was released within one hour whereas in the case of IBU:HP55 1:2 dispersion only 80% drug was released within one hour and it took 4 hours to release all IBU present within the dispersion.

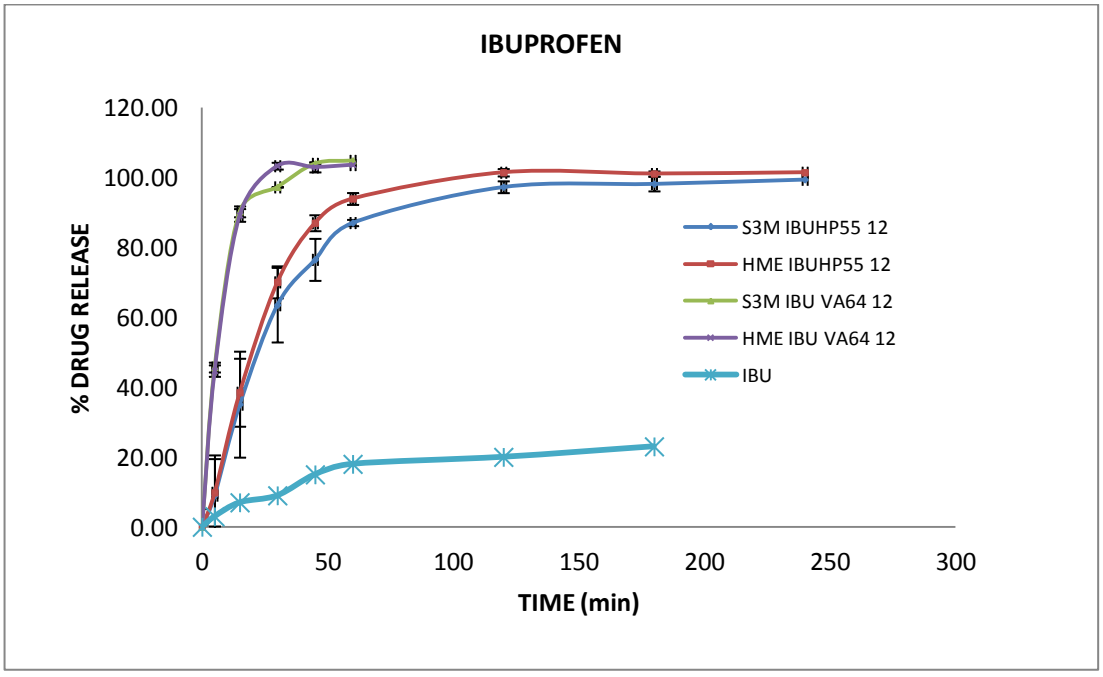

Figure 5.10 Dissolution profile for IBU solid dispersions processed by HME and S3M

There was not much difference in IBU release in the case of PVP VA64 solid dispersions as shown in Figure 5.10. This might be due to the dispersions

produced in both being converted into a solid viscous mass. In the case of IBU dispersion with HP55 although the S3M3 processed dispersion was highly porous compared to the HME processed dispersion there was relatively minor difference in drug release. The solid dispersions were crushed to powder form prior dissolution studies, which might have contributed to the smaller difference in drug release between dispersions processed by HME and S3M3.

A T test was applied to IBU: HP55 1:2 solid dispersion drug releases at 60mins and the calculated p values used to test if there was significant difference between HME and S3M3 processed dispersions. The T test gave a p value of 0.22 which is higher than 0.05, this concludes that there is no significant statistical difference between two processes with regard to drug release at given time points for IBU: HP55 1:2 dispersion.

5.2 GLIBENCLAMIDE

5.2.1 Glibenclamide calibration

The calibration curve for GLIB was linear over the concentration range of 1-10 ug/ml. The linearity equation was calculated using calibration curve, slope of the equation was 0.0526, constant 0.0044 and R^2 0.9998. From the calibration equation it can be confirmed that absorbance v/s concentration follows Beer's law (Figure 5.11).

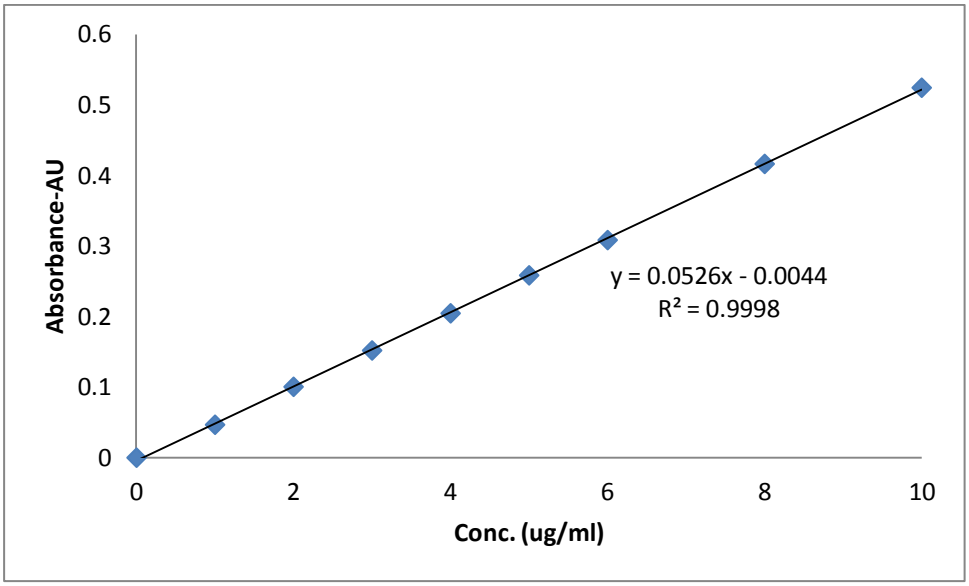

Figure 5.11 Glibenclamide calibration curve by UV spectrophotometer at 240nm

5.2.2 Processing of solid dispersion

Accurately weighed GLIB and respective polymers PVP VA64 and ethyl cellulose in the ratio 1:2 were mixed well and sieved through 80 mesh to achieve uniform particle size. The mixture was then subjected to turbula mixer for 10mins to get a uniform homogenous dispersion. Material feeding to S3M3 was good in the case of both the polymers. First and second cycle gave end product in the form of small agglomerated granular mass which was converted into a solid agglomerated molten mass at the end of the third cycle in case of PVP VA64. In the case of ethyl cellulose the end product was achieved in the third cycle. HME for GLIB solid dispersion batches were carried out using the temperature profiles as mentioned in Section 3.5.2. The extrusion processing for GLIB dispersions was smooth and plasticisers used helped to get good extrudate product in the form of cylindrical extruder die shaped extrudates with low processing torque levels.

5.2.2 Characterisation of solid dispersion

The GLIB solid dispersions processed by HME and S3M3 were subjected to various characterisations

5.2.2.1 PXRD

PXRD for GLIB solid dispersions were carried out as described in Section 3.4.2.

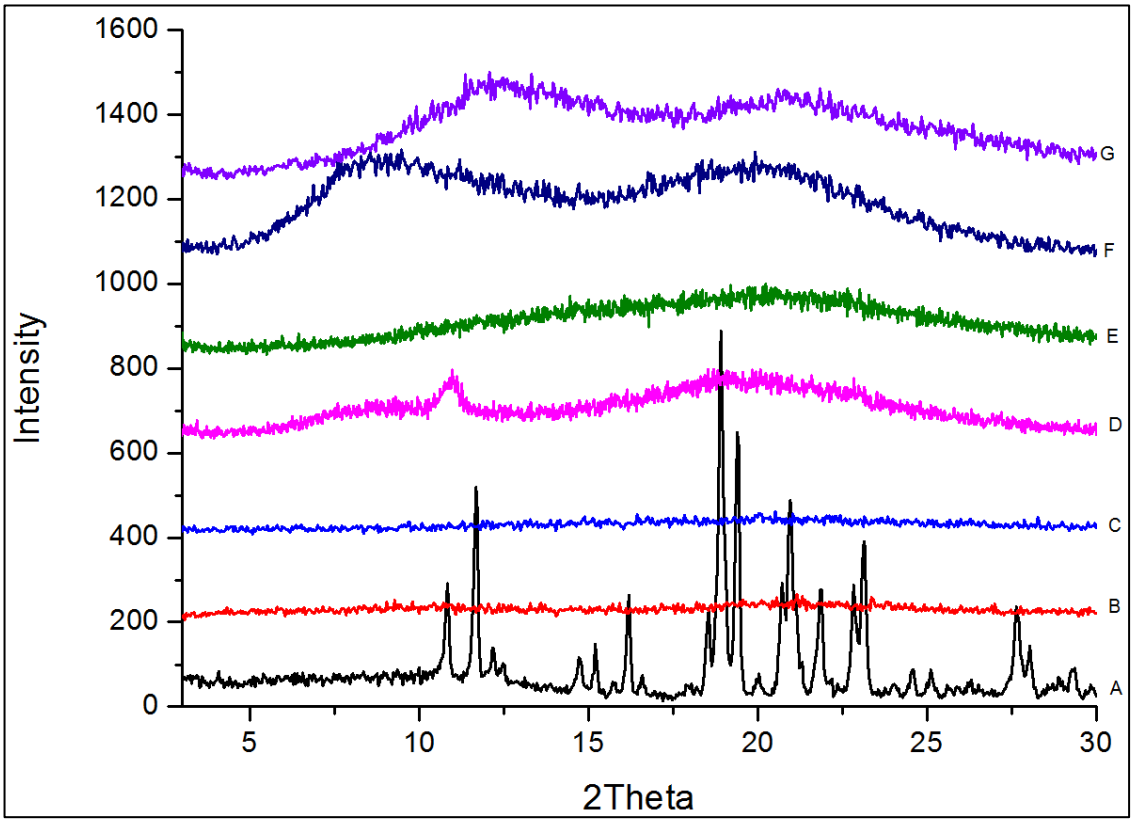

[**A**-Glibenclamide, **B**- HME Glibenclamide:Ethyl Cellulose 1:2, **C**-HME Glibenclamide: VA64 1:2 , **D**-S3M Glibenclamide:Ethyl Cellulose 1:2 , **E**-S3M Glibenclamide:VA64 1:2 , **F**-Ethyl Cellulose , **G**- PVP VA64]

Figure 5.12 PXRD for glibenclamide solid dispersion processed by HME and S3M

The PXRD pattern for GLIB shows all crystalline peaks at respective 2θ values with respective intensities (Table 4.1). Solid dispersions with VA64 and ethyl cellulose processed by HME and S3M not show any crystalline peaks for GLIB (Figure 5.12). The plain polymers showed absence of any

characteristic peak due to their amorphous nature. This confirms that in the case of both the solid dispersions, drug particles were completely covered within the polymer chains. This will be confirmed upon DSC analysis.

5.2.2.2 DSC

DSC was carried out as mentioned in Section 3.4.1. The DSC thermogram for GLIB shows a sharp melting endotherm at 175 °C (A). A physical mixture of GLIB with VA64 (B) and ethyl cellulose (C) also shows a characteristic endotherm for GLIB (Figure 5.13).

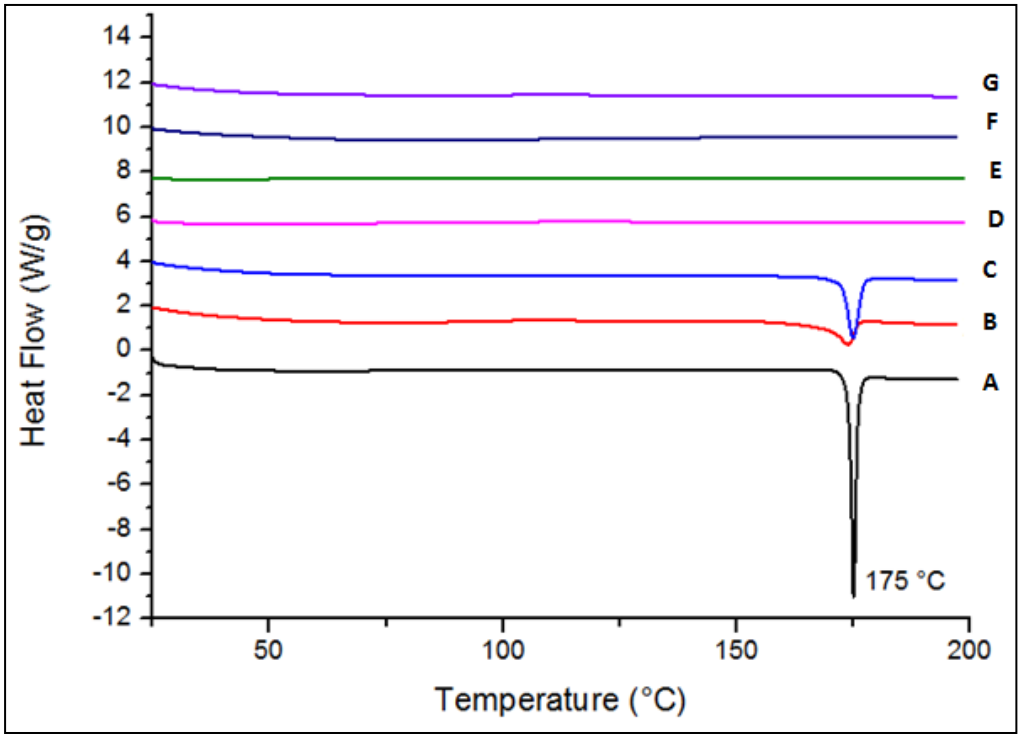

[**A**- Gilbenclamide, **B**- Glibenclamide:VA64 physical mixture, **C**- Glibenclamide:Ethyl cellulose physical mixture, **D**- HME Glibenclamide:VA64 1:2, **E**- HME Glibenclamide:Ethyl cellulose 1:2, **F**- S3M Glibenclamide:VA64 1:2, **G**- S3M Glibenclamide:Ethyl cellulose 1:2]

Figure 5.13 DSC thermograms of Gilbenclamide solid dispersions processed by HME and S3M

Solid dispersions with these both polymers processed by HME and S3M process showed an absence of any crystalline endotherms for GLIB. The

results show that in the case of physical mixtures of GLIB and polymers, a solid solution was not formed just by application of heat in DSC. Upon HME and S3M3 processing GLIB was completely solubilised in the polymer matrix and did not show any melting endotherm.

5.2.2.3 SEM

Surface features for GLIB solid dispersions were performed according to the procedure given in Section 3.4.5.

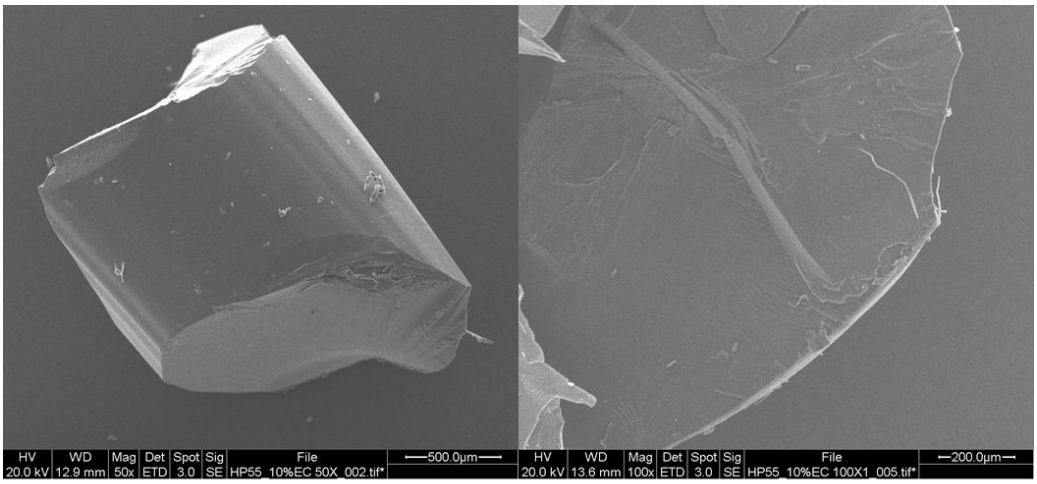

HME GLIB VA64

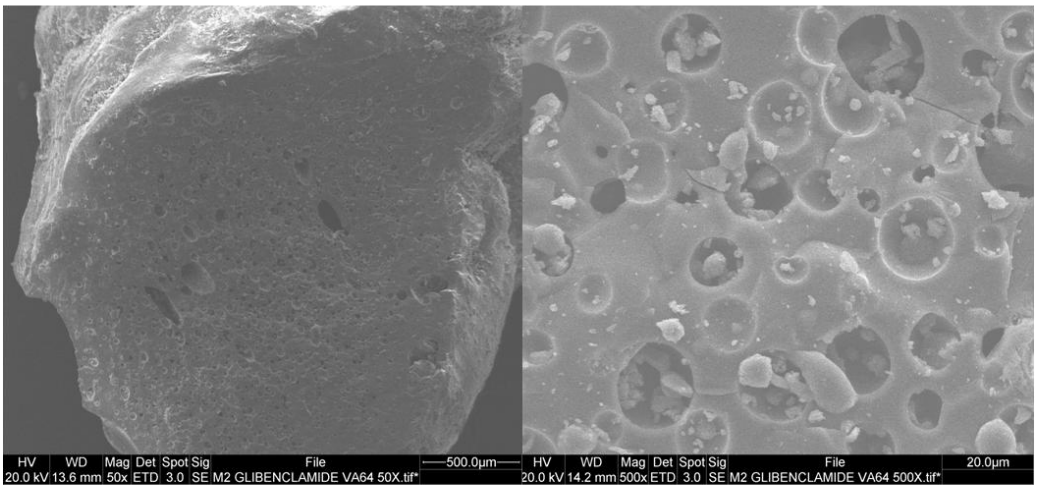

S3M GLIB VA64

Figure 5.14 Surface morphology by SEM of glibenclamide solid dispersions processed by HME and S3M

SEM analysis of HME processed solid dispersions showed very smooth and plain surface features whereas in the case of S3M, highly irregular and porous structures were observed on the surface (Figure 5.14). As discussed in IBU: HP55 dispersion case similar thing happened in GLIB dispersions, S3M3 processed solid dispersions with a porous structure can be attributed to trapped moisture or release of other gases during high shear processing.

5.2.2.4 FT-IR

FT-IR analysis was done according to procedure given in Section 3.4.3.

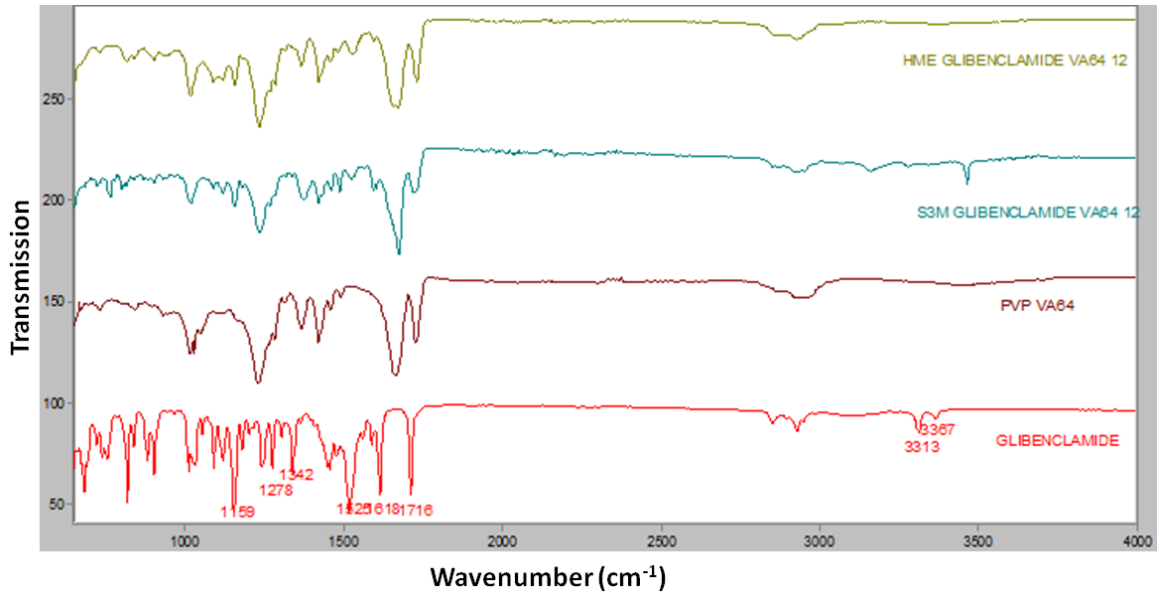

Figure 5.15 FT-IR spectra for glibenclamide: PVP VA64 1:2 solid dispersions processed by HME and S3M

In the case of glibenclamide solid dispersions processed by S3M and HME the characteristic spectral stretching for glibenclamide at 3367 cm^{-1} and 3313 cm^{-1} for strong -NH stretching disappeared in the case of PVP VA64 dispersions and in case of S3M processed dispersions the peak at 3367cm^{-1} shifted to a higher wavenumber which can be due to the strong intermolecular interaction between glibenclamide and VA64 (Chauhan *et al*. 2005) (Figure 5.15).

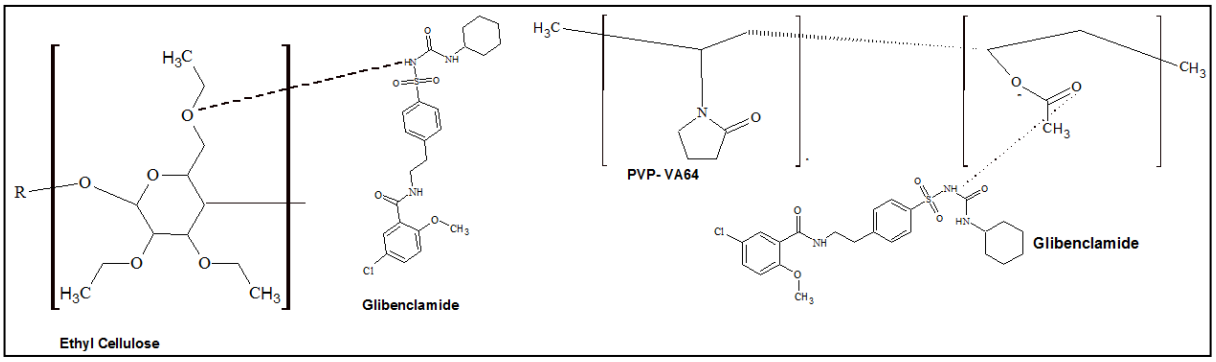

Figure 5.16 Hydrogen bonding between glibenclamide with ethyl cellulose and PVP VA64

The typical amide stretching vibration at 1716cm^{-1} completely disappeared and only showed characteristic spectra for VA64 at 1710 cm^{-1}, possibly due to strong -H bonding between glibenclamide and VA64. The urea -NH stretching vibration at 1278 cm^{-1}, 1618 cm^{-1}, 1525 cm^{-1} and -SO_2 stretching vibrations at 1342 cm^{-1}, 1159 cm^{-1} were distinct in pure glibenclamide spectra but were broadened and shifted in the case of amorphous dispersions due to hydrogen bonding between the functional groups between the drug and polymer (Figure 5.16).

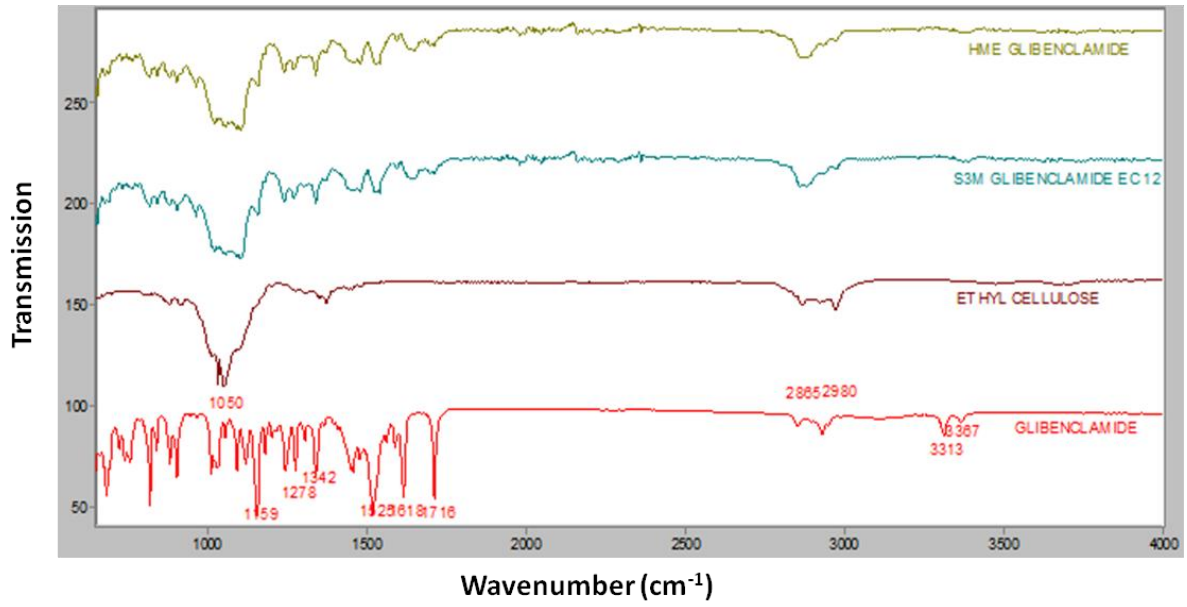

Figure 5.17 FT-IR spectra for glibenclamide: ethyl cellulose 1:2 solid dispersions processed by HME and S3M

In the case of GLIB:EC 1:2 solid dispersions characteristic amide peak stretching vibrations at 3367 cm^{-1} and3313 cm^{-1} completely disappeared, and stretching at 1716 cm^{-1}, 1618 cm^{-1}, 1525 cm^{-1} were broadened and significantly reduced in the case of solid dispersion due to strong intermolecular hydrogen bonding between the drug and polymer (Figure 5.17).

5.2.2.5 NIR

NIR was carried out as described in section 3.4.4. Glibenclamide showed characteristic NIR absorption at 2043 and 2069 nm in the first overtone region whereas in the same region PVP VA64 showed good absorption at 2141 nm and moderate absorption for ethyl cellulose at 2046 nm (Figure 5.18).

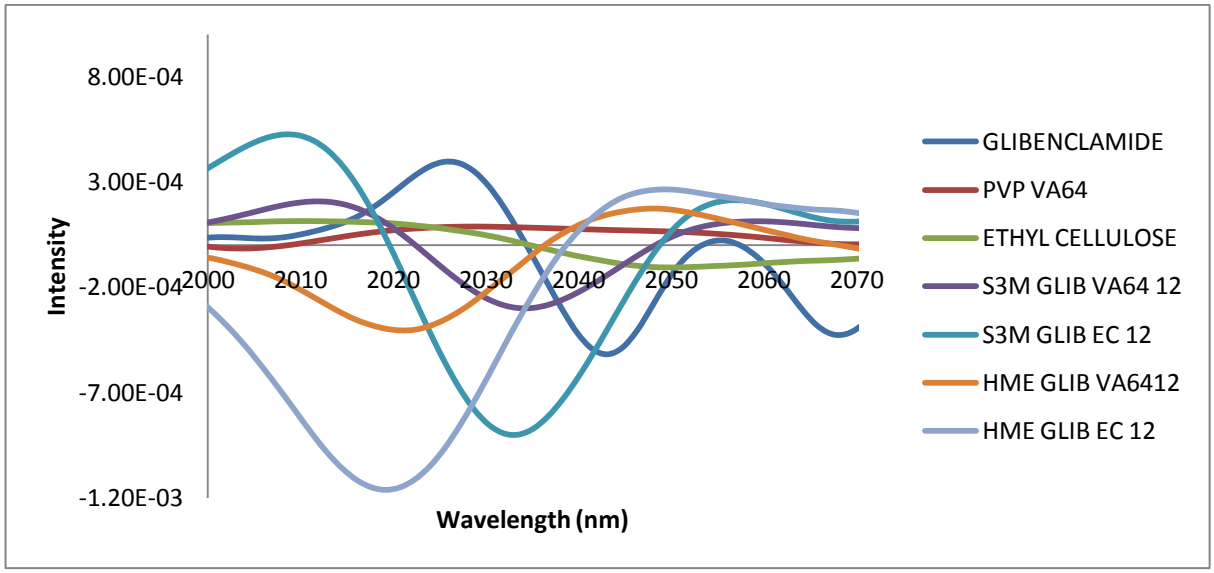

Figure 5.18 NIR spectra for glibenclamide solid dispersions processed by HME and S3M

Glibenclamide solid dispersions with PVP VA64 processed by S3M showed a peak shift at 2035 nm and in the case of HME processed at 2021 nm which can be attributed to the presence of hydrogen bonds between the carbonyl group of VA64 and the -NH group of glibenclamide. In the case of solid dispersions of ethyl cellulose processed by S3M the NIR absorption peak shifted to 2032 nm and in the case of HME it showed significant shift to 2018 nm which can be attributed to strong bond formation between -C=O groups of ethyl cellulose and -NH groups of glibenclamide.

5.2.2.6 Dissolution

The content of GLIB in both the solid dispersions processed by HME and S3M3 was assayed by UV spectroscopy. In the case of GLIB: VA64 1:2 the assay for HME 99±1.4% and S3M 99±2.8%, in the case of GLIB: EC 1:2 the assay for HME100+1.41 ±% and S3M 99±1.4%.

Dissolution parameters and procedure were carried out as described in Section 3.5.3.1.Dissolution studies of GLIB solid dispersions with VA64 processed by S3M showed faster release compared to HME dispersion. In the case of dispersions with ethyl cellulose both the HME and S3M showed a similar kind of controlled release over the period of 24 hours. GLIB: VA64 1:2 processed by S3M3 released 100% drug within 3 hours whereas HME processed dispersion showed a slightly delayed release and released 100% drug in 6 hours. This slow release in the case of dispersions processed by HME can be attributed to compact and non-porous surface features of the extrudates whereas in the case of dispersions processed by S3M3 the surface was very rough and porous, although dispersions were converted to powder form prior to dissolution. The higher release in the case of S3M3 can be attributed to distortion of the surface features to particulate level. In the case of GLIB: Ethyl cellulose dispersions it took 10 hours to release 50% of the drug and another next 24 hours to release 100%.

A T test was applied to GLIB: VA64 1:2 solid dispersion drug release at 60mins and p values was calculated to test if there was there statistical difference between HME and S3M3 processed dispersions. The T test gave a p value of 0.0075 which is less than 0.05, this concludes that there was statistically significant difference between the two processes with regards to drug release at given time points.

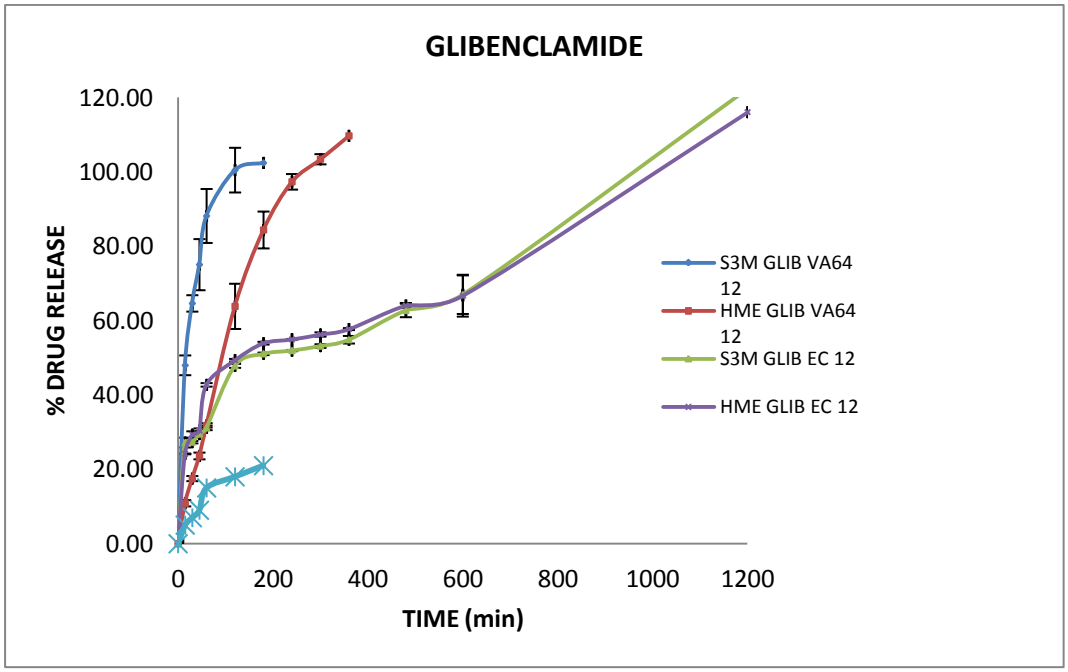

Figure 5.19 Dissolution profiles for glibenclamide solid dispersions processed by HME and S3M

5.3 PARACETAMOL

5.3.1 Paracetamol calibration curve

The calibration curve for PARA was linear over the concentration range of 1-10 ug/ml. The linearity equation was calculated using the calibration curve, the slope of the equation was 0.0679, constant 0.0083 and R^2 was 0.9995 (Figure 5.20). There was good linearity found between concentration v/s absorbance.

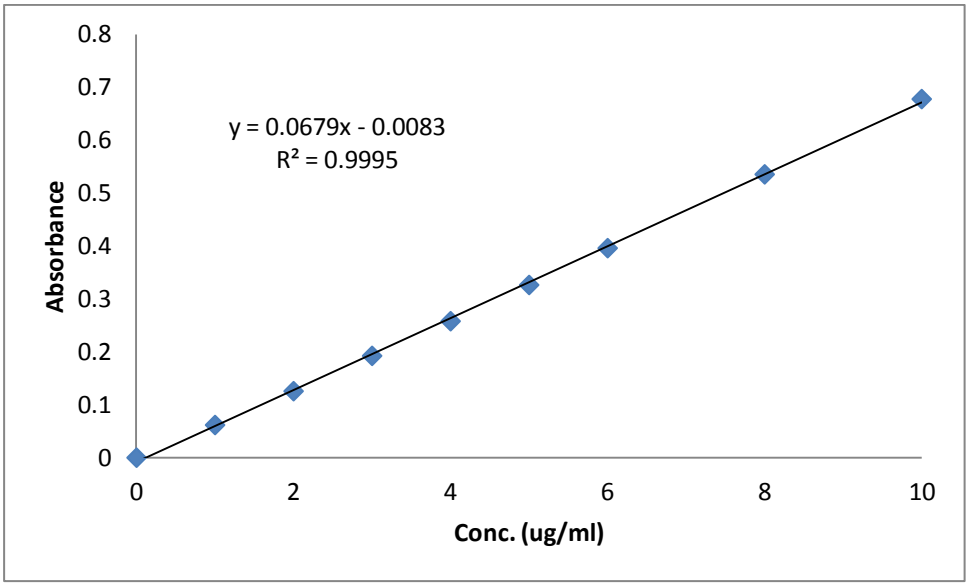

Figure 5.20 Paracetamol calibration curve by UV spectrophotometer at 243nm

5.3.2 Procedure for solid dispersion

Accurately weighed PARA: HP55 mixture in 1:2 ratio was mixed well and passed through an 80 mesh. This mixture was fed to a turbula mixer for 10 mins to ensure homogenous dispersion. This mixture was then fed to S3M3. Material flow was good in the case of PARA dispersion. The end product of 1st and 2nd cycles yielded a small granular mass which was fed to S3M3 for the 3rd cycle. At the end of 3rd cycle the product obtained was molten agglomerated mass. In case of HME for PARA dispersion, TEC was used as a plasticiser in concentration of 10% w/w. The temperature profiles and extrusion parameters were kept as described in section 3.5.2. HME yielded dispersion in the form of a cylindrical extrudates strands at the given extrusion temperature profiles.

5.3.3 Characterisation of the solid dispersion

The end product obtained at the end of 3rd cycle of S3M3 and HME were characterised by various analytical techniques and for drug release.

5.3.3.1 PXRD

PXRD for PARA solid dispersion were carried out as described in Section 3.4.2.

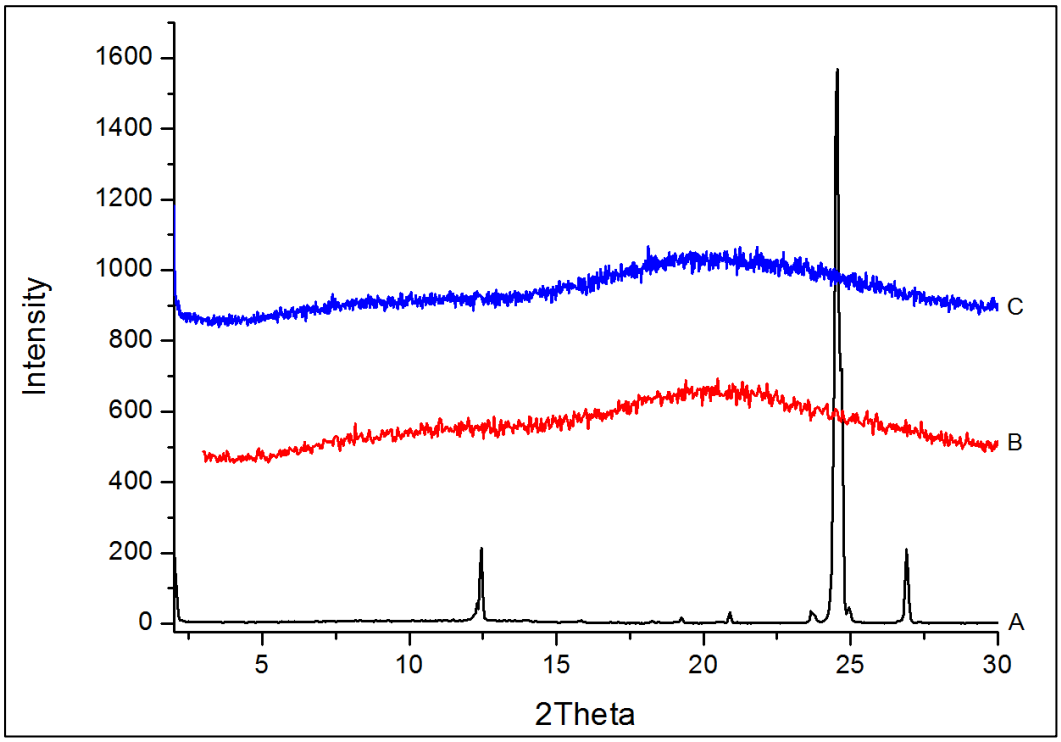

[**A**-Paracetamol, **B**-HME Paracetamol: HP55 1:2, **C**-S3M Paracetamol: HP55 1:2]

Figure 5.21 PXRD for paracetamol solid dispersions processed by HME and S3M

PXRD for PARA showed a sharp characteristic peak at 2θ values with respective intensities (Table 4.1) (Figure 5.21). In the case of PARA solid dispersions all peaks for crystalline PARA were absent. The absence of crystalline peaks in solid dispersions shows that drug particles are completely converted into amorphous form which is further confirmed thermal analysis by DSC.

5.3.3.2 DSC

DSC was carried out as described in Section 3.4.1. The DSC thermograms were analysed for the presence of melting endotherm for PARA.

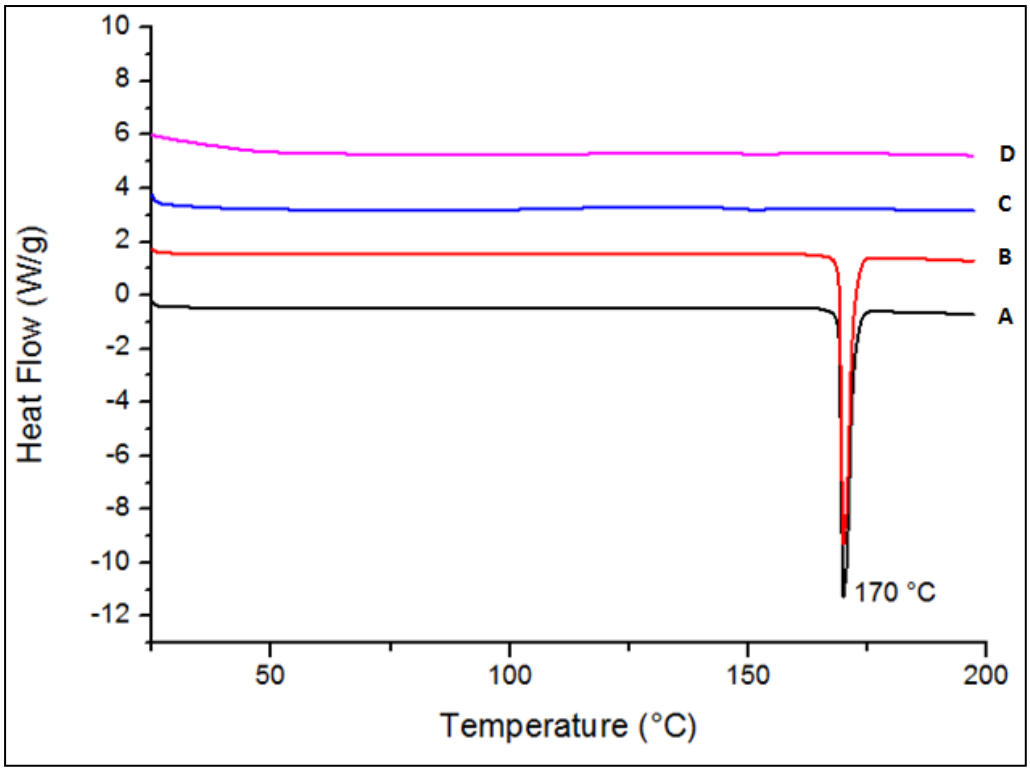

[**A**- Paracetamol, **B**- Paracetamol:HPMCP HP55 physical mixture, **C**- HME Paracetamol:HPMCP HP55 1:2, **D**- S3M Paracetamol:HPMCP HP55 1:2]

Figure 5.22 DSC thermograms of Paracetamol solid dispersions processed by HME and S3M

DSC thermogram for crystalline PARA and physical mixture with HP55 shows a sharp melting endotherm at 170 °C (Figure 5.22). In the case of dispersions processed by HME and S3M there is an absence of crystalline endotherm for PARA. The physical mixture showed similar melting endotherm to PARA which shows that heating of the physical mixture did not yield an amorphous dispersion. The absence of a melting endotherm in solid dispersions shows PARA is completely solubilised in HP55 polymer matrix which made it completely amorphous.

5.3.3.3 SEM

SEM characterisation for various surface features of PARA solid dispersions using procedure as described in Section 3.4.5.

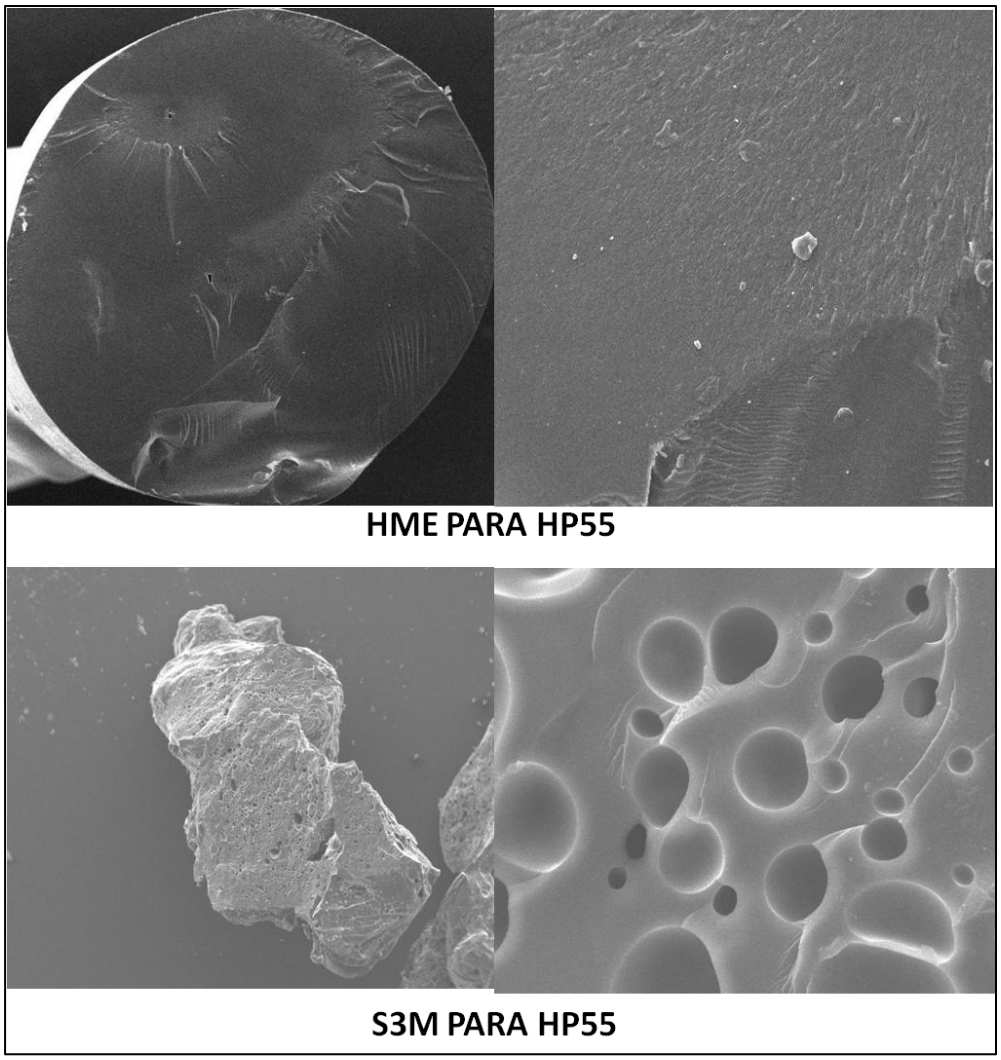

Figure 5.23 Surface morphology by SEM of paracetamol solid dispersions processed by HME and S3M

SEM analysis for HME processed dispersion shows smooth and plain surface features with very low porosity. S3M processed dispersion shows a highly porous surface and surface irregularity (Figure 5.23). Almost all the solid dispersions processed by S3M3 showed distorted and irregular, rough

surface features whereas in the case of HME processed dispersions all the extrudates showed smooth, plain and non-porous surface features.

5.3.3.4 FT-IR

FT-IR characterisations were carried out as described in Section 3.4.3.

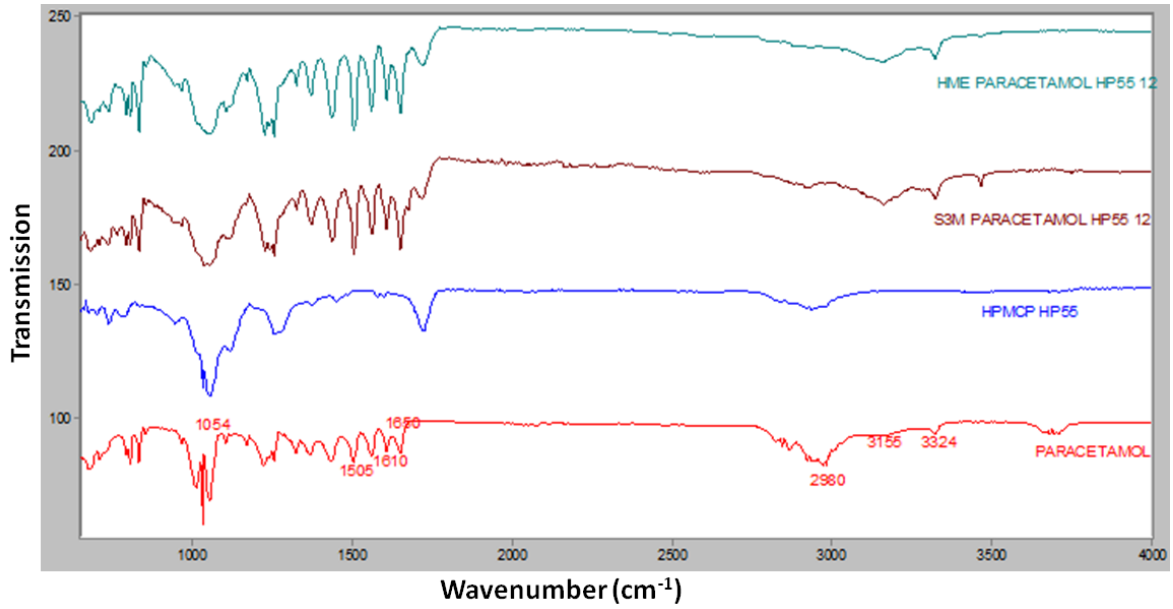

Figure 5.24 FT-IR spectra for paracetamol: HP55 1:2 solid dispersions processed by HME and S3M

In the case of paracetamol amorphous dispersions with HPMCP HP55, Paracetamol showed characteristic -OH stretching at 3324 cm^{-1} and 3155 cm^{-1} out of which 3155 cm^{-1} become prominent in case of dispersions and 3324cm^{-1} showed a similar stretching pattern with no shift in position (Talegaonkar *et al*. 2007) (Figure 5.24).

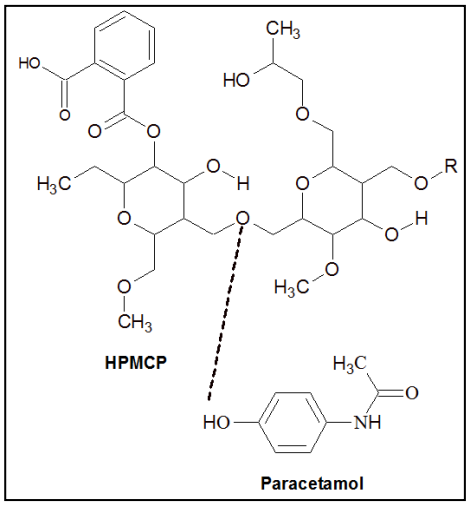

Figure 5.25 Hydrogen bonding between paracetamol and HPMCP HP55

The unsaturated stretching at 1610 cm^{-1}, 1650 cm^{-1} remained similar in dispersion samples. The 1054 cm^{-1} stretching vibration for -C-O-C in HPMCP HP55 showed broaden vibration in case of dispersions. This shows that there is hydrogen bond between –OH of paracetamol and –C-O-C of HPMCP HP55 (Figure 5.25)

5.3.3.5 NIR

NIR analysis was carried out as described in Section 3.4.4. Paracetamol shows high absorption in the second overtone region at wavelengths 1639 and 1670 nm (Figure 5.26).

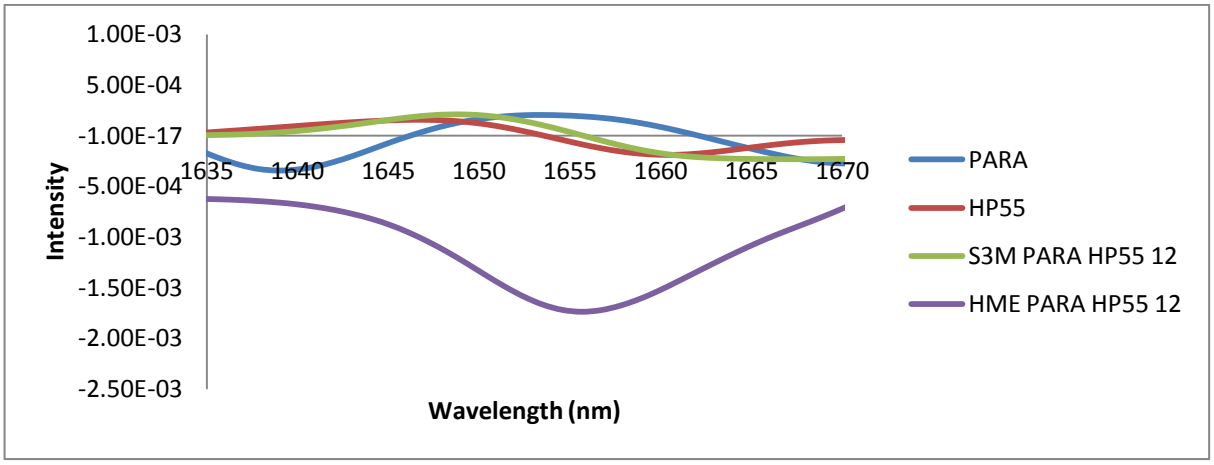

Figure 5.26 NIR spectra for paracetamol solid dispersions processed by HME and S3M

HP55 shows NIR absorption in the second overtone region at 1662 nm. Paracetamol solid dispersion processed by HME show very high NIR absorption at 1639 and 1670 nm whereas in case of S3M processed solid dispersion it shows very low absorptions at 1639 and 1670 nm (Figure 5.26). The change in the intensity and shifts in the absorption for PARA characteristic absorption shows that there is potential hydrogen bond formation between –OH of PARA and –C-O-C of HP55.

5.3.3.6 Dissolution

The content of PARA in solid dispersions processed by HME and S3M3 was assayed by UV spectroscopy. In the case of PARA: HP55 1:2 the assay for HME was 100±1.4% and for S3M was 99.5±2.12%.

Dissolution studies for PARA solid dispersion were carried out as mentioned in Section 3.5.3.1. Drug release pattern over the period of time is shown in Figure 5.27

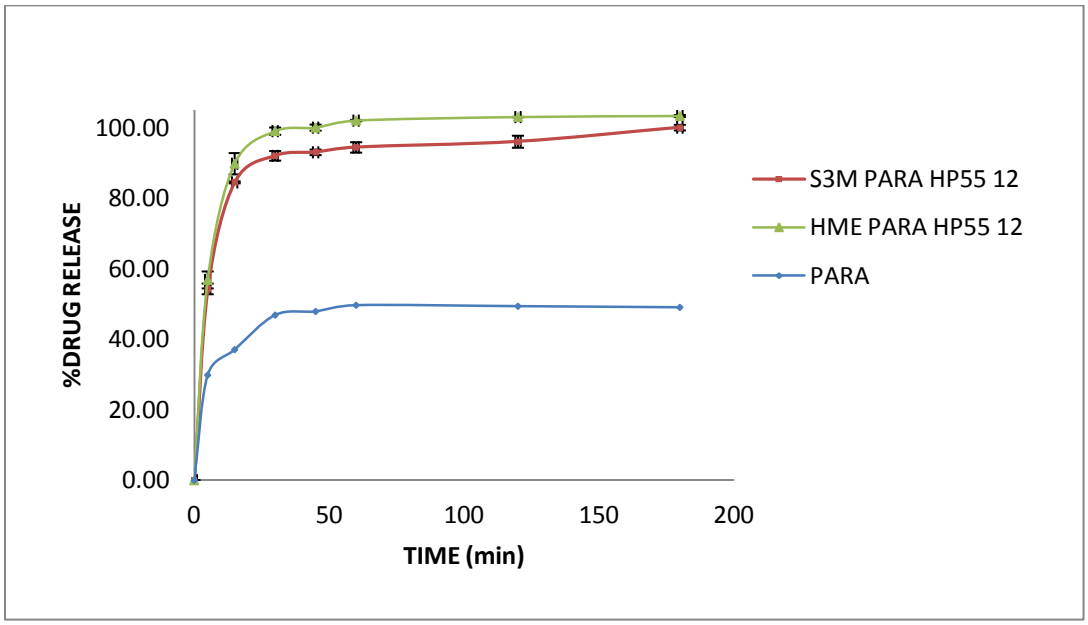

Figure 5.27 Dissolution profile for paracetamol solid dispersions processed by HME and S3M

Dissolution studies for PARA solid dispersion showed slightly faster release in case of HME processed dispersions compared to S3M. There was not much difference in drug release over the time points. Within one hour 90% of drug was released, HME processed solid dispersions showed 100% drug release after one hour whereas in case of S3M3 processed it took 3 hours to release 100% drug.

Statistical analysis in case of PARA: HP55 1:2 was done using a t-test. P value was calculated using the t test to analyse the statistical difference between two processes. The p value from t test was found to be 0.019 which is less than 0.5 which signifies there is statistical difference between the two processes with regards to drug release at given time point.

5.3.3.6 Degradation analysis

PARA yields 4-amino phenol as degradation product when heated or extruded to higher temperatures (Bhimavarapu *et al*. 2011).

5.3.3.6.1 4-amino phenol calibration

The calibration curve for 4-amino phenol was linear over the concentration range of 20-160 ug/ml. The linearity equation was calculated using calibration curve, slope of the equation is 5656.8, constant 53496 and R^2 0.9872 (Figure 5.28). The calibration equation was used to calculate the amount of 4-amino phenol generated.

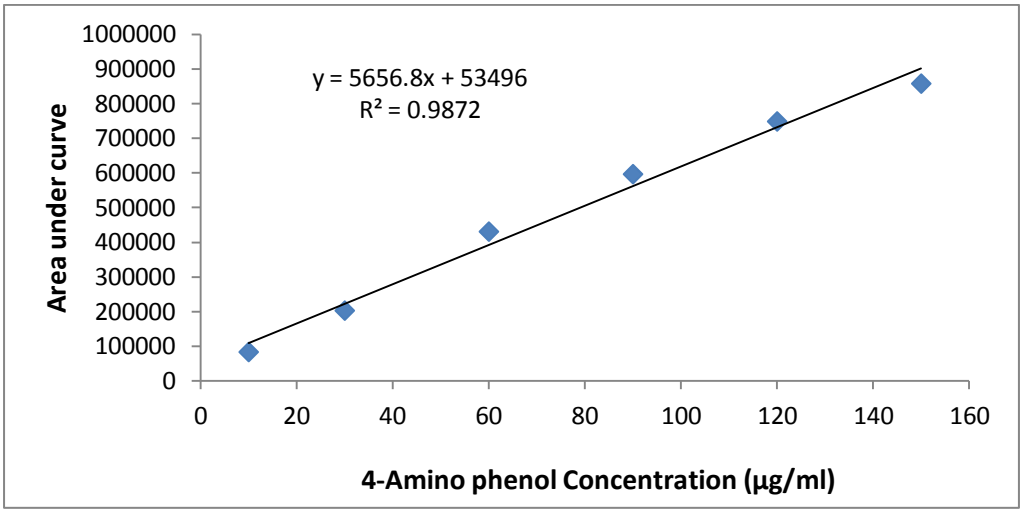

Figure 5.28 Calibration curve for 4-amino phenol by UV spectrophotometer at 227nm

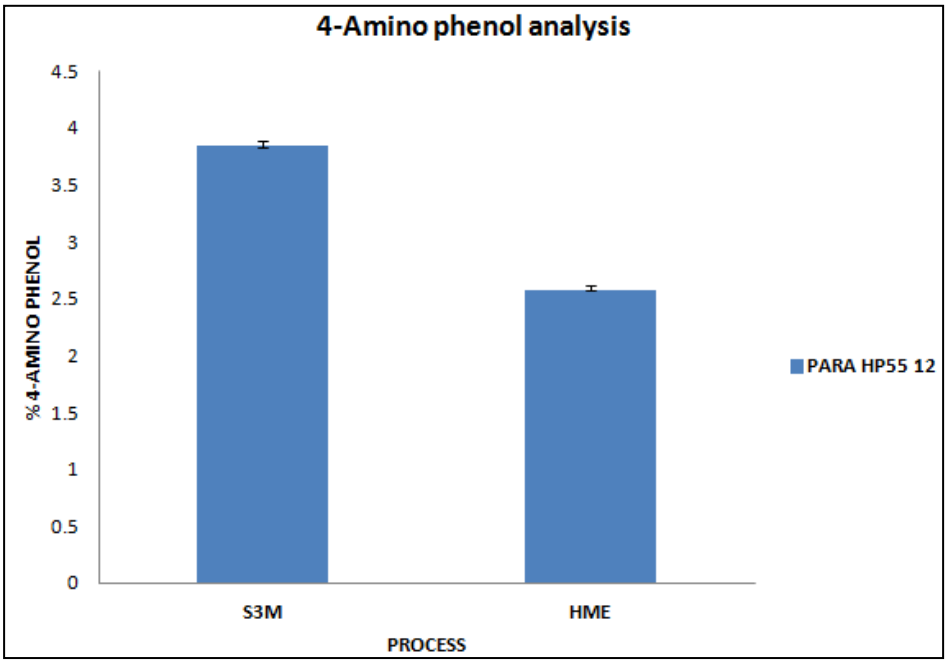

Figure 5.29 4-Amino phenol analysis in paracetamol: HP55 1:2 solid dispersions processed by HME and S3M

The amount of 4-amino phenol generated in S3M3 was higher compared to HME (Figure 5.29). The reason for the higher degradation can be attributed to the uncontrolled rise in temperature during S3M processing as it does not have any opportunity to control temperature, it can also attributed to extremely high shear.

5.4 Carbamazepine

5.4.1 Calibration curve for carbamazepine

The calibration curve for CBZ was linear over the concentration range of 1-10 ug/ml. The linearity equation was calculated using calibration curve, slope of the equation is 0.0506, constant 0.0016 and R^2 0.9996 (Figure 5.30). The calibration equation due to good linear range was used for the calculation of drug release.

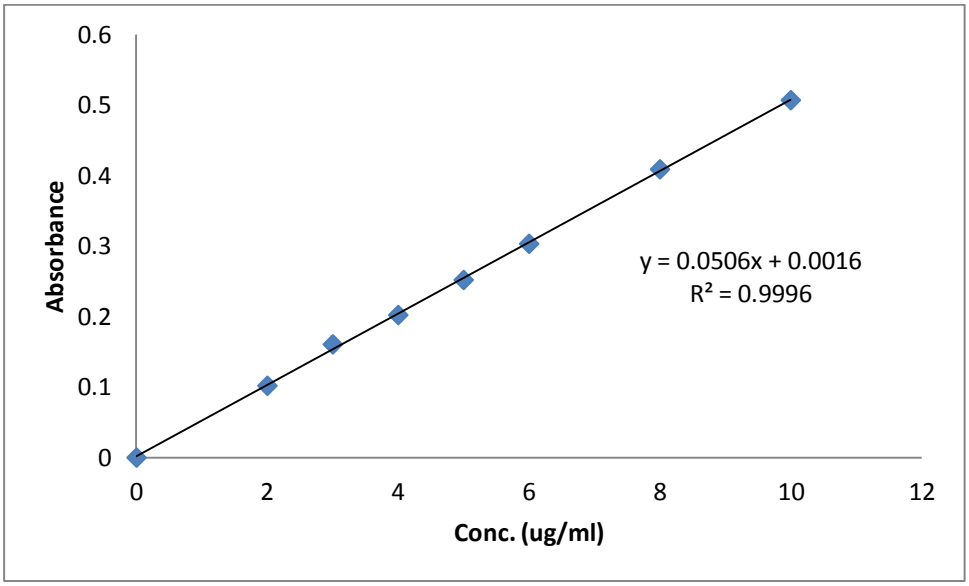

Figure 5.30 Carbamazepine UV spectrophotometry calibration curve at 288nm

5.4.2 Procedure for solid dispersion

CBZ with different polymers were explored to form solid dispersion in this study. As described in section 3.5.1 CBZ solid dispersions were attempted with all four selected polymers i.e. PVP VA64, HPMCP HP55, HPMCAS and ethyl cellulose. In the case of HPMCP HP55 and PVP VA64 two different

ratios were attempted for solid dispersions which are 1:1 and 1:2. All other CBZ dispersions were carried out in 1:2 CBZ: polymer ratio. All the drug: polymer blends obtained after mixing in a turbula mixer showed good flow in the S3M3 process. The formation of agglomerated mass was observed at the end of the 3rd cycle during S3M3 process. In the case of CBZ:HP55 1:1 and 1:2 batches there was formation yellow coloured mass with a distinctive smell at the end of the 3rd cycle. Similar products were obtained in case of CBZ: HPMCAS solid dispersion. In the case of PVP VA64 and ethyl cellulose products were in the form of a white coloured molten agglomerated mass. In the case of HME different temperature profiles and extrusion parameters were used as described in Section 3.5.2.

5.4.3 Characterisation of solid dispersion

All the CBZ solid dispersions obtained in S3M3 and HME processing were subjected to various characterisation techniques described as follows.

5.4.3.1 PXRD

Powder X-ray characterisation for both HME and S3M processed solid dispersion showed no crystalline peak for CBZ as shown in the figure below. Powder X ray diffraction for plain polymer samples did not show any crystalline peaks. The powder X-ray diffraction pattern for pure CBZ showed characteristic high intensity peaks at 2θ values of 13.2, 14.28, 15.44, 15.96, 17.24, 18.8, 19.6, 20.48, 23.52, 24.24, 25.08 and 26.84º which matched the powder diffraction pattern reported for CBZ (Figure 5.31). All the solid dispersions showed the absence of the characteristic peaks for CBZ which confirms all solid dispersions were in a completely amorphous state which

can be again confirmed by DSC thermograms. Except for one solid dispersion, 50% drug loaded CBZ: PVP VA64 1:1 which showed a reduced intensity peak for CBZ at the same 2θ in case of both processes. This finding was contradictory when compared to DSC thermogram of 50% drug loaded CBZ: PVP VA64 1:1 batch as the DSC did not show a presence of endotherm for crystalline CBZ.

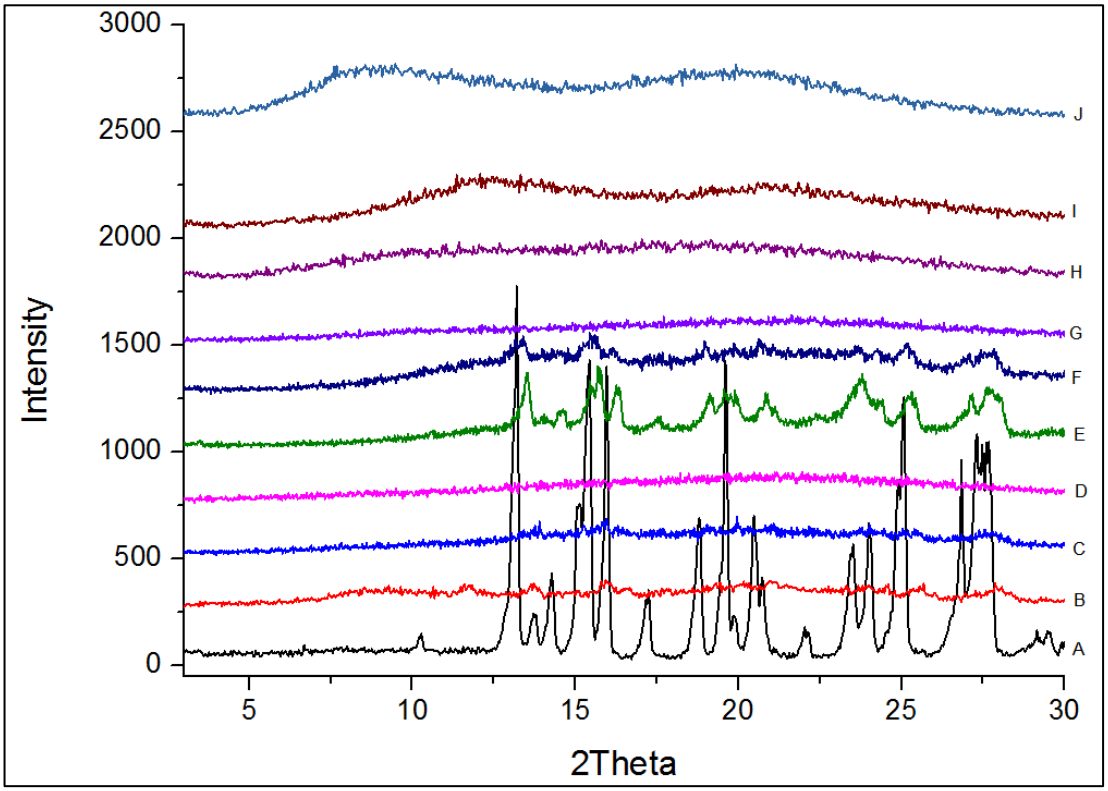

[**A**-Carbamazepine, B-Ethyl cellulose, **C**-HPMCP HP55, **D**-PVP VA64, **E**-HME carbamazepine:VA64 1:1, **F**-HME carbamazepine: HP55 1:1, **G**-HME carbamazepine:HP55 1:2, **H**-HME carbamazepine:HPMCAS 1:2 , **I**- HME carbamazepine:Ethyl Cellulose 1:2, **J**-HME Carbamazepine:VA64 1:2]

Figure 5.31 PXRD for carbamazepine solid dispersions processed by HME

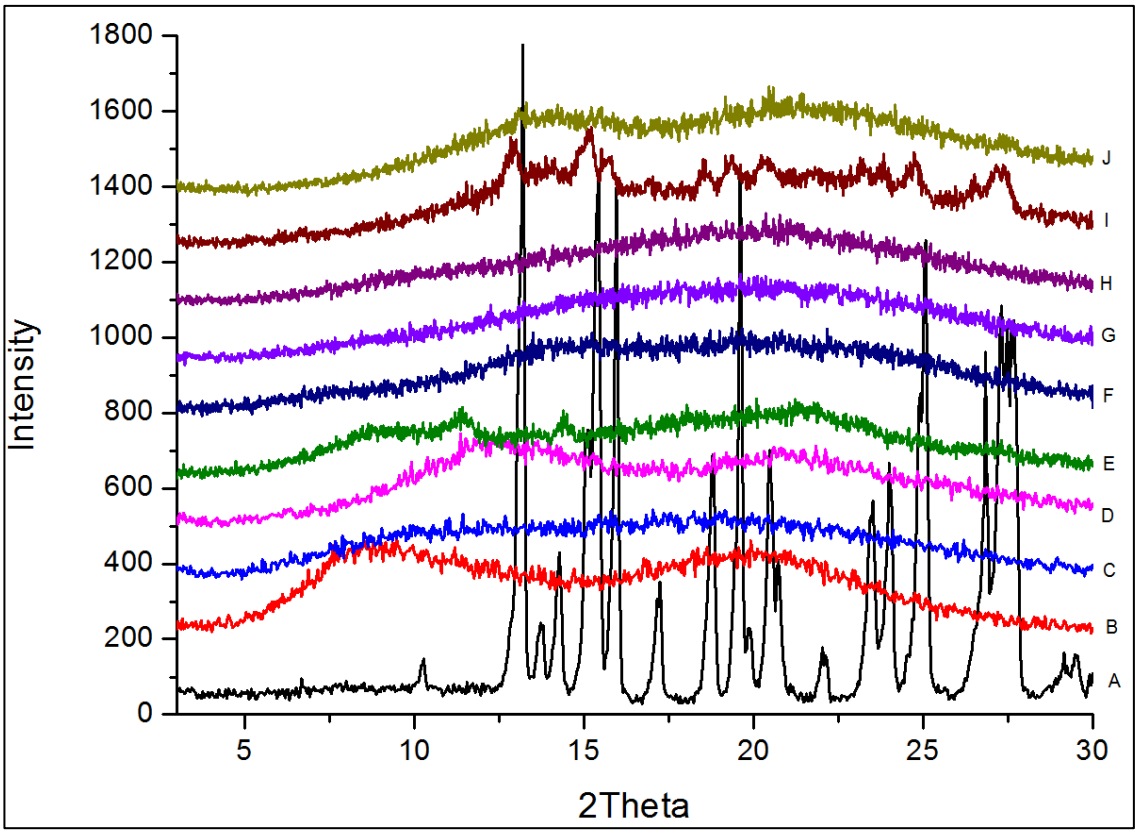

[**A**-Carbamazepine, B-Ethyl cellulose, **C**-HPMCP HP55, **D**-PVP VA64, **E**-S3M carbamazepine:Ethyl Cellulose 1:2,**F**-S3M carbamazepine: HP55 1:1, **G**-S3M carbamazepine:HP55 1:2, **H**-S3M carbamazepine:HPMCAS 1:2 , **I**-S3M carbamazepine:VA64 1:1, **J**-S3M Carbamazepine:VA64 1:2]

Figure 5.32 PXRD for carbamazepine solid dispersions processed by S3M

5.4.3.2 DSC

All samples for solid dispersions and pure drug molecules were subjected to DSC analysis. The presence or absence of the characteristic melting endotherm for the API gives an idea whether the drug is completely dissolved or dispersed in the polymer matrix. Crystalline CBZ shows two melting endotherms, at 175 ºC and at 191 ºC due to the polymorphic change. It is considered to relate to the polymorphic transformation of CBZ from form III to CBZ form I. The physical mixture shows a small endotherm at 170º C and there is absence of another endotherm which shows that the molten

polymer has dissolved the crystalline CBZ with the absence of the polymorphic transformation into CBZ form I (Figure 5.33). All the melt extruded amorphous dispersions showed an absence of either of the peaks for CBZ forms, which clearly shows that the drug has completely dissolved into the polymer matrix or converted into a polymer matrix of HPMCP HP55 and HPMCAS polymer in both the concentrations 33% and 50% of CBZ. The high shear and temperature encountered during melt extrusion helped the solubilisation of CBZ into the respective polymer matrices of HPMCP HP55 and HPMCAS. In the case of S3M processed CBZ dispersions a similar trend was observed, despite the fact that in S3M only shear caused a rise in temperature as there is no external heating or cooling available or applied during S3M. All the S3M processed CBZ dispersions were amorphous in nature as shown in Figure 5.34.

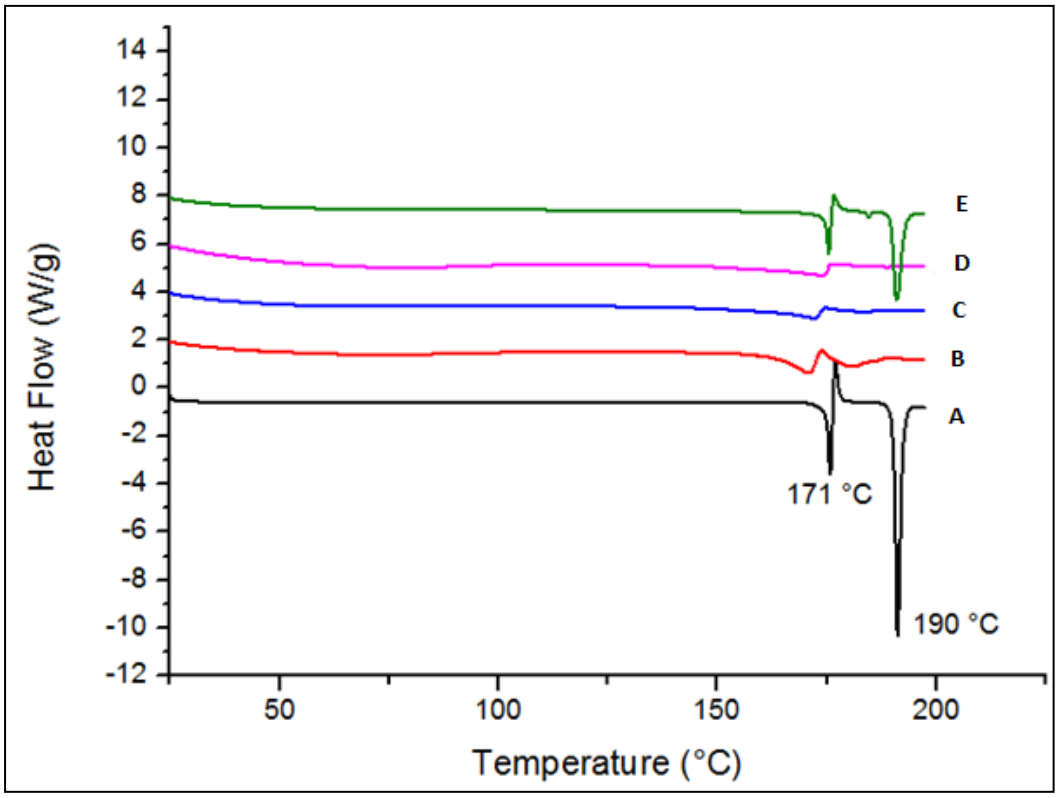

[**A**- Carbamazepine, **B**- Carbamazepine: HP55 physical mixture, **C**- Carbamazepine:HPMCAS physical mixture, **D**- Carbamazepine:PVP VA64 physical mixture, **E**- Carbamazepine:Ethyl cellulose physical mixture]

Figure 5.33 DSC thermograms for physical mixtures of carbamazepine and selected polymers to be processed by HME and S3M

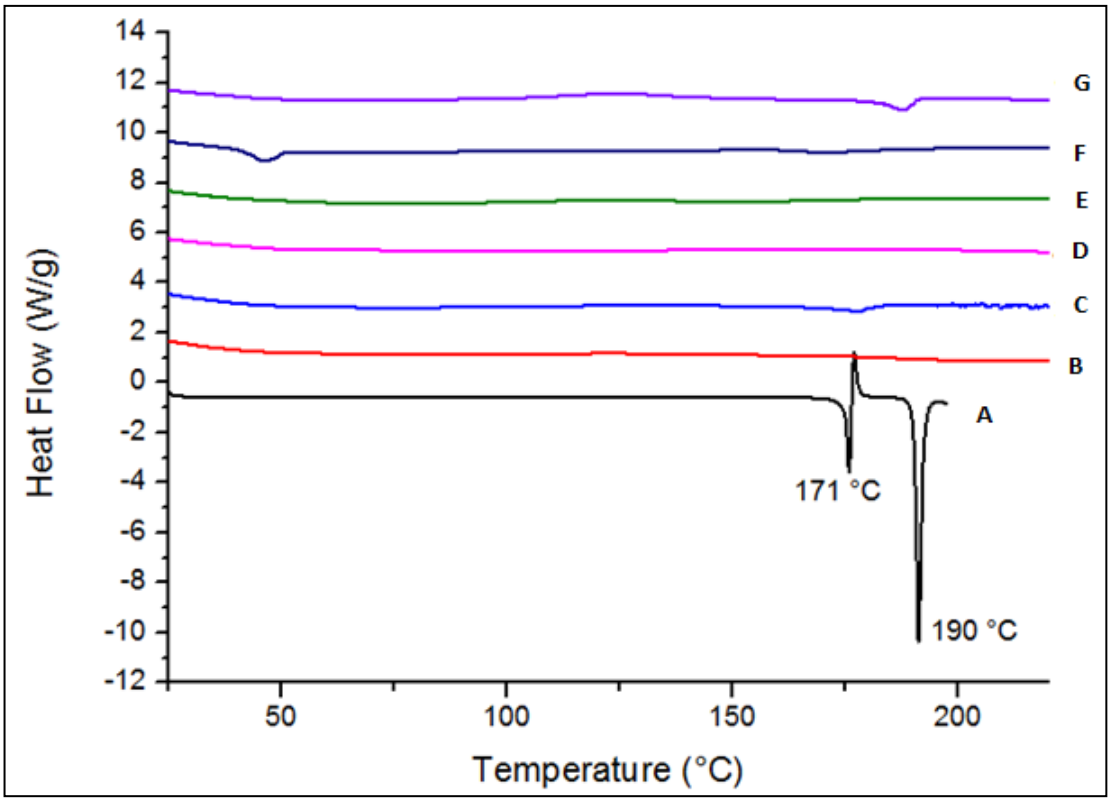

[**A**- Carbamazepine, **B**- HME carbamzepine:HP55 1:2, **C**- HME carbamazepine:HP55 1:1, **D**- HME carbamazepine:HPMCAS 1:2, **E**- HME carbamazepine:VA64 1:2, **F**- HME CBZ VA64 11, **G**- HME CBZ Ethyl cellulose 1:2]

Figure 5.34 DSC thermograms for carbamazepine solid dispersions processed by HME

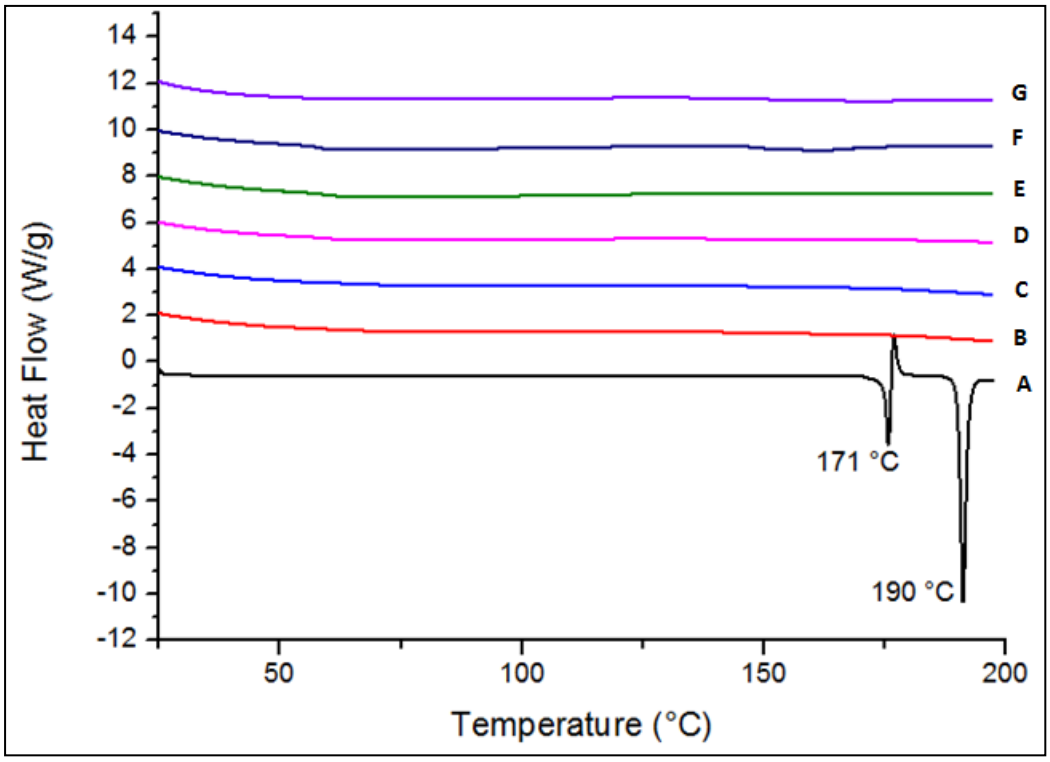

[**A**- Carbamazepine, **B**- S3M carbamzepine:HP55 1:2, **C**- S3M carbamazepine:HP55 1:1, **D**- S3M carbamazepine:HPMCAS 1:2, **E**- S3M carbamazepine:VA64 1:2, **F**- S3M CBZ VA64 11, **G**- S3M CBZ Ethyl cellulose 1:2]

Figure 5.35 DSC thermograms for carbamazepine solid dispersions processed by S3M

In the case of CBZ dispersions with PVP VA64 and ethyl cellulose both the dispersions processed by HME and S3M showed absence of both the endotherm in thermogram (Figure 5.34 and Figure 5.35).

The processing temperature in hot melt extrusion needed to be modified according to the softening point of the respective polymer for PVP VA64 and ethyl cellulose. To achieve melt temperature profile for PVP VA64 at 110 ºC and for ethyl cellulose at 140 ºC required addition of plasticisers using PEG 2000 and TEC respectively. Processing at these temperatures made the drug miscible in the polymer matrix and was not dispersed which can be

confirmed from absence of crystalline endotherm in the solid dispersion processed by both techniques.

5.4.3.3 SEM

SEM anaylysis for various CBZ solid dispersions showed various morphological features.

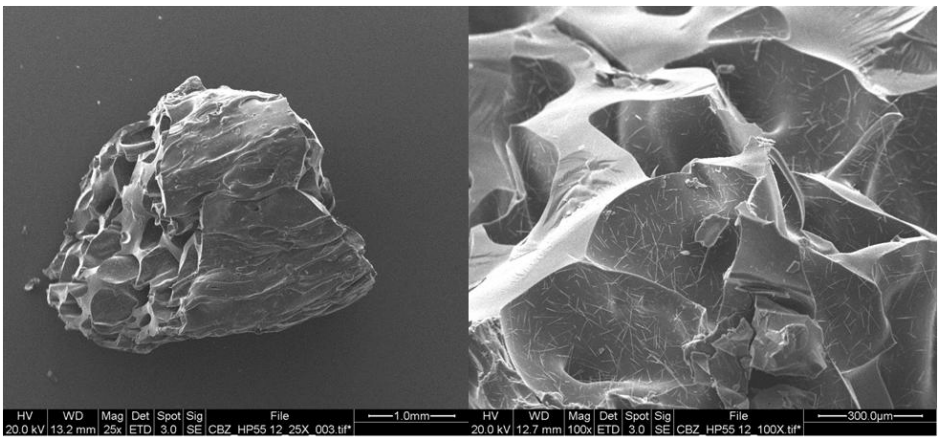

Figure 5.36 Surface morphology by SEM of carbamazepine solid dispersions processed by HME and S3M

SEM analysis for CBZ solid dispersion with HP55 showed distorted surface features in the case of HME processed samples whereas S3M processed dispersion showed a very irregular surface feature with a porous structure (Figure 5.36).

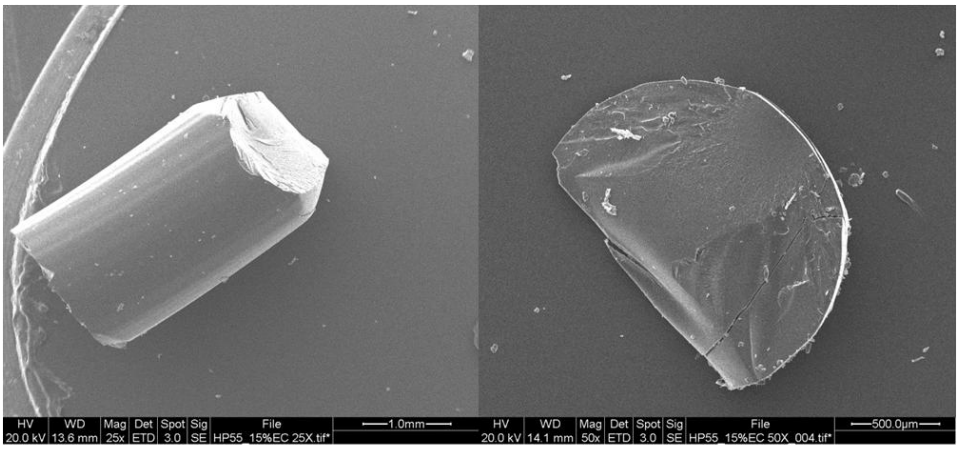

HME CBZ VA64

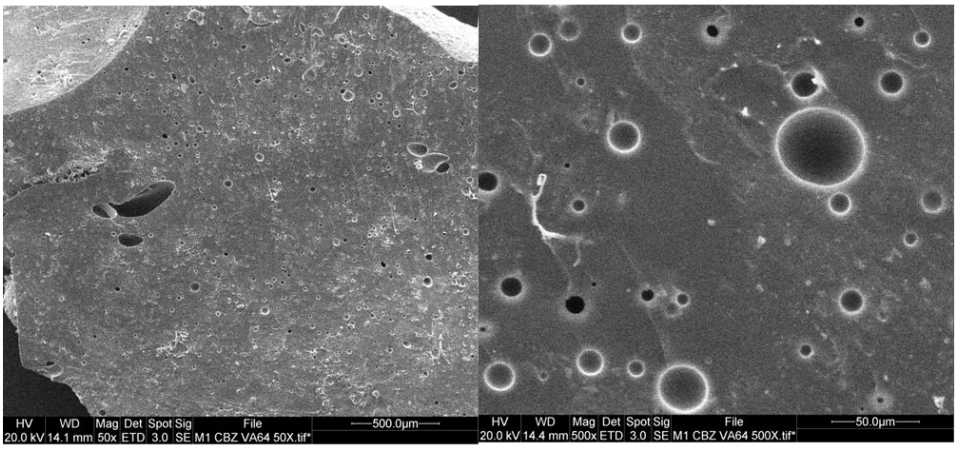

S3M CBZ VA64

Figure 5.37 Surface morphology by SEM of carbamazepine solid dispersions with PVP VA64 processed by HME and S3M

SEM analysis of CBZ dispersions with VA64 showed smooth and plain surface features in the case of HME processed samples with very low surface porosity whereas in the case of S3M processed dispersions the surface shows high porosity and surface roughness (Figure 5.37).

5.4.3.4 FT-IR

FT-IR analysis for carbamazepine solid dispersions were done as described in Section 3.4.3. S3M processed CBZ and PVP VA64 solid dispersion samples are shown in figure below. CBZ shows characteristic stretching for -NH at 3462 cm^{-1} with sharp peak and shows spectra for -NH asymmetrical

stretching at 3159 cm^{-1} which are reduced in the solid dispersion samples in case of 33% drug loading and 50% drug loading. CBZ stretching at 1382 cm^{-1} typically shows -C-NH_2 vibrations which are broadened in the case of solid dispersion samples (Figure 5.38 and Figure 5.40). Spectra broadening or shifting can be considered as bonding between respective functional groups of drug and polymer. The PVP VA64 spectra showed typical stretching at 1728 cm^{-1} and 1672 cm^{-1} for carbonyl bonds. 1672 cm^{-1} stretching shows reduced intensity in the case of solid dispersion samples which can be owed to hydrogen bonding present in CBZ and PVP VA64 (Patterson *et al*. 2008).

In the case of HME processed solid dispersion batches all the spectra showed similar behaviour to the S3M processed dispersions (Figure 5.41). The characteristic -H bond stretching near 3000 cm^{-1} spectrum was broadened in the case of solid dispersion batches as compared to pure polymer which suggested the presence of hydrogen bonding between CBZ and PVP VA64.

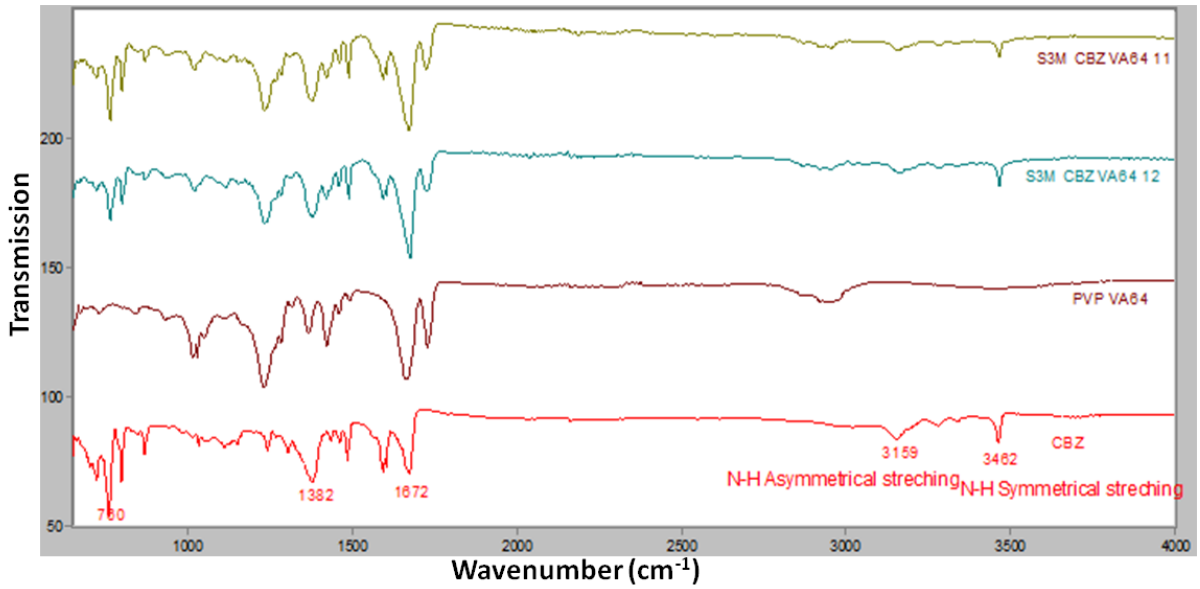

Figure 5.38 FT-IR spectra for carbamazepine:PVP VA64 solid dispersions processed by S3M.

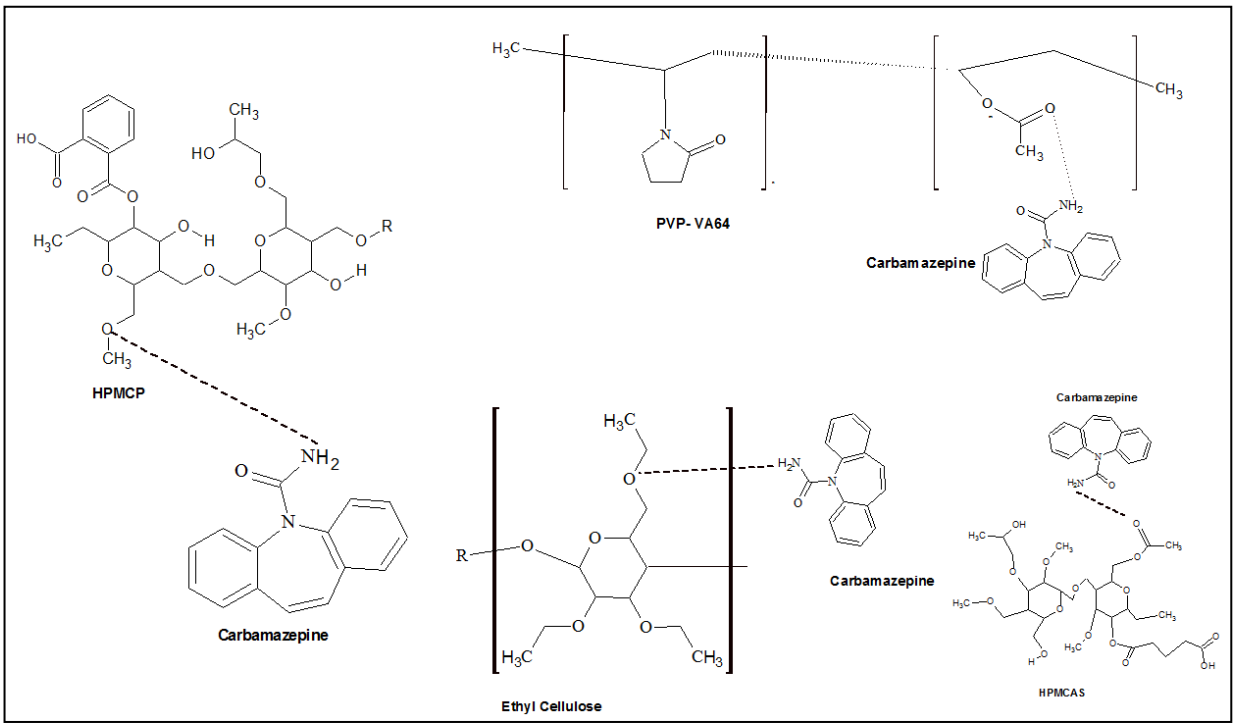

Figure 5.39 Hydrogen bond formation between carbamazepine and respective functional groups of polymers PVP VA64, HPMCP HP55, HPMCAS and ethyl cellulose

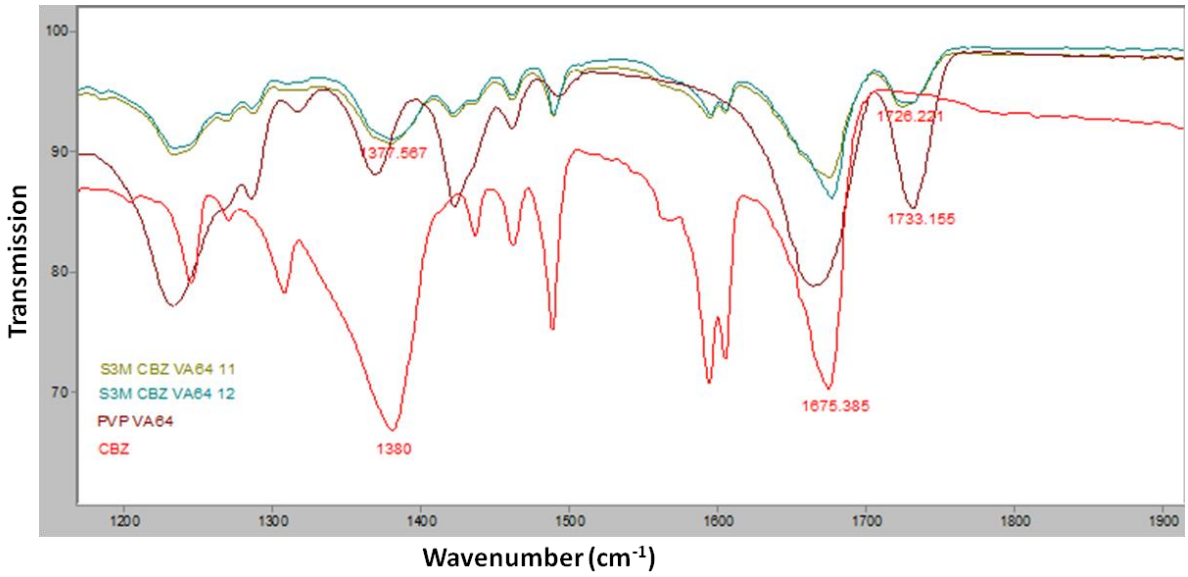

Figure 5.40 FT-IR modified spectra for carbamazepine: PVP VA64 solid dispersions processed by S3M

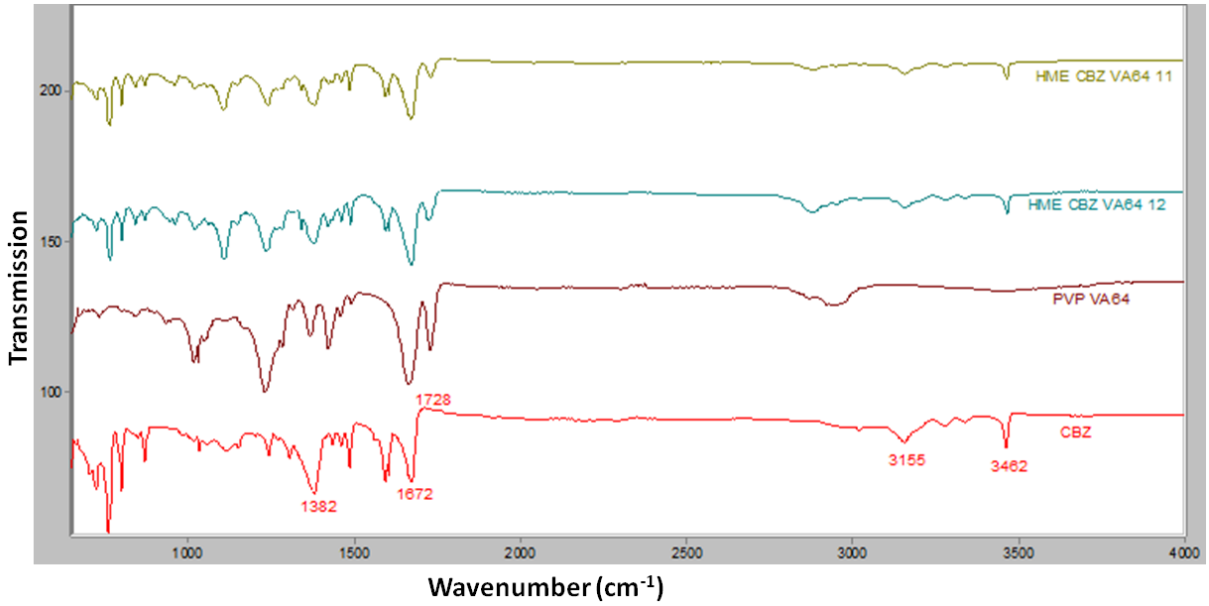

Figure 5.41 FT-IR spectra for carbamazepine:VA64 solid dispersions processed by HME

In the case of HPMCP HP55 solid dispersion samples with both S3M and HME samples, the characteristic stretching at 1054cm^{-1} shows -C-O-C vibrations which shows broadening in solid dispersion spectra. In particular broadening in HME processed dispersions was more significant as

compared to S3M processed which can be due to the possible hydrogen bonding between HPMC and CBZ (Douroumis *et al*. 2007). Characteristic stretching at 1731cm^{-1} in pure HPMCAS and HPMCP HP55 spectra shows reduced intensity in the case of all the dispersions (Figure 5.42 and Figure 5.43).

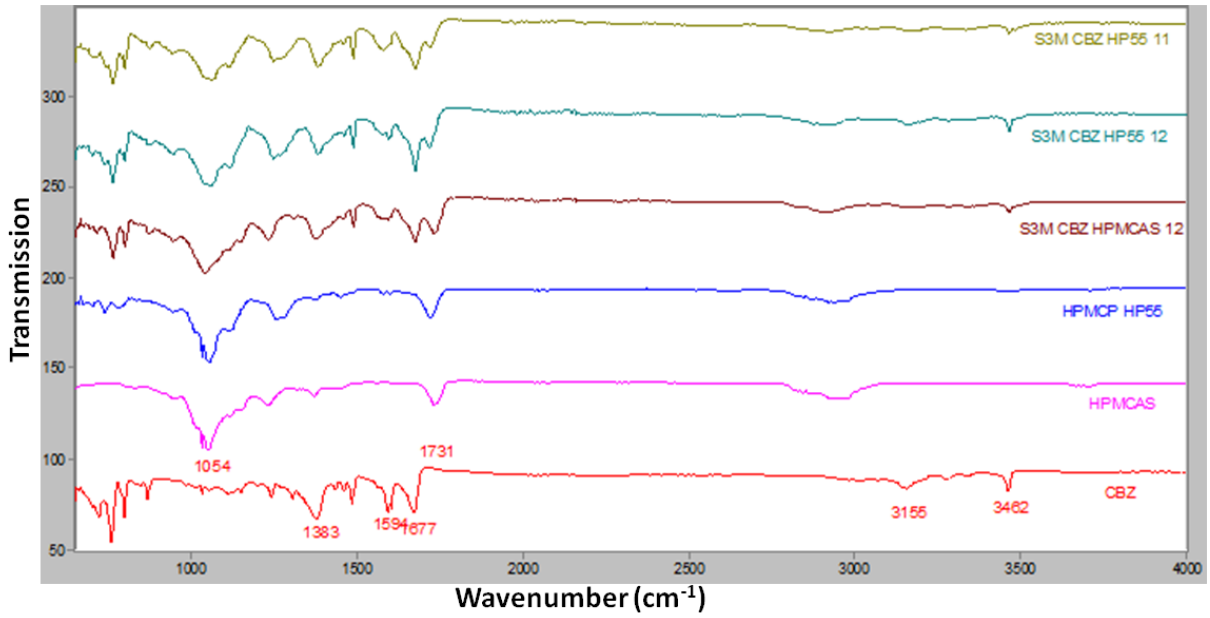

Figure 5.42 FT-IR spectra for carbamazepine solid dispersions with HPMCAS and HPMCP HP55 processed by S3M

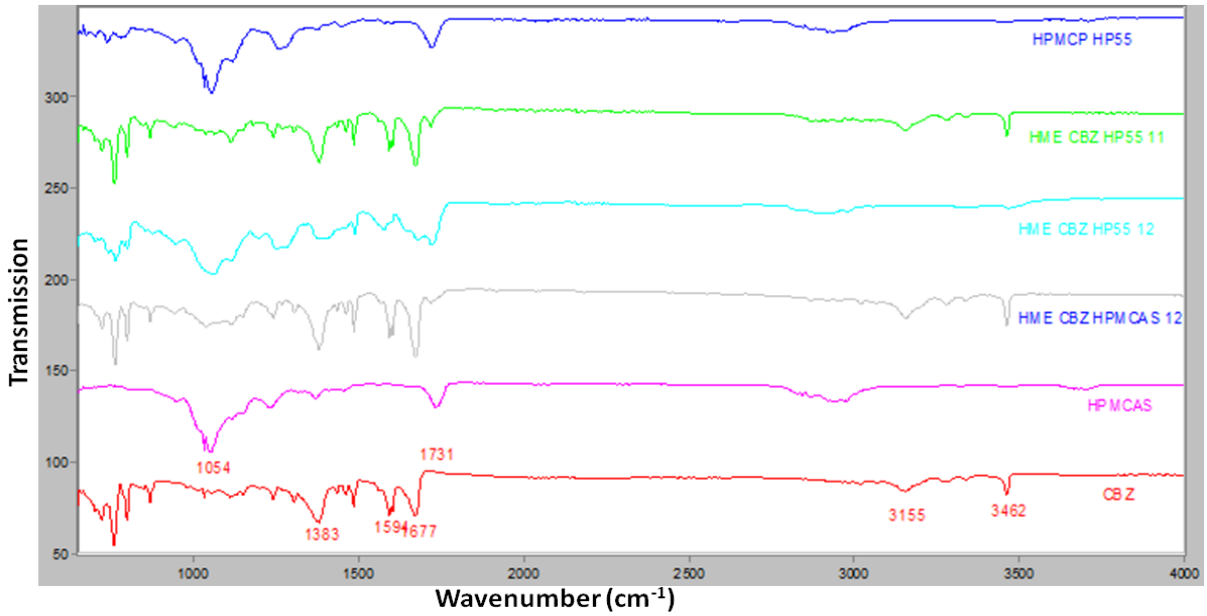

Figure 5.43 FT-IR spectra for carbamazepine solid dispersions with HPMCAS and HP55 processed by HME

In the case of CBZ:EC 1:2 solid dispersion batches, EC shows a characteristic stretching at 1050cm^{-1} due to -C-O-C vibration stretch in cyclic ether which remained the same or slightly broadened in the case of amorphous dispersion in both processes (Figure 5.44). The asymmetric stretching vibrations at 2980cm^{-1} and 2865cm^{-1} showed similar spectra for both types of dispersions. The characteristic spectra in CBZ at 3462cm^{-1} for -NH stretching showed a reduced intensity which might be due to molecular level interaction between CBZ and EC.

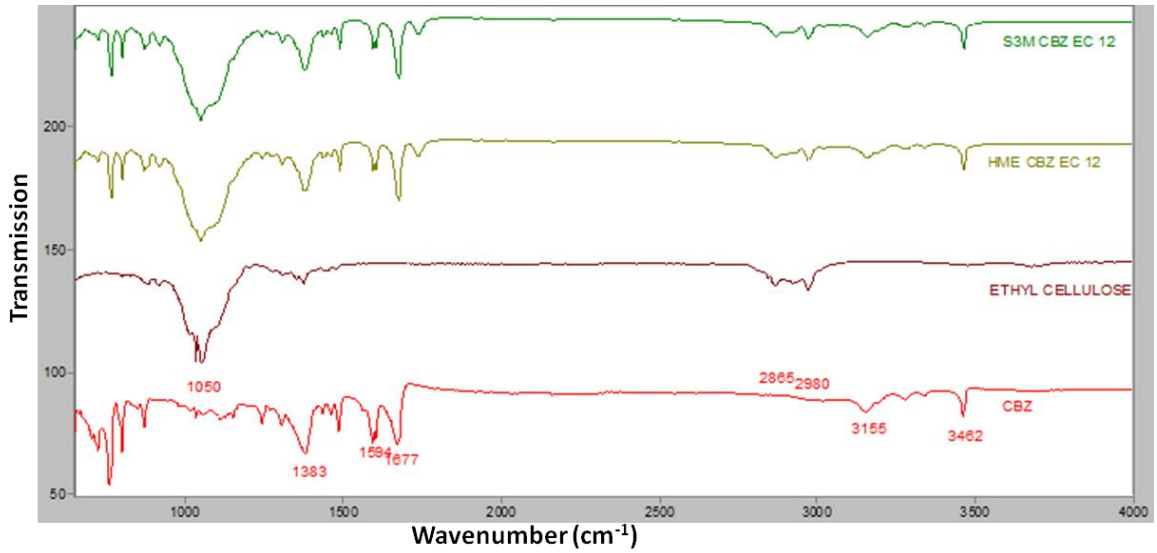

Figure 5.44 FT-IR spectra for carbamazepine: Ethyl cellulose solid dispersions processed by HME and S3M

5.4.3.5 NIR

NIR spectra for CBZ show characteristic absorbance in the second overtone region at a wavelength 1468 nm (Figure 5.45).

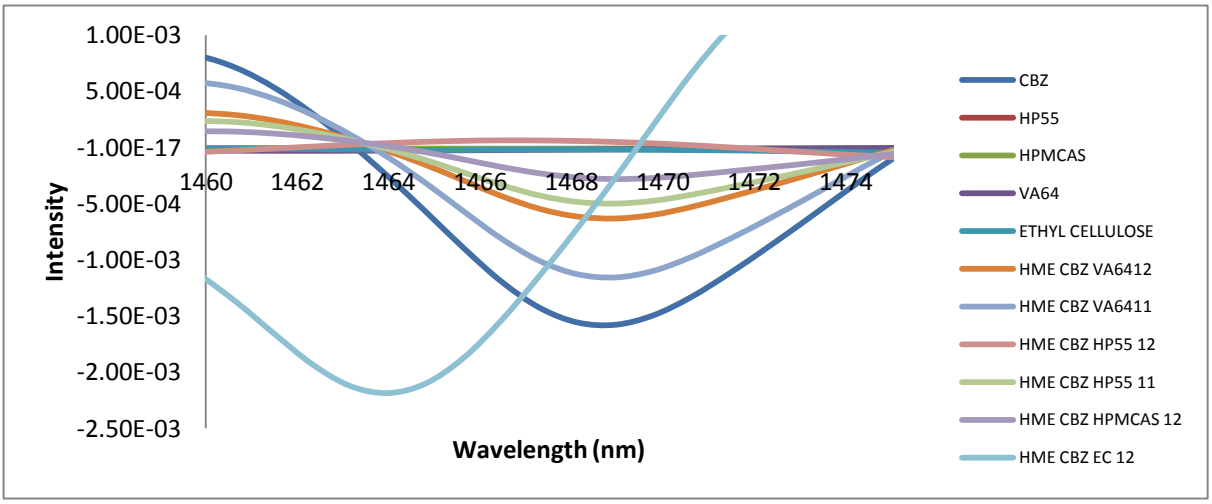

Figure 5.45 NIR spectra for carbamazepine solid dispersions processed by HME

CBZ solid dispersions processed by HME showed similar absorption at 1468 nm in the order of highest absorption for CBZ: VA64 1:1 solid dispersion and the lowest for CBZ: HPMCAS 1:2 solid dispersions. In the case of CBZ: Ethyl cellulose 1:2 the absorption showed a peak shift to 1464 nm. The reduced intensities owing to the solid dispersion of CBZ with different polymers can be due to change in the intensity and nature of hydrogen bonding present in CBZ and respective polymer, which needs to be confirmed by FT-IR analysis.

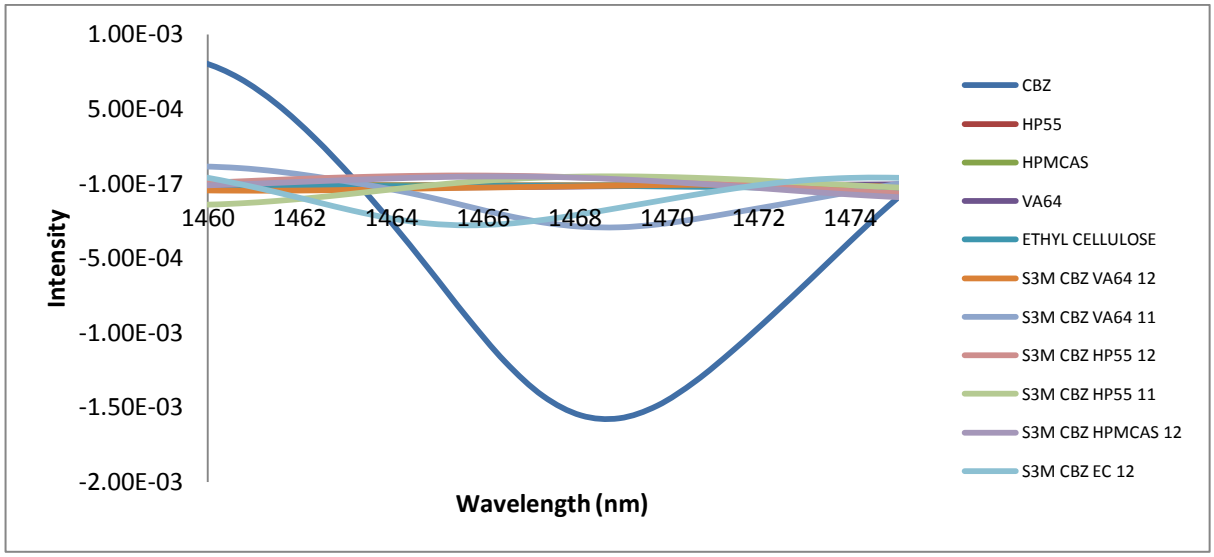

Figure 5.46 NIR spectra for carbamazepine solid dispersions processed by S3M

In the case of NIR absorption spectra for S3M processed CBZ solid dispersions, the spectra were similar but with reduced intensity absorption at wavelength 1468 nm in case of CBZ: VA64 1:1 only whereas there was a shift in peak absorption at 1459 nm in the case of solid dispersions CBZ: HP55 1:1, at 1521 nm for CBZ: HP55 1:2 and CBZ: HPMCAS 1:2 and at 1466 nm for CBZ: Ethyl cellulose 1:2 (Figure 5.46). The shifts in NIR spectra explain that there is formation of hydrogen bonds between –NH of CBZ and respective functional groups of the polymers.

5.4.3.6 Dissolution

Assay: The content of CBZ in both solid dispersions processed by HME and S3M3 was assayed by UV spectroscopy. The assay values are shown in Table 5.1

Table 5.1 Assay values for carbamazepine solid dispersions

Solid dispersion	HME assay	S3M assay
CBZ:HP55 1:1	99±1.4%	99.5±2.12%

CBZ:HP55 1:2	100±2.8%	99±2.8%
CBZ:VA64 1:1	98.5±2.1%	99±0.7%
CBZ:VA64 1:2	99.5±0.7%	101±2.8%
CBZ:HPMCAS 1:2	98.5±0.7%	100±1.4%
CBZ:EC 1:2	99.5±2.1%	97.5±2.12%

All CBZ solid dispersion dissolutions were carried out as detailed in Section 3.5.3.1.

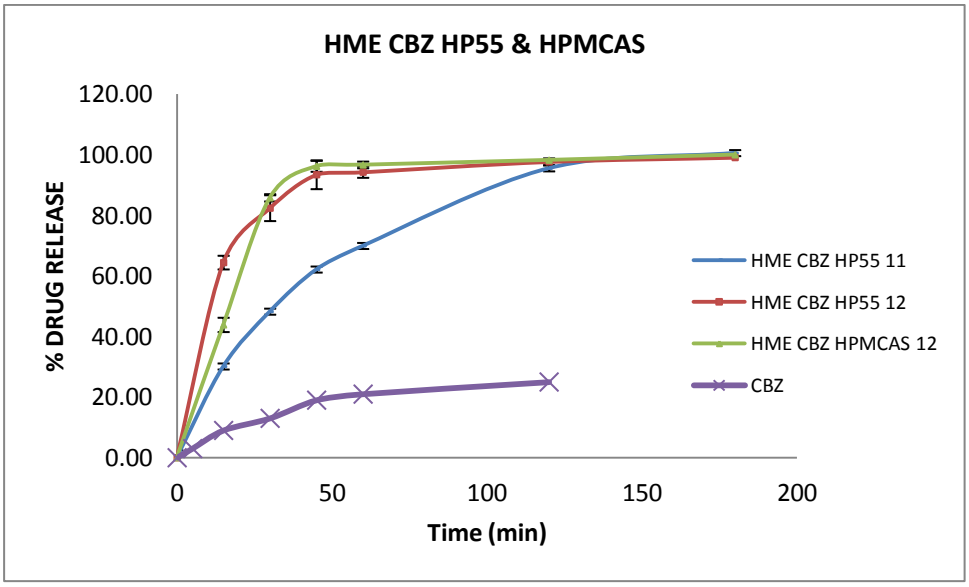

Figure 5.47 Dissolution profiles for carbamazepine solid dispersions with HPMCAS and HP55 processed by HME

HME processed CBZ dispersions with HP55 (1:2) and HPMCAS show 100% drug release within two hours whereas HP55 (1:1) showed slightly slow release (Figure 5.47).

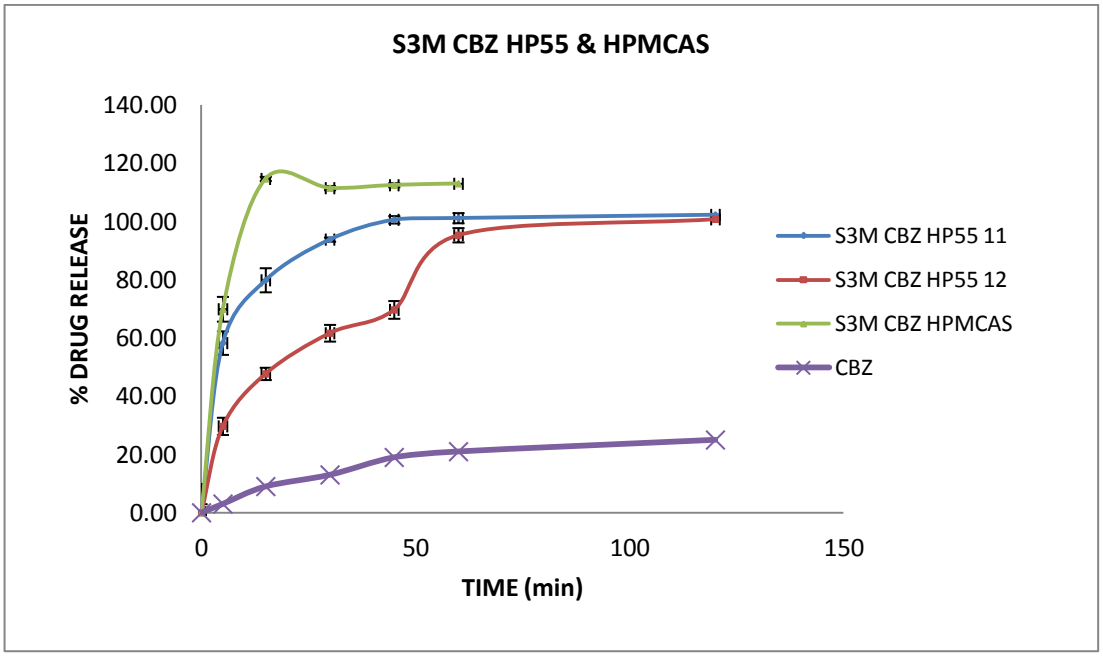

Figure 5.48 Dissolution profiles for carbamazepine solid dispersions with HPMCAS and HP55 processed by S3M

Dissolution studies for S3M processed solid dispersions with HPMCAS showed faster and complete drug release within one hour, whereas 33% drug loaded HP55 dispersion showed slower but complete release after two hours (Figure 5.48). In the case of 50% drug loaded HP55 dispersion, complete drug release occurred after one hour.

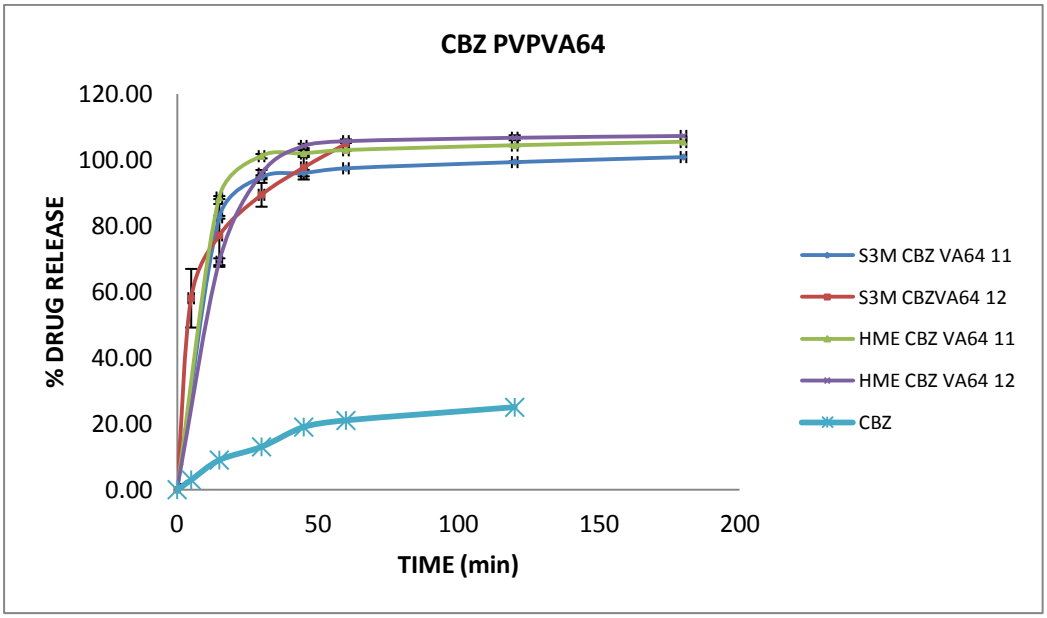

Figure 5.49 Dissolution profiles for carbamazepine solid dispersions with PVP VA64 processed by HME and S3M

Dissolution profiles for CBZ dispersions with VA64 in both cases and both drug loading ratios showed complete drug release after one hour (Figure 5.49). Statistical analysis and variance was calculated at a given point in the dissolution by a t test and p value was calculated to analyse the variance between two processes. The T test was applied to the drug release at 30 mins and the p value was found to be 0.421 which shows that drug release by two processes at the given point have good correlation and are statistically similar.

Dissolution profiles for CBZ solid dispersion with ethyl cellulose showed slow release over a period of 48 hours which was slightly higher in case of S3M processed dispersion (Figure 5.50).

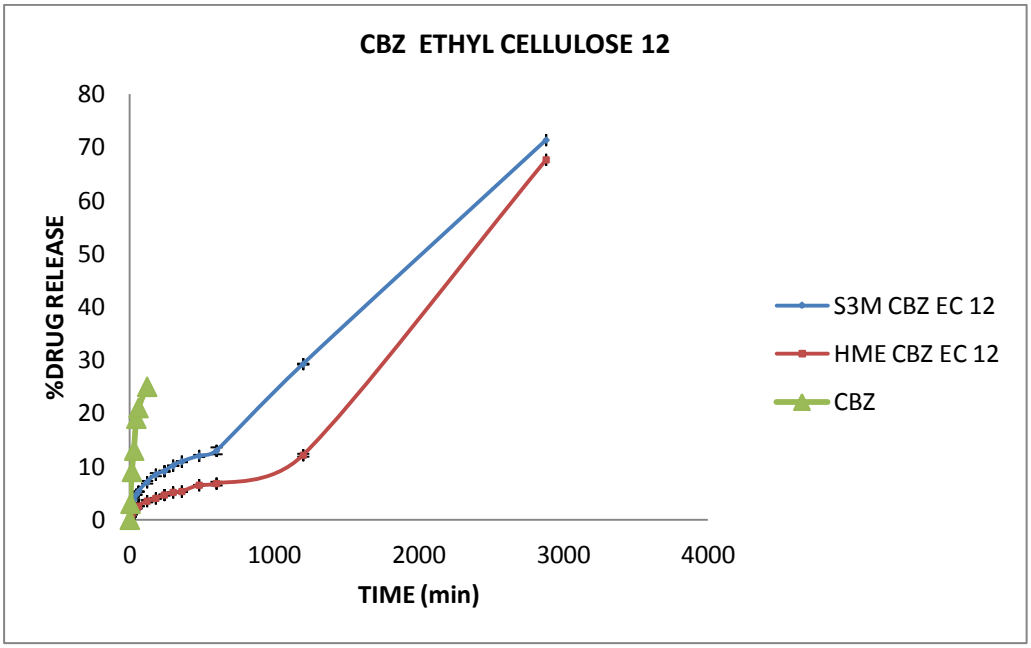

Figure 5.50 Dissolution profile for carbamazepine solid dispersions with ethyl cellulose processed by HME and S3M

5.4.3.7 Degradation analysis

5.4.3.7.1 Iminostilbene determination

The United State Pharmacopoeia (USP) have recommended 0.2% w/w of iminostilbene as a maximum allowable limit in CBZ or its formulations (USP 30/ NF 25). The thermal degradation of CBZ into iminostilbene is known and thus it is important to know the extent of degradation of CBZ into iminostilbene during HME and S3M processing (Figure 5.51).

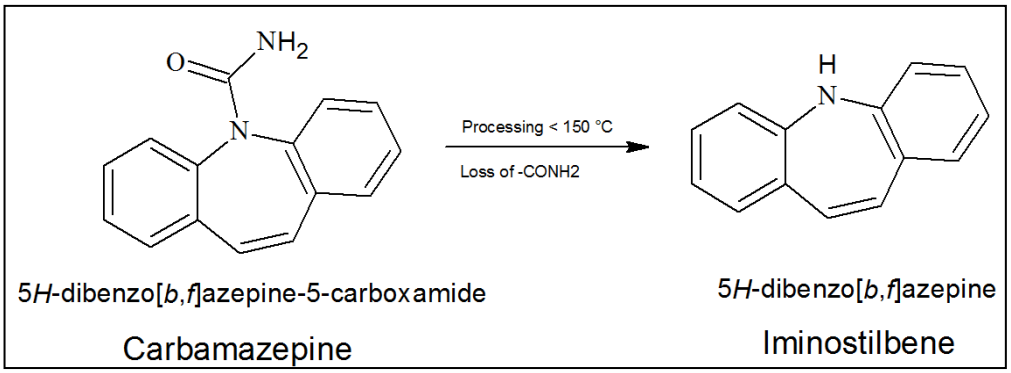

Figure 5.51 Carbamazepine to iminostilbene conversion as degradation product

The estimation of iminostilbene in HME and S3M processed samples was performed using HPLC analysis. First, the calibration curve for iminostilbene was constructed and the generated regression equation was used for calculating the amount of iminostilbene in the processed samples.

Figure 5.52 shows the calibration curve for iminostilbene.

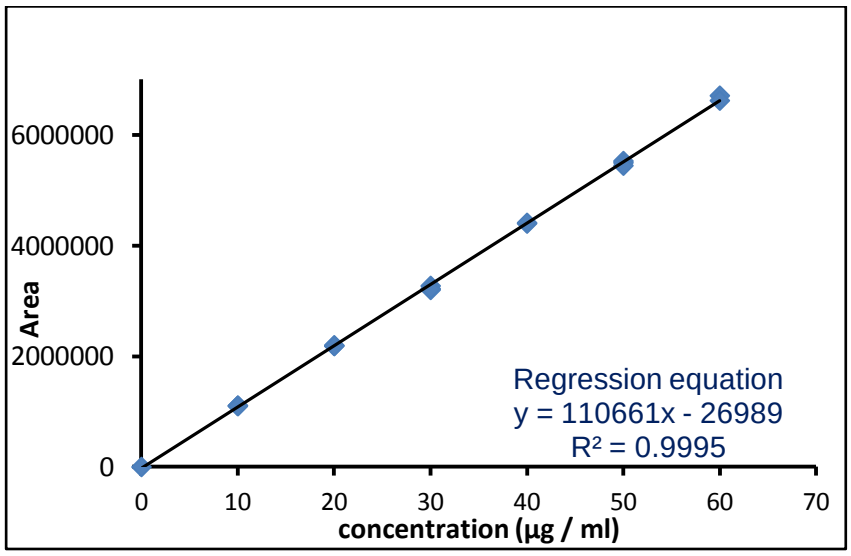

Figure 5.52 Calibration curve for iminostilbene by UV spectrophotometer at 253nm

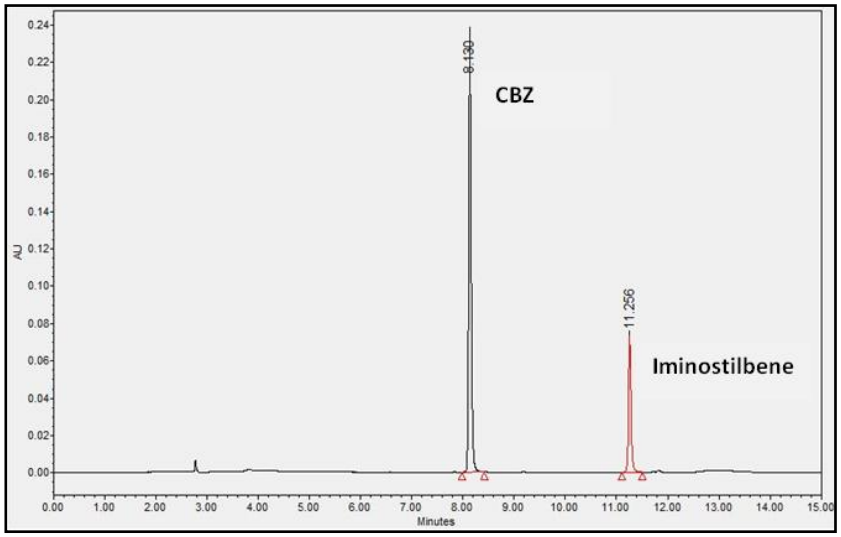

Figure 5.53 Chromatogram for carbamazepine and iminostilbene

Figure 5.53 shows a representative chromatogram where CBZ and iminostilbene eluted at different retention times suggesting that the capability of developed HPLC for detecting CBZ and iminostilbene simultaneously.

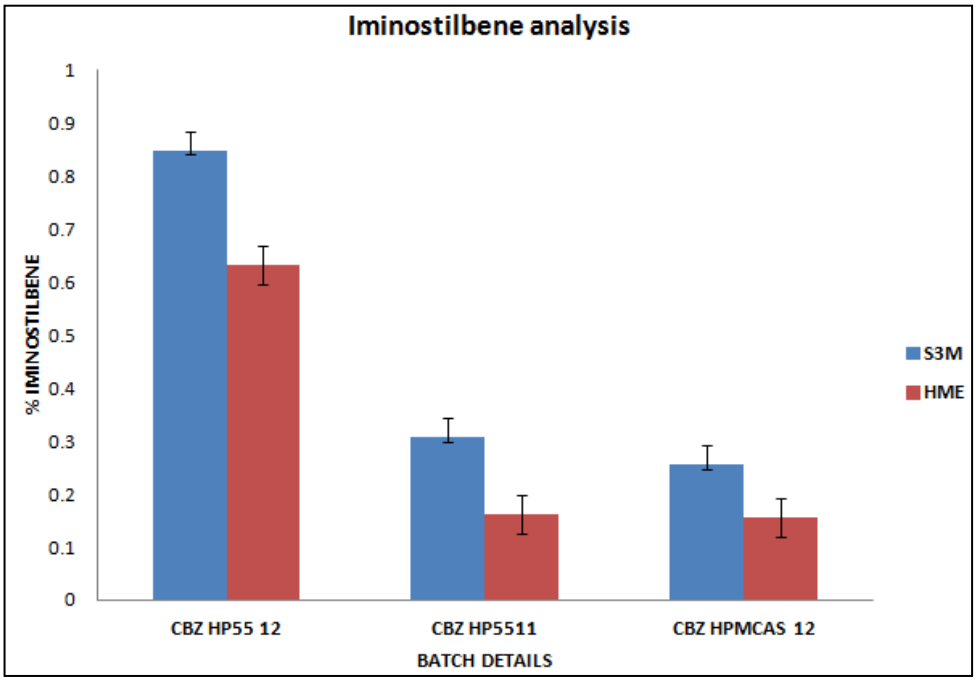

Figure 5.54 Degradation analysis of carbamazepine by imminostilbene determination in carbamazepine solid dispersions processed by HME and S3M

From Figure 5.54 it can be observed that generation of iminostilbene was consistently higher in the case of S3M processed dispersions compared to HME processed solid dispersions. Highest CBZ degradation was observed in case of the CBZ: HP55 1:2 solid dispersions batch which is contradictory to the amount of degradation observed in CBZ: HP55 1:1 solid dispersions, whereas the CBZ degradation was least in case of CBZ: HPMCAS 1:2. It can be observed that the amount of polymer present in mixture plays an important role for drug degradation during high shear processes such as HME and S3M3. As the concentration of polymer increased in dispersions the amount of shear exerted on the material was higher which resulted in more degradation of drug. The polymer chains were stretched and entangled during S3M and HME process whereas CBZ being small molecular weight drug which cannot experience shear or stress as itself, stretching of polymer chains under high stress environment of S3M and HME made drug experience same amount of shear which caused higher degradation of API.

Similarly HPMCP HP55 polymer was analysed for degradation by calculating the amount of phthalic acid and subsequently phthalic anhydride generated during HME and S3M3 processing.

5.4.3.7.2 Phthalic acid determination

Phthalic acid is generated as a degradation product when HPMCP is processed at higher temperatures and the generated phthalic acid further degrades into phthalic anhydride (Figure 5.55)

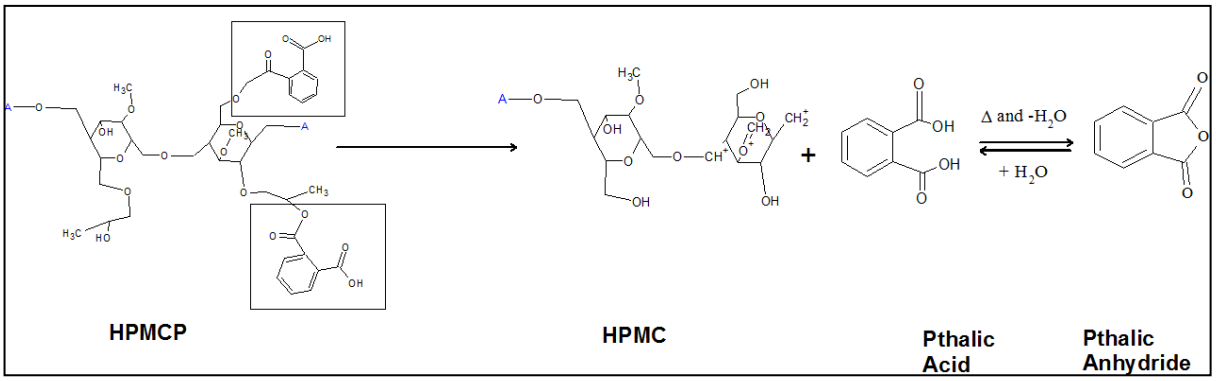

Figure 5.55 HPMCP degradation into phthalic acid and subsequent phthalic acid degradation into phthalic anhydride

Calibration curve

The HPLC calibration curve for phthalic acid was linear over concentration range of 10-60 ug/ml. The linearity equation was calculated using calibration curve, slope of the equation is 72667.3377, constant -16465.8202 and R^2 0.9998 (Figure 5.56). The calibration equation was used to calculate the amount of the phthalic acid generated.

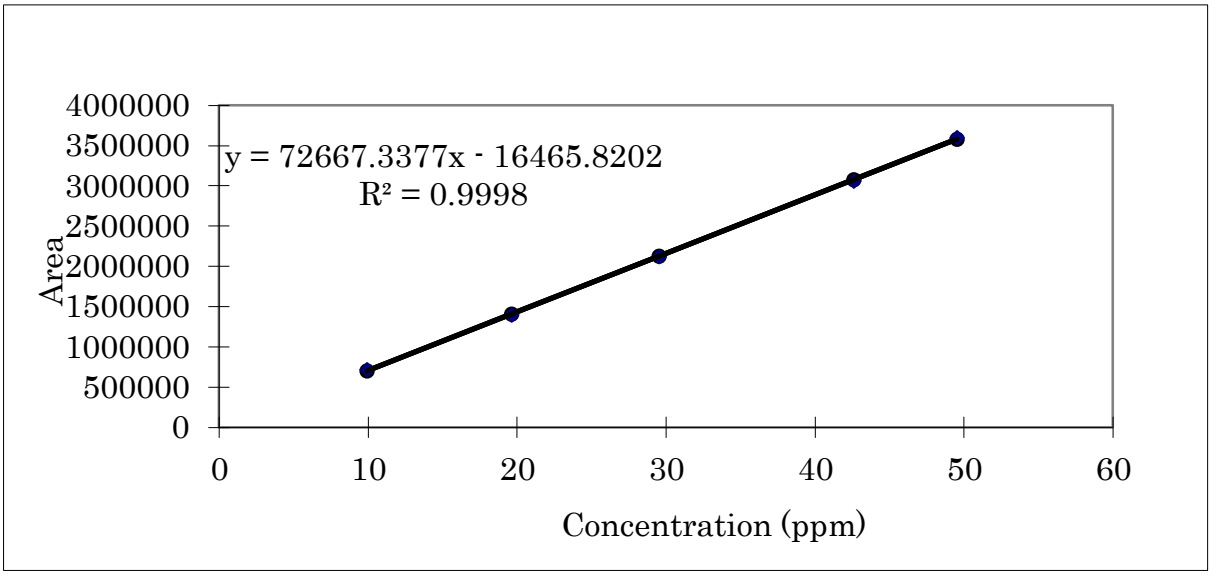

Figure 5.56 Calibration curve for phthalic acid

The degradation analysis by HPLC showed that the melt extruded and pan milled amorphous dispersion has phthalic acid content below 1% as shown in Figure 5.57

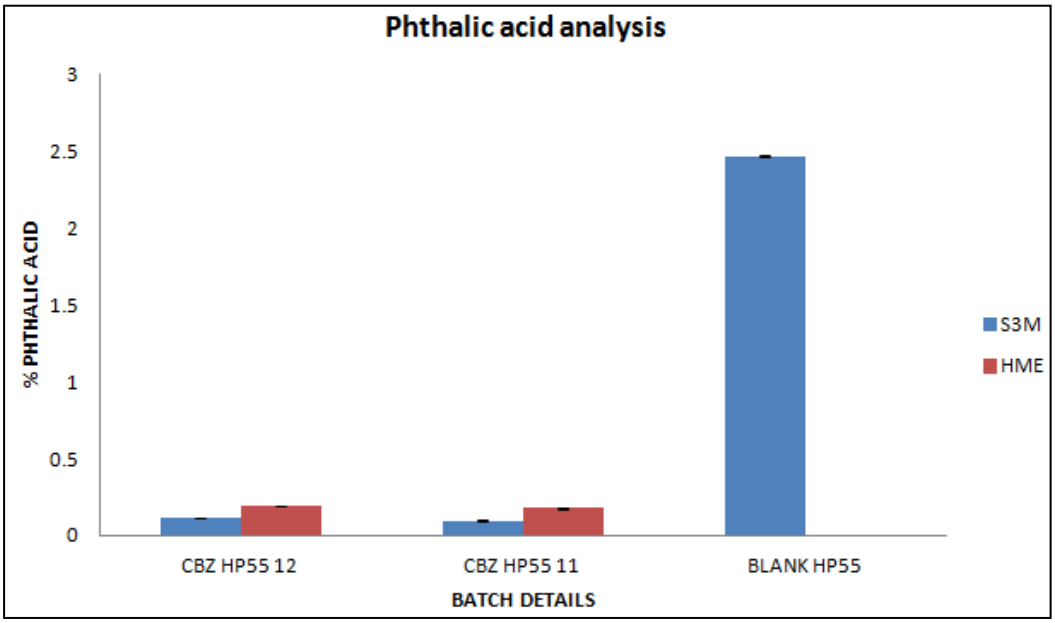

Figure 5.57 phthalic acid determinations in carbamazepine: HP55 solid dispersions processed by HME and S3M

The amount of phthalic acid generated was higher in the case of HME processed CBZ: HP55 dispersions. The amount of phthalic acid generated did not vary with the polymer concentration. It was slightly higher in case of CBZ: HP55 1:2 compared to CBZ: HP55 1:1, this finding is complementary to generation of iminostilbene. The degradation of polymer and drug is dependent on the amount of polymer and not on the drug. The higher generation of phthalic acid may have enhanced the generation of more iminostilbene in the case of CBZ: HP55 1:2 dispersion. Blank HPMCP HP55 showed highest degradation and generated 2.5% of phthalic acid. Shear exerted by S3M3 is based on the amount of polymer which clearly showed in case of phthalic acid generated in the case of blank HP55.

5.4.3.7.3 Phthalic anhydride analysis

Phthalic anhydride calibration curve

The HPLC calibration curve for phthalic anhydride was linear over concentration range of 10-60 ug/ml. The linearity equation was calculated using calibration curve, slope of the equation was 162467.1299, constant -51355.1665 and R^2 0.9989 (Figure 5.58).

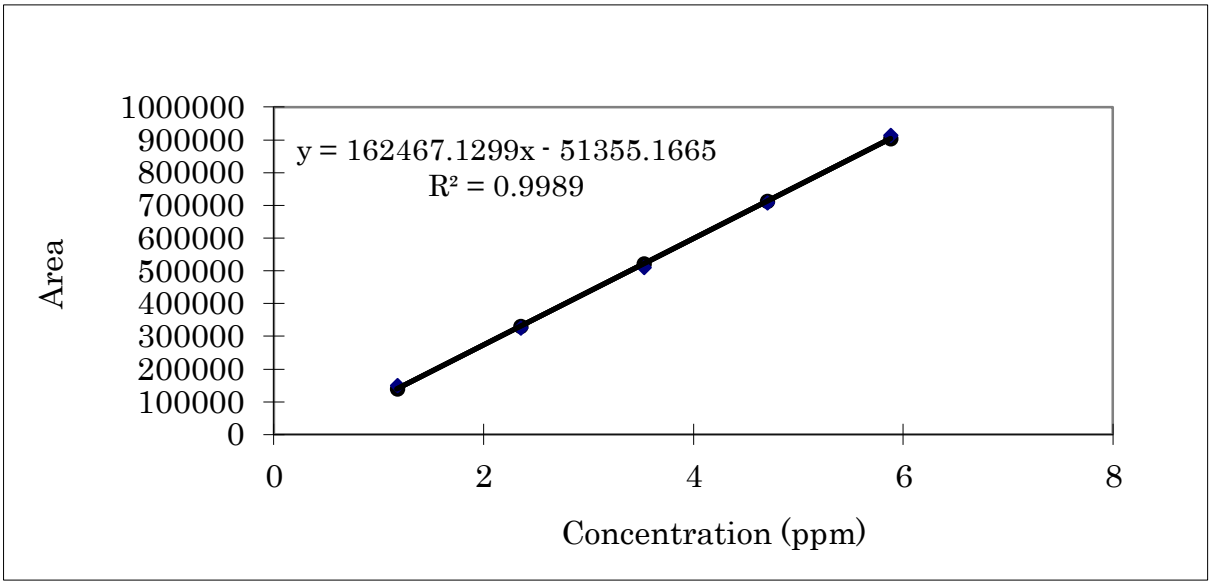

Figure 5.58 Phthalic anhydride calibration curve

The amount of phthalic anhydride generated was expected to be higher where phthalic acid generation is higher (Karandikar, *et al.* 2014), the formed phthalic acid is unstable and will try to convert it into more stable phthalic anhydride form. S3M processed CBZ: HP55 1:2 dispersion showed higher generation of phthalic anhydride compared to HME processed dispersions (Figure 5.59).

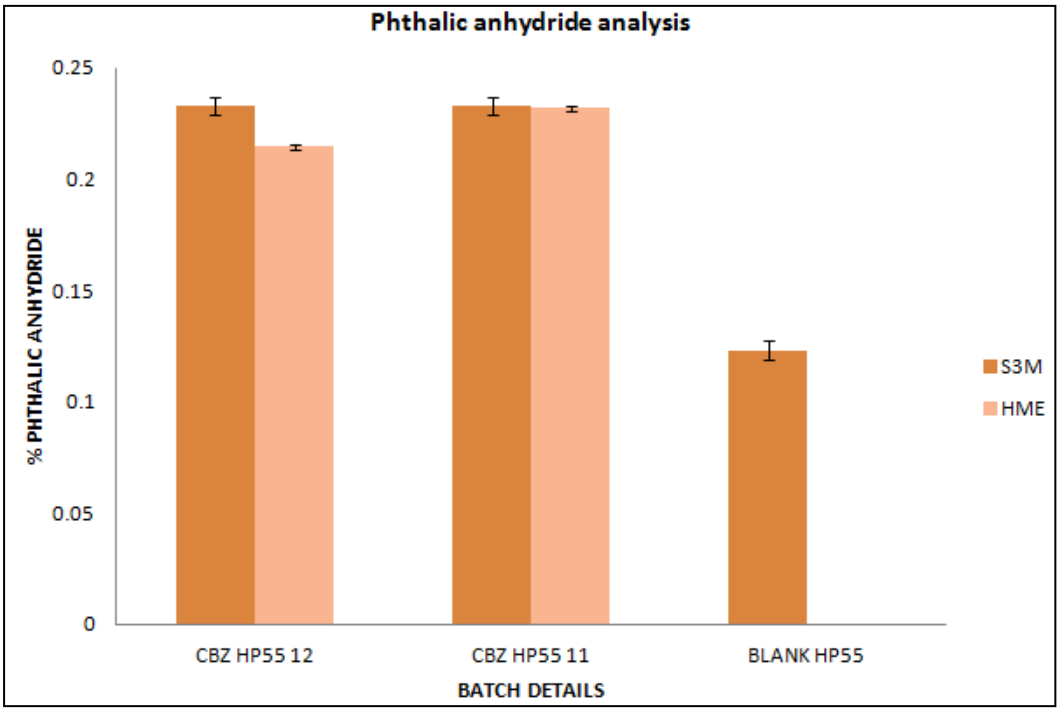

Figure 5.59 Phthalic anhydride determination in carbamazepine: HP55 solid dispersions processed by HME and S3M

5.4.3.8 *DVS*

DVS was carried out as described in Section 3.4.6. For this purpose selected carbamazepine solid dispersions were analysed for amount of vapour sorption and desorption at different humidity conditions. CBZ: VA64 solid dispersions processed by HME and S3M with variable drug concentrations showed significant vapour sorption at 60% RH (Figure 5.60). In both the cases CBZ:VA64 1:1 and 1:2 S3M processed solid dispersions showed lower vapour sorption compared to HME processed dispersions. Plain PVP VA64 showed highest vapour sorption being hygroscopic in nature. The higher vapour sorption values in HME processed solid dispersions may have contributed to the use of PEG as plasticiser.

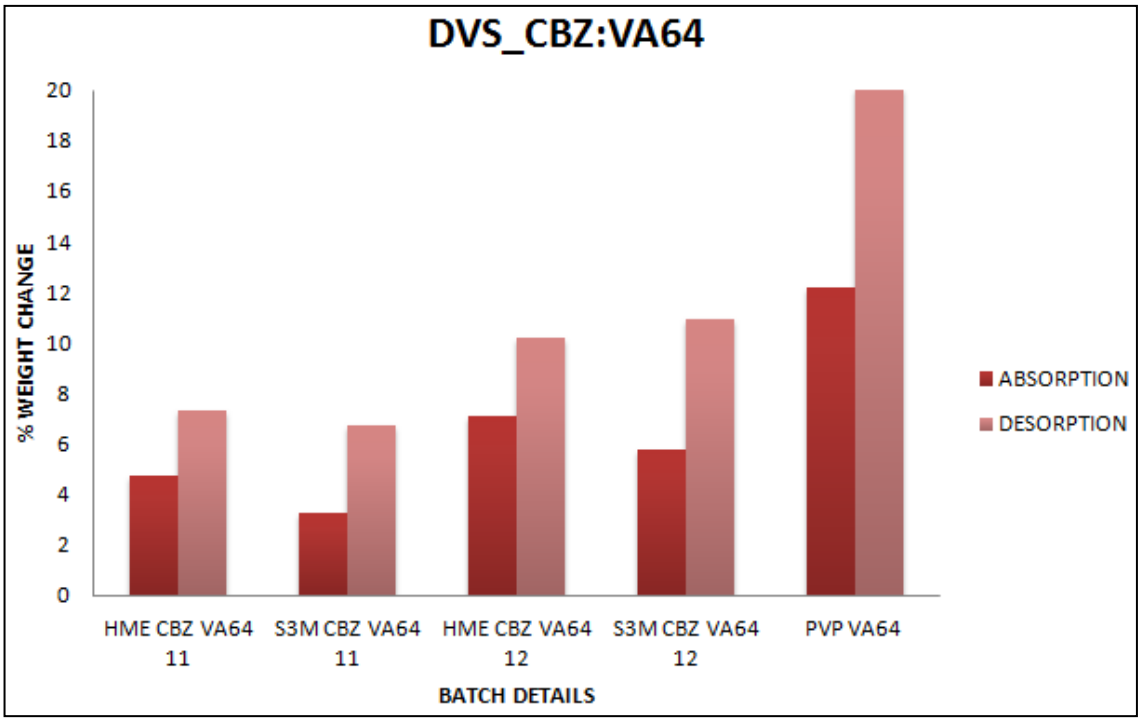

Figure 5.60 DVS at 60% RH for carbamazepine: VA64 solid dispersions processed by HME and S3M

In the case of CBZ: HP55 solid dispersions the vapour sorption was independent of concentration of drug and polymer. In case of CBZ: HP55 1:1 case the vapour sorption was higher in case of HME processed solid dispersion which can be contributed to the plasticiser (TEC) used in HME solid dispersion. In the case of CBZ:HP55 1:2 solid dispersions the vapour sorption showed the opposite behaviour to 1:1 solid dispersions, S3M processed solid dispersion showed higher vapour sorption compared to HME processed (Figure 5.61). Plain HPMCP HP55 showed higher vapour sorption which changed significantly on incorporation of drug.

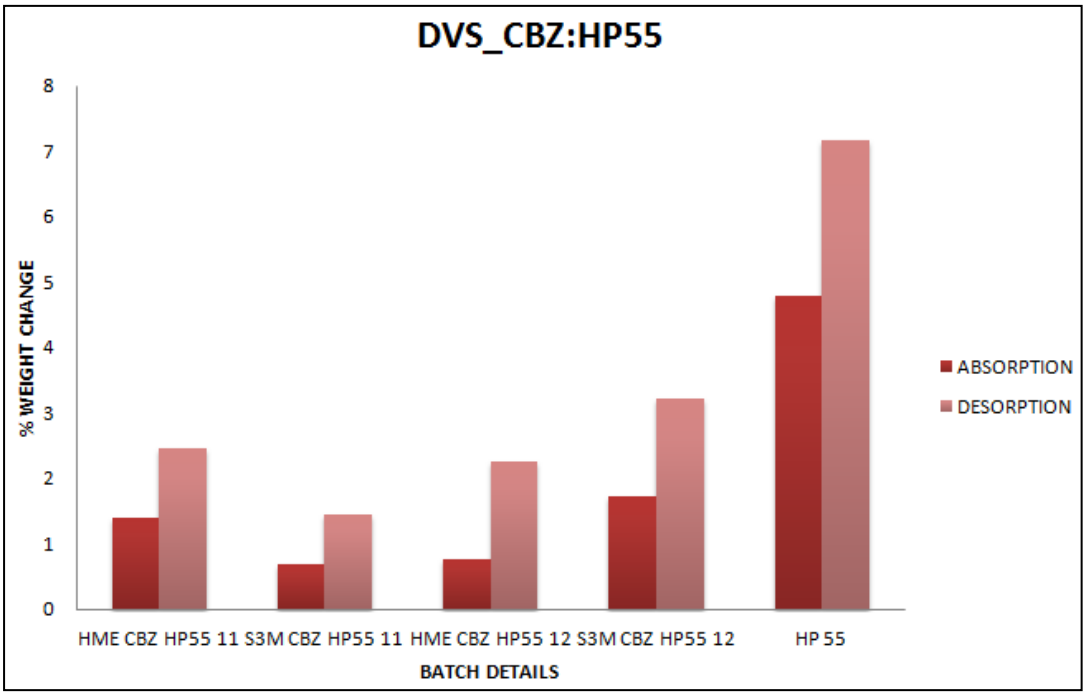

Figure 5.61 DVS at 60% RH for carbamazepine: HP55 solid dispersions processed by HME and S3M

In the case of CBZ:HPMCAS 1:2 solid dispersions HME processed dispersions showed slightly higher vapour sorption compared to S3M processed dispersion, the higher vapour sorption values can be attributed to the presence of plasticiser (TEC) in the case of HME processed dispersion. Plain HPMCAS showed higher vapour sorption as compared to CBZ dispersions (Figure 5.62), the weight change observed in plain polymer is almost double which shows that plain polymer has higher vapour sorption value which changes or reduces on incorporation of CBZ.

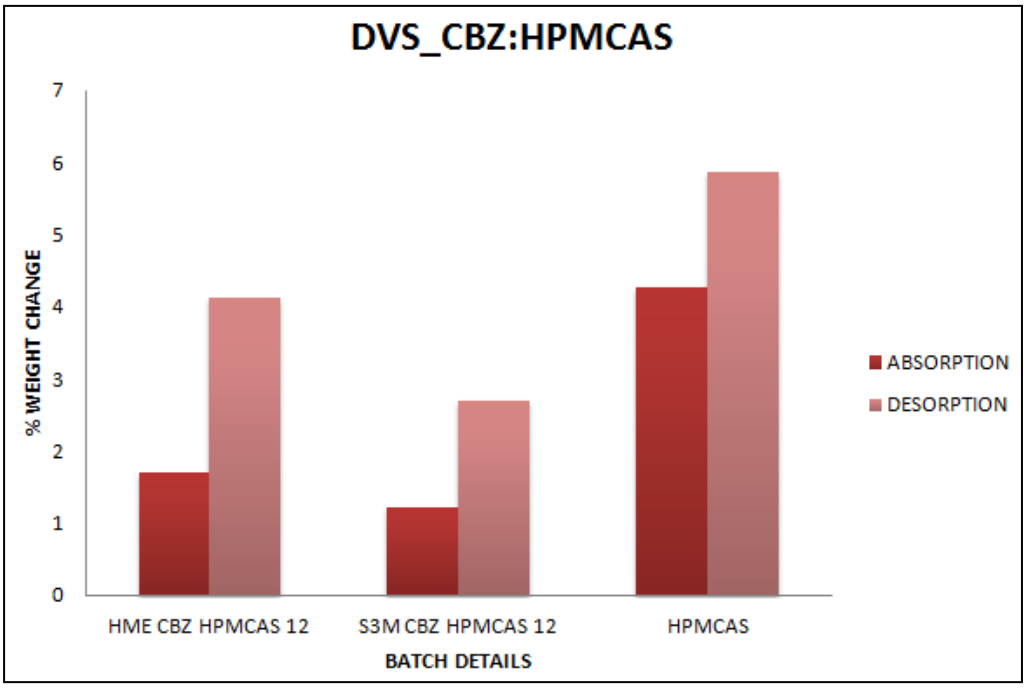

Figure 5.62 DVS at 60% RH for carbamazepine: HPMCAS 1:2 solid dispersions processed by HME and S3M

In the case of CBZ: EC 1:2 solid dispersion vapour sorption was slightly higher for S3M processed dispersions as compared to HME. The presence of plasticiser (PEG) in HME processed dispersions did not have a significant effect on vapour sorption (Figure 5.63). Plain ethyl cellulose showed higher vapour sorption values at all % relative humidity.

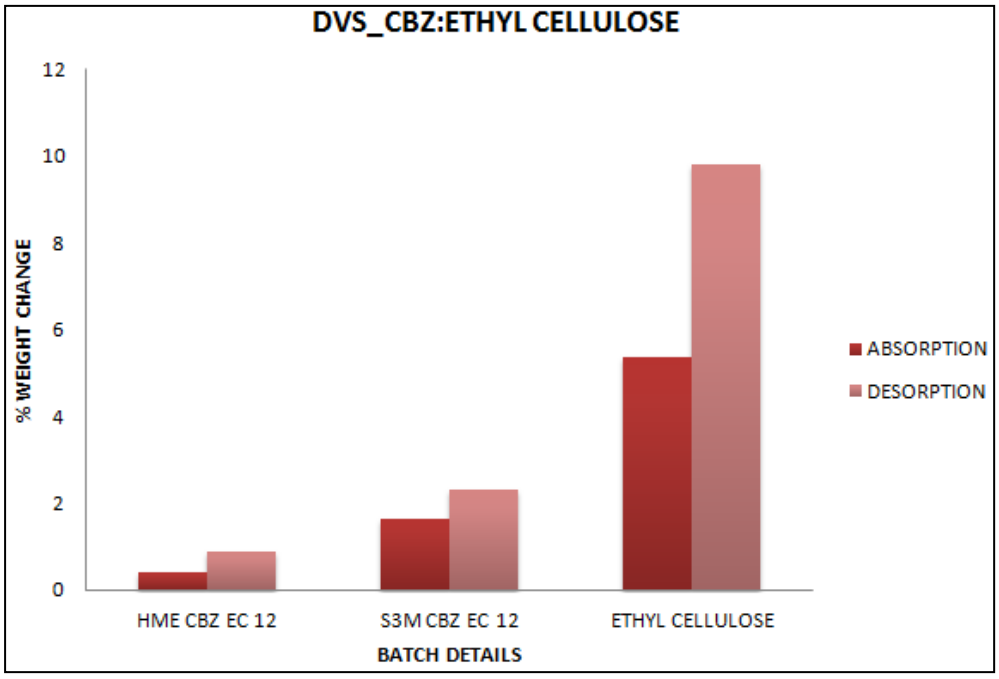

Figure 5.63 DVS at 60% RH for carbamazepine: HPMCAS 1:2 solid dispersions processed by HME and S3M

5.4.3.9 *Surface energy*

Surface energy analysis was done for few samples to check whether there was a difference in surface energies between solid dispersions processed by HME and S3M3 and whether it had an effect on performance of solid dispersions. Surface energy analysis was done as described in Section 3.4.7.

The surface energy values for CBZ: HP55 1:2 processed by HME showed positive correlation with the area, value of the surface energy goes on increasing with as surface area coverage goes on increasing (Figure 5.64). The reverse was observed in for S3M3 processed CBZ: HP55 1:2 solid dispersion which showed a good correlation up to limited area coverage.

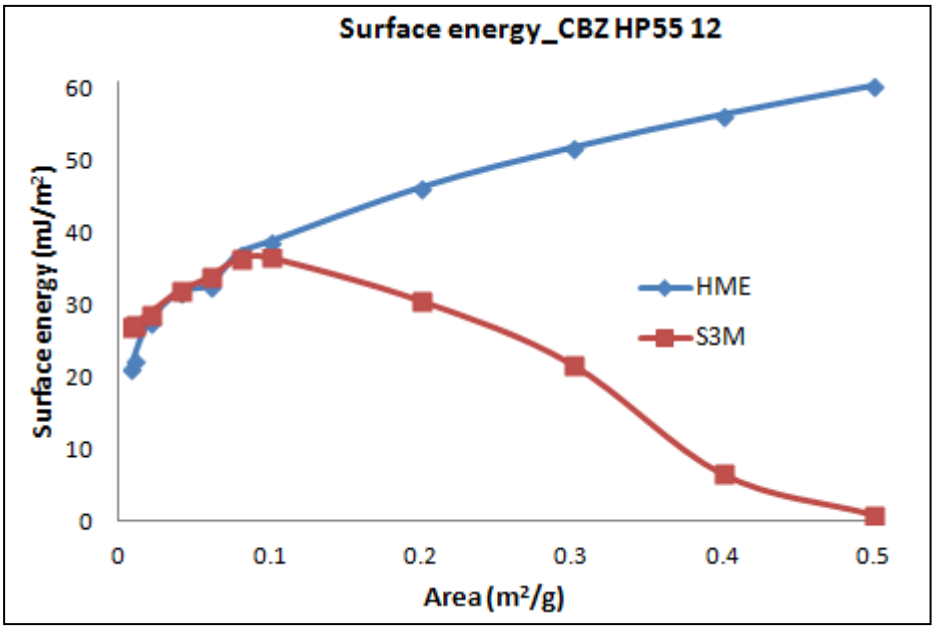

Figure 5.64 *i*GC analysis for carbamazepine: HP55 1:2 solid dispersion processed by HME and S3M

The irregularity in the surface features area may have caused improper area coverage which hinders the effective surface energy of the dispersion. Surface hydrophobicity can be the reason for the variations in surface energy values between dispersions produced by two processes; this can be contributed to surface groups on the dispersions exposed experimental environment. The drop in surface energy in case of S3M processed sample can be contributed to surface relaxation due to aging of the surface (Hasegawa and Buckton, 2008).

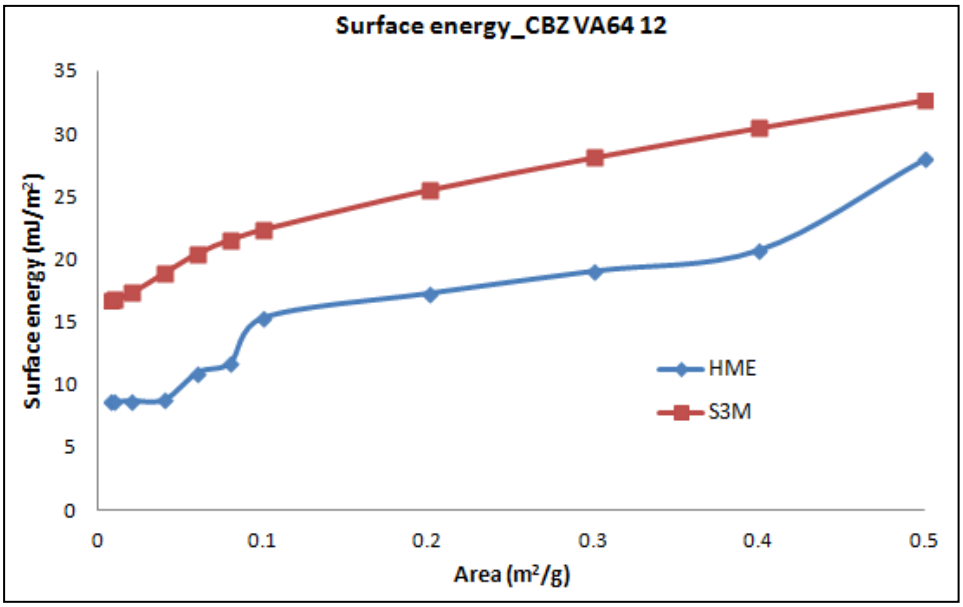

Figure 5.65 *i*GC analysis for carbamazepine: PVP VA64 1:2 solid dispersion processed by HME and S3M

The area coverage for CBZ: PVP VA64 1:2 solid dispersions processed by HME and S3M3 showed good surface exposure. The surface energy showed good correlation with the area covered which increased with increasing area (Figure 5.65). The solid dispersions with PVP VA64 exhibited a higher number of surface groups which resulted in higher surface area coverage and in turn higher surface energy values.

In the case of CBZ: EC 1:2 solid dispersions processed by HME and S3M3, these showed similar surface energy behaviour as CBZ: HP55 1:2 dispersions (Figure 5.66). Previously Shah, *et al*. 2012 has shown the effect of particle size and particle defects on the extent of change in surface energy as particle size or surface defects goes on increasing surface energy increases with it.

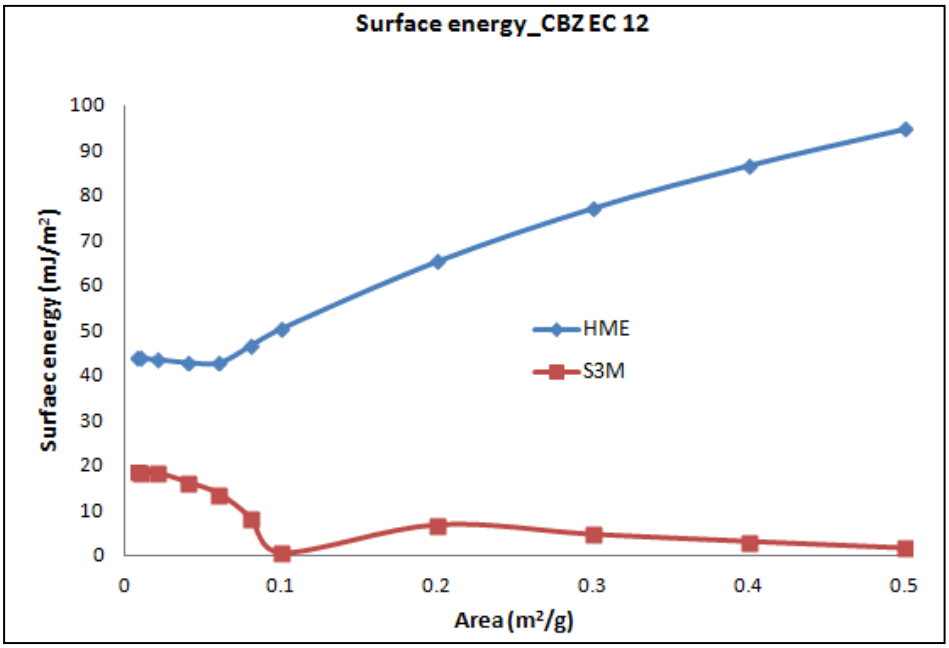

Figure 5.66 *i*GC analysis for carbamazepine: ethyl cellulose 1:2 solid dispersion processed by HME and S3M

This irregular behaviour in the surface energy in CBZ solid dispersions processed by HME and S3M3 can be due the extreme processing conditions with high shear in case of S3M3 which yield a dispersion with surface properties with variable properties with exposure of different groups on the surface, whereas surface properties in case of HME processed solid dispersions are very regular and smooth. There is no direct correlation between extent of surface energy shown by CBZ solid dispersions with drug release and its amorphous nature.

HME and S3M being high shear processes showed lot of variability in there processing conditions and resultant end product. Various analytical characterisations were used to compare processes for the drug: polymer combination pairs. This helped to understand how product characteristics change with respect to amorphous nature of the end product and its

pharmaceutical performance. HME is being widely explored for the formation of amorphous dispersions was very useful as comparative method to explore S3M as new technology for manufacturing amorphous dispersions. HME and S3M have various comparative advantages and disadvantages over each other, such as it was possible to process drug: polymer mixture without plasticiser which is not always possible in HME. Another example in process variability is process control features in HME and S3M; in case of HME process control parameters are excellent which helps to have very good control on the outcome of the end product, whereas in for S3M process parameters or process parameters cannot be controlled as well as in HME. A simple comparative example to understand the difference in product characteristic with respect to drug release from solid dispersions processed by HME and S3M is given in Table 5.2. Table has given the release of respective drug from solid dispersions from HME and S3M.

Differences in processing of solid dispersion and cocrystals were basically depending upon the respective polymer and co-former present in the mixture. The processing conditions in case of solid dispersions were majorly based on the Tg of the polymer present and were processed at respective temperatures as described in experimental section. In case of cocrystals the processing of mixture was dependent on the eutectic temperature of the drug and co-former or at the melting temperature of the co-former and all the cocrystal batches were processed at respective temperatures. The effect of these processing conditions in case of solid dispersions was complete softening of polymer to solubilise the present drug into it and convert system

into complete amorphous form whereas in case of cocrystals the processing conditions made drug:co-former mixture to convert them into phase pure cocrystalline end product.

Table 5.2 Comparative drug release from solid dispersions with respective time points

Sr. No.	Solid dispersion	Time point (min)	HME (% drug release)	S3M (%drug release)
1	IBU:VA64 1:2	5	45%	43%
2	IBU:HP55 1:2	45	86%	76%
3	GLIB: VA64 1:2	60	31%	88%
4	GLIB: EC 1:2	60	42%	31%
5	PARA: HP55 1:2	30	99%	92%
6	CBZ: VA64 1:1	15	88%	82%
7	CBZ:VA64 1:2	15	69%	58%
8	CBZ: HP55 1:1	15	30%	58%
9	CBZ: HP55 1:2	15	64%	29%
10	CBZ: HPMCAS 1:2	15	43%	69%
11	CBZ: EC 1:2	1200	29%	12%

Table 5.2 shows how the drug releases from different drug: polymer composition changes at given time point, this can be attributed to the nature of product characteristics and process characteristics of HME and S3M.

The two high shear processes HME and S3M are continuous (S3M potentially if used in series), solvent free and has good potential for scalability and production of the amorphous formulations for various pharmaceutical APIs. In similar way S3M has been explored for the production of pharmaceutical cocrystals and how it differs from HME is given in Chapter 6.

Chapter 6. Results and discussions of co crystals

This chapter will deal with the formation and performance of different cocrystals of ibuprofen, caffeine, paracetamol and carbamazepine with range of co-formers. Cocrystals produced by S3M3 and HME will be compared with each other as well as with cocrystals generated by solution crystallisation.

6.1 Ibuprofen: nicotinamide 1:1 cocrystal (IBU: NIC 1:1)

IBU: NIC 1:1 was chosen as first pair for cocrystal formation during S3M processing. The product quality varied significantly in the sense with physicochemical properties and drug release processed by S3M and HME. IBU:NIC 1:1 cocrystal with 10% PEO and 10% PVP VA64 yielded a good agglomerated product but with HME processed batches a molten mass was formed through agglomeration with 10% of PEO and 10% PVP VA64. IBU being a low Tg drug as discussed in chapter 5, in combination with PEO and VA64 may have further affected to the Tg of the mixture and turned into a viscous molten mass in HME. Residence time in HME is significantly high compared to S3M3; this longer residence in HME might have caused homogenisation of the molten IBU with polymer to form molten lump. HME end product was in the form molten liquid which made product collection difficult whereas in the case of S3M3 processing IBU:NIC 1:1 cocrystals with 10% PEO and 10% VA64 showed good product characteristics. S3M processed IBU:NIC with polymers gave phase pure cocrystals (Figure 6.1).

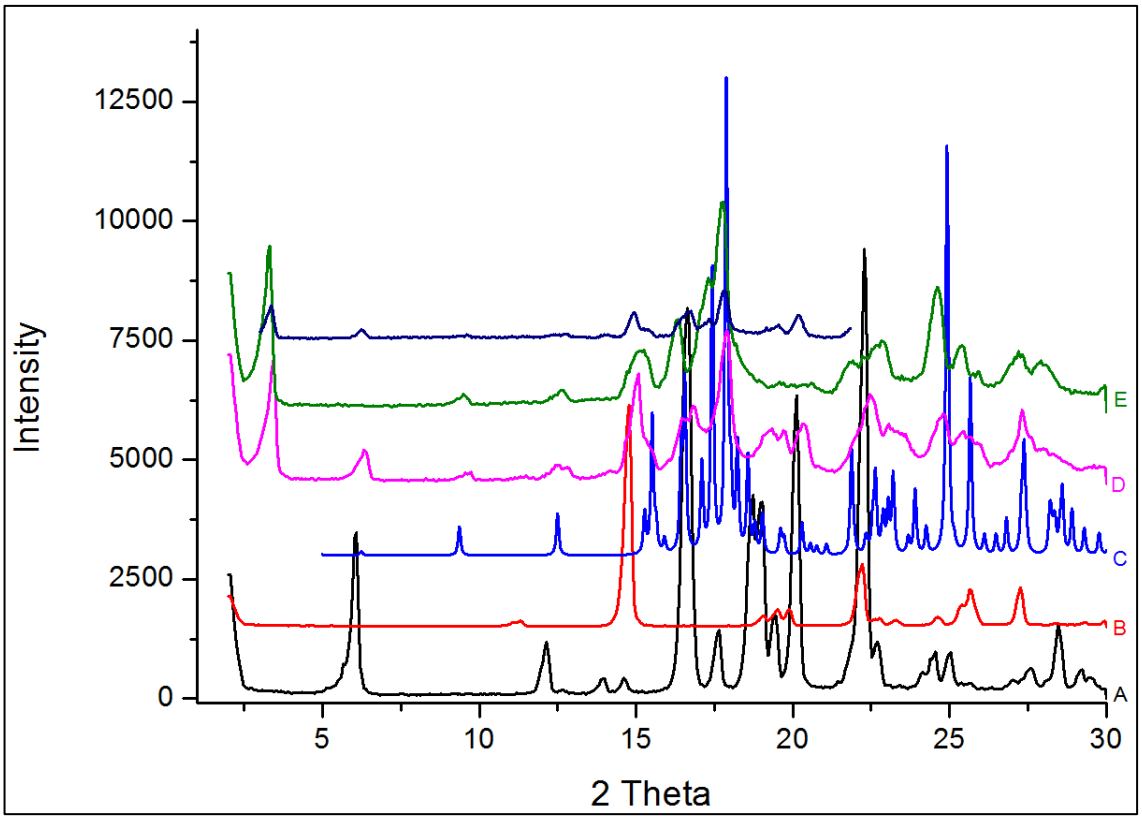

[A- Ibuprofen, B- Nicotinamide, C-IBU: NIC 1:1 cocrystal reference CSD, D) S3M IBU:NIC 1:1 10% VA64, E) S3M IBU:NIC 1:1 10% VA64, F) HME IBU:NIC 1:1 without polymer]

Figure 6.1 PXRD patterns for Ibuprofen: Nicotinamide 1:1 cocrystal processed by HME and S3M

Further analysis was not done for this cocrystal pair due to the liquid end product in HME processing which made direct comparison between two processes difficult.

6.2 Caffeine: maleic acid 1:1 cocrystal (CAF: MAL 1:1)

6.2.1 Crystal structure data

The CAF: MAL 1:1 cocrystal crystallises as a monoclinic form. Hydrogen bonding is one of the attractive forces involved in the formation of cocrystals. The reactive group responsible for the hydrogen bond formation are –N

(imidazole) of CAF and –COOH of the MAL (Trask *et al*., 2005). There is intramolecular hydrogen bonding within the two *cis* oriented carboxylic acid groups of MAL that has retained in the cocrystal from MAL precursor. The crystal structure data, calculated PXRD pattern and important space group details for this cocrystal form is shown in Figure 6.2, Figure 6.3 and Table 6.1. The PXRD pattern shows characteristic peaks at 2θ = 9, 11.18, 13.2, 14.4 and 15.5 °.

Table 6.1Crystal structural database and space group details for CAF:MAL 1:1 cocrystal

Empirical formula	**C8 H10 N4 O2,C4 H6 O5**
Crystal system	Triclinic
Space group	P 1
a (Å)	9.139
b (Å)	9.306
c (Å)	9.771
α (°)	85.131
β (°)	65.297
γ (°)	71.185

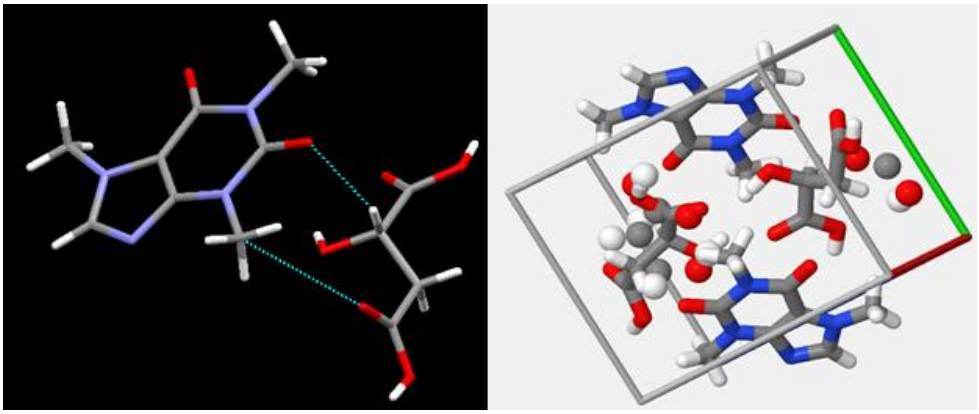

Figure 6.2 Crystal structure of caffeine: maleic acid 1:1 cocrystal and crystal packing in unit cell. (adopted from CSD)

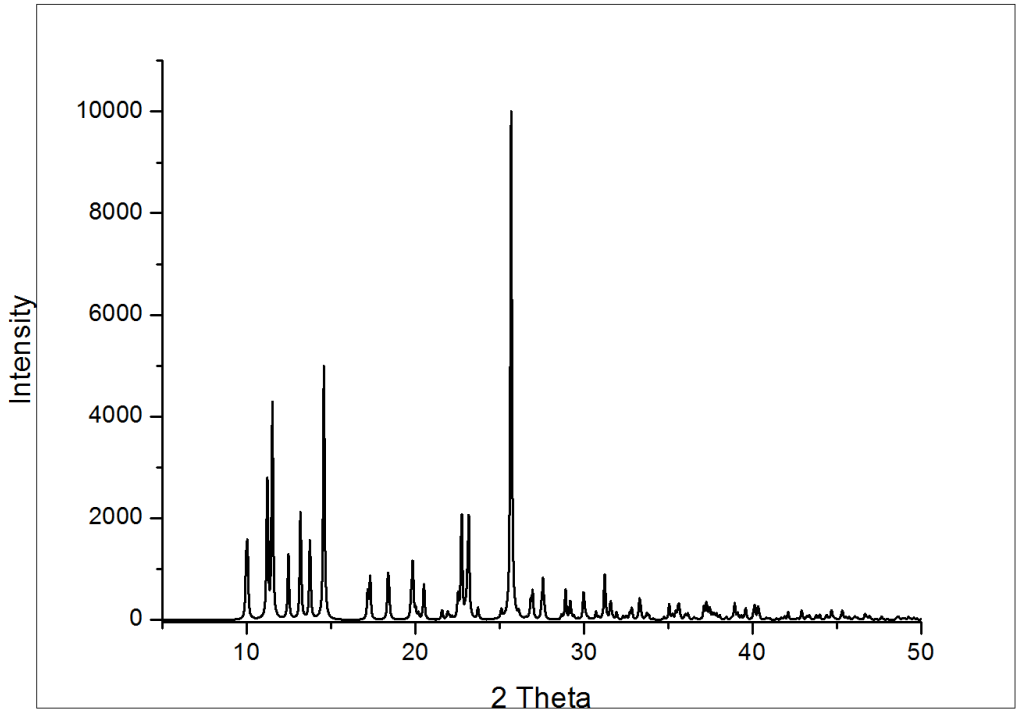

Figure 6.3 Calculated PXRD pattern for caffeine: maleic acid 1:1 cocrystal Form I. (adopted from CSD-HOLVOV and processed in OriginPro 8)

6.2.2 Processing of cocrystal

Accurately weighed CAF and MAL in molar ratios were mixed well and 15% w/w HPMCP HP55 polymer was added as a process aid. This mixture was then seived through an 80 mesh seive and blended in a turbula mixer for 10mins. The blended mixture was subjected to S3M3, material flow was good, HPMCP HP55 help to improve the S3M3 process flow. At the end of the 1st and 2nd cycle there was no tranformation in physical form of the material, when end product of 2nd cycle fed to S3M3 for 3rd cycle there was rise in temperature of the mill and at the end of the third cycle of a hard cake mass was formed as the end product. HME of CAF:MAL 1:1 cocrystal was carried out as per temperature and extrusion profiles given in Section 3.7. It was possible to extrude and process blank CAF:MAL without the aid of

polymer, so CAF:MAL 1:1 with and without polymer were processed. Pure cocrystals for CAF:MAL were produced using a microwave reactor for comparitive purpose and performance was evaluated (Section 3.7.1). The resultant end products of both processes were analysed by various characterisation techniques.

6.2.3 Calibration

6.2.3.1 Caffeine calibration

The calibration curve for CAF was linear over the concentration range of 10-70 ug/ml. The linearity equation was calculated using calibration curve, slope of the equation was 270214, constant 38365 and R^2 0.9998 (Figure 6.4). The calibration was used to calculate the release of CAF.

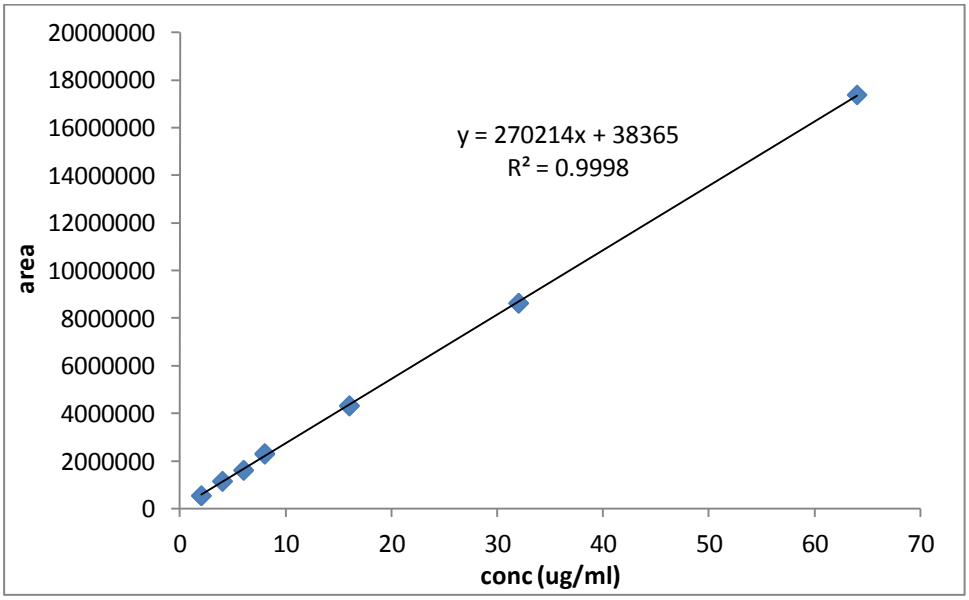

Figure 6.4 Calibration curve for caffeine using HPLC at 209nm

The HPLC retention time of CAF was 12 mins. The chromatogram for CAF is shown in Figure 6.5

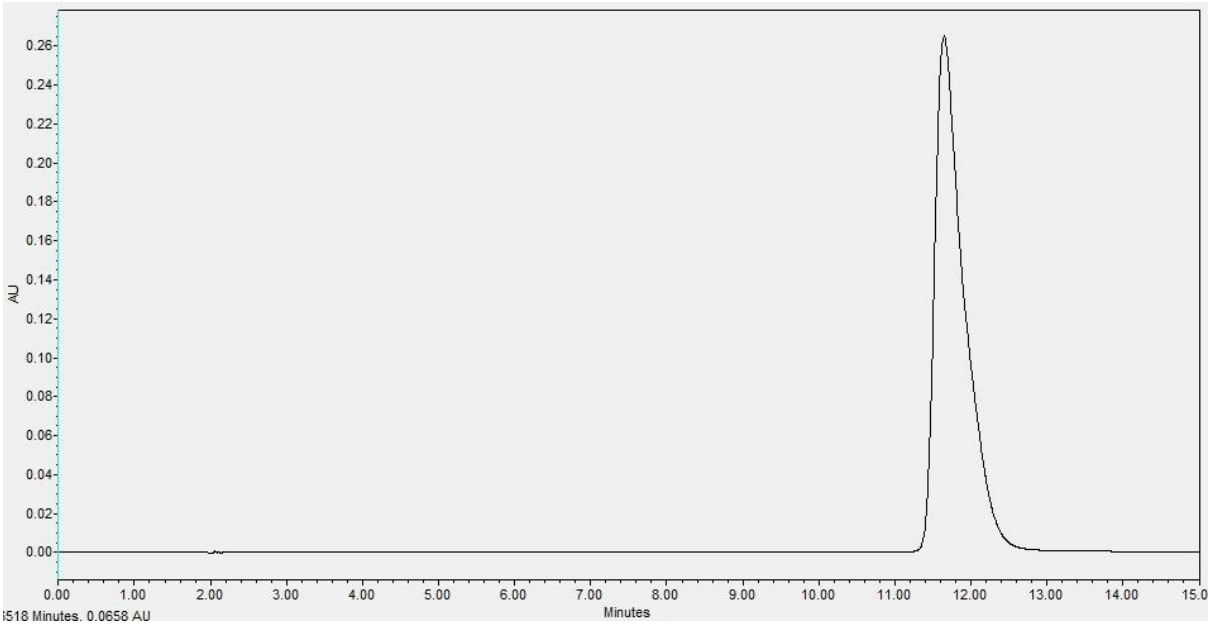

Figure 6.5 Caffeine chromatogram in HPLC analysis

6.2.3.2 MAL calibration

The calibration curve for MAL was linear over the concentration range of 1-20 ug/ml. The linearity equation was calculated using calibration curve, slope of the equation was 267609, constant -20204 and R^2 0.9988 (Figure 6.6).

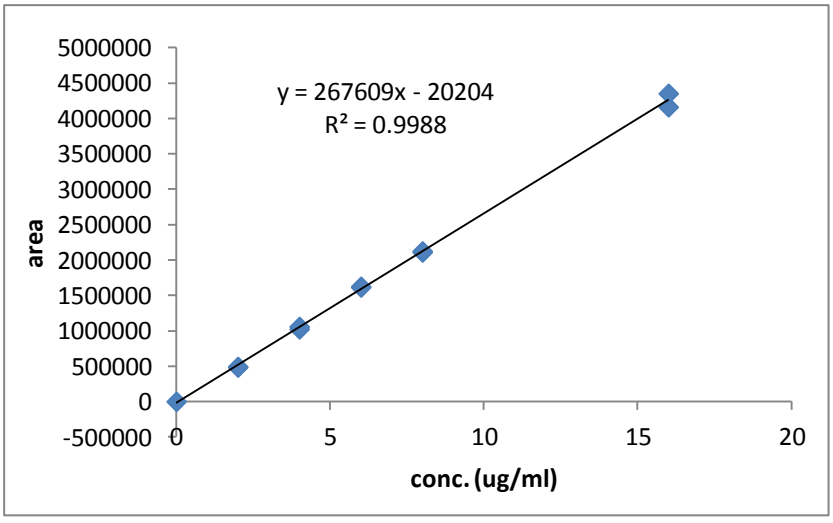

Figure 6.6 Calibration curve for maleic acid using HPLC at 209nm

The HPLC retention time for maleic acid was 5min, the HPLC chromatogram is given in Figure 6.7.

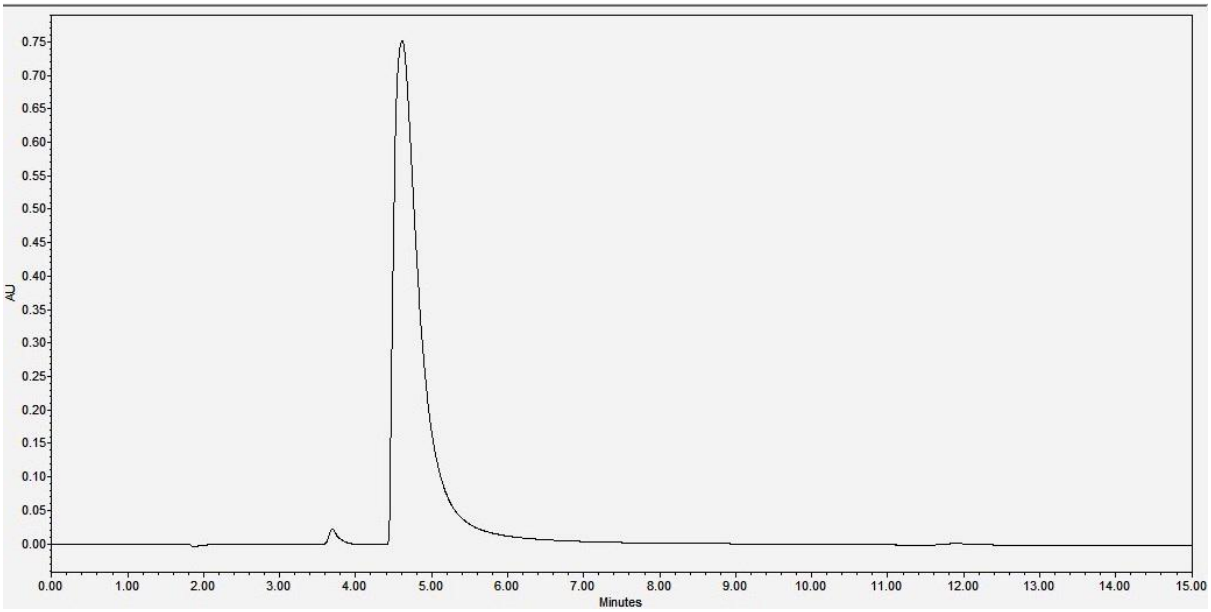

Figure 6.7 Maleic acid chromatogram in HPLC analysis

6.2.4 PXRD

The PXRD procedure was followed as described in Section 3.4.2. The PXRD pattern for pure CAF: MAL shows 2θ values at 9, 11.18, 13.2, 14.4 and 15.5 ° respectively. Figure 6.8 clearly shows that all cocrystal samples processed by HME and S3M matched with the phase pure CAF: MAL 1:1 cocrystal (A) as well as with the 2θ values given in the CSD database (Figure 6.8). The CAF: MAL 1:1 cocrystal with HP55 shows slightly suppressed characteristic peaks at given 2θ values which might be attributed to the effect of polymer chains which must have affected the exposed crystallinity to X-rays (D,E). Use of polymer as a process aid in S3M3 made it possible for plain drug and co-former blend to flow smoothly. It can be concluded that use of HP55 acted as shear aiding material during S3M3 and when shear was applied to polymer approaching at its melting point, the polymer it may have acted as a

solvent for solubilising CAF and MAL in molar ratio to yield phase pure cocrystal.

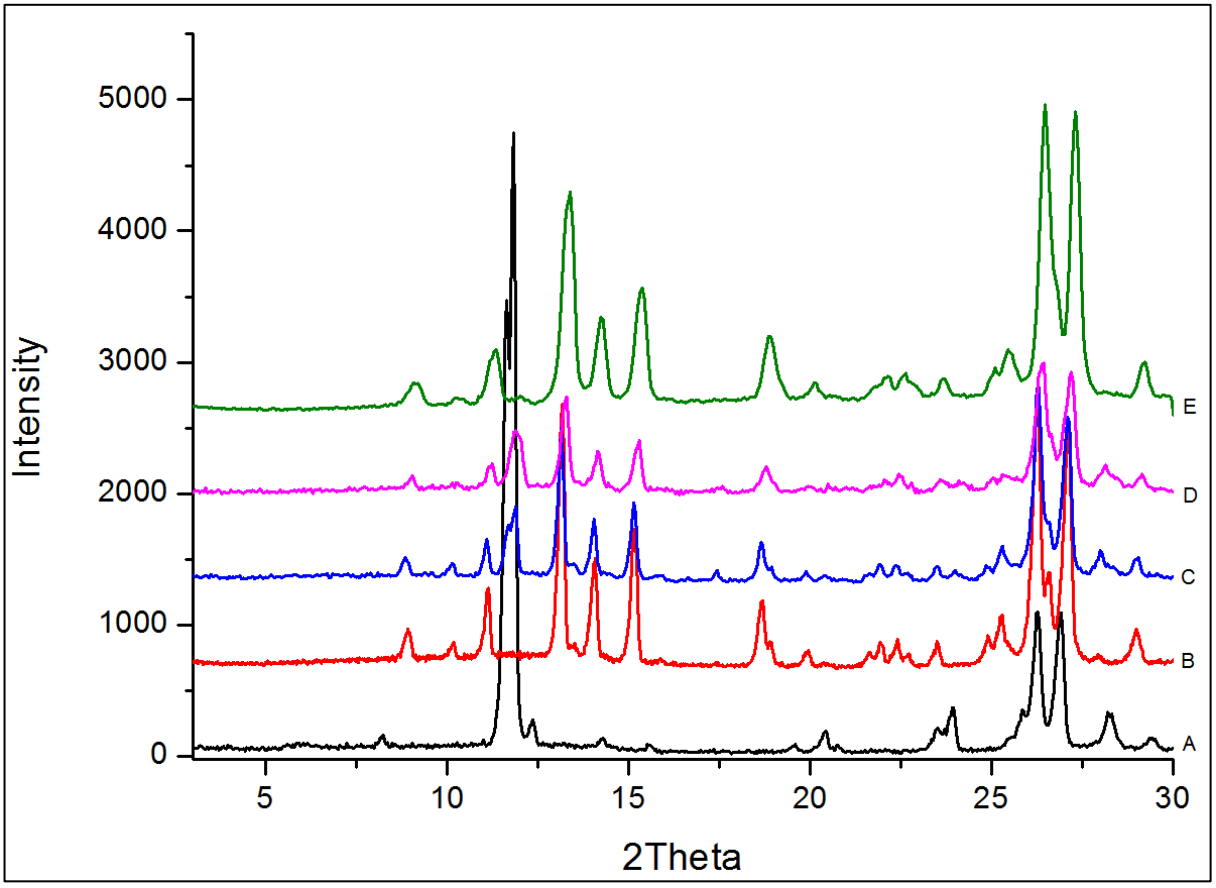

[A: Caffeine, B: CAF:MAL 1:1 PURE CC, C: HME CAF:MAL 1:1, D: HME CAF:MAL 1:1 15% HP55, E: S3M CAF:MAL 1:1 15% HP55]

Figure 6.8 PXRD for caffeine: maleic acid 1:1 cocrystals processed by HME and S3M

These PXRD findings were confirmed by thermal analysis of CAF:MAL 1:1 cocrystal by DSC

6.2.5 DSC

DSC analysis for CAF: MAL 1:1 cocrystal was carried out as described in Section 3.4.1. Crystalline CAF gives a sharp melting endotherm at 238 °C and MAL at 143.26 °C. The phase pure CAF: MAL 1:1 cocrystal shows a sharp melting endotherm at 105 °C (Figure 6.9). The HME and S3M

processed CAF: MAL 1:1 cocrystal with HP55 showed melting endotherms at 103.77 °C and 104.66 °C respectively which confirmed that those are phase pure crystal and support PXRD findings. The HME processed CAF: MAL 1:1 cocrystal without HP55 shows two melting endotherms (C) first one at 100 °C and 105.7 °C. The melting endotherm at 105.7 °C confirms that it has formed phase pure cocrystal, the first endotherm might be due to some eutectic of mixture CAF:MAL 1:1.

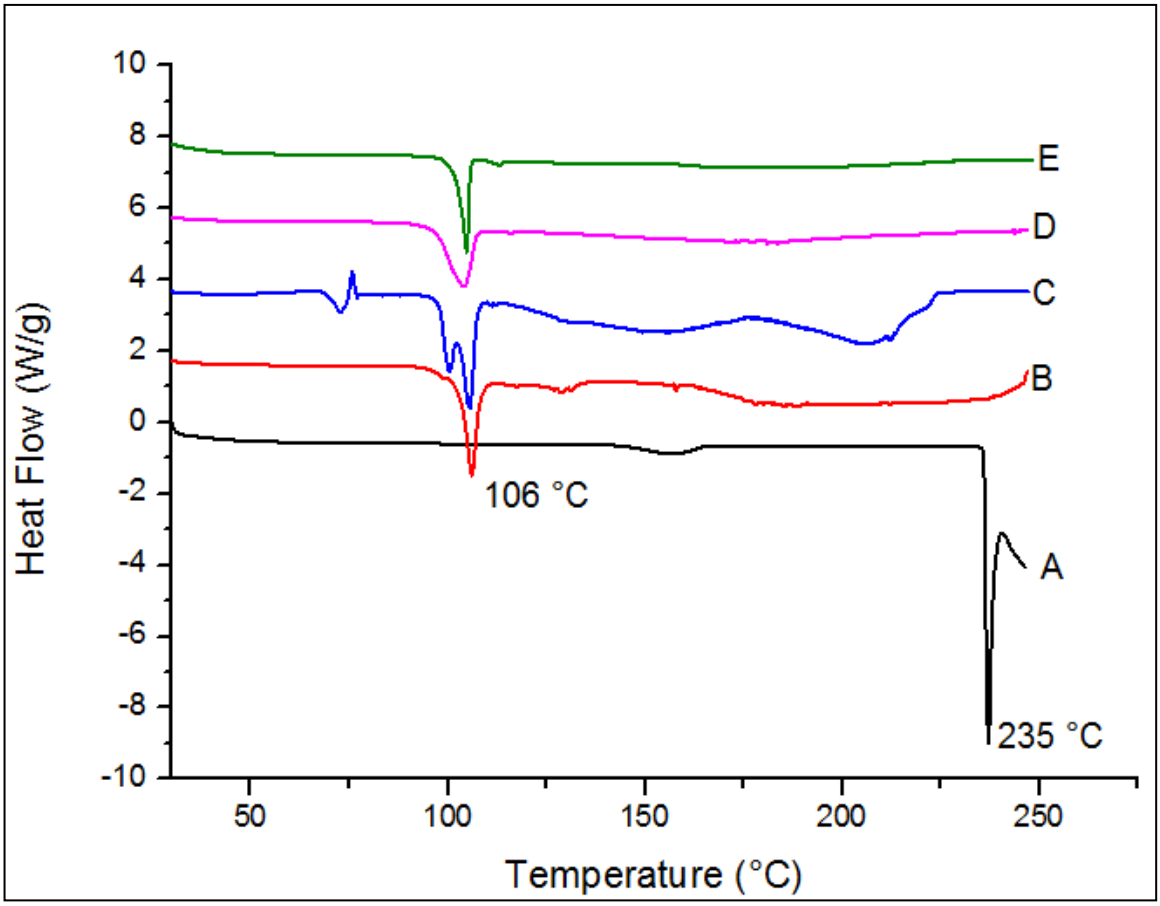

[A: Caffeine, B: CAF:MAL 1:1 PURE CC, C: HME CAF:MAL 1:1, D: HME CAF:MAL 1:1 15% HP55, E: S3M CAF:MAL 1:1 15% HP55]

Figure 6.9 DSC thermograms for caffeine: maleic acid 1:1 cocrystals processed by HME and S3M

6.2.6 SEM

Surface morphology for CAF: MAL 1:1 cocrystals were analysed by SEM as described in Section 3.4.5. Figure 6.10 shows how cocrystals generated by three different processes vary in morphology and surface features.

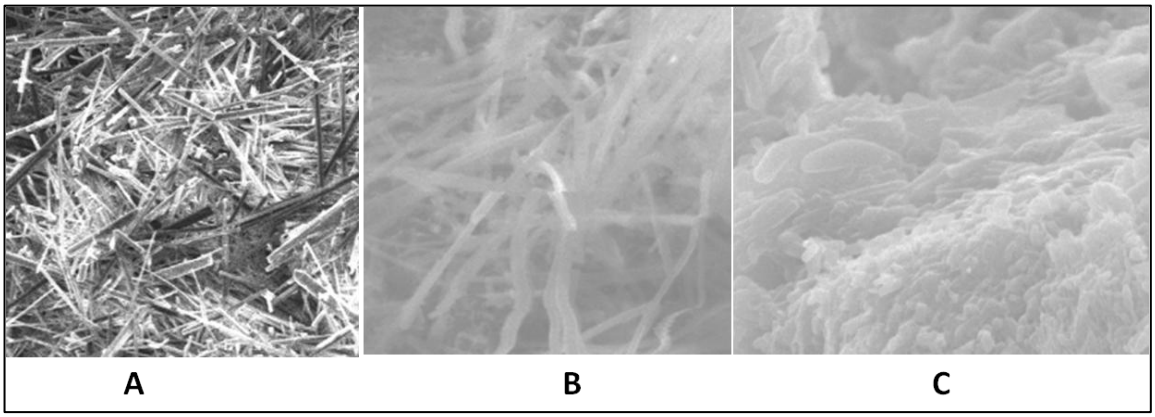

[A- CAF: MAL 1:1 PURE CC, B- S3M CAF: MAL 1:1, C-HME CAF: MAL 1:1]

Figure 6.10 Surface morphology by SEM of caffeine: maleic acid 1:1 cocrystals processed by HME and S3M

CAF: MAL 1:1 pure cocrystals formed a sharp needle like structure and pointed features whereas S3M3 processed cocrystals showed thread like structures distributed within in a matrix like structure. In case of HME processed cocrystals, a compressed form of morphology was observed somewhat like crystals embedded in polymer matrix. This can be due to uniform and highly compacting nature of the extruder screw geometry, which formed the product like a flighted screw shape.

6.2.7 FT-IR

FT-IR analysis for CAF: MAL 1:1 cocrystals was done by as described in Section 3.4.3. As Trask, *et al*. Explained CAF and MAL has excellent hydrogen bonding which exist between their respective functional groups, between –N (imidazole) from CAF and –COOH from MAL. FT-IR for CAF

shows -OH⋯N stretching at 1237 cm^{-1} and 1282 cm^{-1} and -O-C = O stretching in MAL at 1703 and weaker stretching at 1213 due to C-O (Figure 6.11 and Figure 6.12). Pure CAF: MAL cocrystal showed a reduction in the intensity to 1230 and an increase to 1285 cm^{-1} whereas peak intensity for MAL increased to 1707 cm^{-1}, CAF: MAL 1:1 cocrystal processed with HP55 showed exactly similar stretching as pure cocrystal which confirms that cocrystals processed with HP55 are pure in structure and exhibit similar hydrogen bonding as pure cocrystals (Figure 6.12).

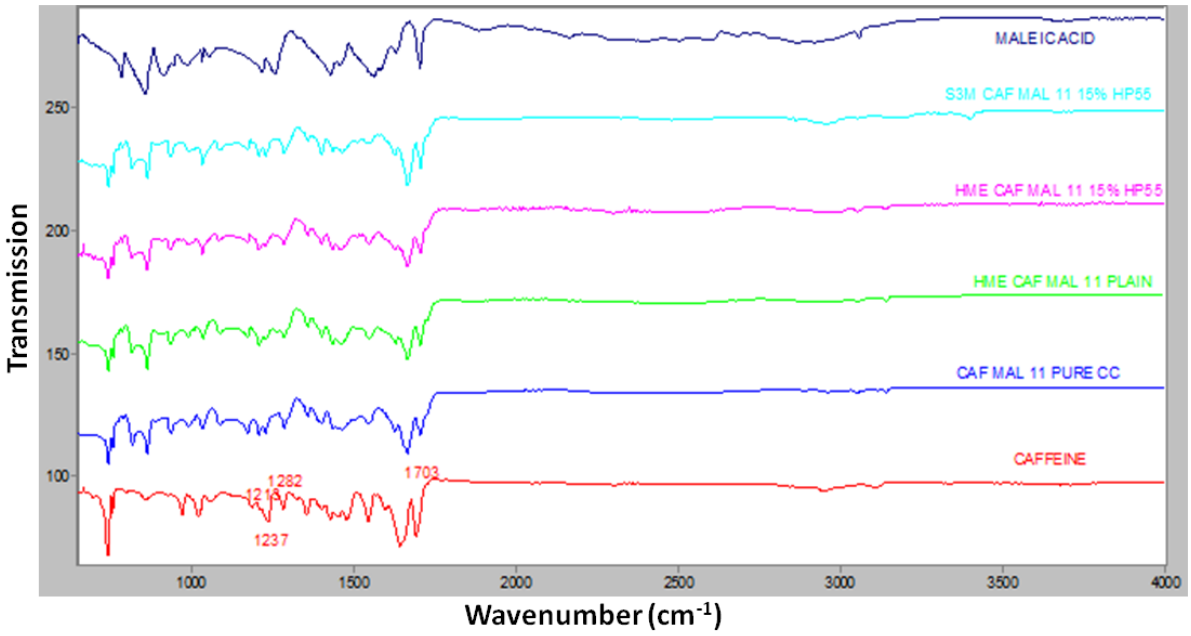

Figure 6.11 FT-IR spectra for caffeine: maleic acid 1:1 cocrystals with HPMCP HP55 processed by HME and S3M

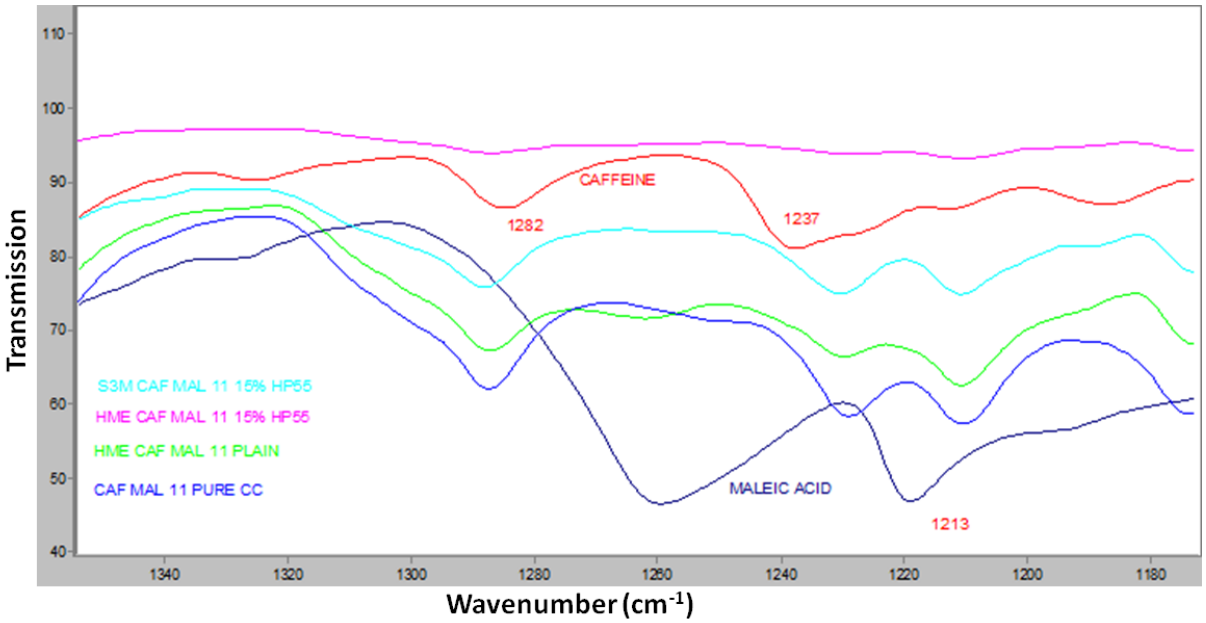

Figure 6.12 FT-IR spectra for caffeine: maleic acid 1:1 cocrystals with HPMCP HP55 processed by HME and S3M

6.2.8 NIR

NIR analysis for CAF: MAL 1:1 cocrystals was carried out as described in Section 3.4.4.

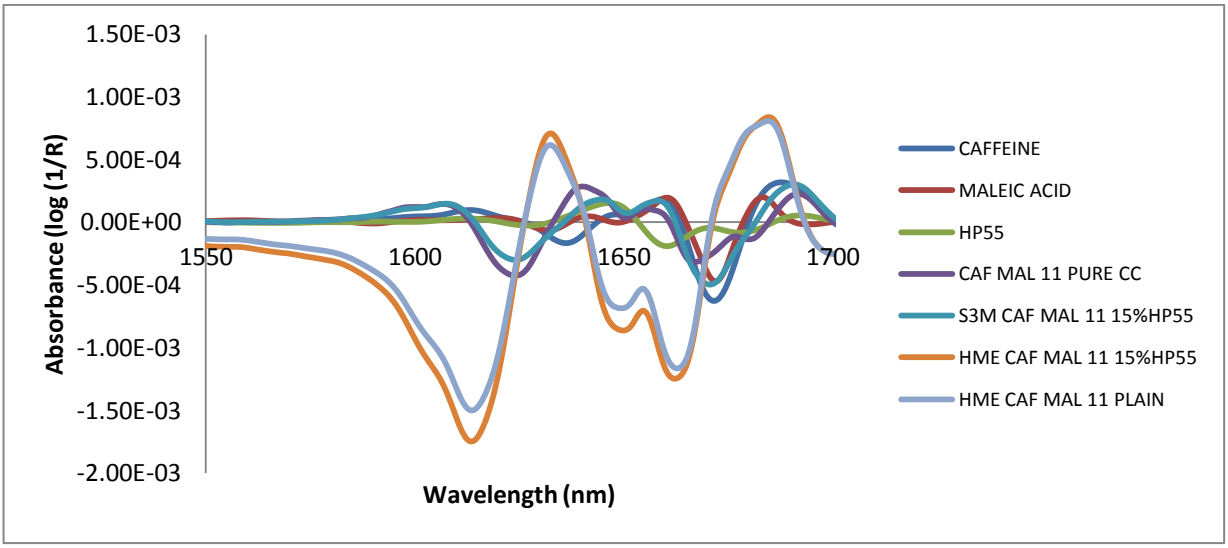

Figure 6.13 NIR spectra for caffeine: maleic acid 1:1 cocrystal with HPMCP HP55 processed HME and S3M

Caffeine showed good NIR absorption in the second overtone region at 1670 and 2249 nm (Figure 6.13) whereas maleic acid showed NIR absorption in first overtone region at 2093 nm. The pure cocrystals of CAF:MAL 1:1 shows NIR absorption at wavelengths 1625 and 2249 nm. These shifts in NIR absorption can be attributed to the hydrogen bond formation between -CONH of caffeine and -COOH of maleic acid. HME processed CAF:MAL 1:1 cocrystals without polymer and cocrystals with 15% HP55 which showed peak shifts to 1665 and 1612 which deviates further absorption shift from pure cocrystals this can be attributed to extent of hydrogen bonding present in the cocrystals. In case of S3M processed cocrystals did not show any change in NIR peak absorption spectra when compared to pure cocrystals which showed that formed cocrystals have good intermolecular bonding.

6.2.9 Dissolution

CAF: MAL 1:1 cocrystal dissolution studies were carried out using HPLC. The dissolution profiles and HPLC method details are described in Section 3.7.1 and 3.7.2 respectively.

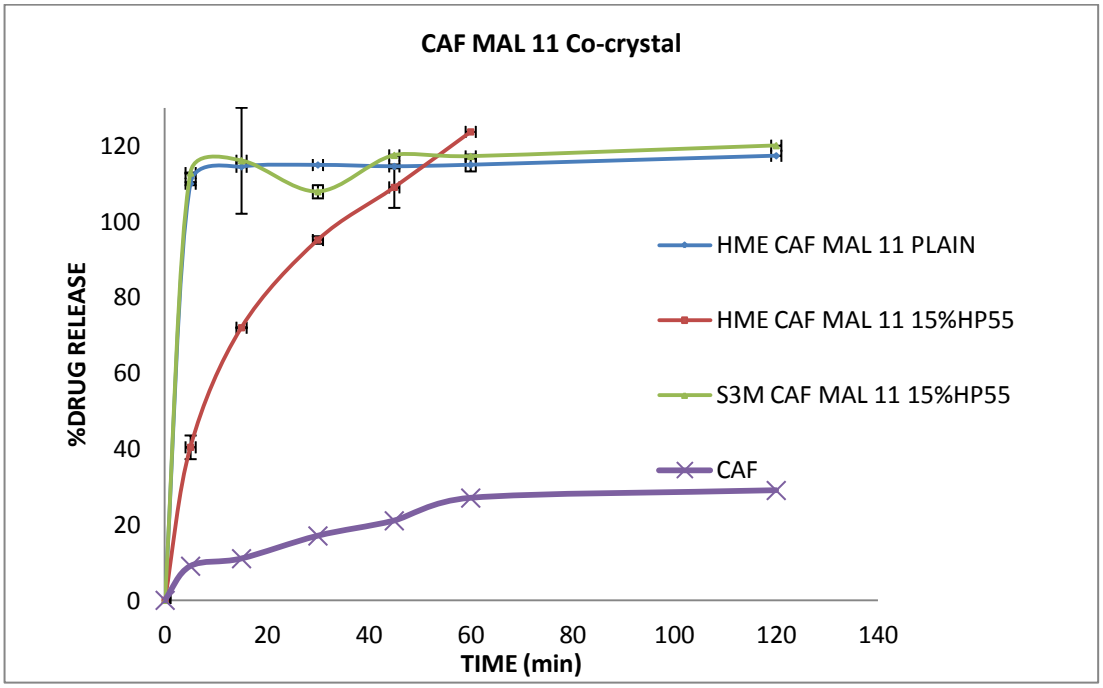

Figure 6.14 Dissolution profiles for caffeine: maleic acid 1:1 cocrystals with HPMCP HP55 processed by HME and S3M

CAF: MAL 1:1 cocrystal processed by HME without polymer and S3M processed with HP55 showed fastest release and released all CAF within 15 mins whereas CAF:MAL 1:1 with 15% HP55 processed by HME showed slow CAF release and took one hour to release 100% drug (Figure 6.14). The delayed release of HME processed cocrystal with polymer can be attributed to the highly compact nature of cocrystal extrudates. Polymer has covered the formed cocrystal during HEM and reduced exposure to surrounding media during dissolution studies. S3M processed cocrystal the

distribution of the formed cocrystal in polymer matrix is such that allowed the dissolution media to penetrate inside the cocrystal matrix and improve overall wettability and hence dissolution.

6.3 Paracetamol: oxalic acid 1:1 cocrystal (PARA: OXAL 1:1)

6.3.1 Crystal structure data

Paracetamol forms good hydrogen bonding with oxalic acid upon solution crystallisation and exhibits a 1:1 cocrystal, Karki *et al*., studied the effect of co-former on compression properties of PARA by forming cocrystal with various co-formers including OXAL.

The crystal structure database bond length and angle details between the PARA: OXAL 1:1 cocrystal are given in Table 6.2

Table 6.2 Crystal structural database and space group details for PARA: OXAL 1:1 cocrystal

Empirical formula	**C8 H9 N O2,C2 H2 O4**
Crystal system	Monoclinic
Space group	P 2_1/c
a (Å)	5.164
b (Å)	11.732
c (Å)	17.593
α (°)	90.000
β (°)	94.329
γ (°)	90.000

The cocrystal structure structure exhibit a hydrogen bond between the functional groups –OH of PARA and –COOH of OXAL as shown in single crystal structure in Figure 6.15

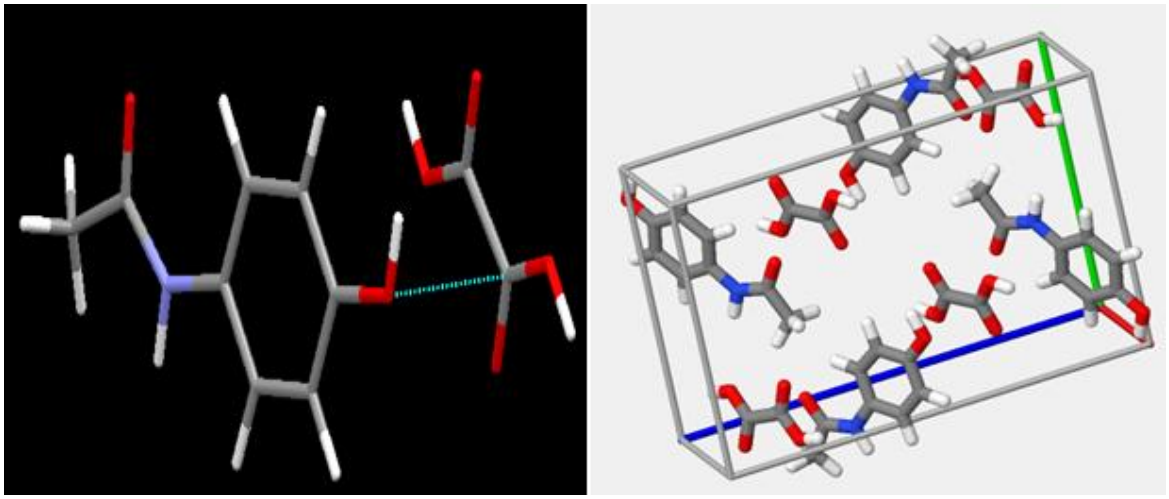

Figure 6.15 Crystal structure of paracetamol: oxalic acid 1:1 cocrystal and crystal packing in unit cell. (adopted from CSD)

Calculated characteristic 2θ values for PARA:OXAL 1:1 cocrystal can be observed in Figure 6.16, showing respective peaks at θ, 9.02, 15.92, 18.18, 21.42 and 27.68

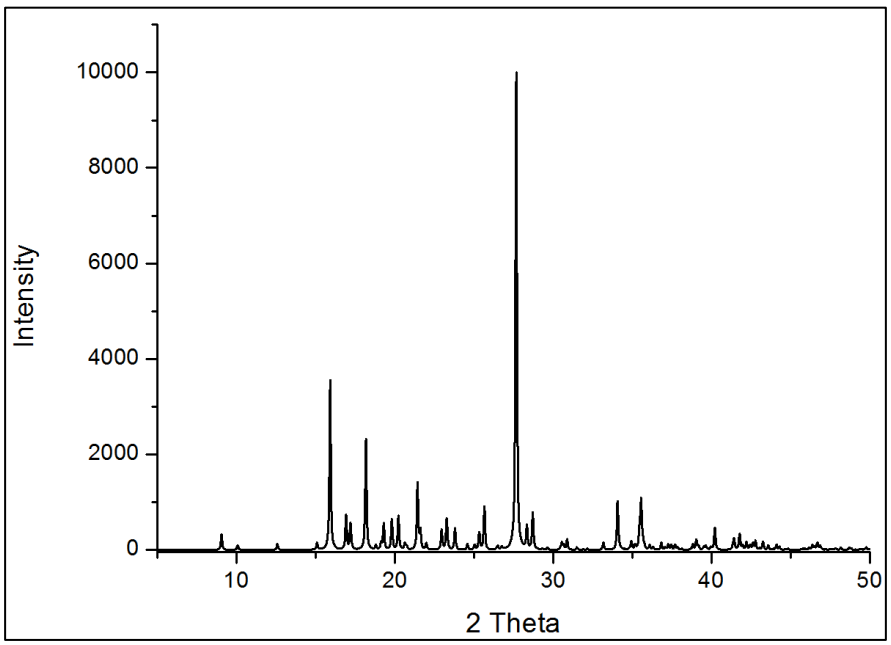

Figure 6.16 Calculated PXRD pattern for paracetamol: oxalic acid 1:1 cocrystal (adopted from CSD-LUJTAM and processed in OriginPro 8).

6.3.2 Processing of cocrystal

Accurately weighed PARA and OXAL in 1:1 molar ratio were mixed well and 15% PEO was added as a processing aid. This mixture was blended using a turbula mixer. The resultant homogenous mixture was fed to S3M3. During the first cycle as soon as the material was fed to the hopper of S3M3 within 10 to 15 secs, the first cycle started to yield an agglomerated thread like product which continued until all material was processed. The difference in processing time of the PEO as aid is highly variable as compared to HP55 in CAF: MAL processing due to variable softening temperatures of two polymers. The short processing time can be attributed to the low melting and low Tg of PEO which made it easier to process PARA:OXAL on S3M3. HME was carried out for PARA: OXAL 1:1 with and without PEO according to the temperature profiles and extrusion parameters described in Section 3.7 and Table 3.10. Resultant end products were analysed by various analytical techniques.

6.3.3 Calibration

As shown in Section 3.6 the PARA and OXAL does not show any overlap between their UV absorbances. Drug release was analysed using UV spectroscopy, and a similar calibration was used for PARA as given in PARA solid dispersion studies.

6.3.4 Characterisation

6.3.4.1 PXRD

PXRD studies for PARA: OXAL were carried out as described in Section 3.4.2. The respective 2θ values for pure PARA: OXAL 1:1 cocrystal shows characteristic peaks at 9.02, 15.92, 18.18, 21.42 and 27.68 as shown in Figure 6.17. The HME and S3M3 processed PARA:OXAL 1:1 with PEO showe identical 2θ values in PXRD with slightly variable intensities which can be attributed to the process variability. The similar 2θ values confirm the HME and S3M3 processes yielded a pure cocrystal. HME processed PARA: OXAL 1:1 without PEO showed very low intensity 2θ values in addition to some characteristic peaks for PARA and OXAL which show that there was partial cocrystal conversion with some impurities from parent materials.

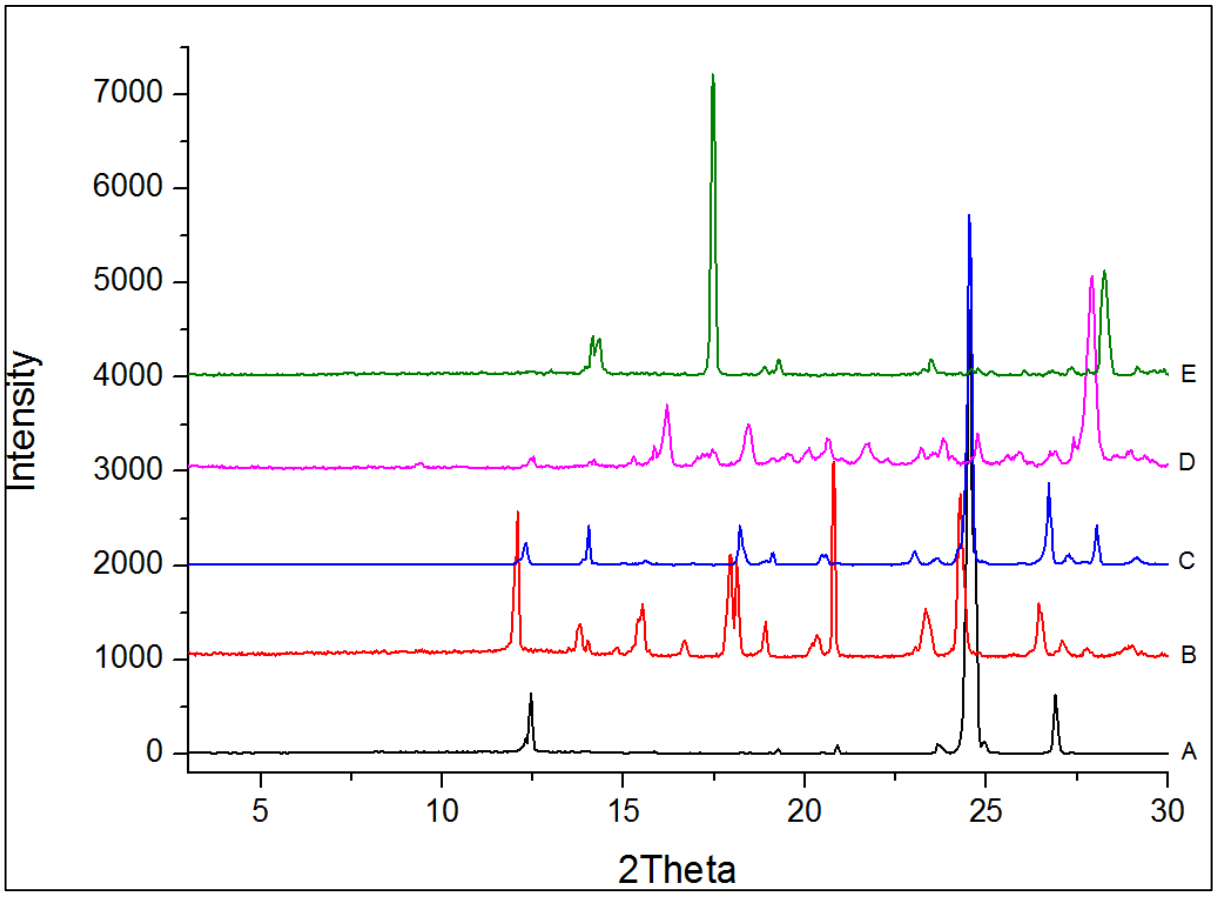

[A: Paracetamol, B: PARA: OXAL 1:1 PURE CC, C:HME PARA:OXAL 1:1, D: HME PARA:OXAL 1:1 15% PEO, E: S3M PARA:OXAL 1:1 15% PEO]

Figure 6.17 PXRD for paracetamol: oxalic acid 1:1 cocrystals processed by HME and S3M

6.3.4.2 DSC

DSC analysis was carried out as described in section 3.4.1. DSC results complement the PXRD findings. PARA showed a sharp melting endotherm at 169.93 °C and OXAL at 100.23 °C, whereas PARA: OXAL 1:1 cocrystal gave a characteristic melting endotherm at 151 °C (Figure 6.18). HME and S3M3 processed cocrystals also show similar endotherms matching calculated melting endotherm values of pure cocrystal at 149.95 in case of HME and 151.06 in case of S3M3. This confirmed formation of phase pure cocrystal.

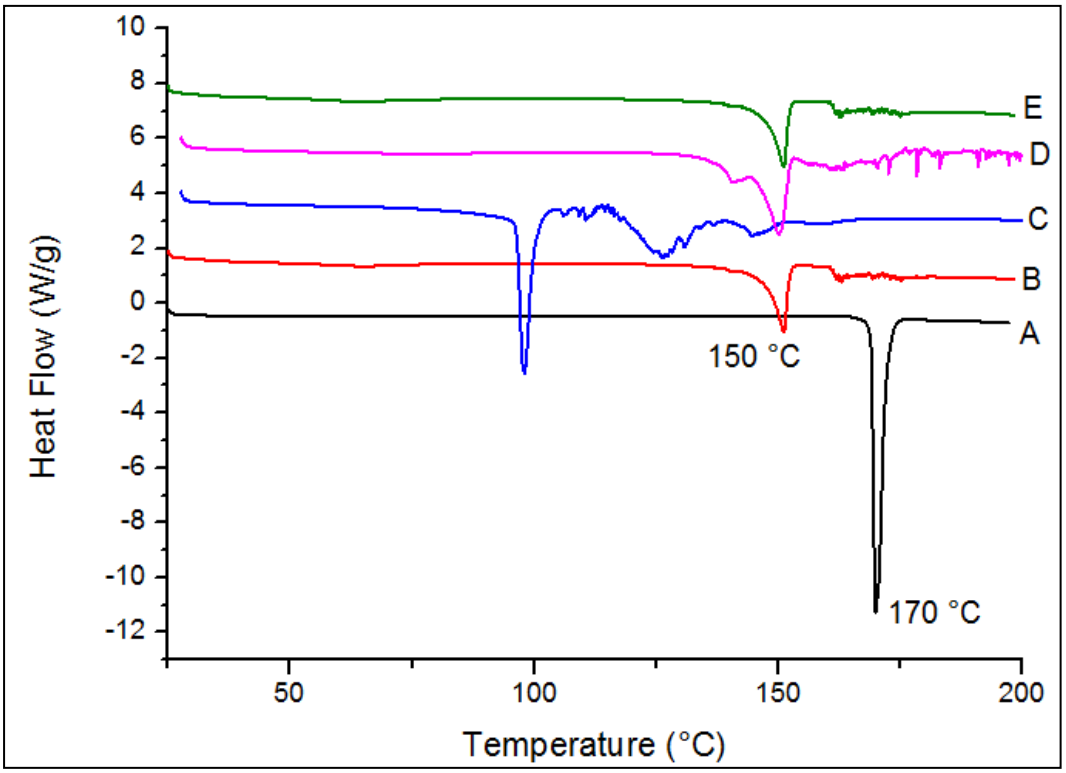

[A: Paracetamol, B: PARA:OXAL 1:1 PURE CC, C:HME PARA:OXAL 1:1, D: HME PARA:OXAL 1:1 15% PEO, E: S3M PARA:OXAL 1:1 15% PEO]

Figure 6.18 DSC thermograms for paracetamol:oxalic acid 1:1 cocrystals processed by HME and S3M

In case of HME processed PARA:OXAL 1:1 cocrystal without PEO shows melting endotherm at 98 °C which differs significantly from pure cocrystal melting endotherm and matches the endotherm of OXAL, which can be attributed to a major OXAL impurity in the formed cocrystal, these findings supports PXRD results for partial cocrystal formation.

6.3.4.3 S3M

Surface morphology studies for PARA: OXAL cocrystals were carried out as described in Section 3.4.5.

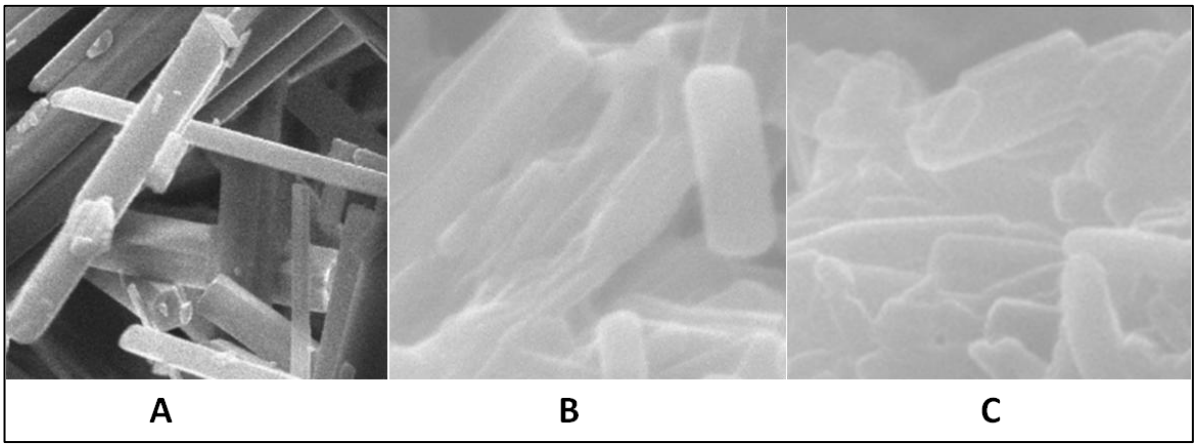

[A- PARA: OXAL 1:1 PURE CC, B- S3M PARA: OXAL 1:1, C-HME PARA: OXAL 1:1]

Figure 6.19 Surface morphology by SEM of paracetamol: oxalic acid 1:1 cocrystals processed by HME and S3M and solution method

As Figure 6.19 shows that cocrystals produced by solution method exhibited sharp, needle like structures whereas, HME and S3M3 processed cocrystals showed compact and broken crystals embedded in the polymer matrix. There was little difference between HME and S3M3 processed cocrystals. It was very difficult to vary the broken crystal size as crystal size was very much different; there was no uniformity in the size and shape of the crystals.

6.3.4.4 FT-IR

FT-IR analysis for PARA: OXAL 1:1 cocrystals was carried out using the method described in Section 3.4.3. PARA showed –OH stretching at 3324 cm^{-1} and 2982 cm^{-1} whereas OXAL showed characteristic –COOH stretching at 3417 and 1686 cm^{-1} and stretching for unsaturation in structure was at 1653 and 1610 cm^{-1}. PARA (Figure 6.20). PARA: OXAL pure cocrystal showed characteristic stretching shift at 3420 whereas cocrystal with 15% PEO showed stretching shifts at 3344 and 3386 cm^{-1} in both the cases HME and S3M3 (Figure 6.21). Karki *et al*., has explained characteristic stretching

at 3384 cm^{-1} can indicate hydrogen bond formation between –CONHR of PARA and –COOH of OXAL which was similarly observed in HME and S3M processed samples and in the case of solution cocrystal as well.

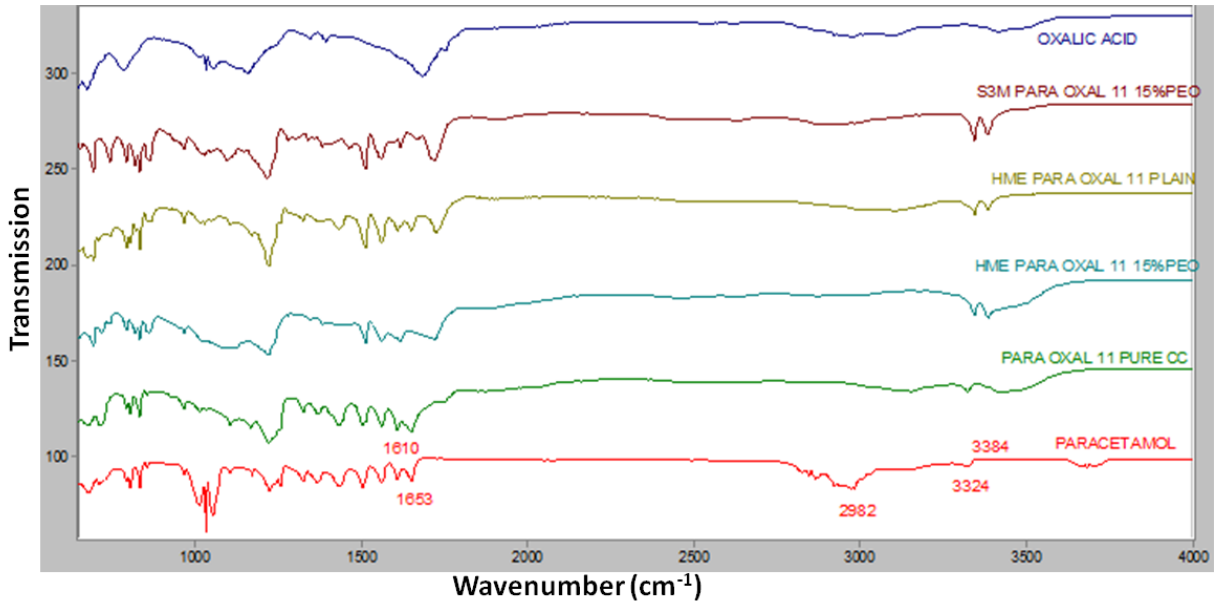

Figure 6.20 FT-IR spectra for paracetamol: oxalic acid 1:1 cocrystals with PEO processes by HME and S3M

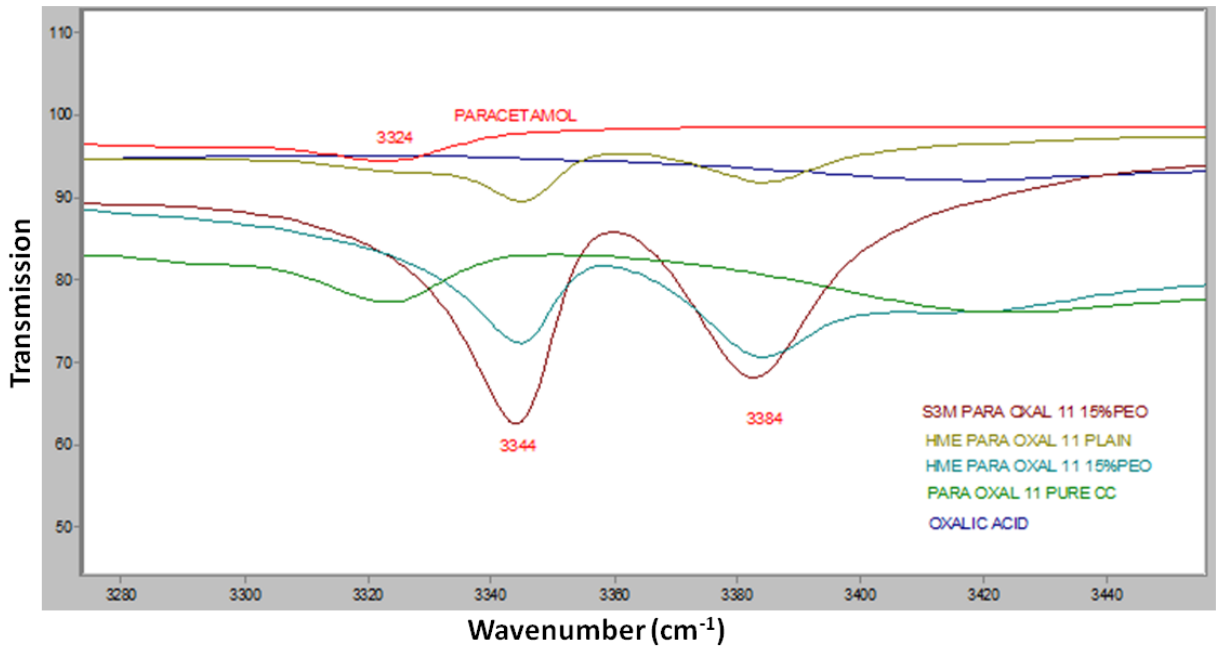

Figure 6.21 FT-IR spectra for paracetamol: oxalic acid 1:1 cocrystal with PEO processed by HME and S3M

6.3.4.5 NIR

NIR analysis was carried out as described in Section 3.4.4.

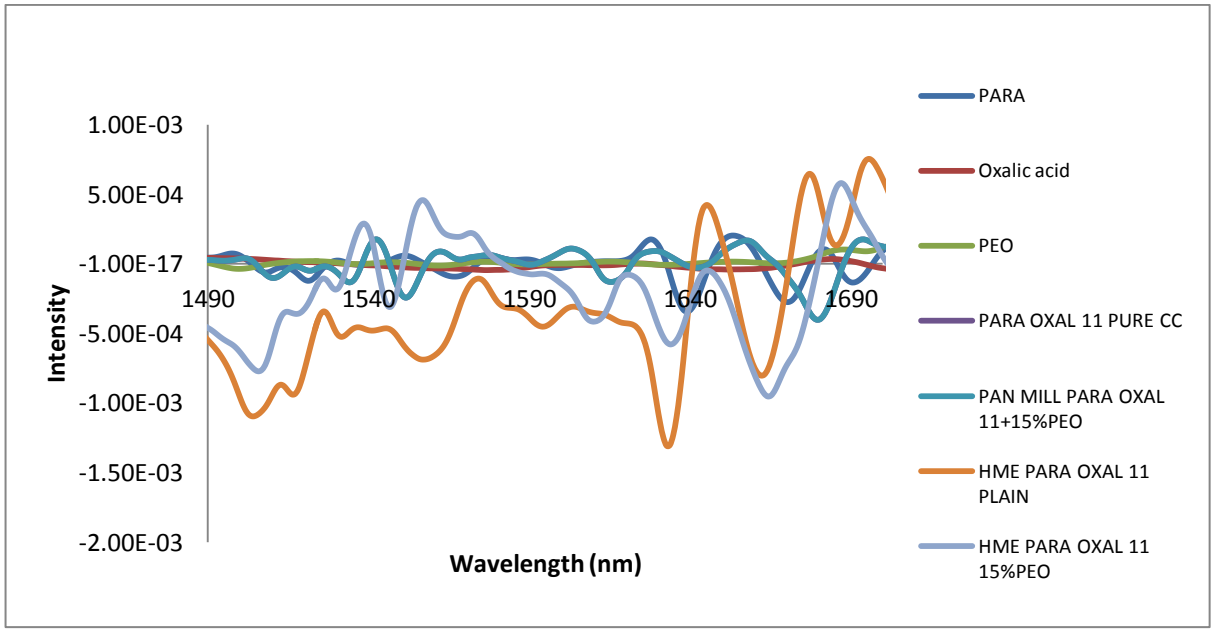

Figure 6.22 NIR spectra for paracetamol: oxalic acid 1:1 cocrystals processed by HME and S3M

Paracetamol shows good NIR absorption spectra in the second overtone region at 1639 and 1670 nm respectively. Oxalic acid owing to its acid functional group (-COOH) did not show NIR absorption spectra which can be attributed to the low sensitivity of detection for oxalic acid in the near infrared region. The pure cocrystal for PARA:OXAL 1:1 showed good NIR absorption at 1615 and 1680 nm which can be attributed to the formation of hydrogen bond between the functional groups of paracetamol (-CONHR) and oxalic acid (-COOH) (Figure 6.22). Cocrystals processed by S3M showed identical NIR spectra absorption at 1615 and 1680 nm whereas HME processed paracetamol cocrystals with and without polymer showed identical NIR spectra absorption at 1634 and 1664. This change in absorption spectra can be attributed to the extent of hydrogen bonding and purity of the cocrystals formed.

6.3.4.6 Dissolution

Dissolution studies for PARA: OXAL cocrystal were carried out as per the dissolution parameters followed for PARA solid dispersion. Dissolution studies showed cocrystal prepared by solution method exhibited fastest drug release and release 100% drug within 10mins. HME processed PARA:OXAL cocrystals without polymer showed second highest dissolution rate; 100% release in 20 mins (Figure 6.23). It was observed that S3M3 and HME processed cocrystal with PEO showed slow drug release; and HME processed cocrystals exhibited slowest release. The slow release of PARA from HME and S3M3 processed cocrystal with PEO was due to the compact and dense nature of product which may have hampered the media penetration inside cocrystal matrix and resulted in slow or less exposure to media.

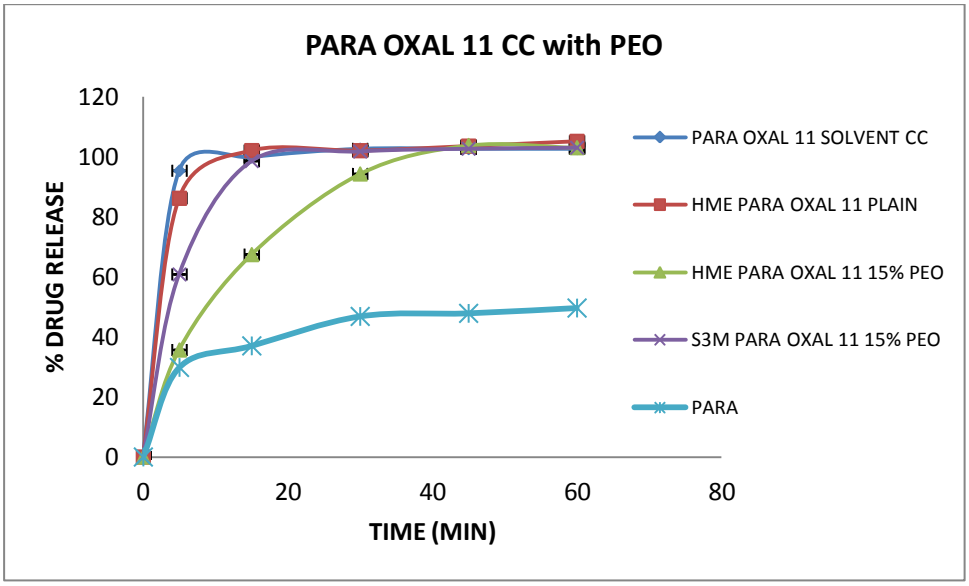

Figure 6.23 Dissolution profiles for paracetamol: oxalic acid 1:1 cocrystals with PEO by HME and S3M

6.4 Carbamazepine cocrystal

CBZ was explored for cocrystal formation with four co-formers salicylic acid, saccharin, nicotinamide and glutaric acid. CBZ: SAL pair was studied with different levels of polymers as processing aid in HME and S3M3 PEO (levels 5-25% w/w) and PVP VA64 (15-25% w/w), CBZ with other co-formers was studied with 15% PEO as a processing aid during HME and S3M3.

6.4.1 Carbamazepine: salicylic acid 1:1 cocrystal (CBZ: SAL 1:1)

6.4.1.1 Crystal structure data

CBZ and SAL forms a cocrystal in 1:1 molar which shows unique structural characteristics different from CBZ and SAL, CBZ SAL forms a cocrystal with a monoclinic form. The cocrystal exhibits hydrogen bonds between the $–NH_2$

of CBZ and –COOH of SAL (Figure 6.24). The cocrystal structural data, group spacing, bond angles and length details are given in Table 6.3.

Table 6.3 Crystal structural database and space group details for CBZ: SAL 1:1 cocrystal

Empirical formula	$C_{15}H_{12}N_2O$, $C_7H_6O_3$
Crystal system	Monoclinic
Space group	$P2_1/n$
a (Å)	5.106
b (Å)	19.783
c (Å)	18.328
α (°)	90.000
β (°)	97.903
γ (°)	90.000

The crystal structure of CBZ: SAL 1:1 cocrystal developed and adopted from CSD database and its crystal packing in unit cell is given in Figure 6.24. Figure 6.25 shows PXRD for CBZ: SAL 1:1 cocrystal which shows characteristic 2θ values at 6.6, 8.92, 9.72 and 13.22.

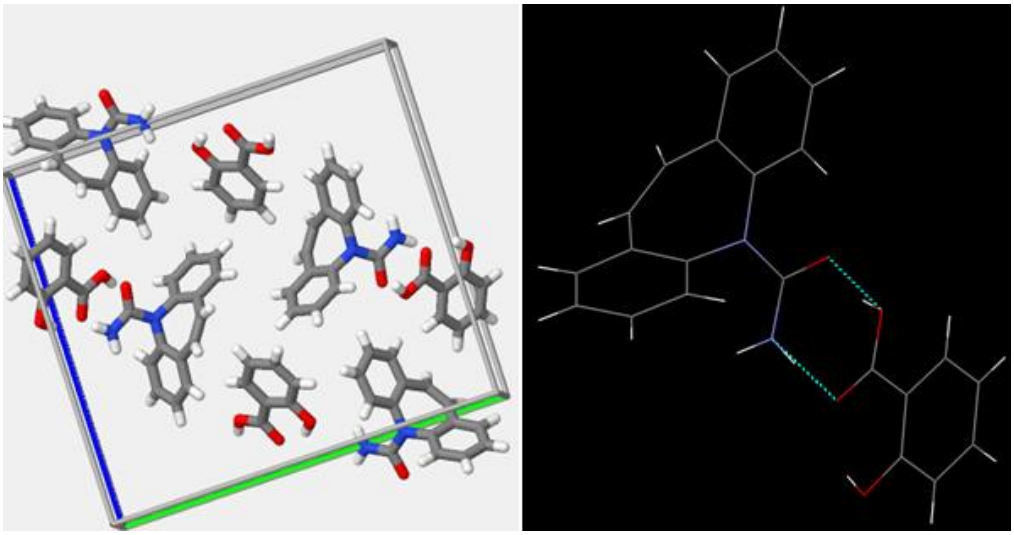

Figure 6.24 Crystal structure of carbamazepine: salicylic acid 1:1 cocrystal and crystal packing in unit cell. (adopted from CSD)

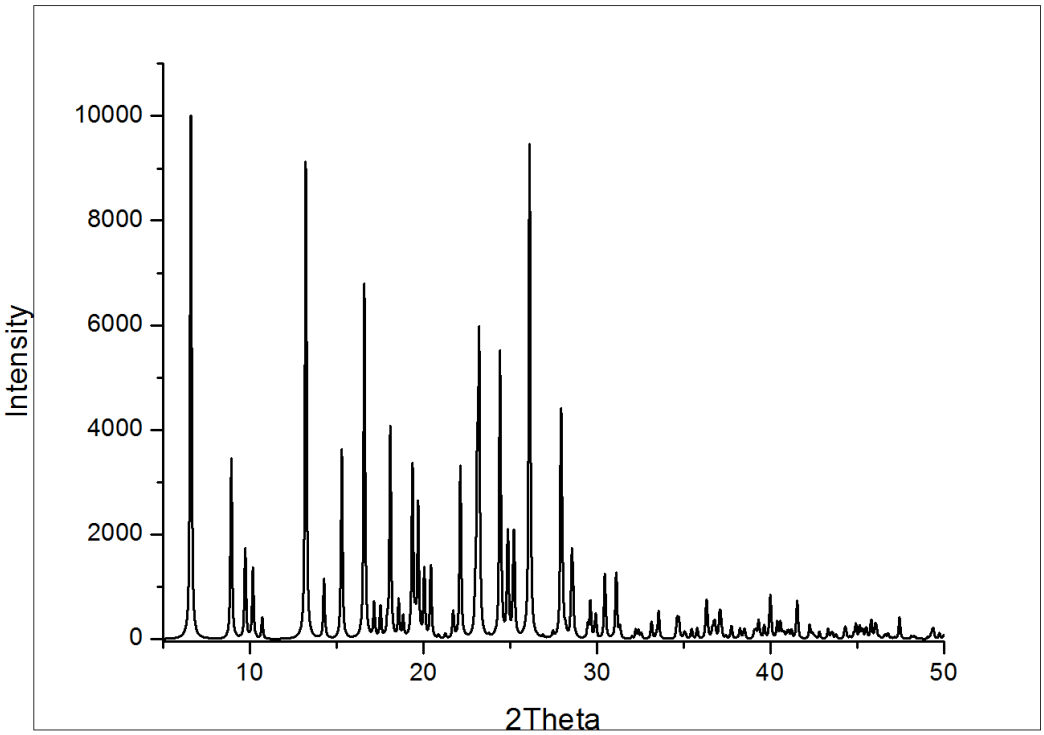

Figure 6.25 Calculated PXRD pattern for carbamazepine: salicylic acid 1:1 cocrystal (adopted from CSD- MOXWAY and processed in OriginPro 8)

6.4.1.2 CBZ UPLC calibration

The UPLC calibration curve for CBZ was linear over concentration range of 10-100 ug/ml. The linearity equation was calculated using calibration curve, slope of the equation was 2146.9, constant 2084.6 and R^2 0.9998 (Figure 6.26). The calibration equation was used to calculate the amount of CBZ released.

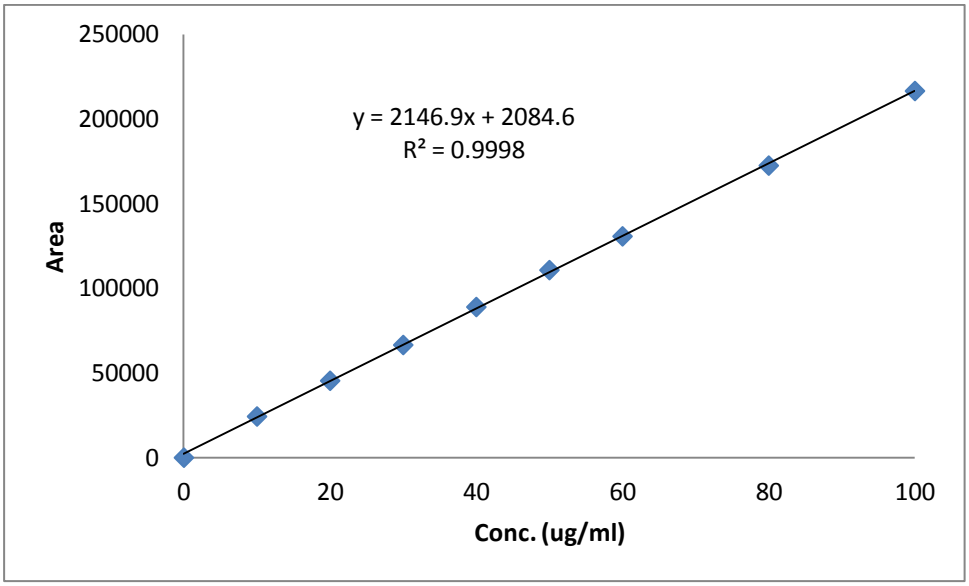

Figure 6.26 Carbamazepine calibration curve using UPLC at 288nm

CBZ shows a retention time in UPLC of 2.3 mins as shown in figure 6.26.

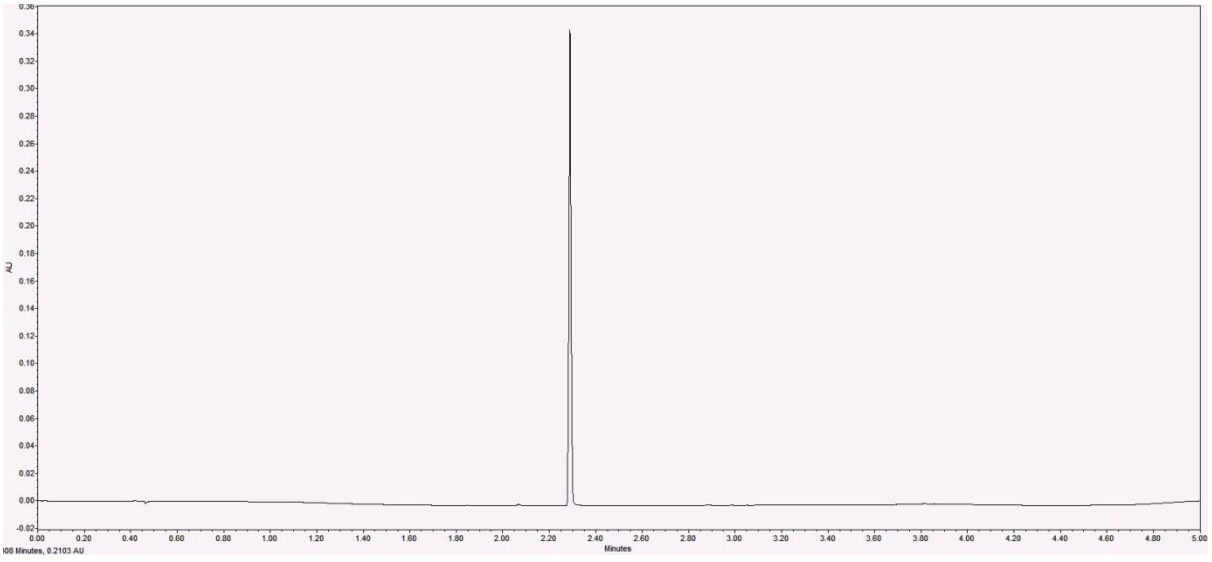

Figure 6.27 Carbamazepine chromatogram from UPLC analysis

The UPLC calibration curve for SAL was linear over concentration range of 10-100 ug/ml. The linearity equation was calculated using calibration curve, slope of the equation was 998.04, constant -1263.6 and R^2 0.9968. SAL shows retention time in UPLC at 1.8 min (Figure 6.28).

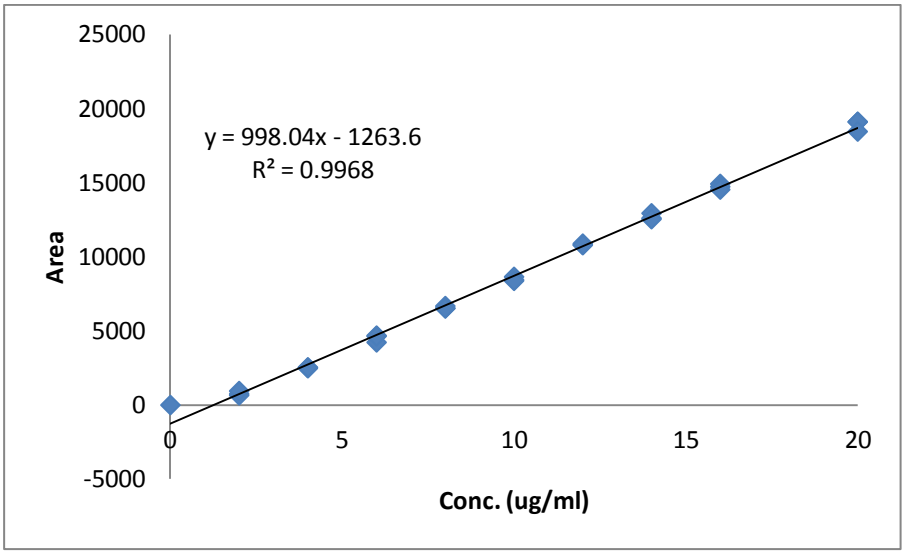

Figure 6.28 Salicylic acid calibration curve using UPLC at 296nm

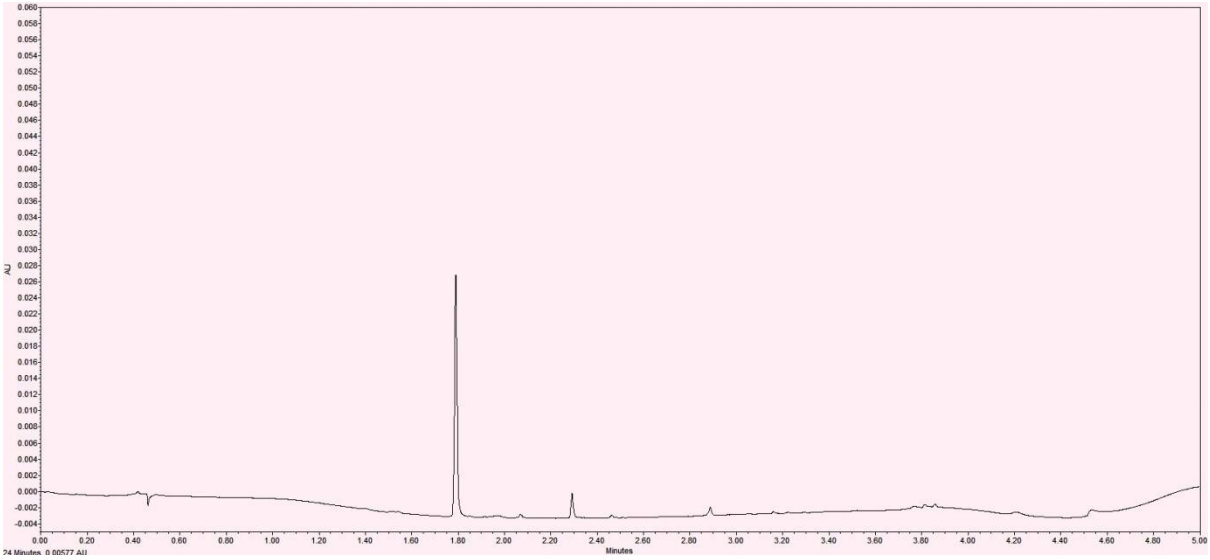

Figure 6.29 Salicylic acid chromatogram in UPLC analysis

6.4.1.3 PXRD

PXRD studies for CBZ: SAL 1:1 cocrystals were carried out as per Section 3.4.2. The PXRD for CBZ: SAL 1:1 pure cocrystal produced using the solution method shows characteristic 2θ values at 6.48, 8.84, 13.08, 16.44 which were similar to those what was observed in the CSD structure for CBZ:

SAL 1:1 cocrystal. CBZ:SAL 1:1 with 5%, 10% PEO and 15%, 25% VA64 showed identical 2θ values to the pure cocrystal which confirms that S3M3 and HME produced pure cocrystal with these polymer aids in given concentrations (Figure 6.30 and Figure 6.31).

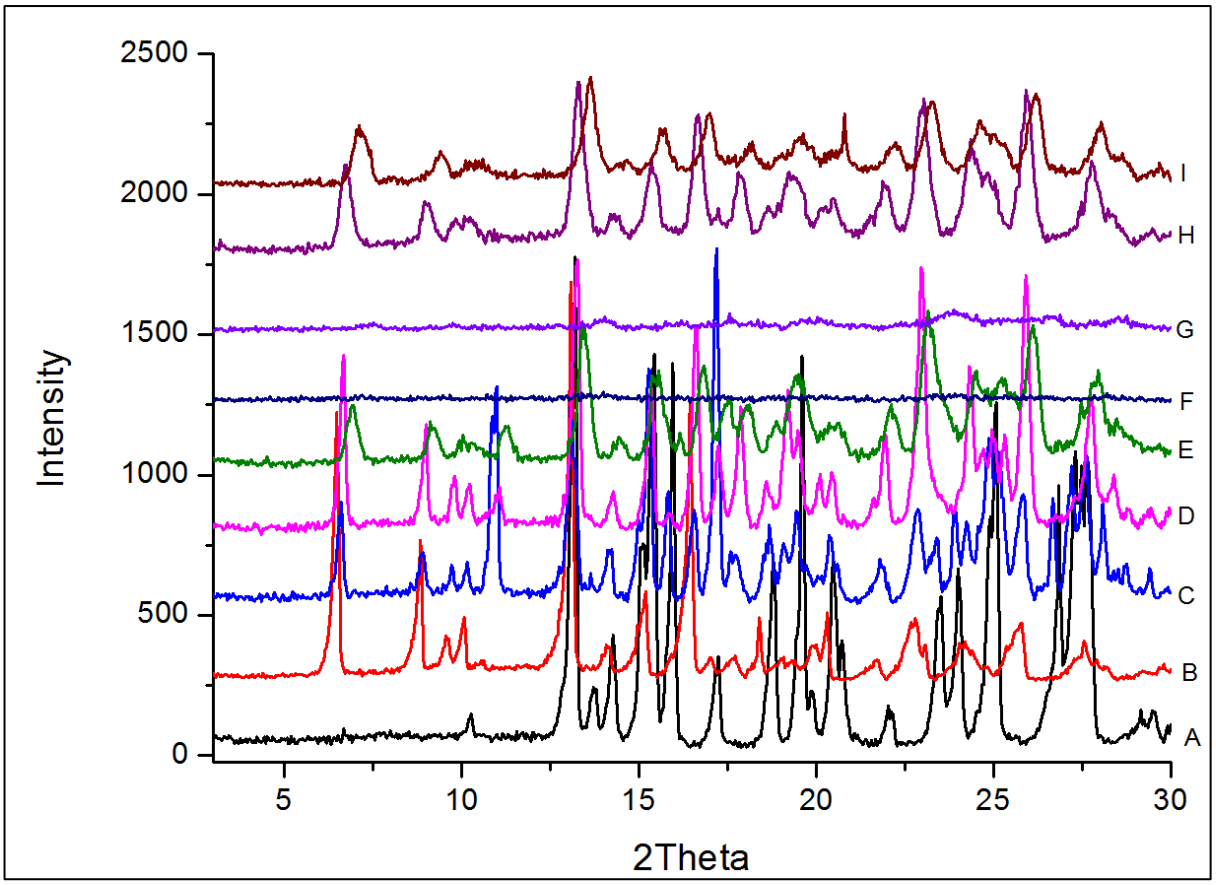

[A: Carbamazepine, B: CBZ:SAL 1:1 PURE CC, C: HME CBZ:SAL 1:1, D: HME CBZ:SAL 1:1 5% PEO, E: HME CBZ:SAL 1:1 10% PEO, F: HME CBZ:SAL 1:1 15% PEO, G: HME CBZ:SAL 1:1 25% PEO, H: HME CBZ:SAL 1:1 15% VA64, I: HME CBZ:SAL 1:1 25% VA64]

Figure 6.30 PXRD for carbamazepine: salicylic acid 1:1 cocrystals processed by HME

15%, 25% PEO in HME and 25% PEO in S3M3 batches showed reduced or non-characteristic intensities in the end product, which can be result of the higher polymer concentrations having solubilised CBZ and SAL and turned into an amorphous system. In the case of the 15% PEO S3M3 batch, strong

characteristic 2θ peaks were observed as shown by pure cocrystal, which shows the formation of pure cocrystal

The PEO polymer added in 15%, 25% in HME and 25% in S3M3 turned the processed CBZ: SAL 1:1 in to an amorphous system. This may have happened due to the high shear applied in S3M3 and HME which made the crystalline CBZ and SAL soluble in PEO at its softening/ melting, PEO acted as a solvent in the melt state which solubilised CBZ and SAL. The surface of the end product showed smooth features with very less exposure to X-rays during PXRD studies. Addition of a polymer processing aid plays an important role during these high shear processes and thus polymer concentration and type of polymer should be selected carefully as these types of results were not observed with PVP VA64.

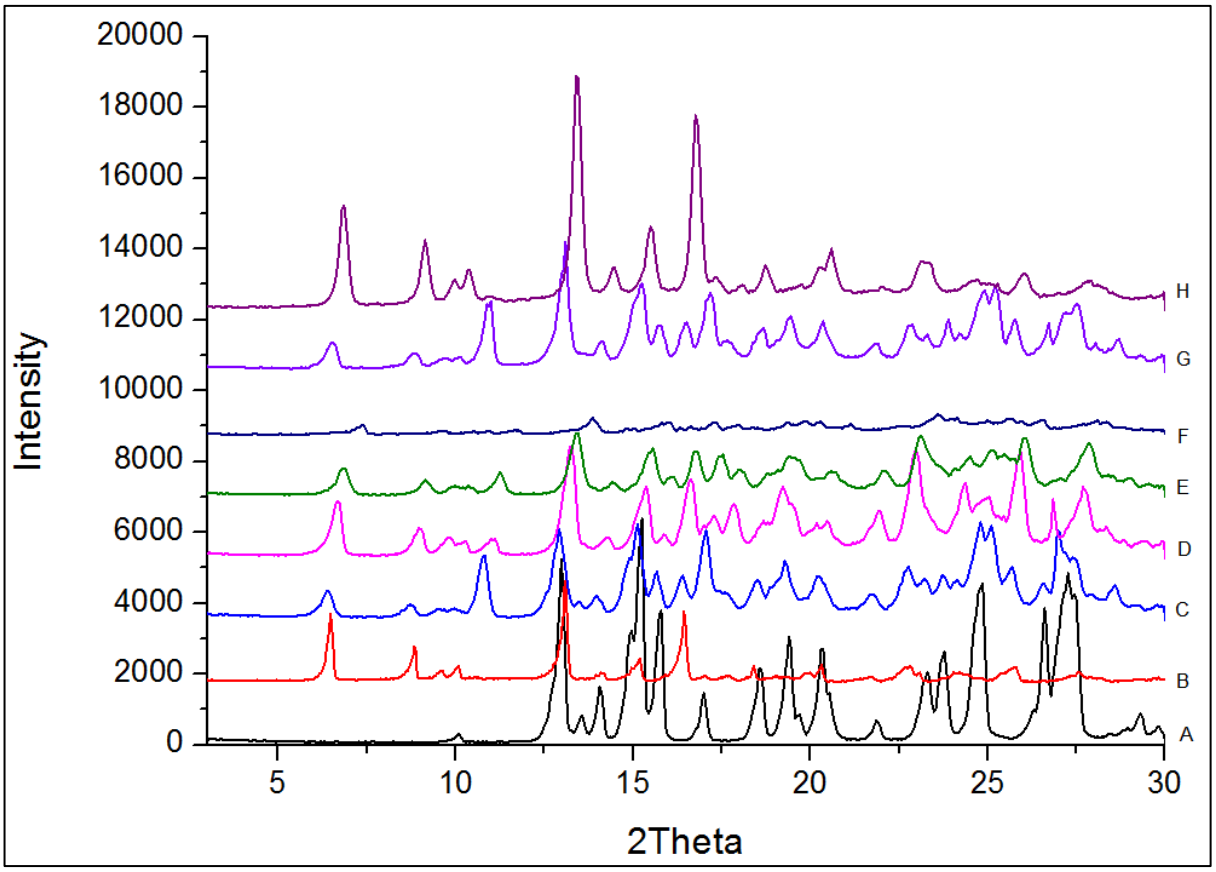

[A: Carbamazepine, B: CBZ:SAL 1:1 PURE CC, C: S3M CBZ:SAL 1:1 5% PEO, D: S3M CBZ:SAL 1:1 10% PEO, E: S3M CBZ:SAL 1:1 15% PEO, F: S3M CBZ:SAL 1:1 25% PEO, G: S3M CBZ:SAL 1:1 15% VA64, H: S3M CBZ:SAL 1:1 25% VA64]

Figure 6.31 PXRD for carbamazepine: salicylic acid 1:1 cocrystals processed by S3M

6.4.1.4 DSC

DSC analysis was carried out for CBZ: SAL 1:1 as described in Section 3.4.1. Crystalline CBZ showed a sharp melting endotherm at 191.26 °C and a small melting endotherm at 175 °C due to conversion of form III to I as discussed in chapter 5. SAL shows a melting endotherm at 160 °C, CBZ: SAL 1:1 cocrystal shows melting endotherm at 159 °C which is close to SAL's endotherm (Figure 6.32 and Figure 6.33). All the polymer aided

CBZ:SAL 1:1 cocrystal by HME and S3M3 showed similar melting endotherms with slightly variable intensities.

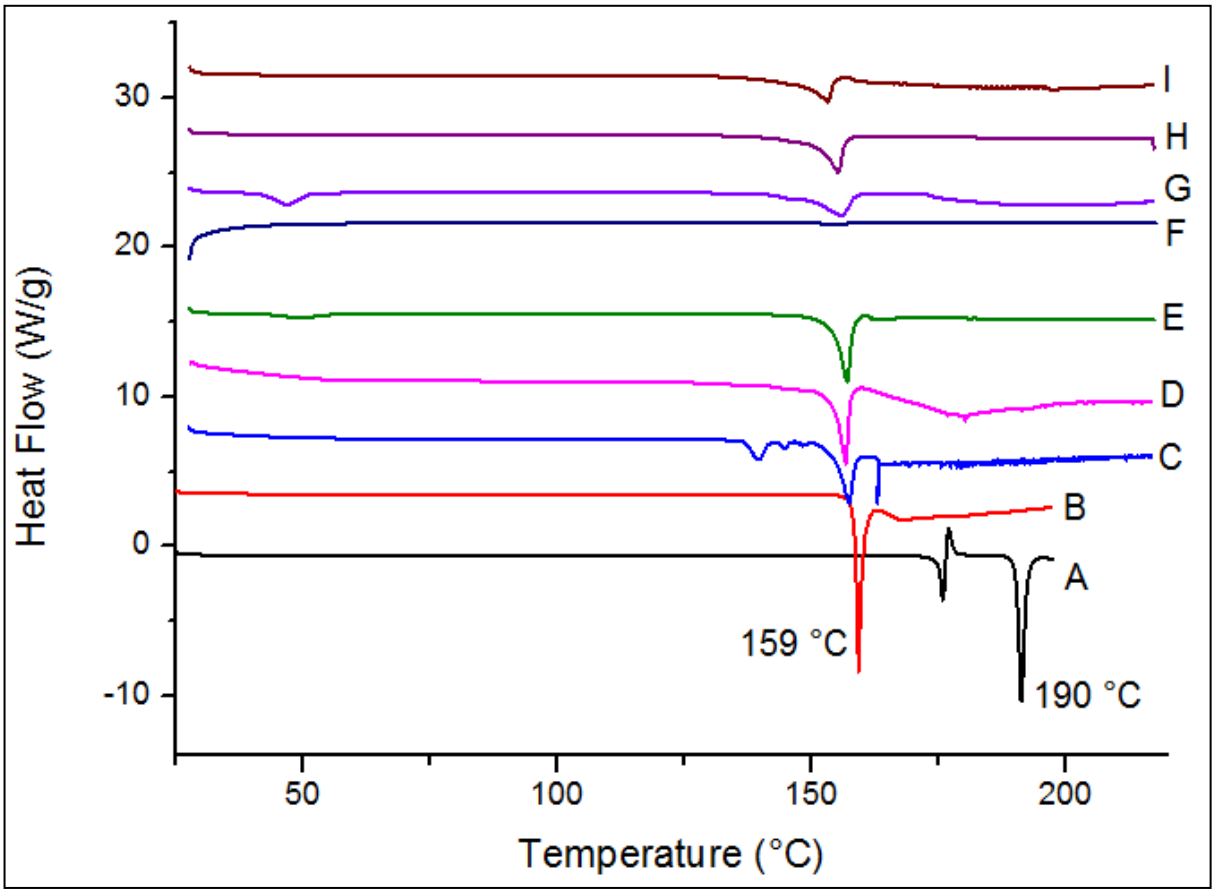

[A: Carbamazepine, B: CBZ:SAL 1:1 PURE CC, C: HME CBZ:SAL 1:1, D: HME CBA:SAL 1:1 5% PEO, E: HME CBZ:SAL 1:1 10% PEO, F: HME CBZ:SAL 1:1 15% PEO, G: HME CBZ:SAL 1:1 25% PEO, H: HME CBZ:SAL 1:1 15% VA64, I: HME CBZ:SAL 1:1 25% VA64]

Figure 6.32 DSC thermograms for carbamazepine:salicylic acid 1:1 cocrystals processed by HME

No melting endotherm was observed for processing aid polymers (PEO and VA64) which showed that at the polymers melting point, CBZ and SAL may have utilised all the polymer as a solvent system to convert whole system in cocrystal matrix. DSC findings complement PXRD results and also confirmed

that a higher concentration of PEO was also able to form cocrystal which was bit difficult to understand from PXRD.

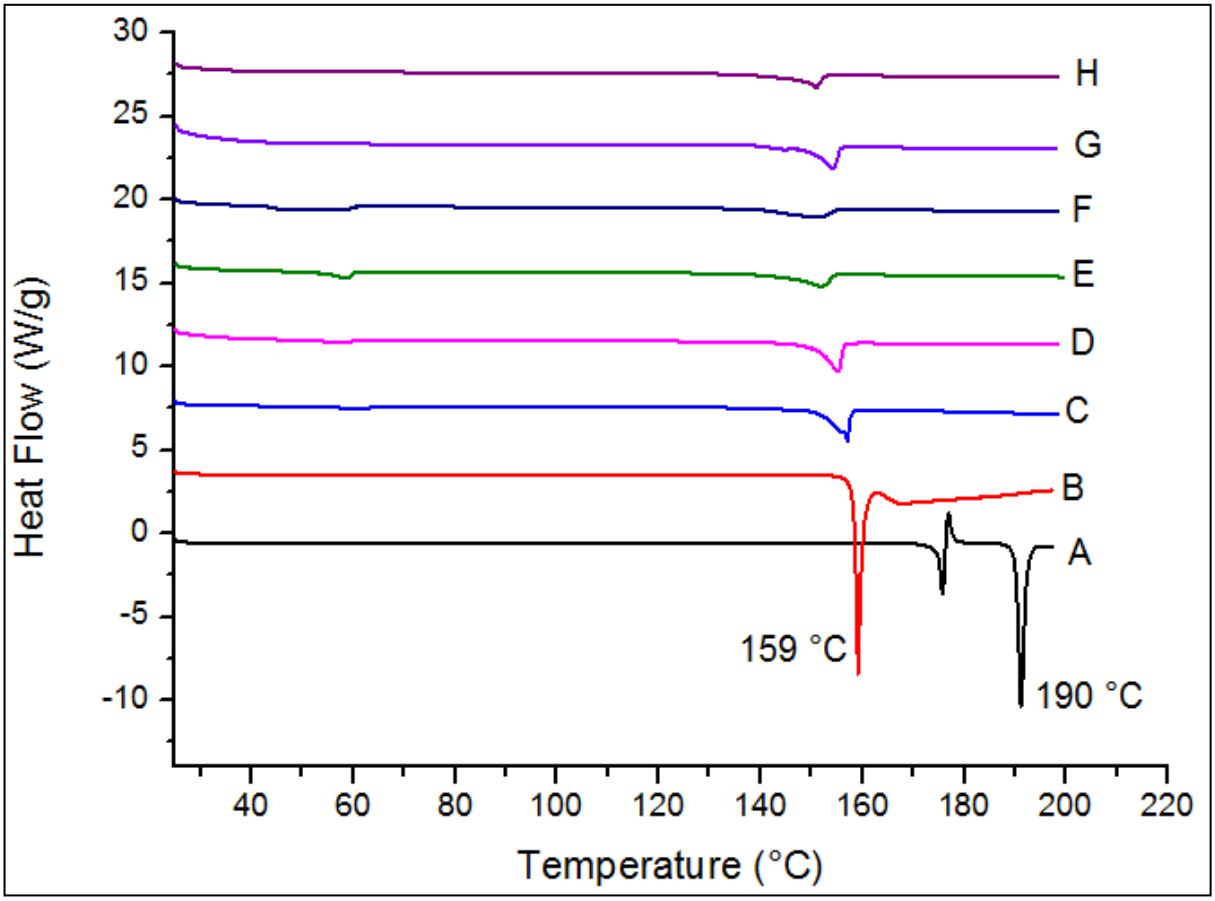

[A: Carbamazepine, B: CBZ:SAL 1:1 PURE CC, C: S3M CBA:SAL 1:1 5% PEO, D: S3M CBZ:SAL 1:1 10% PEO, E: S3M CBZ:SAL 1:1 15% PEO, F: S3M CBZ:SAL 1:1 25% PEO, G: S3M CBZ:SAL 1:1 15% VA64, H: S3M CBZ:SAL 1:1 25% VA64]

Figure 6.33 DSC thermograms for carbamazepine: salicylic acid 1:1 cocrystals processed by S3M

6.4.1.5 SEM

Surface morphology for CBZ: SAL cocrystals was done as described in Section 3.4.5. As shown in Figure 6.34 it shows that as polymer concentration increase there was a significant change in cocrystal structure on polymer surfaces. At lower polymer concentrations, the structure looked

more compact whereas there seemed to be good crystal growth as polymer content increased. These variable structural morphologies will affect the dissolution of these cocrystals, and polymer concentration will influence the drug release.

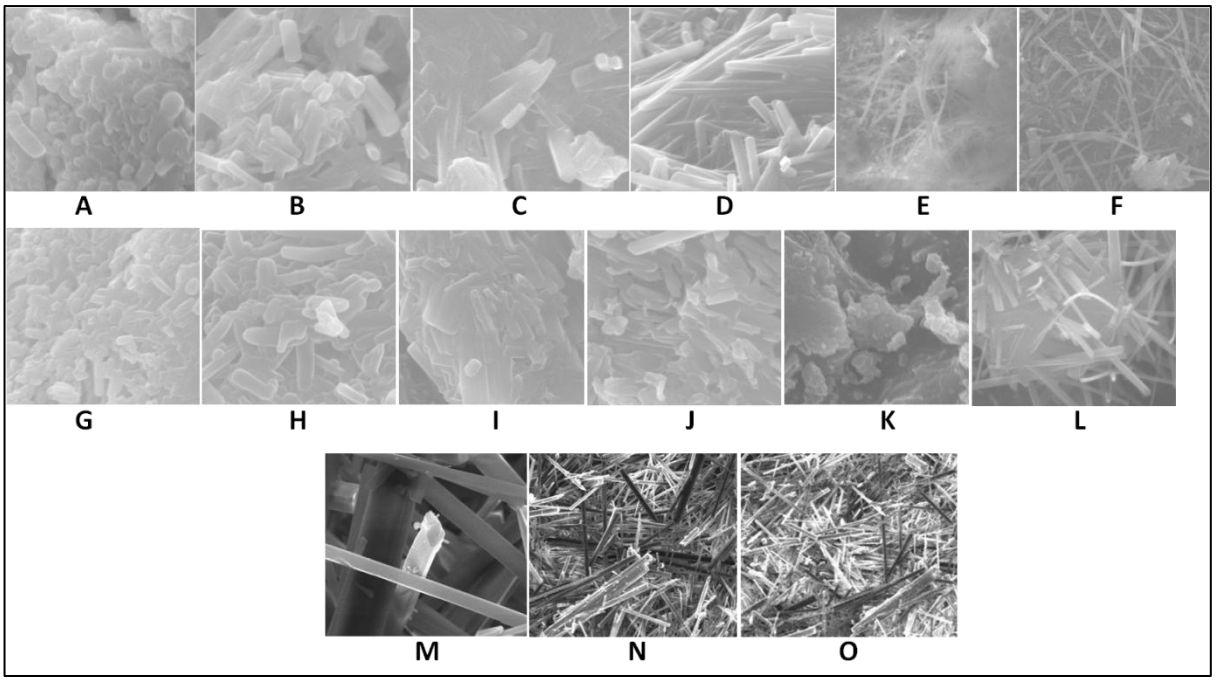

[A- S3M 5% PEO, B- S3M 10% PEO, C- S3M 15% PEO, D- S3M 25% PEO, E- S3M 15% VA64, F- S3M 255 VA64; G- HME 5% PEO, H- 10% PEO, I- 15% PEO, J- 25% PEO, K- 15% VA64, L- 25% VA64; M,N,O- Solution cocrystal]

Figure 6.34 Surface morphology by SEM of carbamazepine: salicylic acid 1:1 cocrystals processed by HME and S3M

Cocrystals produced by the solution method shows needle type long crystals which were difficult hard to observe in the case of polymer assisted cocrystals.

6.4.1.6 FT-IR

FT-IR studies were carried out as described in Section 3.4.3. CBZ shows strong amide group stretching which can be symmetrical or asymmetrical in nature (Childs *et al*. 2008; Schultheiss and Newman, 2009). These amide

vibrations are observed at 3465, 3155 cm^{-1}, -C=O stretching are observed at 1677 cm^{-1} and C=C and –NH deformation vibrations at 1593 and 1603 cm^{-1} respectively (Figure 6.35). Similarly SAL shows characteristic stretching vibrations for –C-H at 3069, 3037 and 3019 cm^{-1}, -O-H stretching at 1292 cm^{-1} and strong stretching at 1651 cm^{-1} for C=O (Figure 6.36). HME and S3M3 processed cocrystals showed identical vibrations to pure cocrystals at 3504 cm^{-1} for –NH stretching, -C=O stretching were reduced to 1661 in both the processes which shows the presence of hydrogen bond between –NH of CBZ and –C=O of SAL.

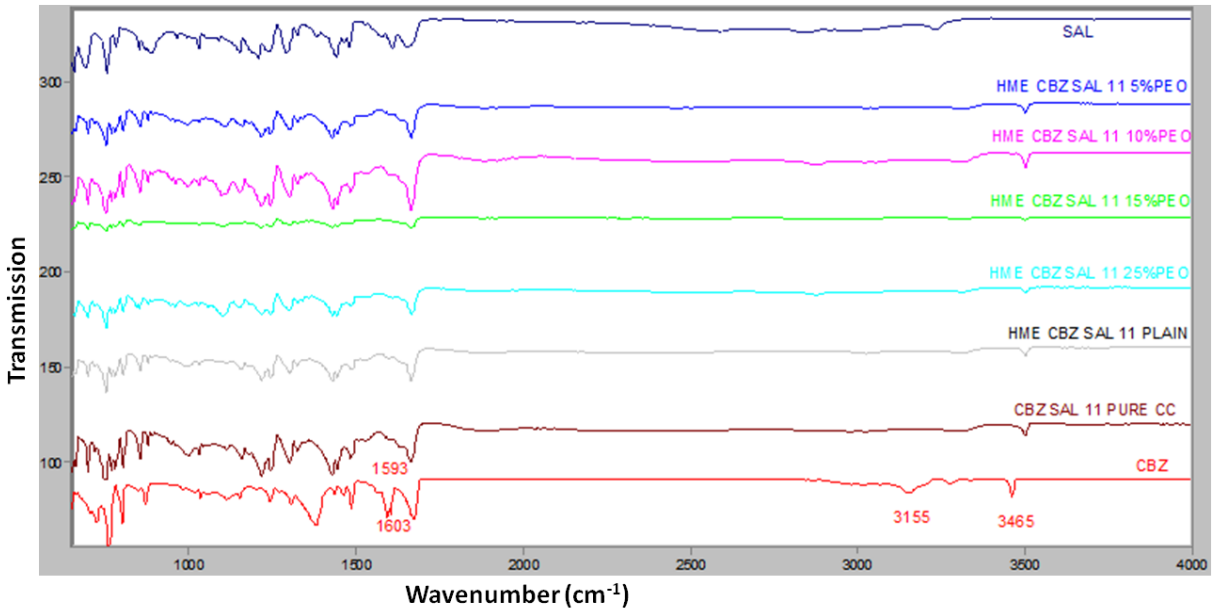

Figure 6.35 FT-IR spectra for carbamazepine: salicylic acid 1:1 cocrystals with PEO by HME

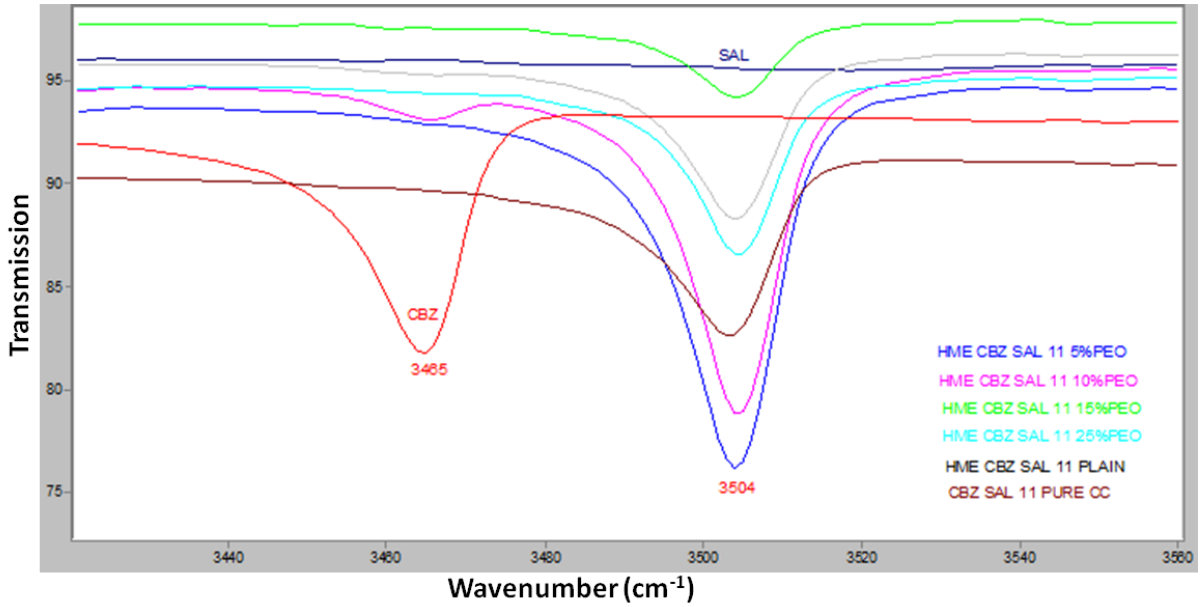

Figure 6.36 FT-IR spectra for carbamazepine: salicylic acid 1:1 cocrystals with PEO by HME

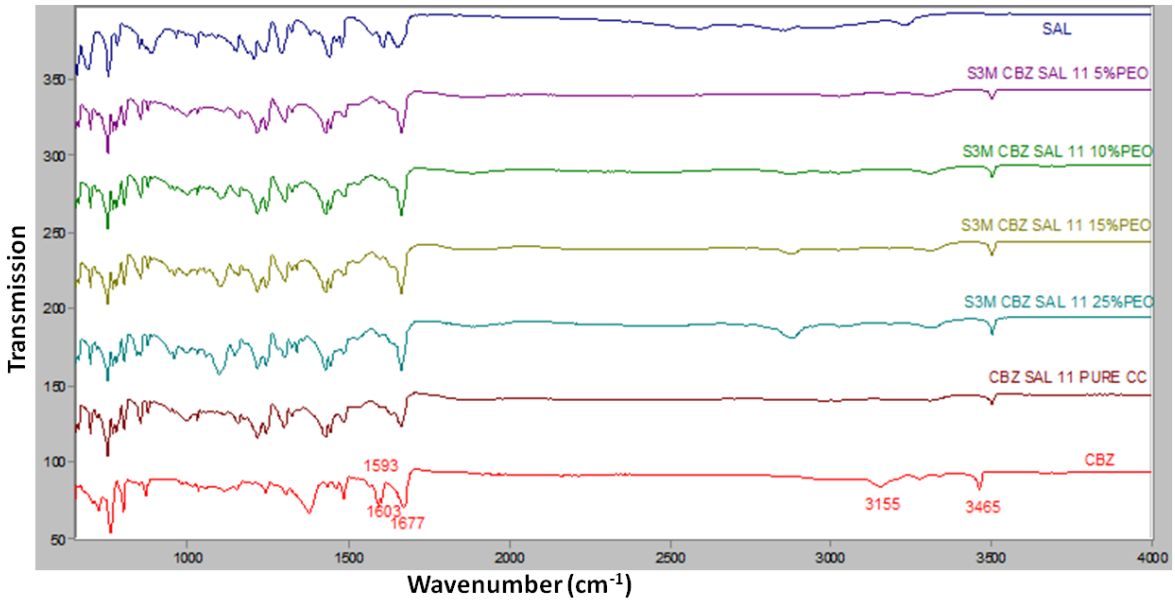

Figure 6.37 FT-IR spectra for carbamazepine: salicylic acid 1:1 cocrystals with PEO by S3M

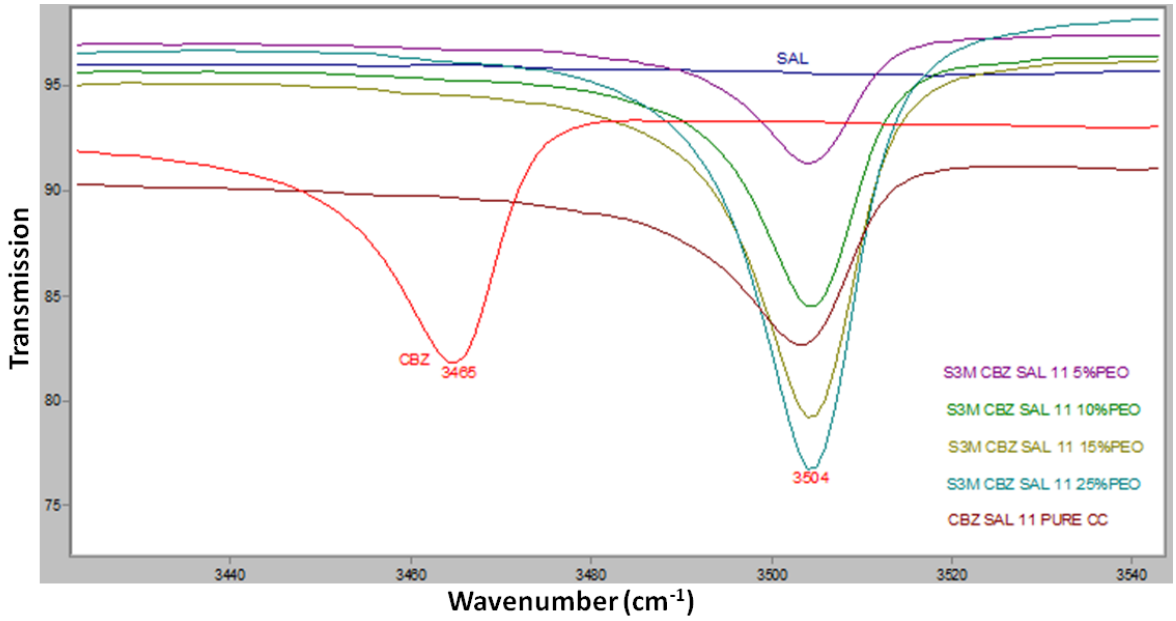

Figure 6.38 FT-IR spectra for carbamazepine: salicylic acid 1:1 cocrystals with PEO by S3M

In FT-IR studies of CBZ: SAL cocrystals processed with VA64 as a processing aid, the strong symmetrical vibrations for –NH at 3465 and 3155 cm^{-1} the 3155 cm^{-1} vibrations disappeared from pure cocrystal and also in VA64 processed cocrystal batches processed by HME and S3M3 (Figure

6.39 and Figure 6.40). C=C and –C=O vibrations at 1593 and 1603 cm^{-1} disappeared completely in pure cocrystal and VA64 based cocrystal batches processed by HME and S3M3. The effect of the presence of PEO or VA64 cannot be directly determined by the FT-IR analysis as its total concentration is less in final cocrystal matrix, or its effect on hydrogen bond formation.

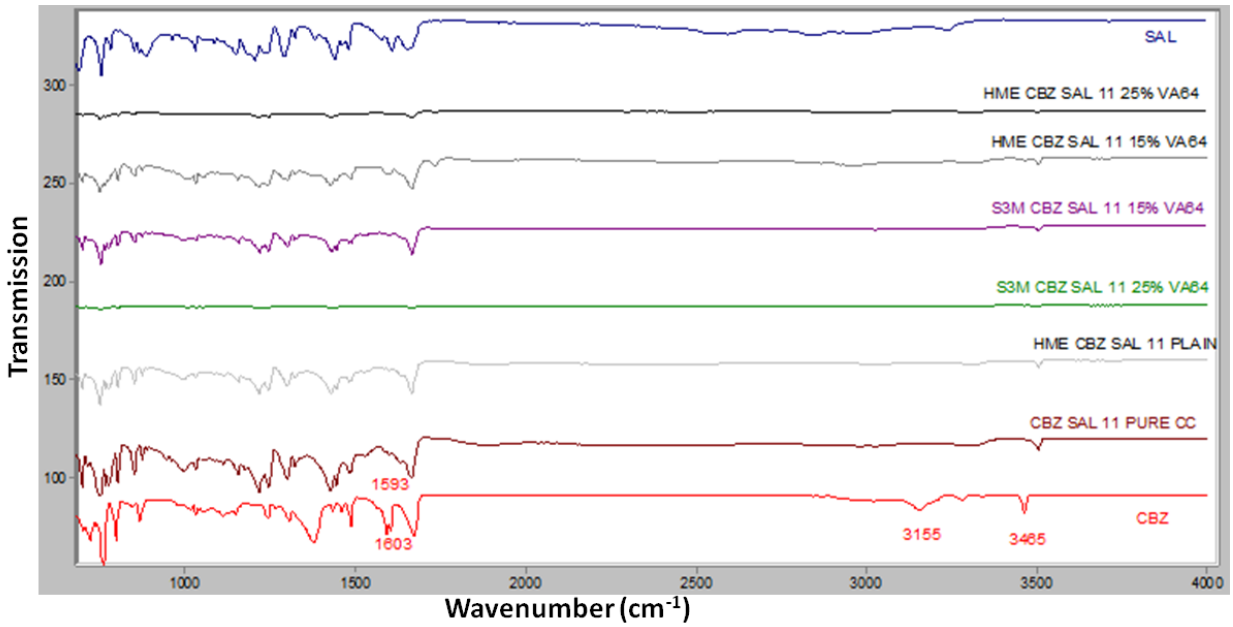

Figure 6.39 FT-IR spectra for carbamazepine: salicylic acid 1:1 cocrystals with PVP VA64 by HME and S3M

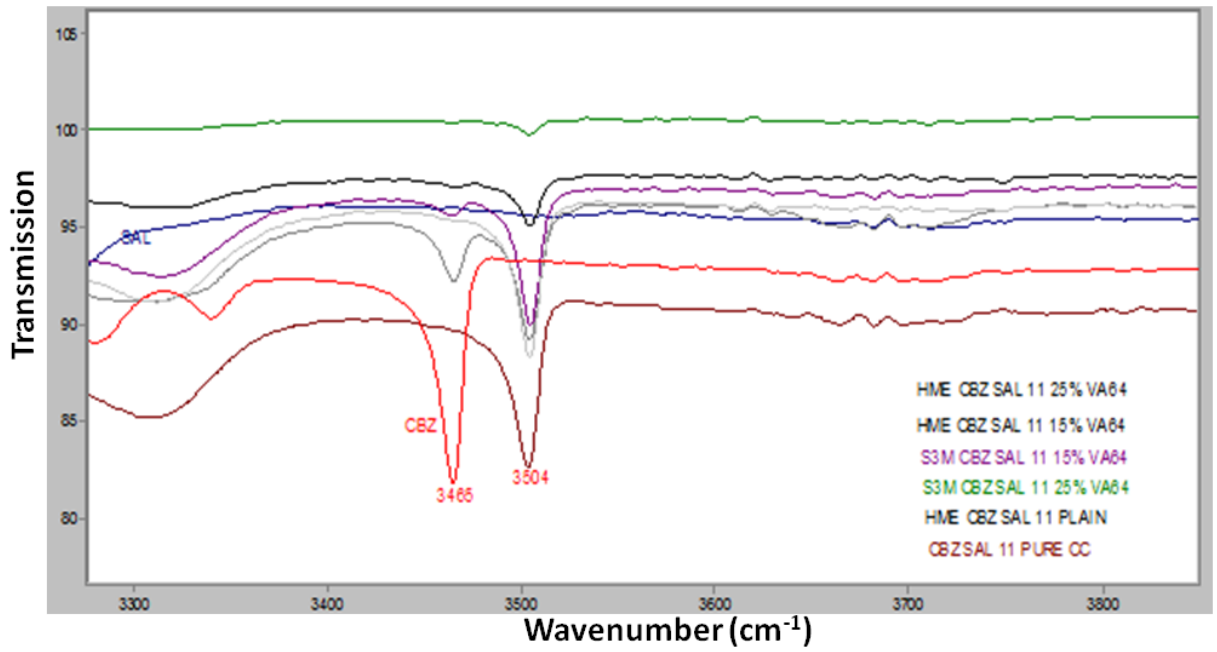

Figure 6.40 FT-IR spectra for carbamazepine: salicylic acid 1:1 cocrystals with PVP VA64 by HME and S3M

6.4.1.7 NIR

NIR analysis for CBZ: SAL cocrystals was carried out as described in Section 3.4.4.

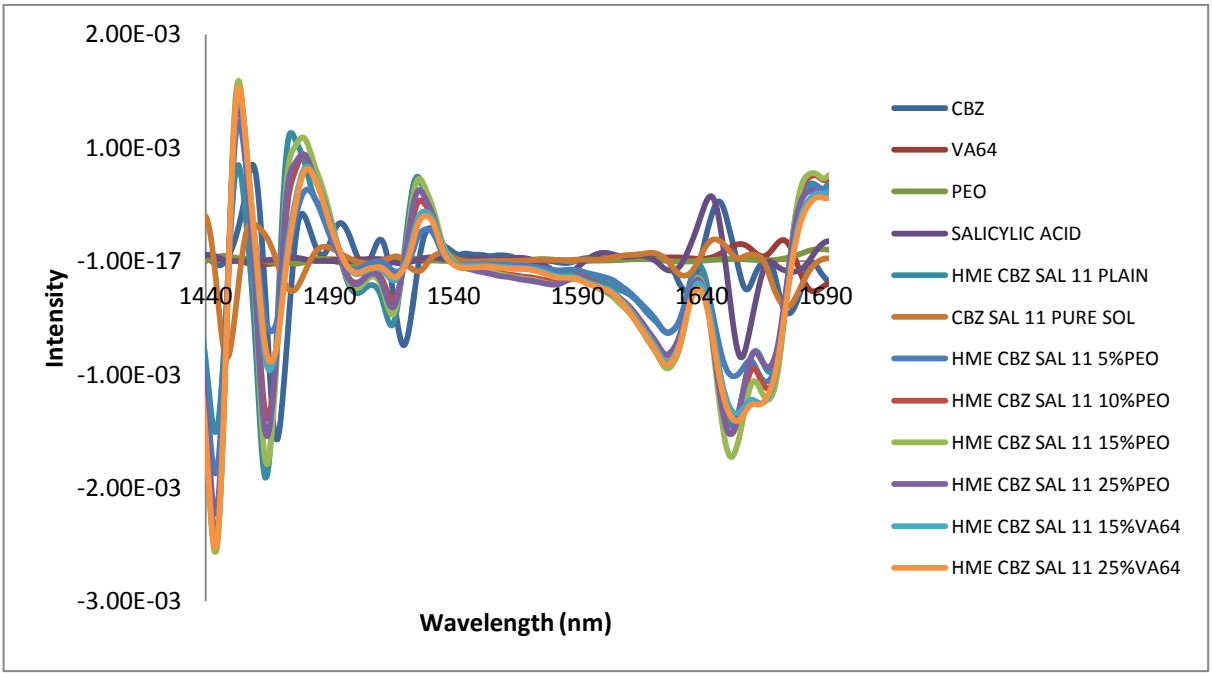

Figure 6.41 NIR spectra for carbamazepine: salicylic acid 1:1 cocrystals with PEO and VA64 by HME

As discussed in the carbamazepine solid dispersions, NIR analysis shows characteristic absorption in second overtone region at 1468 nm. Salicylic acid owing to its acid functionality shows good NIR absorption in the first overtone region at 1656 nm. Pure cocrystals of CBZ:SAL 1:1 showed good NIR absorption spectra in the second overtone region at 1448 and 1474 nm which is completely different than the starting components (Figure 6.41). This distinct change in NIR absorption peaks may due to hydrogen bond formation between -NH of carbamazepine and -COO of salicylic acid. All the CBZ:SAL 1:1 cocrystals processed by HME with PEO and PVP VA64 showed identical NIR absorption at 1445, 1465, 1651 and 1670 nm with highest peak intensity for CBZ:SAL 1:1 15% PEO and lowest for CBZ:SAL 1:1 cocrystals without polymer. This drastic change in intensity can be attributed to the extent of hydrogen bonding between the formed cocrystals.

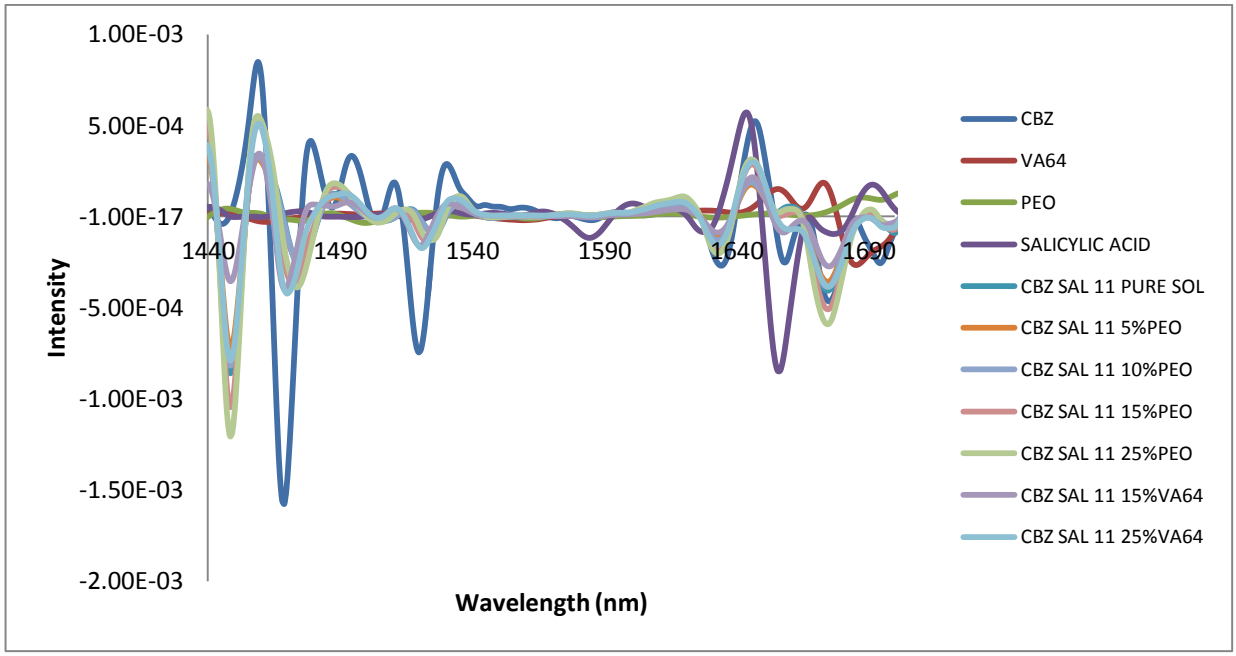

Figure 6.42 NIR spectra for carbamazepine: salicylic acid 1:1 cocrystals processed by S3M

In the case of S3M processed CBZ:SAL 1:1 cocrystals, unlike HME processed these cocrystals showed identical NIR absorption in the second overtone region at 1448 and 1474 nm. The intensity for NIR absorption was highest in the case of CBZ: SAL 1:1 25% PEO but lowest for CBZ: SAL 1:1 25% VA64 (Figure 6.42). This identical NIR absorption can be attributed to the similar pattern of hydrogen bonding between parent components as with pure cocrystals.

6.4.1.8 DISSOLUTION

Dissolution studies for CBZ:SAL 1:1 cocrystal were carried out as per parameters explained in section 3.7.2. Dissolution behaviour of the cocrystal processed by HME and S3M3 with variable amount of polymers were of particular interest.

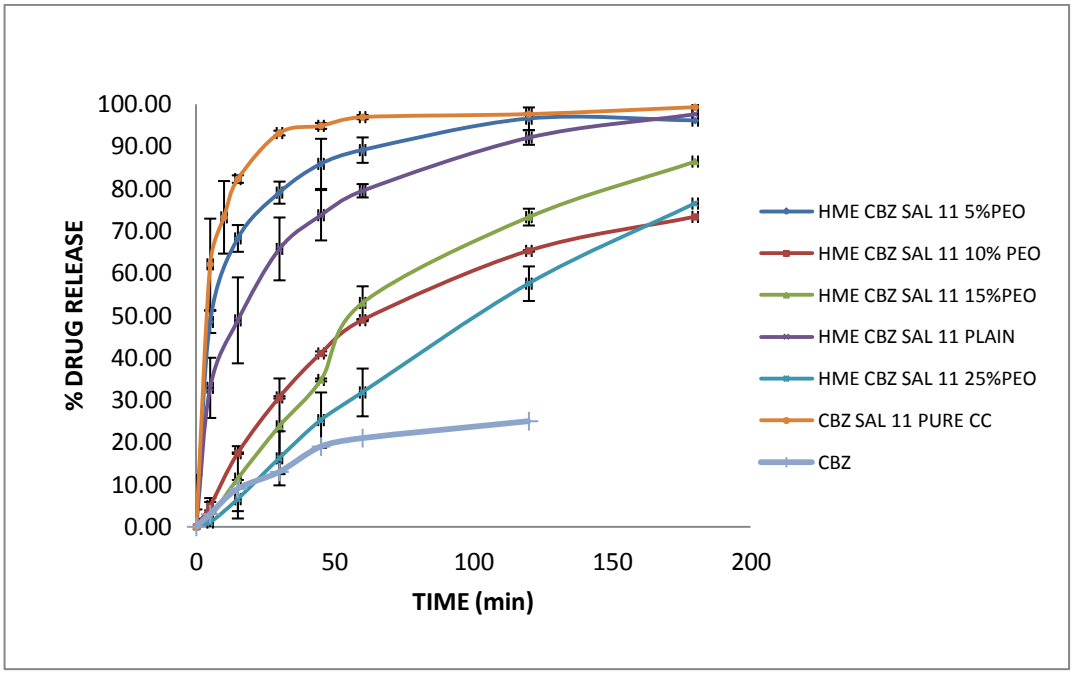

Figure 6.43 Dissolution profiles for carbamazepine: salicylic acid 1:1 cocrystals with PEO by HME

Figure 6.43 clearly shows drug release from HME processed CBZ:SAL 1:1 cocrystal batches with PEO. CBZ:SAL 1:1 cocrystals produced by the solution method showed fastest release and released 100% drug within 20 mins, HME processed cocrystals with 5% PEO show the second fastest release followed by HME processed cocrystals without any polymer, only above three batches were able to release 100% CBZ; polymer aided batches with 10%, 15%, 25% PEO showed the slowest release among all and took almost 3 hours and to release about 80% of the total drug. Similar observations were made in HME processed cocrystal batches with VA64 as the aiding polymer. 15% VA64 cocrystal batch showed slightly higher release of 75% of the drug within 3 hours, whereas cocrystal batches with 25% VA64 showed slower release only 50% of CBZ in 3 hours (Figure 6.44).

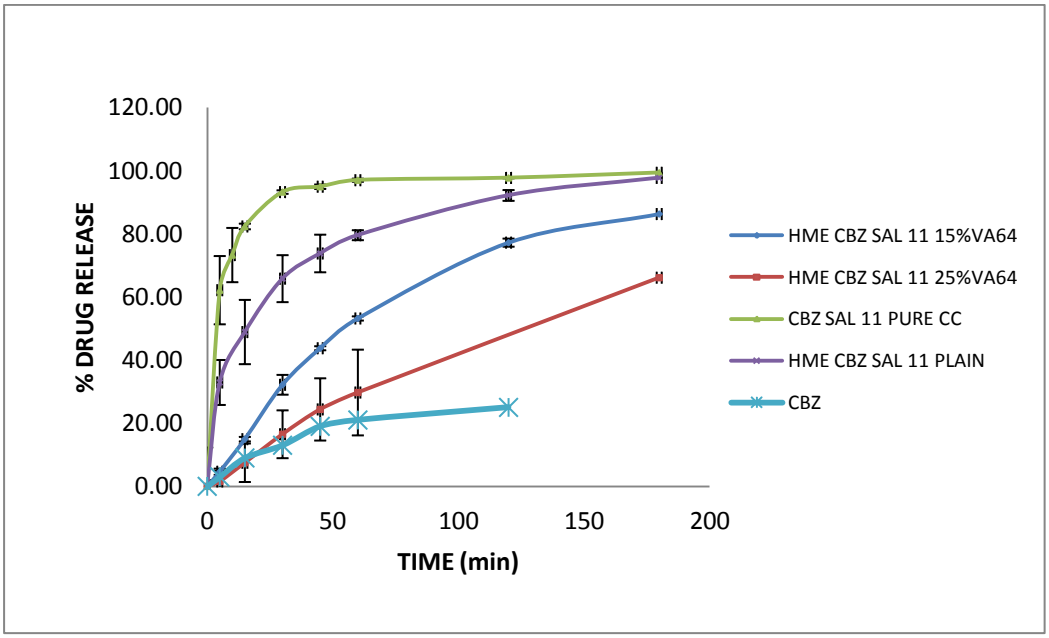

Figure 6.44 Dissolution profiles for carbamazepine: salicylic acid 1:1 cocrystals with PVP VA64 by HME

Slower release of the CBZ through cocrystal batches with higher polymer concentration can be explained by the surface properties of respective cocrystals. The higher concentration polymer cocrystal batches were more compact in nature which not allows dissolution media to penetrate through the polymer chains into the cocrystal matrix. This reduced overall wettability and exposure which resulted in slower and incomplete CBZ release from those batches.

CBZ:SAL 1:1 cocrystal batches processed by S3M3 showed more complex results which differed from HME processed batches. In the case of S3M3, fastest release was observed batches with 10% and 25% PEO whereas for 5% and 15% it was observed that CBZ release was slower and could only release around 80% of the total drug (Figure 6.44).

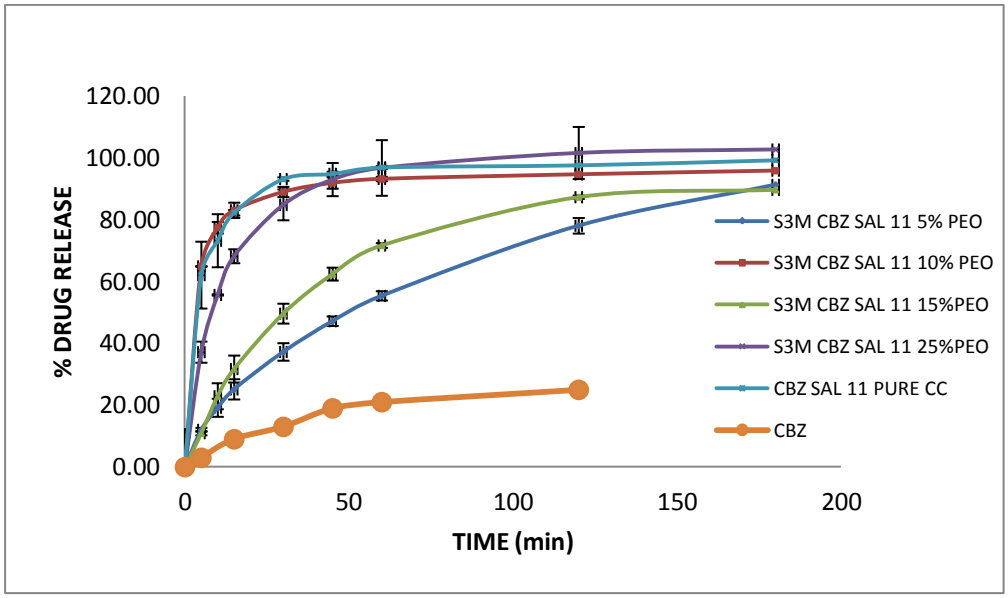

Figure 6.45 Dissolution profile for carbamazepine: salicylic acid 1:1 cocrystals with PEO by S3M

For S3M3 cocrystal batches with VA64 showed similar kind of release as observed in HME processed batches (Figure 6.45). Cocrystal batches with 15% VA64 showed 100% release over 3 hours whereas the 25% VA64 batch which could only release 45% of CBZ in 3 hours.

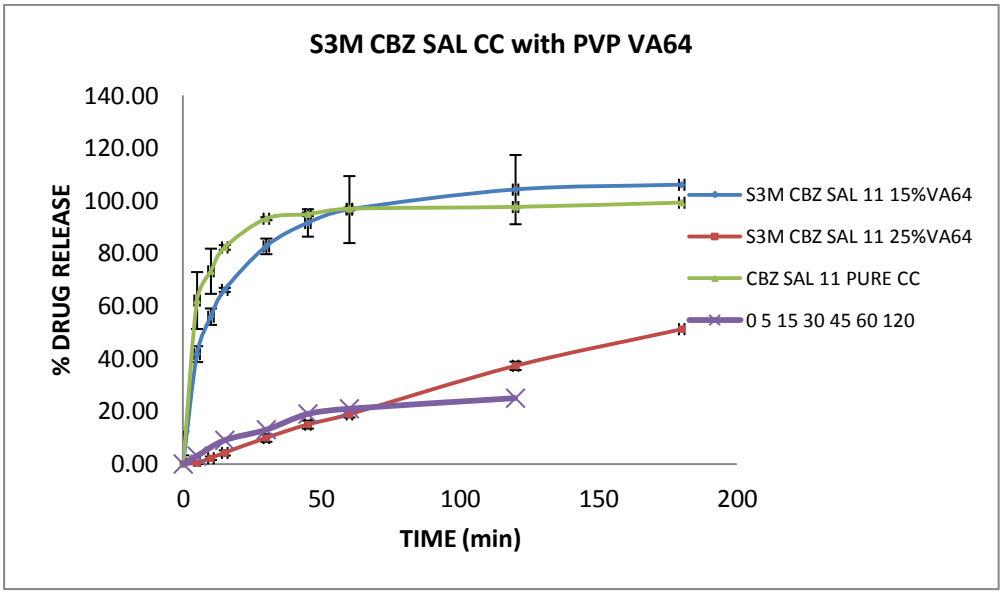

Figure 6.46 Dissolution profile for carbamazepine: salicylic acid 1:1 cocrystals with PVP VA64 by S3M

Drug release results of S3M3 processed cocrystal batches with PEO could not be correlated with the amount of polymer present. This may be due to the total amount of polymer present at the ɗ surface of S3M3 during its three dimensional scissoring action made it less or more available. The part of material used from the cocrystal batches may have different amount of polymer present which are used for dissolution studies. The other reason for this can be explained as some parts of the aid polymer may have experience very high shear which might have caused degradation of either polymer or drug or it would have formed highly dense structure specially in case of the samples used for dissolution studies.

6.4.1.9 DVS

DVS analysis for CBZ: SAL 1:1 cocrystals showed variable vapour sorption behaviour. HME processed plain CBZ:SAL 1:1 cocrystal without polymer

vapour sorption results were similar to pure cocrystal and the weight change contributed to less than 0.01% w/w. CBZ:SAL 1:1 cocrystals with 10% PEO processed by S3M showed higher vapour sorption as compared to HME processed. Weight change in the case of S3M processed cocrystal was more than 0.2 % w/w whereas in case of HME processed cocrystal it was less than 0.2% w/w (Figure 6.47). The higher value for vapour sorption in S3M processed cocrystal batches can be attributed to the three dimensional scissoring shear actions on material during processing. Due to this highly distorted structure the vapour penetration might have increased for S3M3 processed cocrystal samples with 10% PEO. PEO is highly hygroscopic in nature, In the case of HME processed cocrystal batches it formed a very compact product and surface with low porosity which made all the crystal embedded in polymer layer of PEO and hindered the overall exposure to the vapour during DVS analysis.

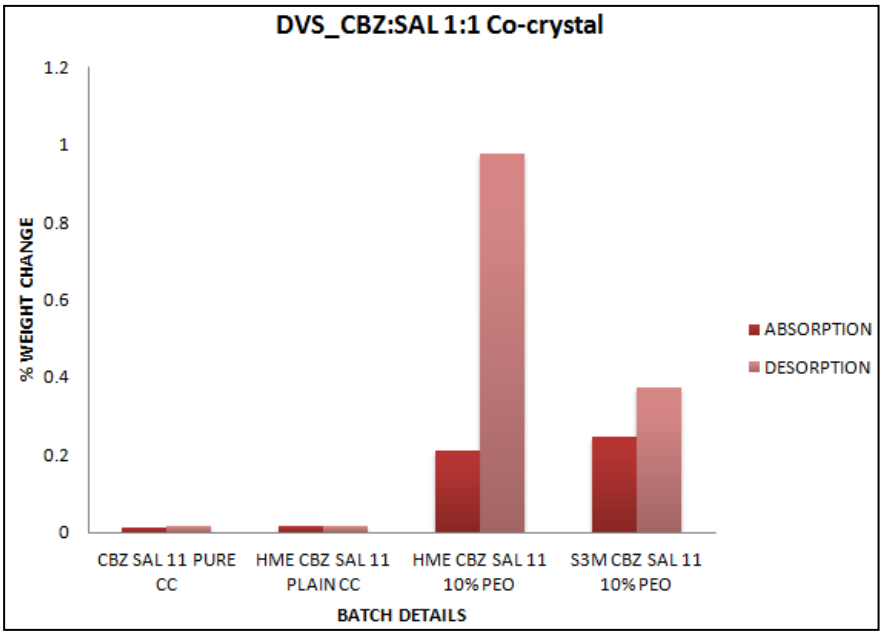

Figure 6.47 DVS analysis at 60% RH for carbamazepine: salicylic acid 1:1 cocrystals processed by HME and S3M

In the case of S3M3 processed cocrystal batches the distribution of PEO was uniform all over the cocrystal matrix and overall exposure to the environment with high surface roughness and porosity made it absorb more vapours.

6.4.1.10 Surface energy

Surface energy analysis was carried out for the batches which were analysed for DVS. Surface energy analysis was kept similar for all the batches and the procedure followed as described in Section 3.4.5. Surface energy analysis was carried out to analyse the effect of two different high shear processes on respective product surfaces and their related surface energies.

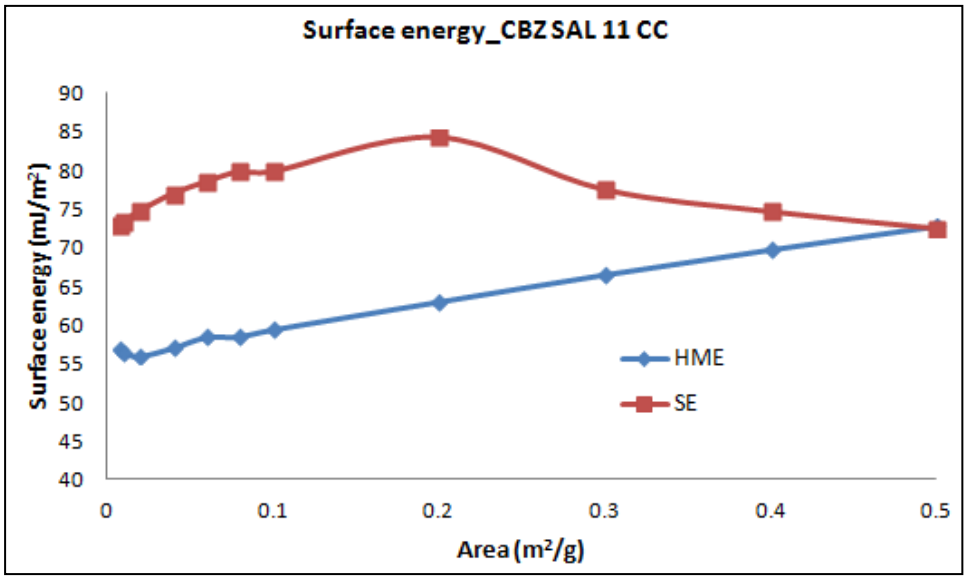

Figure 6.48 *i*GC analysis for carbamazepine: salicylic acid 1:1 cocrystals processed by HME and solution crystallisation

As Figure 6.48 shows pure cocrystal shows high surface energy values and HME processed cocrystal batch without polymer also shows surface energy values increasing with increase in surface coverage area. This can be attributed to the surface groups available on these cocrystals, surface hydrophobicity has a positive effect on surface energy and these cocrystals without polymer have shown lowest vapour sorption in DVS studies. These findings can be directly correlated to drug release, higher the surface energy the higher is the release.

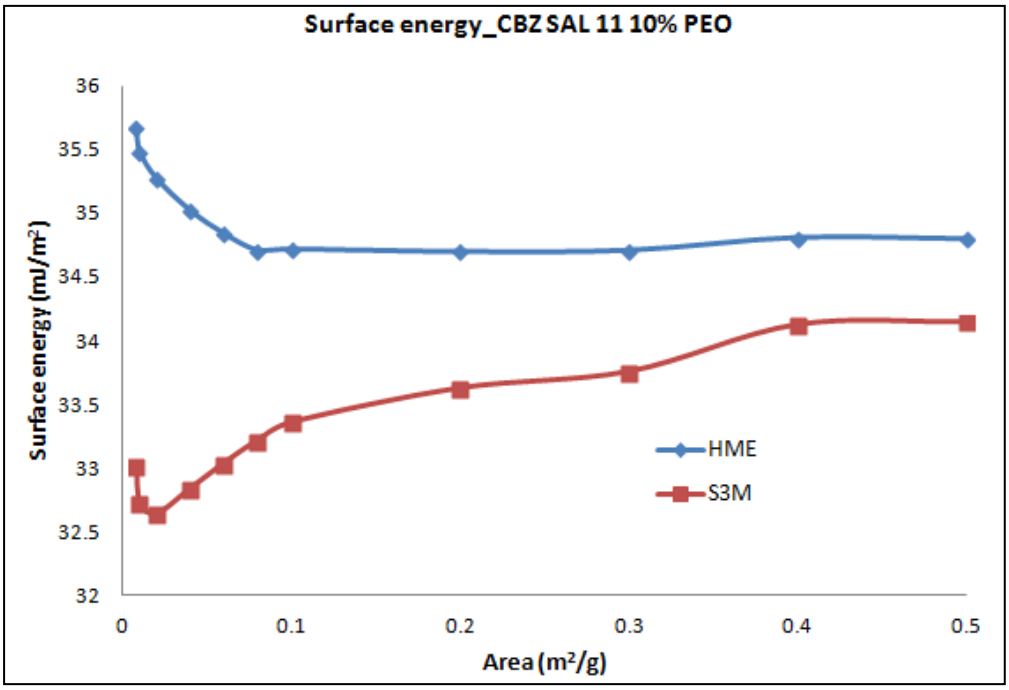

Figure 6.49 *i*GC analysis for carbamazepine: salicylic acid 1:1 cocrystals with 10% PEO processed by HME and S3M

In case of cocrystals with 10% PEO, HME processed cocrystals surface energies showed higher values compared to S3M and was consistent as the coverage area increased (Figure 6.49). The cocrystal produced by S3M3 had highly compacted features with uneven or irregular crystal distribution at the surface embedded in the polymer matrix. These findings cannot be directly correlated to drug release or vapour sorption studies.

6.4.2 Carbamazepine: saccharin 1:1 cocrystal (CBZ: SACC 1:1)

6.4.2.1 Crystal structure data

Carbamazepine forms a monoclinic 1:1 cocrystal with saccharin. The CBZ: SACC cocrystal pair is extensively studied among the CBZ cocrystals. CBZ: SACC 1:1 cocrystal exhibit in two polymorphic forms Form I and II

respectively. As shown in Figure 6.50 the CBZ and SACC form a hydrogen bond between their respective functional groups, -NH of CBZ and -SO2N of SACC. The single crystal data and space group features with other important crystal parameters are given in Table 6.4

Table 6.4 Crystal structural database and space group details for CBZ: SACC 1:1 cocrystal

Empirical formula	$C_{15}H_{12}N_2O$, $C_7H_5NO_3S$
Crystal system	Monoclinic
Space group	C2/c
a (Å)	35.719
b (Å)	6.837
c (Å)	16.111
α (°)	90.000
β (°)	98.026
γ (°)	90.000

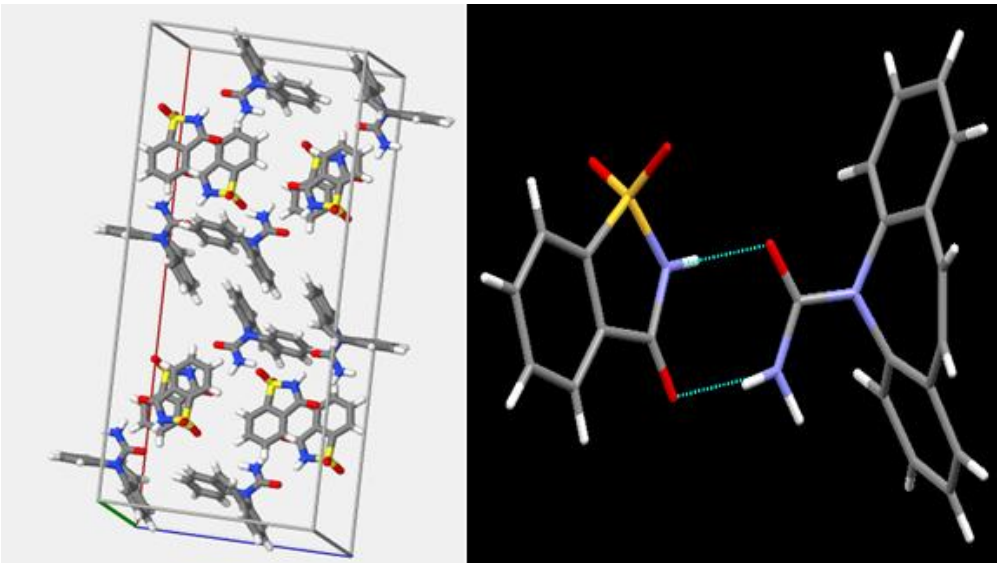

Figure 6.50 Crystal structure of carbamazepine: maleic saccharin 1:1 cocrystal and crystal packing in unit cell. (adopted from CSD)

The CBZ: SACC 1:1 cocrystal exhibits characteristic 2θ peaks at 6.46, 11.76, 13.36, 13.8° respectively as shown in Figure 6.51.

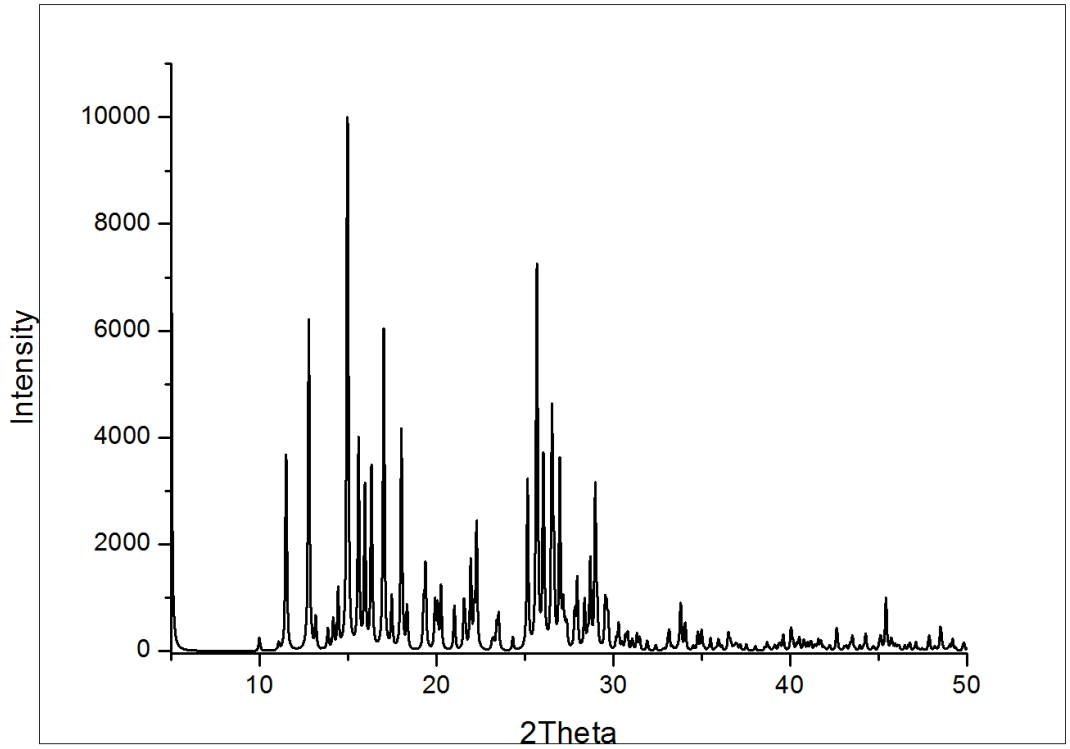

Figure 6.51 Calculated PXRD pattern for carbamazepine: saccharin 1:1 cocrystal. (adopted from CSD- UNEZAO01 and processed in OriginPro 8)

6.4.2.2 Processing of cocrystal

CBZ and SACC were weighed accurately and mixed in molar ratios; to this 15% w/w PEO was added as a processing aid. This mixture was subjected to turbula mixer for making all three components homogenous; this was then transferred to S3M3 hopper. Material flow was excellent. Product started coming out in the form of agglomerated threads as soon as the material was added to the feeder. It took only 10-15 secs during first cycle to start giving out the product. Agglomerated threads varied in the size length (0.5 mm to 1 cm) and overall structural features. HME for CBZ:SACC cocrystal was carried out according to the temperature profile and extrusion parameters given in section 3.7 (Table 3.10). Extrusion was carried out for CBZ: SACC 1:1 with and without PEO as it was feasible to process drug polymer alone

on HME. The end product was half broken screw type structural features. The end product of both processes was characterised by various analytical tools and for drug release.

6.4.2.3 SACC Calibration

The calibration curve for SACC was linear over the concentration range of 10-100 ug/ml. The linearity equation was calculated using calibration curve, slope of the equation was 347.78, constant -359.94 and R^2 0.9996 (Figure 6.52). The SACC release was calculated using calibration equation.

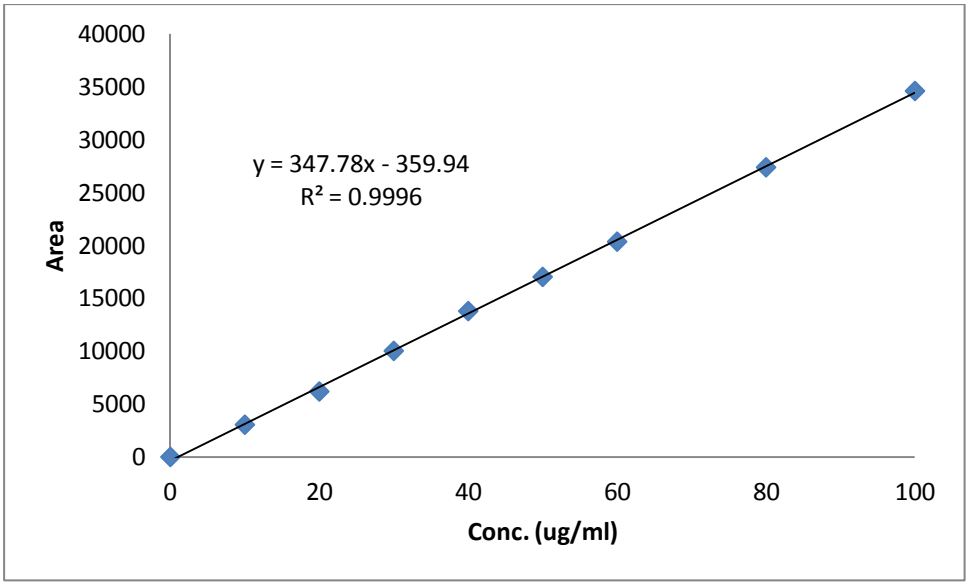

Figure 6.52 Saccharin calibration curve using UPLC at 269nm

The retention time for saccharin in UPLC was 1.30 mins in the total runtime of 5mins as shown in Figure 6.53.

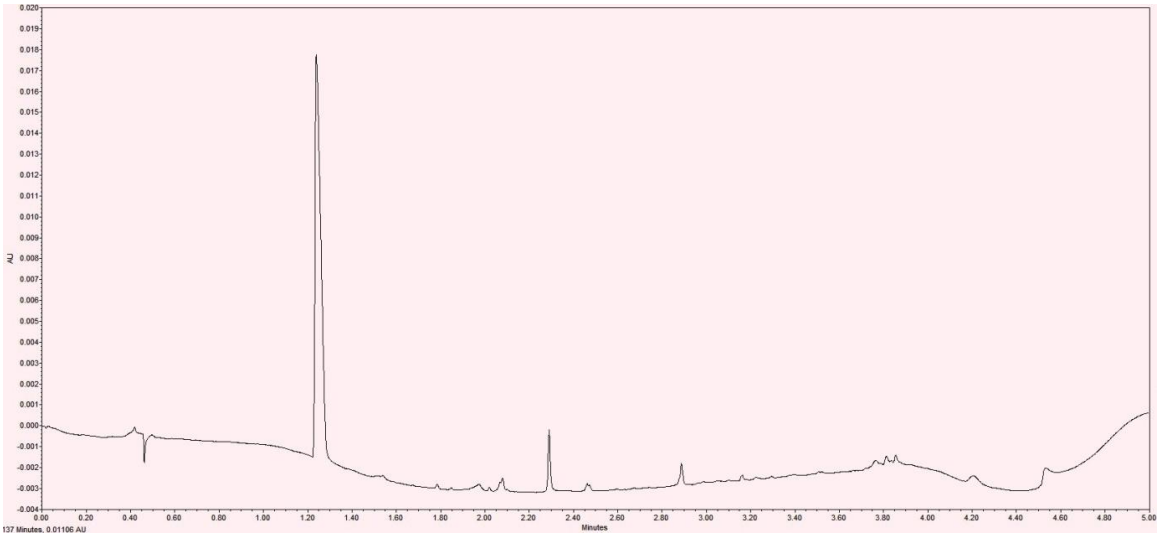

Figure 6.53 saccharin chromatogram in UPLC analysis

6.4.2.4 PXRD

PXRD studies for CBZ: SACC 1:1 cocrystals were carried out as described in Section 3.4.2. The characteristic 2θ values for CBZ: SACC 1:1 cocrystals were observed at 6.46, 11.76, 13.36, 13.8° which matches the structural data from CSD. Characteristic 2θ values for CBZ at 13.16, 14.2, 15.36, 15.92, 18.72, 19.56, 20.4 and SACC were observed at 9.44, 16.04, 18.92, 20.12°, which completely differs from the cocrystal values. CBZ: SACC cocrystals without polymer processed by HME showed that it has some characteristic peaks at or near 2θ of CBZ and SACC (Figure 6.54) and it also shows characteristic peaks for pure cocrystal also. From this it can be concluded that there is partial conversion into cocrystal and need to modify the HME process to get phase pure cocrystal with more appropriate temperature and shear profile. CBZ: SACC 1:1 cocrystal with 15% PEO as an aid processed by HME and S3M3 shows all the characteristic peaks at 2θ values of pure cocrystals, which confirms that both the processes yielded phase pure

cocrystal. The justification for getting phase pure cocrystal using polymer as aid can be explained as discussed in CBZ: SAL cocrystal study, at very high shear PEO acted as solvent or common media to dissolve CBZ SACC in equal proportion which helped them to form hydrogen bond.

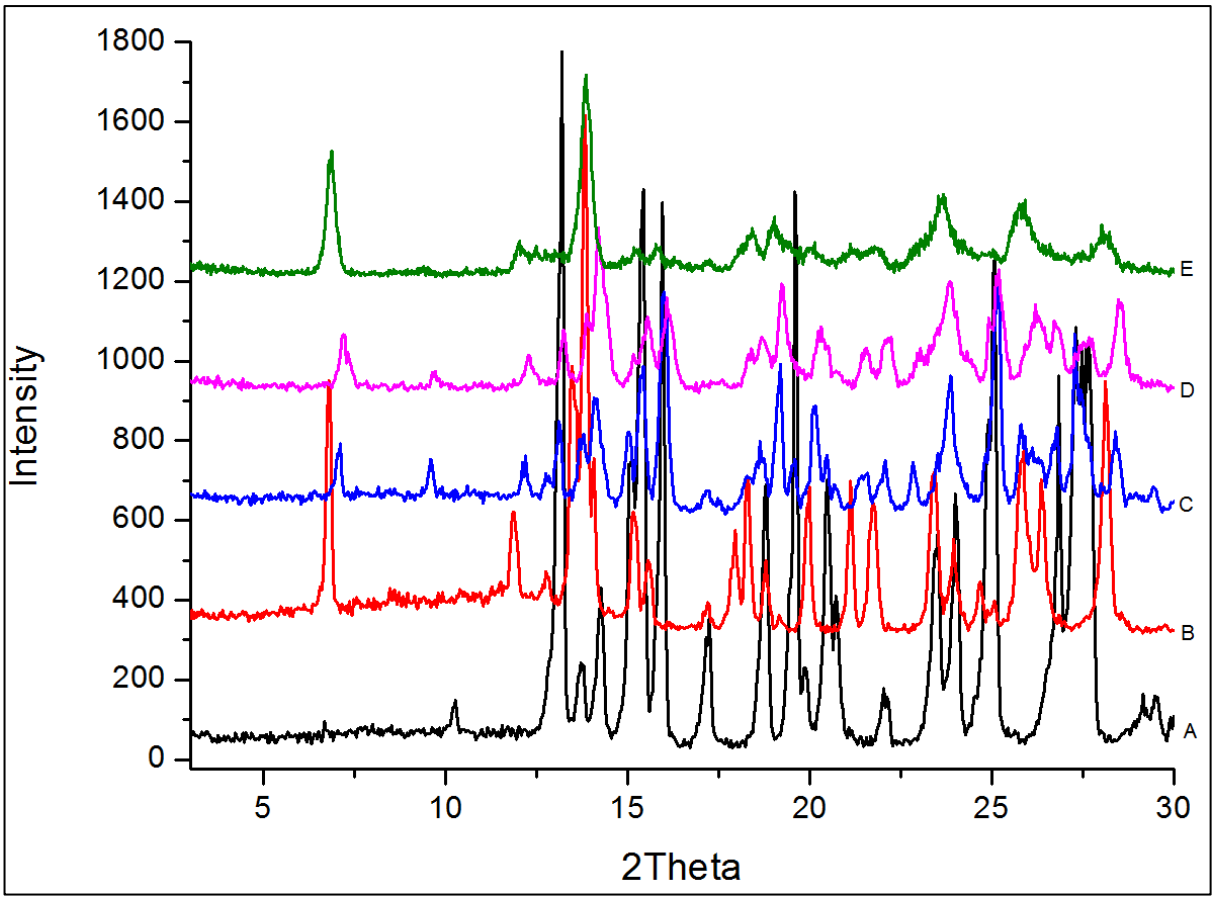

[A: Carbamazepine, B: CBZ:SAC 1:1 PURE CC, C: HME CBZ:SAC 1:1, D: HME CBZ:SAC 1:1 15% PEO, E: S3M CBZ:SAC 1:1 15% PEO]

Figure 6.54 PXRD for carbamazepine: saccharin 1:1 cocrystals processed by HME and S3M

6.4.2.5 DSC

Thermal properties of the cocrystal were studied to support PXRD findings. DSC studies were carried out as described in Section 3.4.1. As discussed earlier CBZ shows characteristic melting endotherm at 175 °C and 191 °C,

whereas SACC shows this at 229 °C. The CBZ: SACC 1:1 pure cocrystal showed a characteristic melting endotherm at 178 °C. HME processed cocrystal without PEO the endotherm was observed at 173°C (Figure 6.55). whereas cocrystal with 15% PEO processed by HME showed endotherm at 172 °C and S3M3 processed at 170 °C. The slight difference in melting endotherm with pure cocrystal can explained as sample for DSC analysis used was small (2-3 mg) and in that respective sample amount of polymer, the amount of cocrystal present might have varied which made endotherms exhbit at different temperatures.

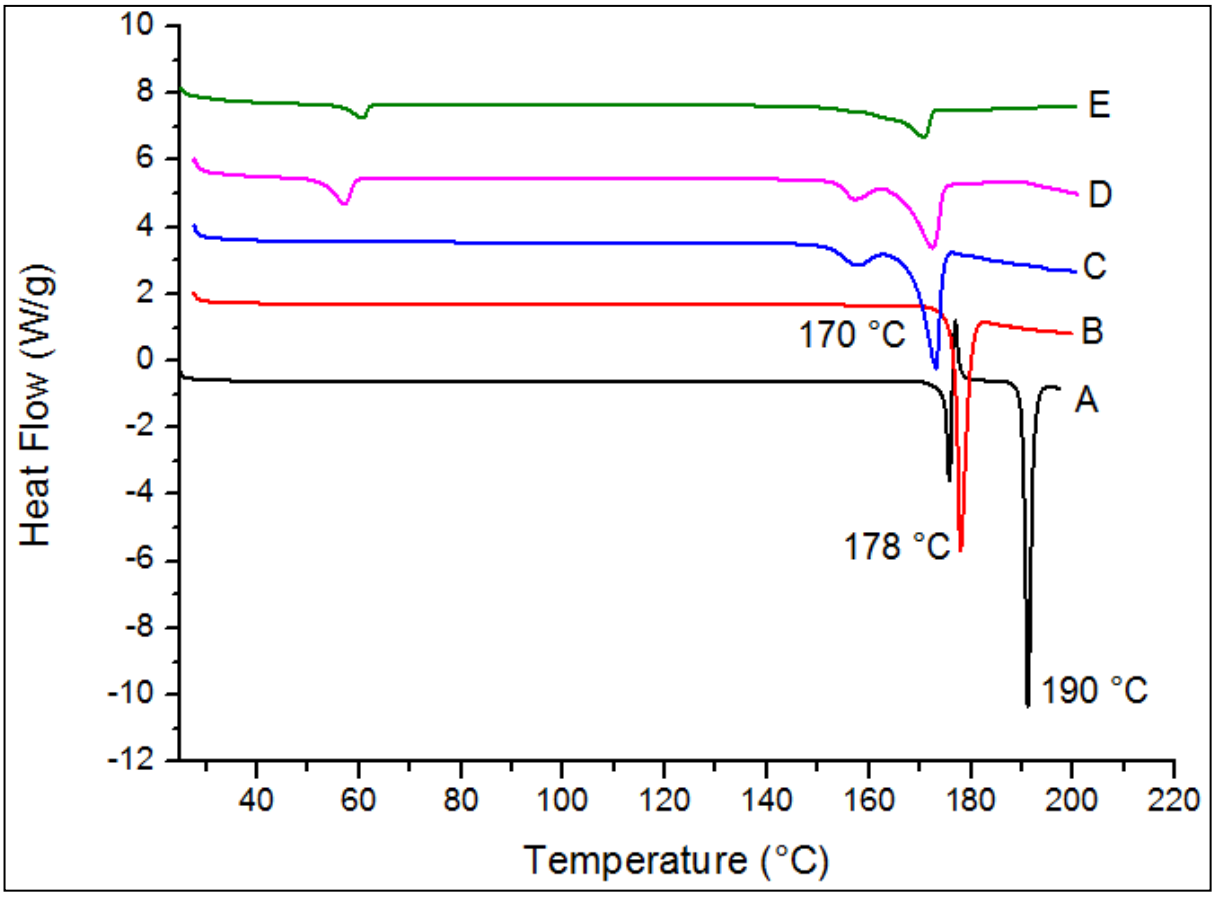

[A: Carbamazepine, B: CBZ:SACC 1:1 PURE CC, C: HME CBZ:SACC 1:1, D: HME CBZ:SACC 1:1 15% PEO, E: S3M CBZ:SACC 1:1 15% PEO]

Figure 6.55 DSC thermograms for carbamazepine: saccharin 1:1 cocrystals processed by HME and S3M

6.4.2.6 SEM

Surface morphology studies were carried out as discussed in Section 3.4.5. The structural surface features and properties were similar to those observed in CBZ: SAL cocrystals with the respective processes. Figure 6.56 shows that the HME processed PEO based cocrystals were more compact in nature whereas S3M3 showed compact but distorted structural features (Figure 6.52).

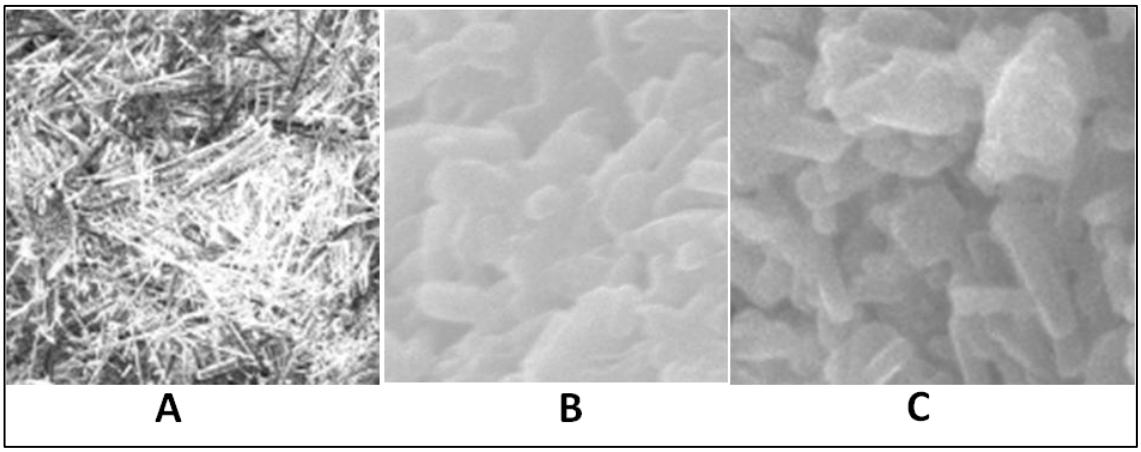

[A- CBZ: SACC 1:1 PURE COCRYSTAL, B- HME, C- S3M3]

Figure 6.56 Surface morphology by SEM of carbamazepine: saccharin 1:1 cocrystals processed by HME and S3M

6.4.2.7 FT-R

FT-IR analysis was carried out as detailed in Section 3.4.3. As discussed earlier CBZ shows characteristic symmetrical or asymmetrical –NH vibrations at 3465 and 3155 cm^{-1}, -C=O stretching at 1677 cm^{-1} and C=C, -C=O vibrations and –NH deformation at 1593 and 1603 cm^{-1} respectively. SACC shows characteristic –NH and C=O secondary amide stretching at 3093 and 1715 cm^{-1} respectively with asymmetric $–SO_2$ streching at 1332 and 1175 cm^{-1} (Figure 6.57). Pure coccrystal there was a shift in stretching at 3496 and 3182 respectively, exactly similar kind of strechings were observed in HME and S3M3 processed cocrystals with PEO. The peaks were broadened in all the cocrystal batches and due to slight change in $–SO_2$ streching vibrations (Figure 6.58).

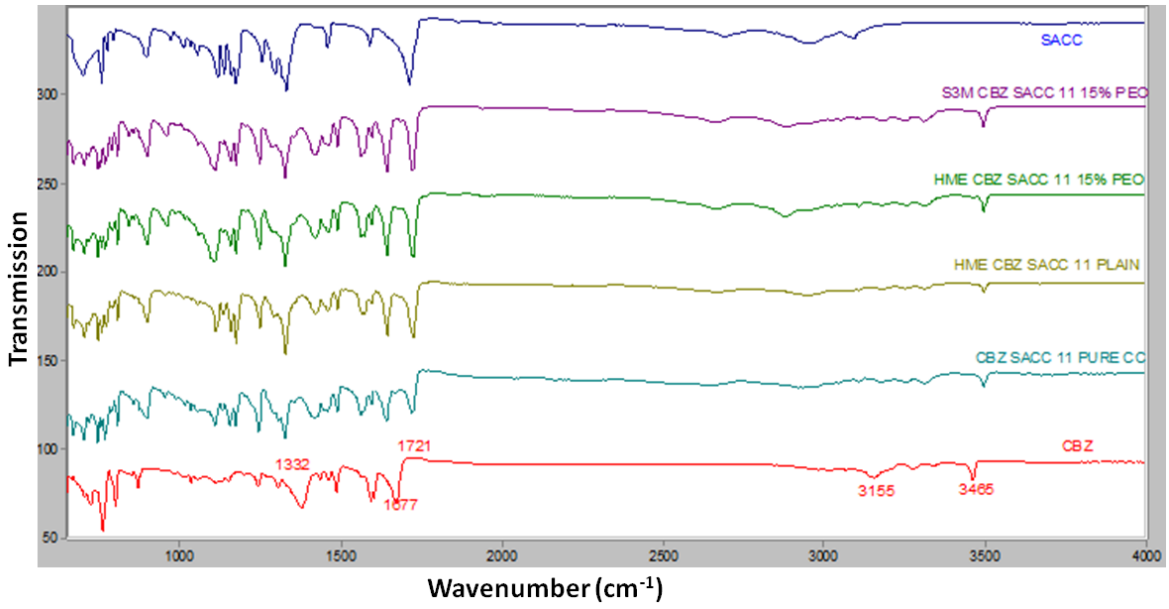

Figure 6.57 FT-IR spectra for CBZ:SACC 1:1 cocrystals by HME and S3M with PEO

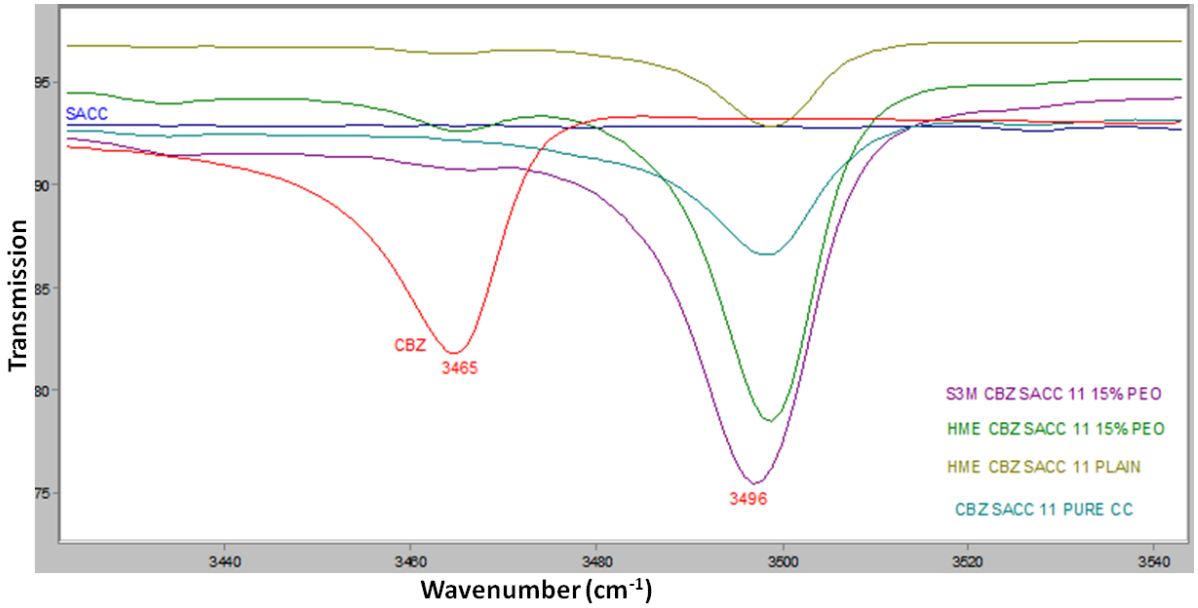

Figure 6.58 FT-IR spectra for carbamazepine: saccharin 1:1 cocrystals processed by HME and S3M with PEO

The shift in the stretching vibrations to such extent can be due to hydrogen bond formation (Schultheiss and Newman, 2009, Maheshwari *et al*. 2009) and it can be concluded that there is hydrogen bond formation between –NH of CBZ and $–SO_2$ of SACC.

6.4.2.8 NIR

NIR analysis was carried out as discussed in Section 3.4.4. Formation of new peak or stretching is generally considered as representative cocrystal peak in NIR analysis.

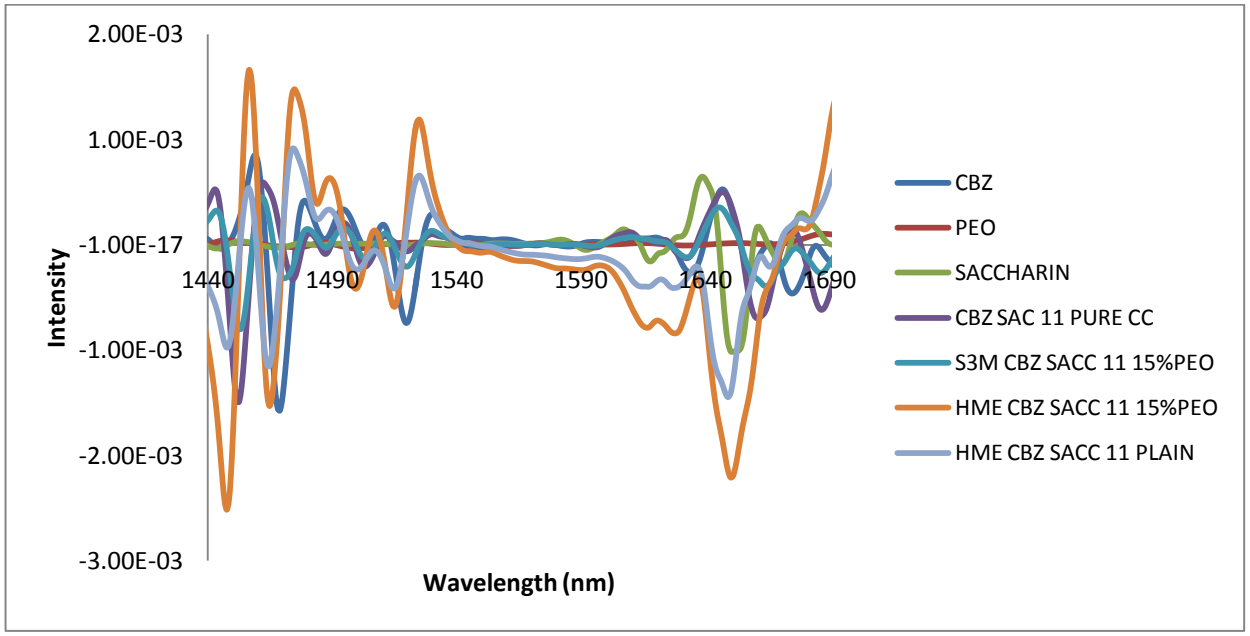

Figure 6.59 NIR spectra for carbamazepine: saccharin 1:1 cocrystals processed by HME and S3M

Saccharin showed good NIR absorption in the first overtone region at 1651 nm. The CBZ:SACC 1:1 pure cocrystal showed high NIR absorption in the second overtone region at 1454 and 1475 nm (Figure 6.59). The S3M processed CBZ:SACC 1:1 with PEO showed identical NIR absorption at 1454 nm whereas HME processed CBZ:SACC 1:1 cocrystals with and without polymer both showed NIR absorption at 1448 and 1465 nm which is a lower wavelength shift compared to pure cocrystal. The NIR findings complemented FT-IR outcomes and the presence of hydrogen bonds can be confirmed.

6.4.2.9 Dissolution

The dissolution profiles were performed as per Section 3.7.2 and the dissolution analysis was done by UPLC. HME processed CBZ: SACC 1:1 cocrystal without PEO showed slow CBZ release compared to PEO based cocrystals released 80% of CBZ in one hour and 100% in next three hours. The CBZ: SACC 1:1 cocrystal with 15% PEO showed 90% of CBZ release within 45mins and 100% within one hour (Figure 6.60).

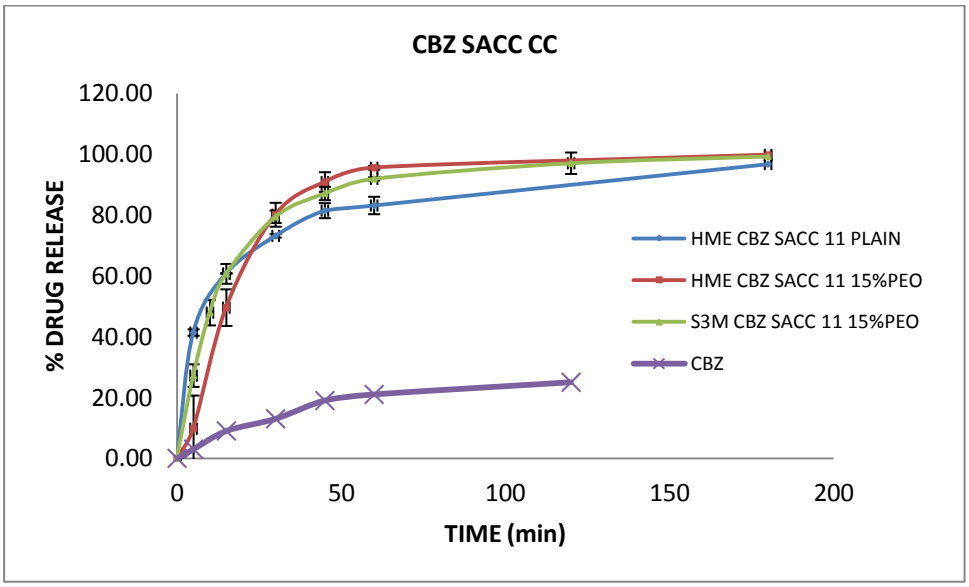

Figure 6.60 Dissolution profile for carbamazepine: saccharin 1:1 cocrystals with PEO processed by HME and S3M

The slow release for cocrystals without polymer can be contributed to a lower wettability due to the absence of polymer. The PEO based cocrystal enabled dissolution media to penetrate cocrystal matrix readily and showed faster dissolution.

6.4.3 Carbamazepine: nicotinamide 1:1 cocrystal (CBZ: NIC 1:1)

6.4.3.1 Crystal structure data

CBZ forms cocrystal with NIC in a 1:1 molar ratio which exhibits in an orthorhombic form. Many researchers have reported this pair as a good solubility improvement medium for CBZ. The crystal structure details, space groups and bond lengths and angles are described in Table 6.5.

Table 6.5 Crystal structural database and space group details for CBZ: NIC 1:1 cocrystal

Empirical formula	$C_{15}H_{12}N_2O$, $C_6H_6N_2O$
Crystal system	Orthorhombic
Space group	$P2_1/n$
a (Å)	5.096
b (Å)	17.595
c (Å)	19.647
α (°)	90.000
β (°)	90.917
γ (°)	90.000

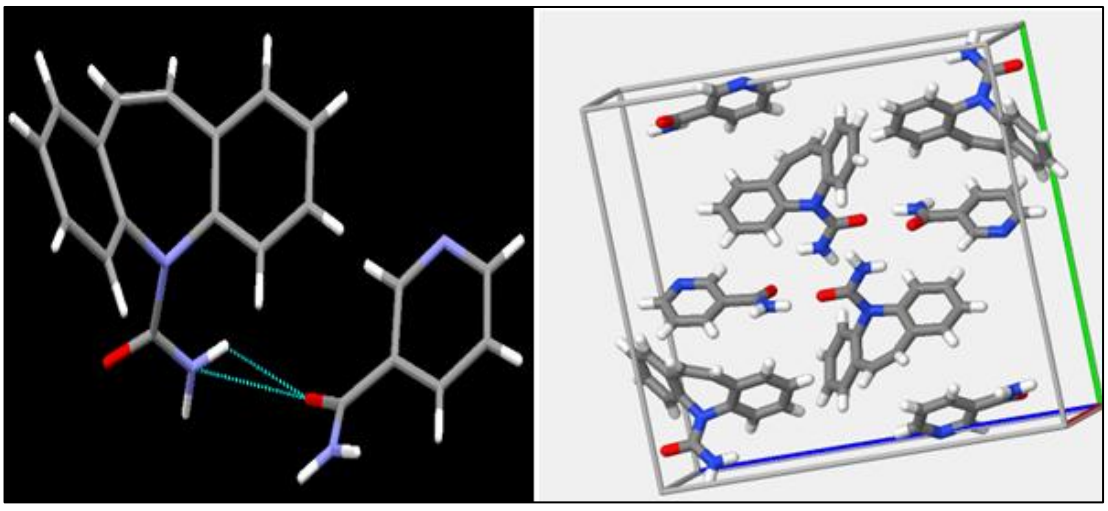

Figure 6.61 Crystal structure of carbamazepine: nicotinamide 1:1 cocrystal and crystal packing in unit cell. (adopted from CSD)

As shown in Figure 6.61 CBZ and NIC forms hydrogen bond with each other between respective functional groups –NH from CBZ and –C=O of NIC (Figure 6.58).

The PXRD for CBZ:NIC 1:1 cocrystal shows characteristic 2θ values at 6.44, 8.64, 9.92° respectively calculated from CSD database (Figure 6.62).

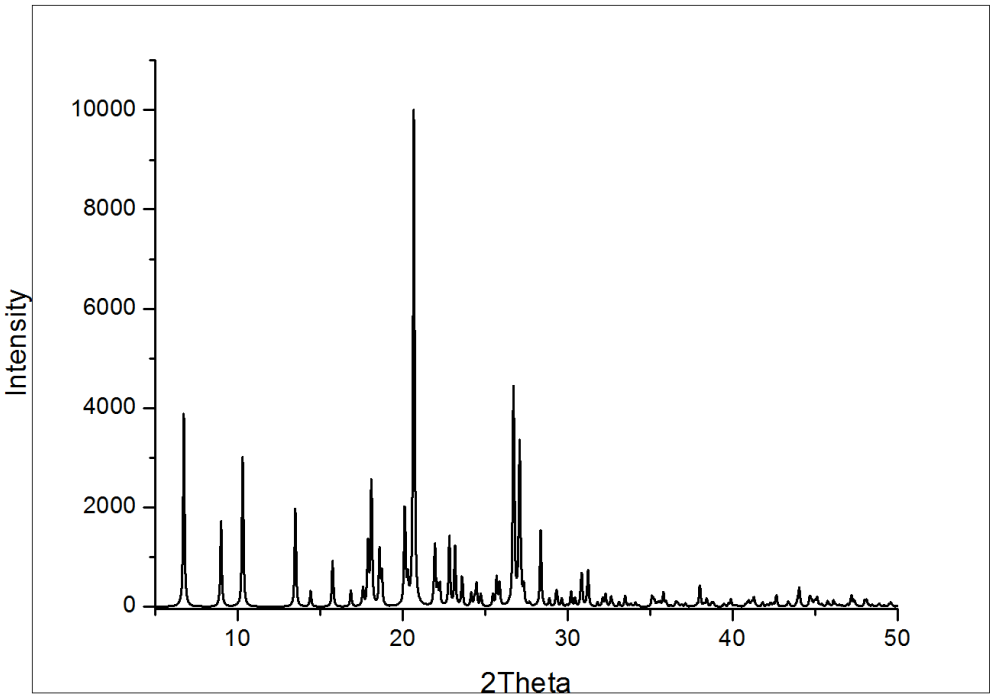

Figure 6.62 Calculated PXRD pattern for carbamazepine: nicotinamide 1:1 cocrystal (adopted from CSD- UNEZES and processed in OriginPro 8)

6.4.3.1 Processing of cocrystal

Accurately weighed CBZ and NIC were mixed in 1:1 proportion and 15% w/w PEO was added to this mixture. Following homogenous blending in a turbula mixer, the mixture was subjected to S3M3 processing. The product characteristics and process time was the same as CBZ: SACC and CBZ:

SAL cocrystals with both the processes HME and S3M3 process. The extrusion and temperature profiles were set as described in Section 3.7 (Table 3.10). The resultant end product of both the processes were analysed by various analytical techniques and for drug release.

6.4.3.2 Nicotinamide calibration

The calibration curve for NIC was linear over concentration range of 10-100 ug/ml. The linearity equation was calculated using calibration curve, slope of the equation is 783.52 and constant 584.4 and R^2 is 0.9982 (Figure 6.63). Calibration equation was used to calculate NIC release.

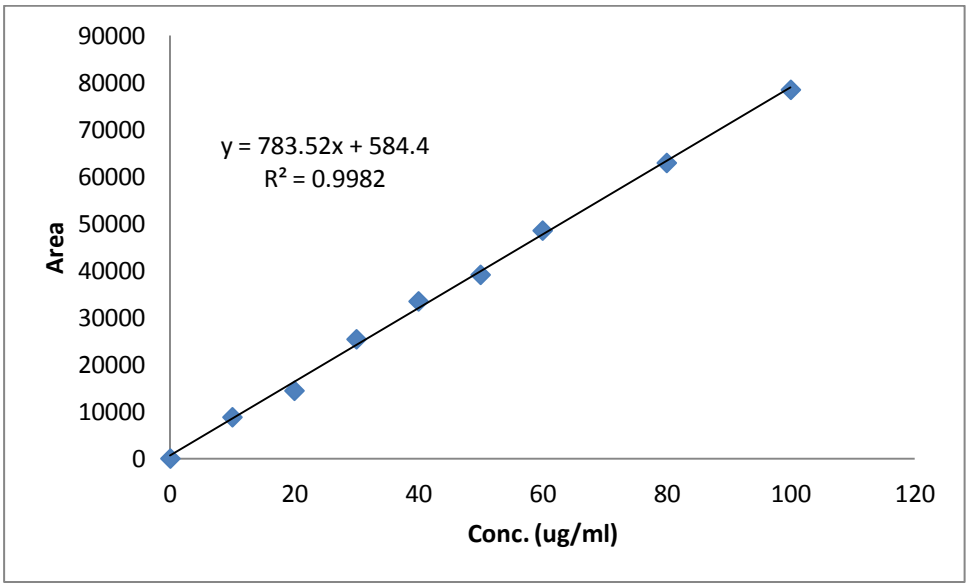

Figure 6.63 Nicotinamide calibration curve using UPLC at 262nm

The retention time for NIC in the UPLC method was found to be 1.3mins as shown in Figure 6.64.

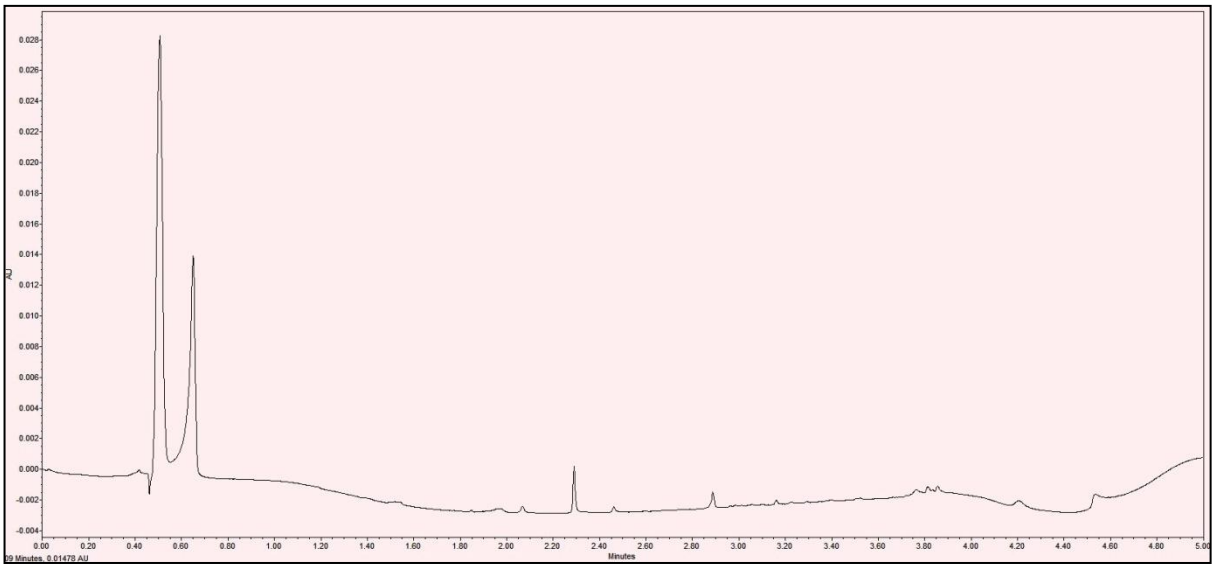

Figure 6.64 Nicotinamide chromatogram in UPLC analysis

6.4.3.3 PXRD

PXRD analysis was carried out as per Section 3.4.2. The characteristic 2θ values for CBZ were observed at 13.16, 14.2, 15.36, 15.92, 18.72, 19.56, 20.4° respectively as discussed earlier whereas pure CBZ:NIC 1:1 cocrystal showed characteristic 2θ values at 6.44, 8.64, 9.92°, similar to the CSD database for CBZ: NIC 1:1 cocrystal. The HME processed CBZ: NIC 1:1 without PEO showed 2θ values at 6.76, 9.83, 10.32° whereas PEO based cocrystal by S3M3 and HME showed 2θ values at 6.34, 8.52, 9.9° and 6.8, 8.92, 10.28 respectively (Figure 6.65). This confirms formation of pure CBZ:NIC 1:1 cocrystal processed by both the processes. The slight change in 2θ values can be attributed to the amount and type of surface exposed to X-rays during PXRD.

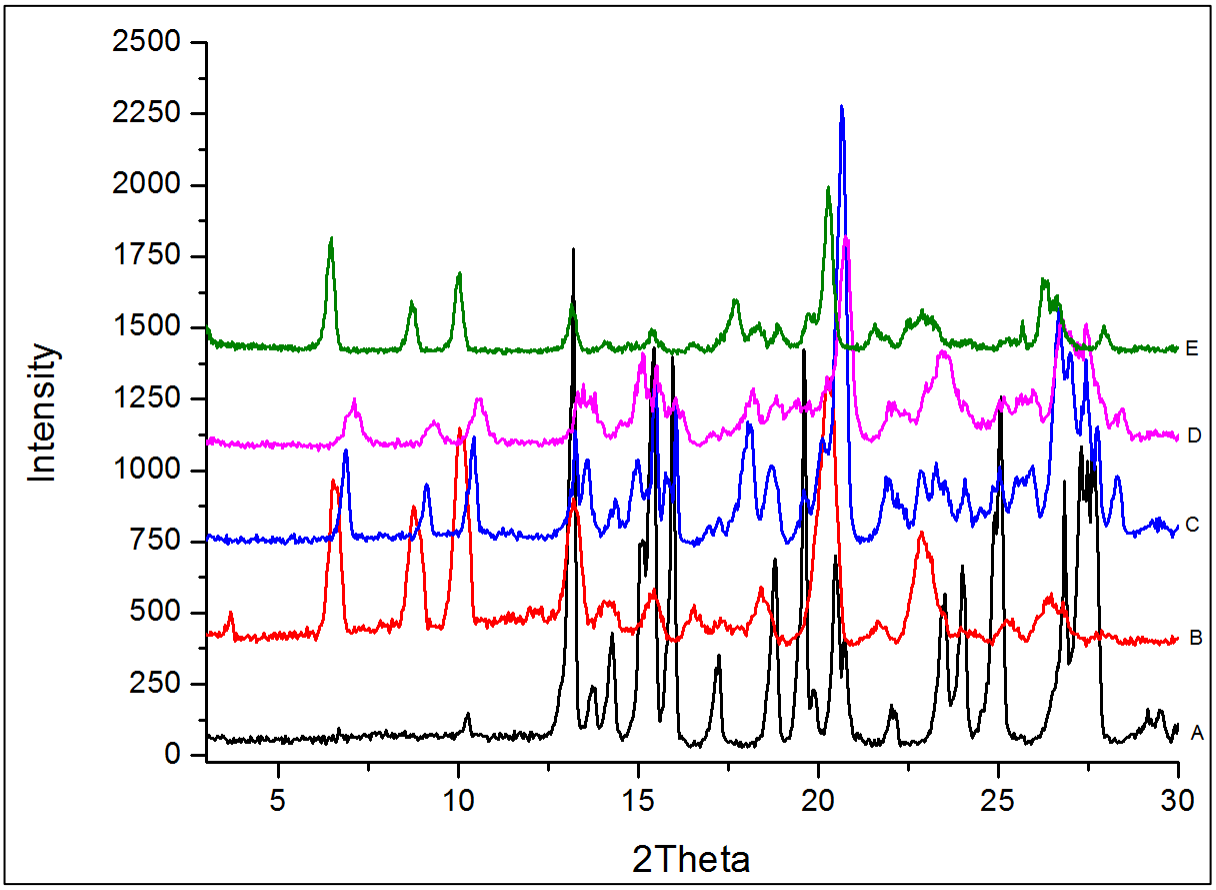

[A: Carbamazepine, B: CBZ:NIC 1:1 PURE CC, C: HME CBZ:NIC 1:1, D: HME CBZ:NIC 1:1 15% PEO, E: S3M CBZ:NIC 1:1 15% PEO]

Figure 6.65 PXRD for carbamazepine: nicotinamide 1:1 cocrystals processed by HME and S3M

6.4.3.4 DSC

Thermal analysis by DSC for CBZ:NIC 1:1 was carried out as described in Section 3.4.1. The CBZ melting endotherms at 175 and 191°C were not observed in any cocrystal batch (Figure 6.66). The CBZ:NIC 1:1 cocrystal shows a typical melting endotherm at 159 °C, which was observed in HME processed CBZ:NIC 1:1 cocrystal without PEO. The melting endotherm in case of S3M3 cocrystal was observed at 157 °C and in case of HME processed it was observed at 159 °C. The slight difference in the melting temperature can be attributed to the amount of polymer present in the DSC

sample. Thermal endotherms for respective cocrystals confirms that there is formation of phase pure cocrystal.

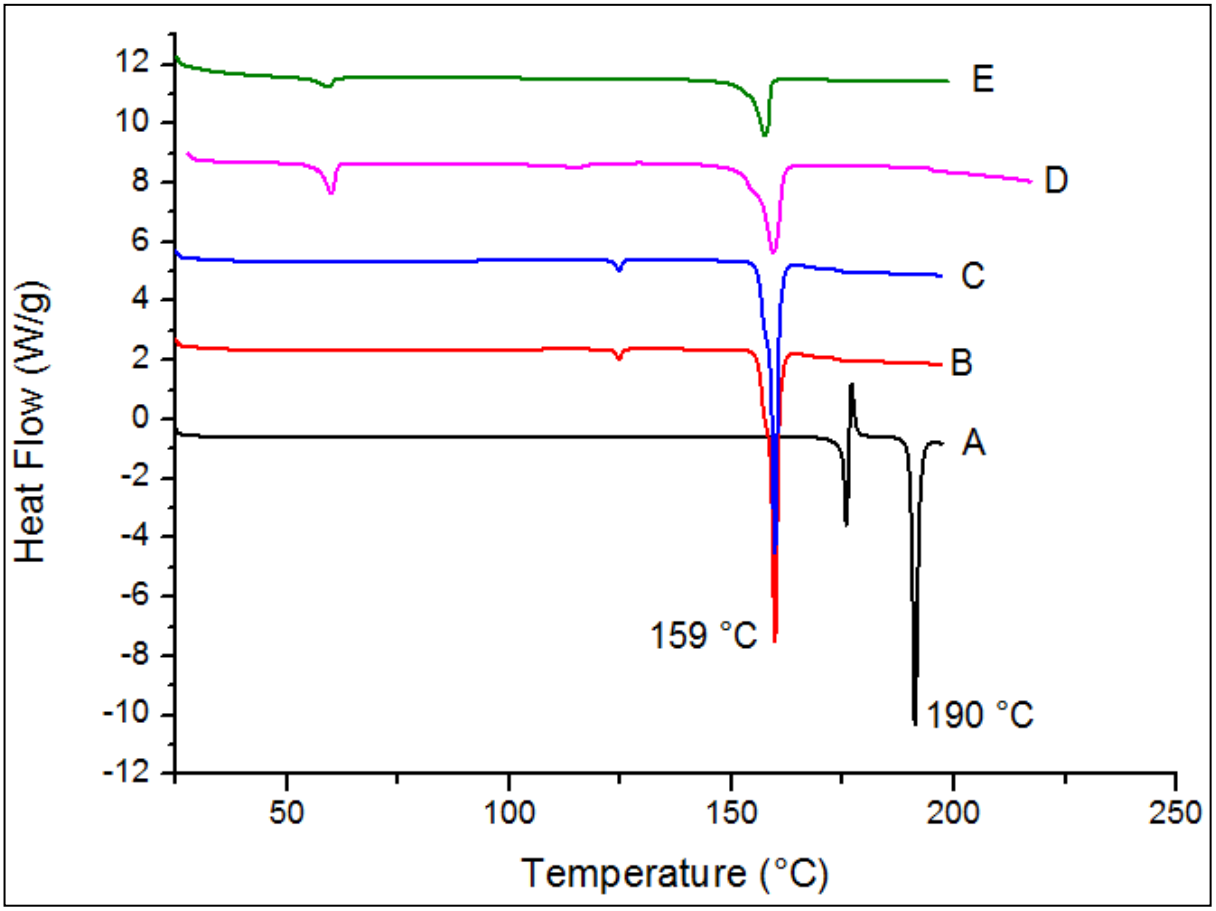

[A: Carbamazepine, B: CBZ:NIC 1:1 PURE CC, C: HME CBZ:NIC 1:1, D: HME CBZ:NIC 1:1 15% PEO, E: S3M CBZ:NIC 1:1 15% PEO]

Figure 6.66 DSC thermograms for carbamazepine: nicotinamide 1:1 cocrystals processed by HME and S3M

6.4.3.5 SEM

Surface morphology studies were carried out as described in Section 3.4.5. CBZ:NIC 1:1 cocrystals showed similar surface features and compacted physical form properties to those seen in CBZ:SAL and CBZ:SACC cocrystal. The HME cocrystals showed a similar compacted structure and

crystal embedded in the polymer matrix whereas S3M3 processed cocrystal had similar properties with distorted surface features (Figure 6.67)

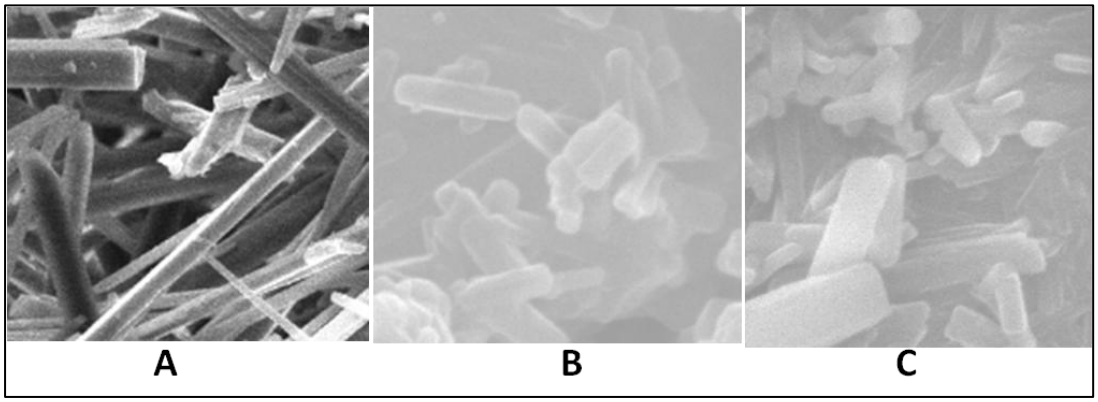

[A- CBZ: NIC 1:1 PURE CC, B- HME, C- S3M]

Figure 6.67 Surface morphology by SEM of carbamazepine: nicotinamide 1:1 cocrystals processed by HME and S3M

6.4.3.6 FT-IR

FT-IR analysis was carried out to confirm the presence of hydrogen bonding between CBZ and NIC. The procedure was carried out as described in Section 3.4.3. CBZ shows characteristic stretching at 3465 and 3155 cm^{-1} for primary amide stretching of –NH. Similar vibrations were also observed for NIC at 3358 and 3146 cm^{-1}, -C=O stretching was observed at 1677 in CBZ and at 1672 cm^{-1} NIC (Figure 6.68). CBZ: NIC 1:1 cocrystal showed stretching vibrations at 3448 and 3210 cm^{-1} typically with peak broadening. The same vibrations were seen in case of CBZ: NIC 1:1 cocrystal processed with 15% PEO by HME and S3M3 (Figure 6.69). The presence of hydrogen

bond between –NH and –C=O of NIC can be confirmed due to the shift in FT-IR vibrations and peak broadening.

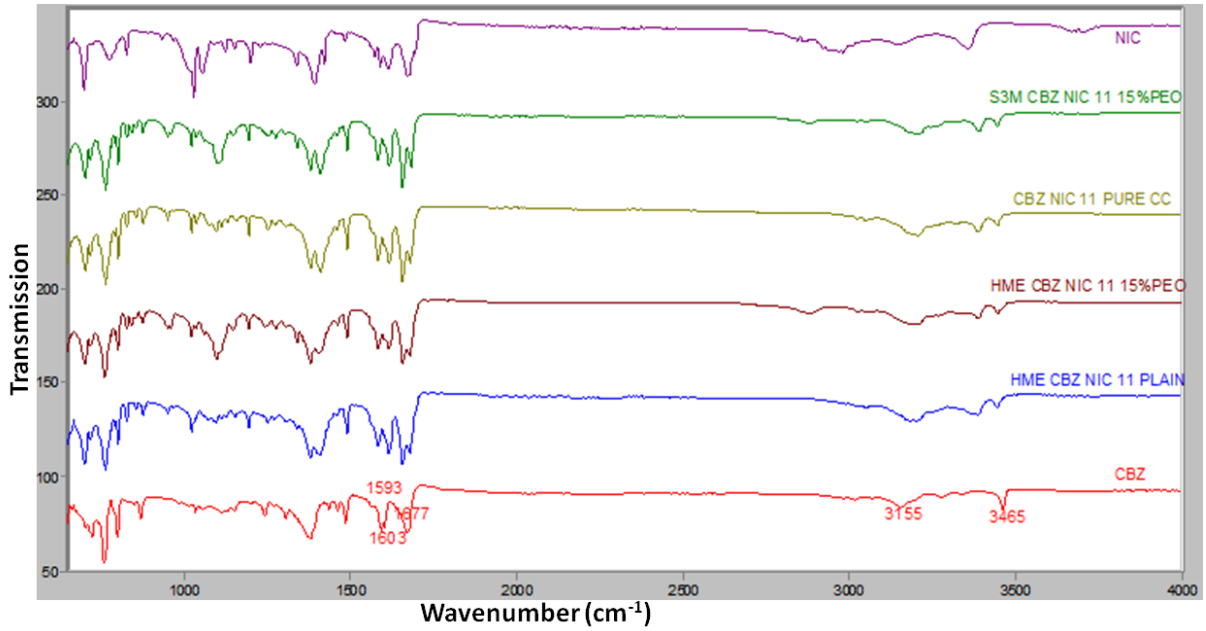

Figure 6.68 FT-IR spectra for carbamazepine: nicotinamide 1:1 cocrystal processed by HME and S3M with PEO

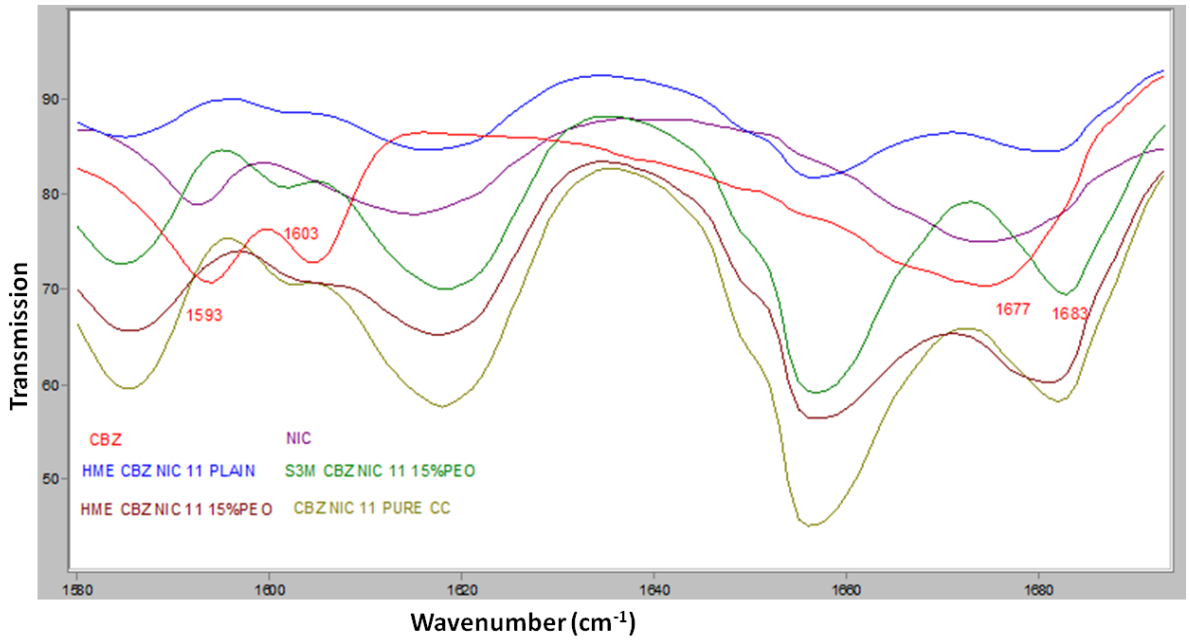

Figure 6.69 FT-IR spectra for carbamazepine: nicotinamide 1:1 cocrystals processed by HME and S3M with PEO

6.4.3.7 NIR

NIR analysis for CBZ:NIC cocrystals was carried out to support the FT-IR findings, procedure was followed as described in Section 3.4.4.

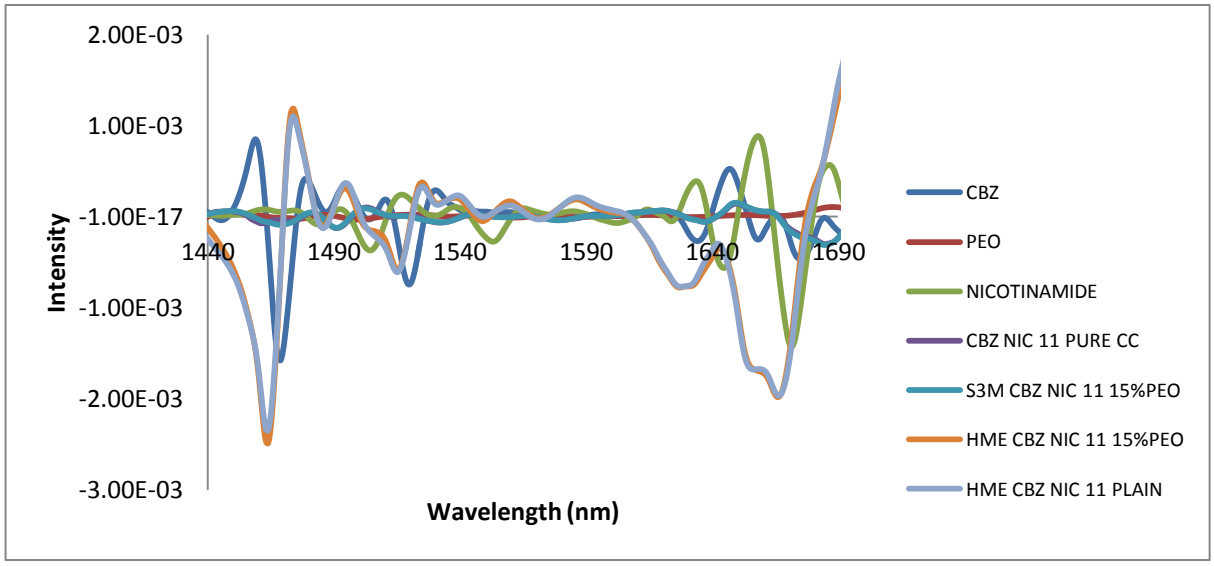

Figure 6.70 NIR spectra for carbamazepine: nicotinamide 1:1 cocrystals processed by HME and S3M

Nicotinamide showed characteristic NIR absorption in the second overtone region at 1505 and 1672 nm. Pure cocrystal CBZ:NIC 1:1 showed good NIR absorption in the first overtone region at 1463 and 1514 nm (Figure 6.70). Similarly way S3M and HME processed cocrystals showed identical NIR absorption as the pure cocrystal which shows that the extent of hydrogen bonding was similar for all CBZ:NIC 1:1 cocrystals.

6.4.3.8 Dissolution

Drug release studies were performed as described in Section 3.7.2. Figure 6.71 shows the drug release from different cocrystals processed by S3M3 and HME. S3M3 processed cocrystal with 15% PEO showed the fastest drug

release compared to HME cocrystals, S3M3 cocrystal exhibited maximum drug release in one hour. For HME processed cocrystals with 15% PEO the drug release was slow, 20% of drug in one hour and 3 hours to release about 70% of total drug. However, HME processed cocrystals without PEO showed good drug release around 70% in one hour and 100% in 3 hours.

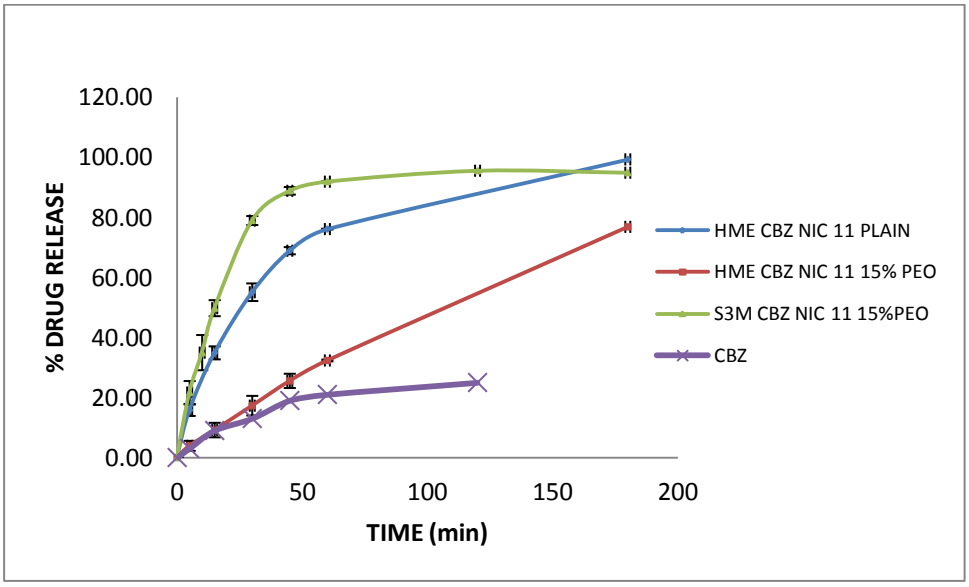

Figure 6.71 Dissolution profile for carbamazepine: nicotinamide 1:1 cocrystals with PEO processed by HME and S3M

The slower release of HME processed cocrystals can be attributed to the highly compacted nature of the end product which produced surface area and low surface porosity, reducing penetration of the dissolution media into the cocrystal matrix. The release of drug from S3M can be attributed to the highly crystalline and distorted, irregular surface features which improved penetration of media in crystal matrix.

6.4.4 Carbamazepine: glutaric acid 1:1 cocrystal (CBZ: GLUT 1:1)

6.4.4.1 Crystal structure data

CBZ forms a monoclinic cocrystal wit GLUT in 1:1 symmetry, this cocrystal exhibits monoclinic symmetry. GLUT has not been extensively studied by researchers as compared to the above discussed co-formers. GLUT, being a dicarboxylic acid and has –COOH functional readily available to form hydrogen bond with –NH of CBZ. The hydrogen bond formation is shown in Figure 6.72. The crystal structural database, space group details are given in Table 6.6.

Table 6.6 Crystal structural database and space group details for CBZ: GLUT 1:1 cocrystal

Empirical formula	$C_{15}H_{12}N_2O$, $C_5H_8O_4$
Crystal system	Monoclinic
Space group	$P2_1/n$
a (Å)	18.562
b (Å)	5.120
c (Å)	19.459
α (°)	90.000
β (°)	106.839
γ (°)	90.000

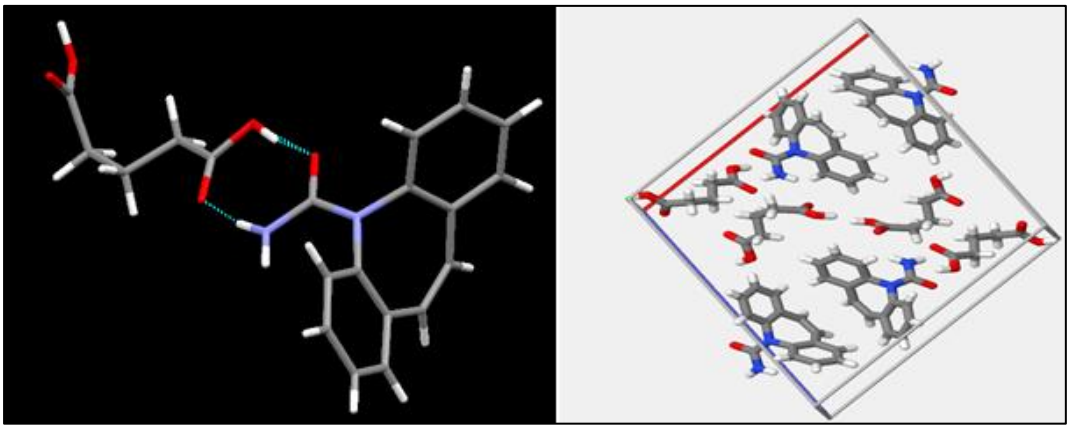

Figure 6.72 Crystal structure of carbamazepine: glutaric acid 1:1 cocrystal and crystal packing in unit cell. (adopted from CSD)

The CBZ:GLUT 1:1 cocrystal shows characteristic 2θ values at 9.48, 9.88, 13.36° respectively as shown in Figure 6.73

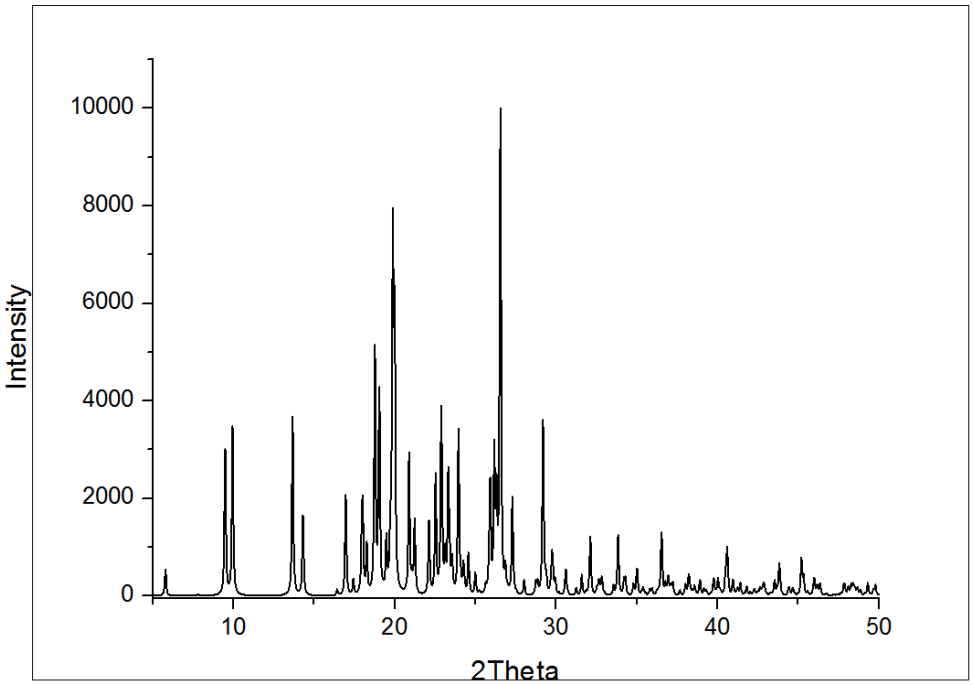

Figure 6.73 Calculated PXRD pattern for carbamazepine: glutaric acid 1:1 cocrystal (adopted from CSD- MOXVOL and processed in OriginPro 8)

6.4.4.2 Processing of cocrystal

The S3M3 procedure for CBZ:GLUT processing and its respective product characteristic were same as seen in case of CBZ: SAL, CBZ: NIC cocrystals. The HME was carried out as per the temperature and extrusion profiles described in Section 3.7 (Table 3.10). No difficulties were found in processing this cocrystal pair like others. End products of both the processes were characterised by various analytical techniques and for drug release

6.4.4.3 Glutaric acid calibration

As GLUT neither shows any UV absorbance nor gave any peak in UPLC analysis. A calibration study was not carried out for GLUT. The drug release studies were restricted to the CBZ release only.

6.4.4.4 PXRD

The PXRD for CBZ: GLUT 1:1 cocrystal was carried out by procedure described in Section 3.4.2. As discussed earlier CBZ shows characteristic 2θ values at 13.16, 14.2, 15.36, 15.92, 18.72, 19.56, 20.4° respectively, whereas GLUT shows at 13.88, 19.76, 21.44, 22.04, 24.12°. The pure CBZ: GLUT 1:1 cocrystal showed characteristic 2θ values at 9.48, 9.88, 13.36° which were identical to those seen in CSD structural database (Figure 6.74). With CBZ: GLUT cocrystal processed by HME without PEO, there was only one 2θ value was seen at 9.15°, with no other peaks observed. This can be attributed to partial transformation into cocrystal and HME process would need to be modified to get phase pure cocrystal. PXRD in the case of HME processed cocrystal with 15% PEO showed 2θ values at 9.72, 10.24, 13.36° and for S3M3 at 9.32, 9.8, 12.96° respectively, which shows that these 2θ values matches with the pure cocrystal. The slight difference in 2θ values can be explained as discussed earlier by the surface area of cocrystal exposed to X-rays during PXRD studies as well as due to process variations between HME and S3M3.

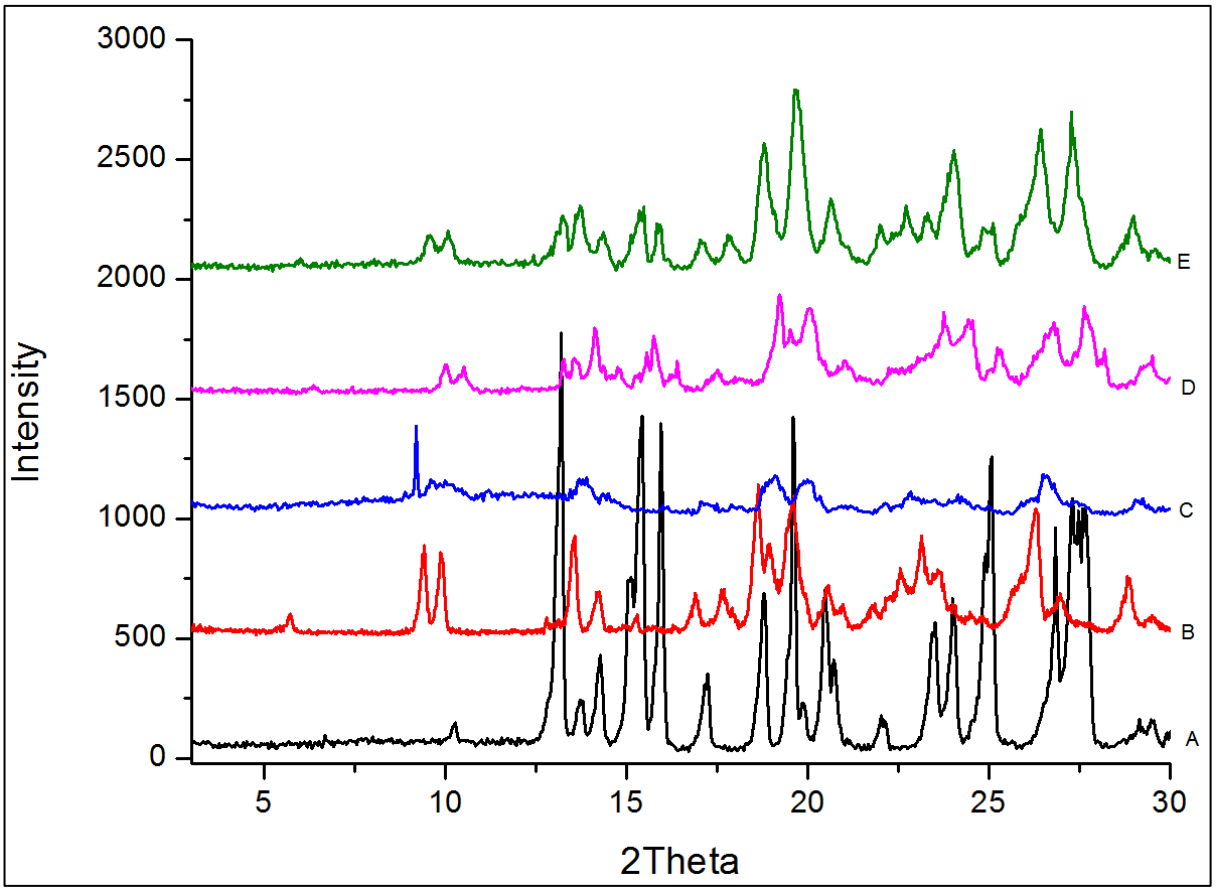

[A: Carbamazepine, B: CBZ:GLUT 1:1 PURE CC, C: HME CBZ:GLUT 1:1, D: HME CBZ:GLUT 1:1 15% PEO, E: S3M CBZ:GLUT 1:1 15% PEO]

Figure 6.74 PXRD for carbamazepine: glutaric acid 1:1 cocrystals processed by HME and S3M

6.4.4.5 DSC

Thermal analysis for CBZ: GLUT 1:1 cocrystals were performed as described in Section 3.4.1. As discussed earlier CBZ shows characteristic endotherms at 175 and 191 °C, in case of GLUT an endotherm was observed at 98 °C. The CBZ: GLUT 1:1 pure cocrystal showed characteristic melting endotherm at 124 °C. For HME processed cocrystal without PEO endotherms were observed 112 and 124 °C, first endotherm at 112 °C can be attributed to GLUT impurity and the endotherm at 124 °C show that there was formation of cocrystal. In the case of S3M3 processed CBZ: GLUT cocrystal with 15%

PEO an endotherm observed at 123.53 °C and in case of HME at 121.89 °C (Figure 6.75), which are near or close to the melting endotherm of pure cocrystal. This confirms the usefulness of PEO as aid in both the processes, which proved to be a good carrier for cocrystal formation.

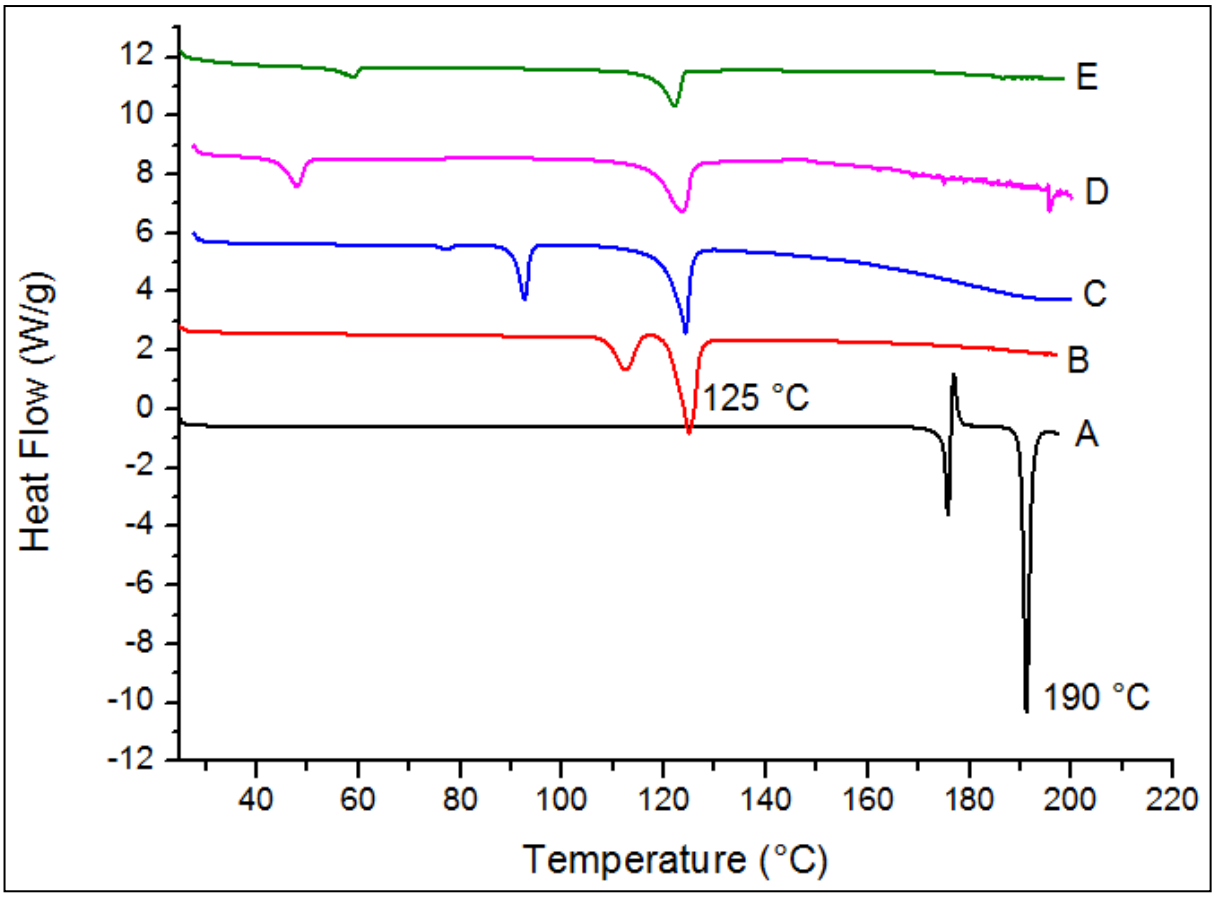

[A: Carbamazepine, B: CBZ:GLUT 1:1 PURE CC, C: HME CBZ:GLUT 1:1, D: HME CBZ:GLUT 1:1 15% PEO, E: S3M CBZ:GLUT 1:1 15% PEO]

Figure 6.75 DSC thermograms for carbamazepine:glutaric acid 1:1 cocrystal processed by HME and S3M

6.4.4.6 SEM

Surface morphology studies for CBZ: GLUT cocrystals were carried out as described in Section 3.4.5. The surface morphology was found to be similar to that in CBZ: SAL and CBZ: NIC cocrystals with PEO. CBZ:GLUT

cocrystals with PEO processed by HME showed a highly compacted structural morphology whereas S3M3 processed equivalents rough surface features with distorted morphology (Figure 6.76)

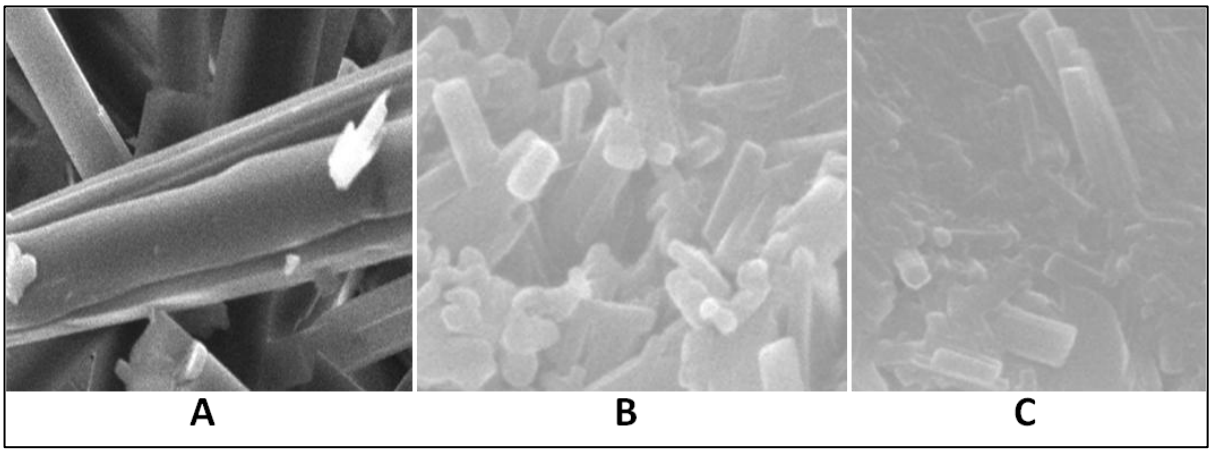

[A- CBZ: GLUT 1:1 PURE CC, B- S3M, C-HME]

Figure 6.76 Surface morphology by SEM of carbamazepine: glutaric acid 1:1 cocrystals processed by HME and S3M

6.4.4.7 FT-IR

FT-IR analysis of CBZ: GLUT 1:1 cocrystal was carried out as described in section 3.4.3. The formation of hydrogen bond between –NH of CBZ and –COOH of glutaric is an essential factor to convert CBZ and GLUT into a cocrystal. As discussed earlier CBZ specific –NH stretching can be seen at 3465 and 3155 cm^{-1} which are primary amide group asymmetrical or symmetrical stretching. GLUT specifically shows stretching at 1686 cm^{-1} (Figure 6.77), the resultant cocrystal shows unique stretching shifts at 3464 and 3182 cm^{-1}. For pure cocrystal generated by solution method whereas cocrystal with 15% PEO processed by S3M3 and HME showed stretching vibrations at 348 and 3182 cm^{-1} respectively with peak broadening (Figure 6.78). These peak shifts and peak broadening can be attributed to the hydrogen bond formation between CBZ and GLUT (Schultheiss, and Newman, 2009, Maheshwari *et al*. 2009).

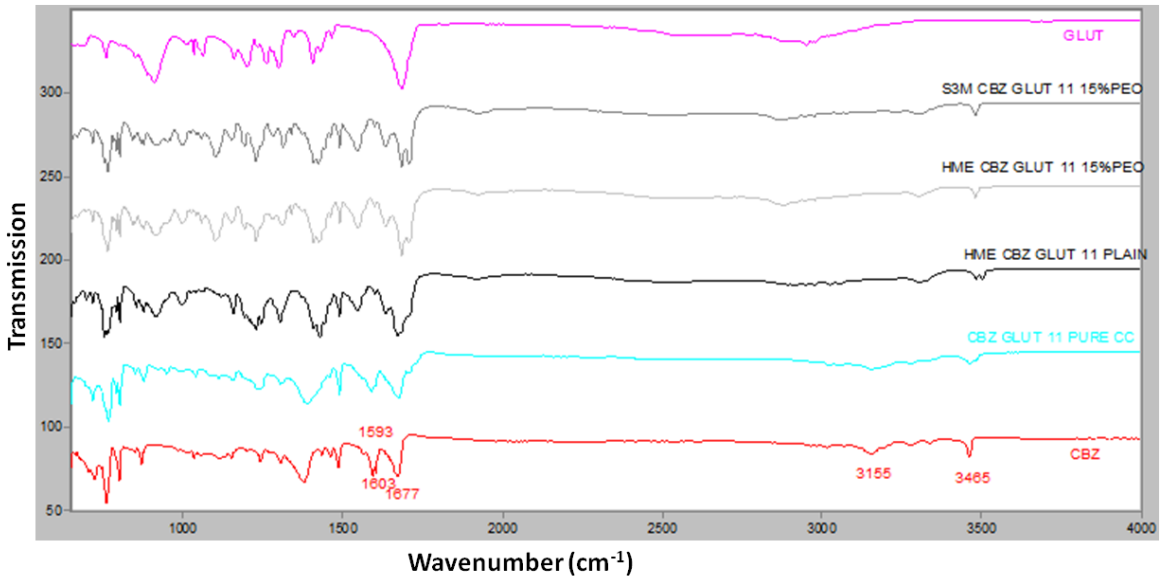

Figure 6.77 FT-IR spectra for carbamazepine: glutaric acid 1:1 cocrystals with PEO by HME and S3M

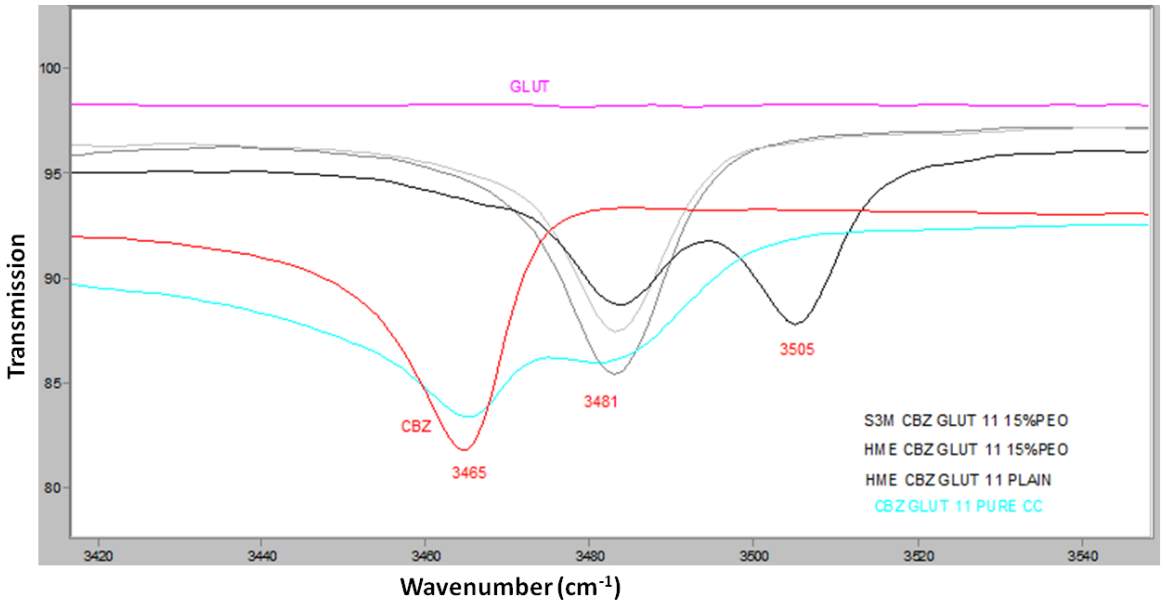

Figure 6.78 FT-IR spectra for carbamazepine: glutaric acid 1:1 cocrystal with PEO processed by HME and S3M

6.4.4.8 NIR

NIR analysis for CBZ: GLUT 1:1 cocrystal was carried out to support the FT-IR results and to confirm the nature and extent of hydrogen bonding.

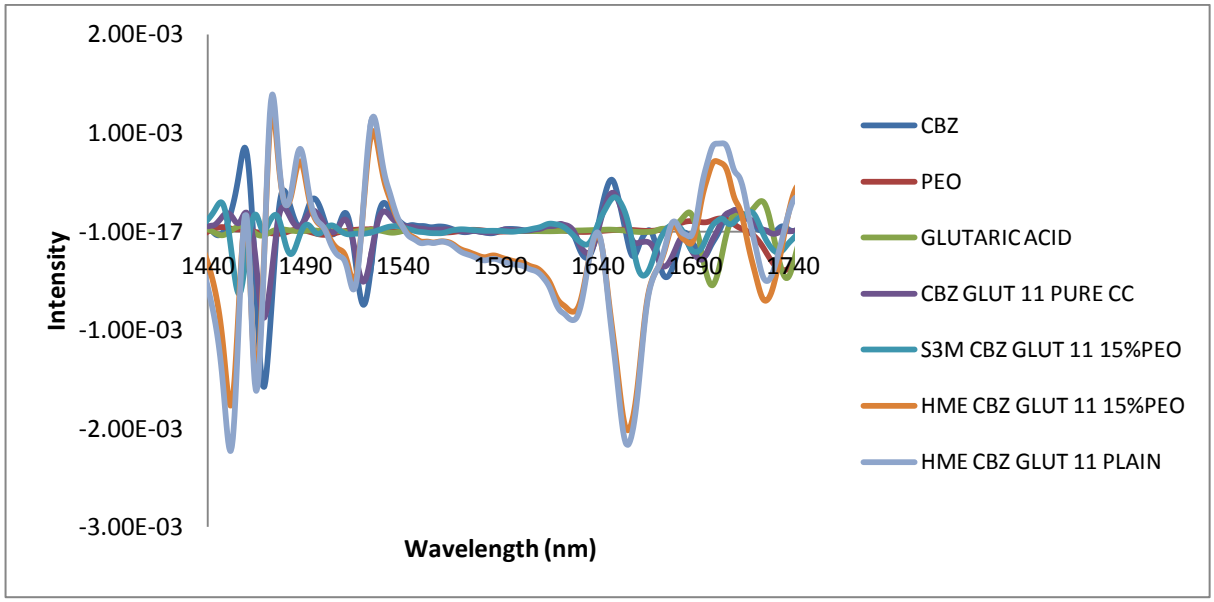

Figure 6.79 NIR spectra for carbamazepine: glutaric acid 1:1 cocrystals processed by HME and S3M

Glutaric acid shows good NIR absorption in the first overtone region at 1701 and 1737 nm. Pure cocrystals of CBZ:GLUT 1:1 showed characteristic NIR absorption at 1467 and 1519 nm. The S3M processed CBZ:GLUT 1:1 cocrystals with 15% PEO showed peaks at 1451 and 1465 nm; similar NIR absorption peaks were observed in case of CBZ:GLUT 1:1 cocrystal without PEO from HME. Cocrystals processed by HME with PEO showed NIR absorption shift to 1457 and 1482 nm respectively (Figure 6.79). The formation of new peaks or this major shift from CBZ and GLUT can be attributed to the formation of hydrogen bond between CBZ and GLUT.

6.4.4.9 Dissolution

The dissolution studies were carried out as per the method and procedure described in Section 3.7.2.

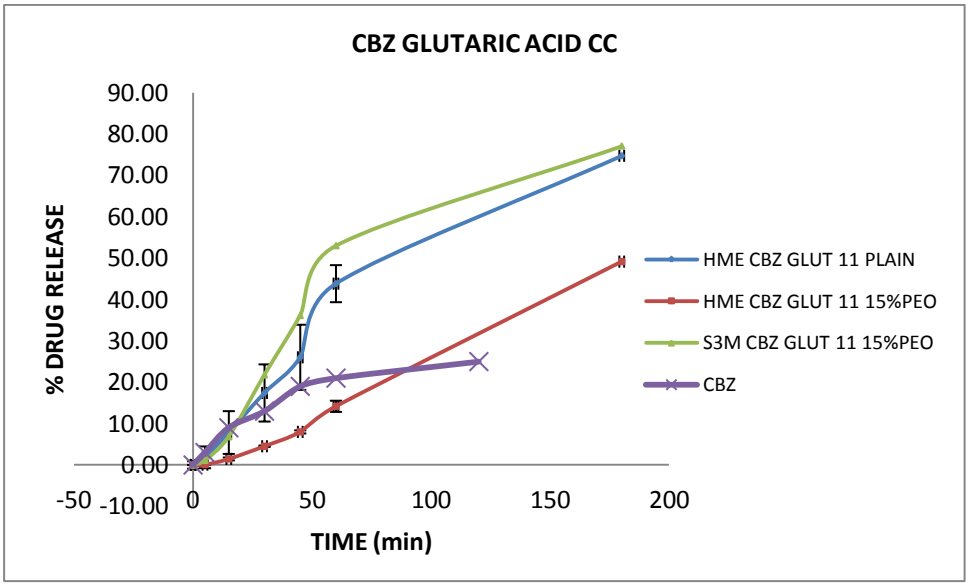

Figure 6.80 Dissolution profile for carbamazepine: glutaric acid 1:1 cocrystal with PEO by HME and S3M

Dissolution profiles for CBZ: GLUT 1:1 cocrystal (Figure 6.80) showed similar drug release to that shown by CBZ: NIC 1:1 cocrystals. The S3M3 processed cocrystal with PEO showed fastest release but slow release as compared to other S3M3 processed cocrystal with SAL, NIC or SACC as co-formers. Only 80% of the drug was released in 3 hours, and a similar kind of observation was made in case of HME processed cocrystal without PEO as an aid. The HME processed cocrystal with PEO showed slowest release as compared to the other two and could release only about 50% of the total drug; this can be attributed to the compacted nature of the extrudates as discussed earlier.

All the cocrystals processed on S3M3 included polymer from 5-25% w/w of total composition, it was very important to see that does this amount of polymer will have any effect on the degradation of drug, co-former or on

polymer itself. Degradation studies were carried out for CBZ cocrystal batches as it is majorly focussed drug in this study.

6.4.5 Degradation analysis

All the CBZ cocrystal batches with and without polymers were subjected to iminostilbene analysis. Most of the CBZ solid dispersion showed degradation by generating iminostilbene during HME and S3M processing. The iminostilbene generation results are shown in Figure 6.81. All S3M processed CBZ cocrystal batches showed none or negligible amount of iminostilbene except for the CBZ:SAL 1:1 with 25% PVP VA64 cocrystal batch, which showed significant iminostilbene generation. HME processed CBZ:SAL 1:1 cocrystal batches also showed significant generation of iminostilbene. The highest generation of iminostilbene was observed in cocrystals with 25% PVP VA64>15% PVP VA64>5% PEO> HME CBZ:SAL 1:1 plain cocrystal without polymer> HME CBZ:SACC 1:1 plain cocrystal without polymer> HME CBZ:GLUT 1:1 15% PEO> HME CBZ:GLUT 1:1 plain cocrystal without polymer> HME CBZ:SACC 1:1 15% PEO> HME CBZ:SAL 1:1 25% PEO> HME CBZ:SAL 1:1 10% PEO.

From Figure 6.81 it can be observed that CBZ degradation for CBZ: SAL cocrystals was seen when 25% VA64 was used as a processing aid during S3M3 and that there was no CBZ degradation observed in the case of the other CBZ: SAL cocrystal batches with other polymer concentrations. This confirms that for drug degradation, the amount of polymer plays an important role, as application of shear on the total drug: polymer system is governed by the polymer and not the drug in S3M3 processing. In HME the reason for

CBZ degradation is likely to be due to the residence time in the extruder barrel during HME processing. The HME process would require modification to control the extent of drug degradation.

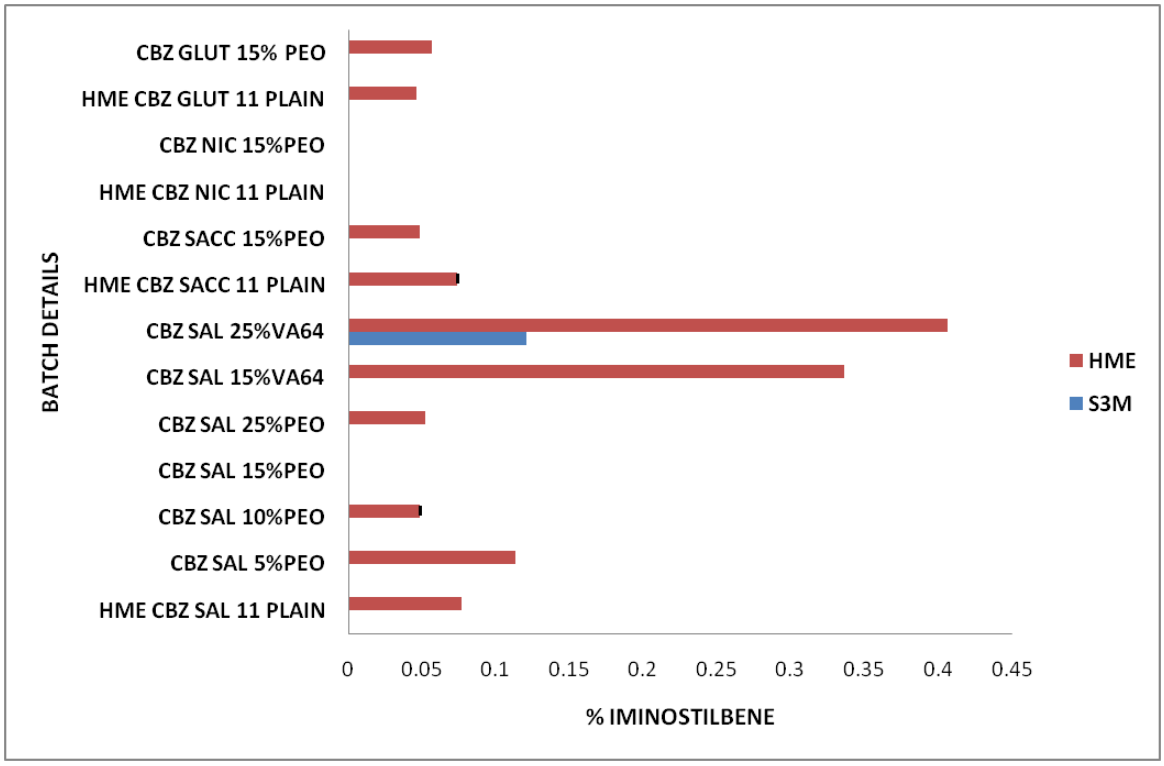

Figure 6.81 Iminostilbene analysis in carbamazepine cocrystals with and without PEO and PVP VA64 processed by HME and S3M

This can be achieved by control on process parameters such as screw configuration and screw rotation speed. The S3M3 process is rather basic in nature, scalable but primarily used for plastics. However, it has shown great potential in producing pharmaceutical cocrystals with minimal degradation.

Cocrystals can be efficiently formed using the S3M3 process, but it has a limitation of a dependency on polymeric processing aids. Without the aid a polymer it is very hard to process the plain drug and co-former mixture. Different concentrations of polymer had different structural effects in various cocrystal pairs; performance of the cocrystals formed can be manipulated by

the concentration and type of polymer used. HME has major advantage over S3M3 as it is not dependent on polymeric processing aids to form the cocrystals.

Processing aid used in case of CBZ cocrystals were PEO and PVP VA64 both the polymer aid was able to form phase pure cocrystals so it was very difficult to differentiate between these two which one is better over other. Both the polymers can be used as processing aids.

In case of solid dispersions, S3M3 has an advantage in the sense that its drug polymer mixtures can be directly processed without use of plasticisers as discussed in previous chapter.

The S3M3 mechanism, its control and its three dimensional scissor shear action need to be understood well, as it governs the product performance in all sense. The overall observations and results from solid dispersions and cocrystals manufactured by both these processes has shown that S3M3 can be a potentially important process for the pharmaceutical industry to manufacture solid dispersions and cocrystal formulations on large scale.

The nature of products and product performance in both solid dispersions and cocrystals showed significant differences; the next chapter will provide a brief explanation and discussion of the understanding between the physicochemical changes in the products developed by two the processes and provide a process comparative study.

Chapter 7. Global discussion

The effect of processing technology on the product properties has been discussed in the chapter 5 and chapter 6. The major aim of this discussion is to develop some understanding based on the difference in the processing requirements for solid dispersions and cocrystals. The solid dispersion batches which are two component systems produced at relatively high polymer concentrations (50-66% w/w) whereas a three component system (drug: co-former: polymer) 5-20% w/w in case of co-crystal batches. The objective in solid dispersion is to achieve miscibility of the solid dispersion as two component system (containing drug and polymer (50-66%w/w), the cocrystal batches were ternary system containing drug-coformer and polymer (5-20%w/w). Though the SFCC technique using HME reported from our lab demonstrated generation of cocrystals from two phases system without polymer. There have been attempts to produce cocrystals in the ternary systems using HME. An attempt has been reported include generate ibuprofen-nicotinamide cocrystals in presence of 50% xylitol, but there is not clear evidence of achieving cocrystals. Hence, xylitol addition shown has limited success. Whereas Boksa *et al*., reported matrix assisted cocrystallisation of carbamazepine-nicotinamide in presence of 20% soluplus using HME technique. This clearly shows that selection of the third component is critical. The third component concentration was maintained constant during batches by both the techniques. The lower concentration of polymer in cocrystal batches was improving processability but above critical concentrations (20%) solid dispersion is favoured.

In the present study carbamazepine was selected as a model molecule due to its degradation challenge at high temp. Carbamazepine is common in cocrystal as well as solid dispersion batches. It was observed that

HME and S3M both being a high shear solid state processing technologies showed a completely different end product characteristics. The solid dispersions and cocrystals produced by these techniques varied in all physicochemical aspects as well as in terms of drug release and degradation. PXRD and DSC analysis showed similar results for HME and S3M processed samples whereas SEM analysis showed a drastic variability in terms of morphology and surface features between end products of these processes. The distorted and highly rough surfaces in case of S3M processed plasticiser free amorphous dispersions can be contributed to the three dimensional scissoring shear actions during S3M processing; these highly rough surfaces affected the dissolution of the amorphous dispersions which was faster than HME processed dispersions. The faster drug release was not observed in all the drugs solid dispersions processed by S3M, some of the dispersions showed similar kind of drug release pattern without any major delay or difference during dissolution studies. The highly rough and porous surfaces will surely help in improving wettability and penetration of dissolution medium into the solid dispersion matrix; this will be very useful during the downstream processing during conversion of milled solid dispersions into powder form due to their easily crushable nature. In case of HME processed solid dispersions due to plasticisation the surface features of solid dispersions were very smooth and completely non-porous and unlike

S3M processed solid dispersions these were very hard to break due to high plasticity, which made them difficult to break into fine powders during milling. This shows that S3M processed product will exhibit easy downstream processing compared to HME. In case of cocrystals both the processes produced phase pure cocrystals. It was possible in HME to process plain drug: co-former blends as such whereas in case of S3M it was mandatory to use polymer aid. The type of end products in HME and S3M processing using polymer aids for cocrystal preparation showed similar structural features but differed in shape size and overall morphology. The polymer aid cocrystals showed crystals embedded in polymer matrix as shown in SEM analysis. The critical polymer concentration needed to form phase pure cocrystal during S3M processing was very important, in case of CBZ: SAL 1:1 cocrystals PEO concentration varied from 5-25%. The 5% PEO aided material showed formation of phase pure cocrystals whereas 25% aided also showed formation of phase pure cocrystals but with reduced intensity crystalline peaks in PXRD analysis and which seems near to get converted into amorphous structure. The 10% and 15% of PEO as polymer aid showed formation of phase pure cocrystals in that 15% PEO aided cocrystals showed good structural morphology. 15% polymer aid was then finalised as standard polymer aid for other cocrystals. In case of HME it's not compulsory to have polymer aid as it is possible to process the drug: conformer blend easily at the eutectic temperature of the mixture. The use of polymer aid might have acted as solvent in molten form at softening or melting temperature of respective polymers (PEO/ PVP VA64/ HP55) during S3M processing, which

eventually made drug: co-former blend to get dissolved in the polymer melt and form a phase pure cocrystals. One more interesting fact is that in case of S3M there is no external heating facility or temperature controlling ability, the polymer aid was melted due to high shear applied during S3M processing, temperature rise in S3M processing was only due to high shear mechanism of S3M and due to friction of two pans over each other. In case of HME plain drug: co-former mixture without external heat application was not able to produce cocrystals, similar observation was found when experiment was carried out without polymer aid. It is compulsory in HME processing to have external heating or temperature controlling facility without that the shear applied by twin screws was not sufficient enough to generated required heat during processing to convert drug: co-former into cocrystals. It was then mandatory to keep the HME processing temperature at or slightly above the melting or softening temperature of polymer aid.

Recently Liu et al., studied the use of cocrystallisation with solid dispersion using HME processing to form chemically stable solid dispersions of CBZ: NIC 1:1 cocrystals. The polymer used was PVP VA64, soluplus and HPMC. They observed that CBZ can be processed at 160 °C i.e. 30° below its melting point to avoid its degradation. As it was discussed in case of CBZ solid dispersions with HPMCP and HPMCAS there was significant CBZ degradation in both the processes S3M and HME whereas in case of all CBZ cocrystals processed at 110 °C which is 80° below melting temperature of CBZ. Though CBZ cocrystal were processed at well below its melting point still there was some degradation found which was quantified by generation of

iminostilbene. In case of S3M processed CBZ cocrystals with polymer aid CBZ degradation was observed when 25% PVP VA64 was used as a polymer aid. All other CBZ cocrystals processed by S3M did not show any CBZ degradation whereas in case of HME all CBZ cocrystals showed CBZ degradation which was increased as polymer aid concentration was increased. These findings were contradictory with Liu et al., findings, as Liu et al., did not show any iminostilbene generation data and did TGA analysis for degradation studies. The HPLC analysis for iminostilbene for quantification of CBZ degradation gives better analysis of CBZ degradation.

It can be concluded that HME is plasticiser dependent and S3M is plasticiser free processing in case of solid dispersions whereas S3M is polymer aid dependent for cocrystal manufacturing whereas HME is independent of polymer aid. As the polymer concentration increases in case of S3M degradation will also be enhanced as seen in CBZ degradation analysis. The main reason for degradation of drug or polymer in case of HME can be contributed to the residence time and temperature profiles used during process as well as plasticiser concentration in case of solid dispersions. The shear applied in S3M processing was same for all the solid dispersions and cocrystals but the residence time and shear applied was mainly dependent on the polymer concentrations.

One aspect which is not clear is whether the energy requirement for disruption of crystal lattice and achievement of a molecular dispersion require more energy compared to formation of cocrystals. This is also evident that formation of cocrystals can be achieved with relatively low

energy input as in ball milling whereas generation of solid dispersions require significantly high energy input. Considering this, an attempt to enhance understanding of energy consumption during processing has been initiated but it is still in a preliminary stage (Figure 7.1)

Milling of the end product in HME and S3M is most important step in downstream processing. Extrudates from HME and agglomerates from S3M need to be reduced to a certain particle size to formulate them into suitable dosage forms such as tablets or capsules. Energy consumption during downstream processing might change the physicochemical structure of the product.

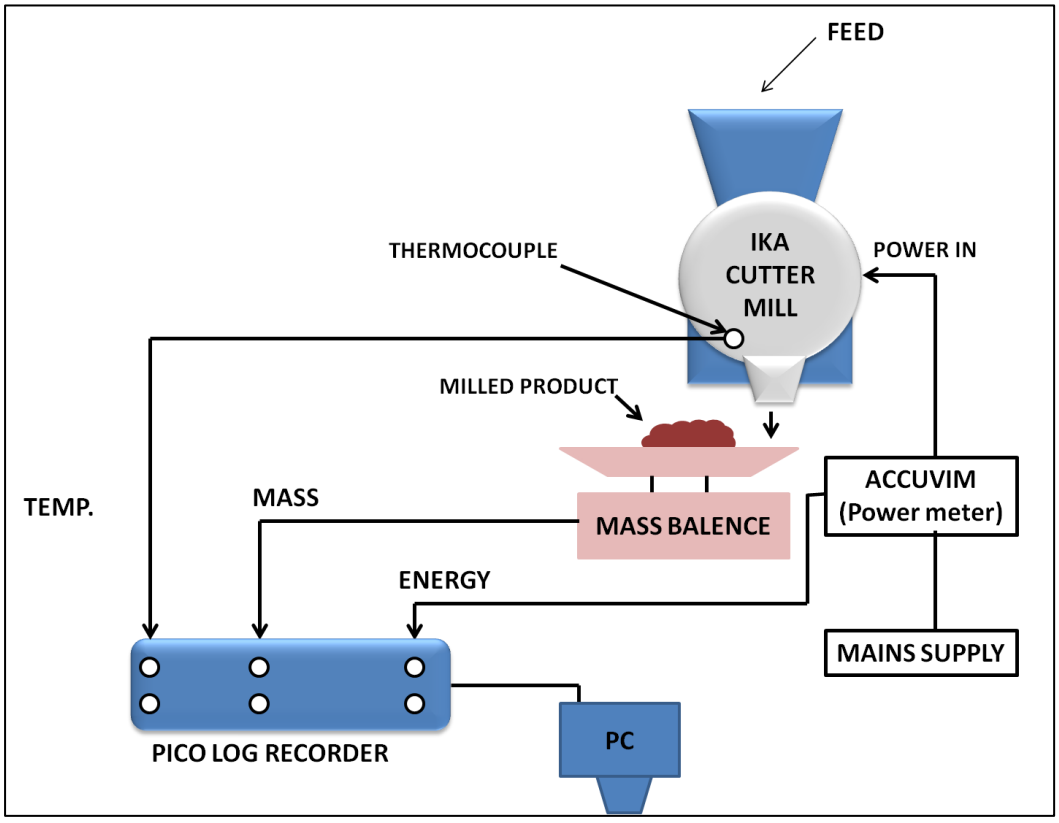

Figure 7.1 Schematics of energy measurement system

Energy measurement components: IKA cutter mill, PICO TECHNOLOGY TC-08, ACCUENERGY ACCUVIM 100, PICO log recorder.

Weighing balance with analogue output: A&D GX-200-EC 210g x 0.001g, Pan size: 128 x 128mm & Analogue Output Option (GX-OP-06).

For simultaneous analysis of energy, mass output and temperature during the milling process, power output was measured by an ACCUVIM 100 directly from the mill which was recorded by a PICO log recorder to convert and log the exact amount of energy. For mass output, the analogue output from the balance connected to PICO recorder which converted the exact mass output into the system. For simultaneous temperature monitoring a thermocouple was fixed beneath sieve of mill which was fixed in PICO log recorder to monitor fluctuations or rise in temperature during milling.

Chapter 8. Conclusion and future work

From the research carried out here, the following conclusion can be drawn:

- S3M has shown great potential in manufacturing of solid dispersions and cocrystals in continuous manner. It shows similar potential as HME and can be a good alternative technology for large scale production of solid dosage forms. HME has proved its potential in many ways to improve the existing pharmaceutical dosage forms and by avoiding conventional upstream processing which is generally followed in production of solid unit dosage forms tablets and capsules. HME being widely accepted technology need to come over some processing hurdles with respect to different pharmaceutical APIs.
- One need a very good process control in terms of temperature profile and different process variable, as we discussed earlier plasticisation is must in some cases to lower down the processing temperatures and avoid subsequent degradation. At present S3M being very basic model and majorly been explored for higher molecular weight plastic polymers and unfit for the pharmaceutical processing at this stage, use of S3M for pharmaceutical processing is at very early stage and being firstly getting noticed and reported here.
- S3M has some major advantages over HME in case of processing times, plasticisation free processing and quality of end products obtained in case of solid dispersions and cocrystals. The pharmaceutical market keeps thriving on existing technologies to

improve them and to look for substantial technologies which can replace existing ones with minimal or no drawbacks.

- S3M can be a successful single step, continuous processing technology for pharmaceutical manufacturing. There was provision of S3M in series (2-3 S3M kept vertically or horizontally in series) for large and continuous processing of polymers which can be implemented while developing pharmaceutical products which will specifically help in product development which need more than one S3M cycles to convert them into suitable product. S3M potential has been explored for production of solid dispersions and cocrystals, development of other and challenging pharmaceutical dosage forms will test the real efficiency in pharmaceutical field.
- Future work will majorly focus on improving S3M process to an pharmaceutical industry standard with an excellent process control in terms of temperature, shear, process time, improved material of S3M construction (Pharma grade SS with low or no wear and tear) and different size, shape and designs of pans will make S3M. This might turn S3M in a new edge technology for pharmaceutical field with very wide applications for development of existing and new kind of pharmaceutical dosage forms.

Chapter 9. References

Abramov, Y.A., Loschen, C., Klant, A. (2012) Rational coformer or solvent selection for pharmaceutical cocrystallization or desolvation. J. Pharm. Sci., 101, 3697.

Aher, S., Dhumal, R., Mahadik, K., Paradkar, A., York, P. (2010) Ultrasound assisted cocrystallization from solution (USSC) containing a non-congruently soluble cocrystal component pair: Caffeine/maleic acid. *Eur J Pharm Sci*., 41(5), 597-602.

Al-Obaidi, H., Lawrence, M. J., Al-Saden, N. and Ke, P. (2013) Investigation of griseofulvin and hydroxypropylmethyl cellulose acetate succinate miscibility in ball milled solid dispersions. *Int J Pharm,* 443 (1-2)**,** 95-102.

Asada, M., Takahashi, H., Okamoto, H., Tanino, H. and Danjo, K. (2004) Theophylline particle design using chitosan by the spray drying. *Int J Pharm.,* 270 (1–2)**,** 167-174.

assesment, P. s. <POLYOX, DOW, 2002.pdf>.

Babu, R. J. and Pandit, J. K. (1999) Effect of aging on the dissolution stability of glibenclamide/beta-cyclodextrin complex. *Drug Dev Ind Pharm,* 25 (11)**,** 1215-9.

Babu, N.J, and Nangia, A. (2011) Solubility Advantage of Amorphous Drugs and Pharmaceutical Cocrystals. *Cryst. Growth Des.*, 11 (7), 2662–2679.

Balaz, P. (2008) High energy milling, Mechanochemistry in Nanoscience and Minerals Engineering, Springer-Verlag Berlin Heidelberg.

Bartolomei M (2000) Solid-state studies on the hemihydrate and the anhydrous forms of flunisolide. J Pharm Biomed Anal., 24(1), 81-93.

Berry, D.J., Seaton, C.C., Clegg, W., Harrington, R.W., Coles, S.J., Horton, P.N., Hursthouse, M.B., Storey, R., Jones, W., Friscic, T., Blagden, N. (2008) Applying hot-stage microscopy to co-crystal screening: a study of nicotinamide with seven active pharmaceutical ingredients. Cryst. Growth Des. 8, 1697–1712.

Bikiaris, D. N. (2011) Solid dispersions, Part I: recent evolutions and future opportunities in manufacturing methods for dissolution rate enhancement of poorly water-soluble drugs. *Expert Opinion on Drug Del.,* 8 (11)**,** 1501-1519.

Boksa, K., Otte, A. and Pinal, R. (2014) Matrix-assisted cocrystallization (MAC) simultaneous production and formulation of pharmaceutical cocrystals by hot-melt extrusion. *J Pharm Sci,* 103 (9)**,** 2904-10.

Bounartzi M, Panagopoulou A, Kantiranis N, Malamataris S, Nikolakakis (2014) Effect of plasticiser type on the hot melt extrusion of venlafaxine hydrochloride. J Pharm Pharmacol., 66(2), 297-308.

Branham, M. L., Moyo, T. and Govender, T. (2012) Preparation and solid-state characterization of ball milled saquinavir mesylate for solubility enhancement. *Eur J Pharm Biopharm,* 80 (1)**,** 194-202.

Brabander, C.DE., Vervaet, C., Remon, J.P. (2002) Characterization of Ibuprofen as a Nontraditional Plasticizer of Ethyl Cellulose. *J Pharm. Sci.,* 91 (7).

Breitenbach, J. (2002) Melt extrusion from process to drug delivery technology.. *Eur J Pharm Sci.,* 54**,** 107-117.

Balaz, P. (2008) Mechanochemistry in Nanoscience and Minerals Engineering. Springer.

Balaz, P. (2008) High energy milling. Mechanochemistry in Nanoscience and Minerals Eng. Chapter 2.

Ball mill, (2013) http://www.grindingmedia.cc/html_news/How-a-Grate-Discharge-Ball-Mill-Works-12.html.

Blagden, N., de Matas, M., Gavan, P.T., York, P. (2007) Crystal engineering of active pharmaceutical ingredients to improve solubility and dissolution rates. Adv. Drug Deliv. Rev. 59, 617–630.

Bin Li, Kim Harich, Lindsay Wegiel, Lynne S. Taylor, Kevin J. Edgar, (2013) Stability and solubility enhancement of ellagic acid in cellulose ester solid dispersions. Carb. Poly., 92(2), 1443–1450.

Bond, F.C. (1952) The third theory of comminution. Transactions of AIME, Minerals Eng. 193, 484–494.

Boksa K., Otte A., Pinal R., (2014) Matrix-assisted cocrystallization (MAC) simultaneous production and formulation of pharmaceutical cocrystals by hot-melt extrusion. J Pharm Sci. 103(9):2904-10.

Burns, D.A. and Ciurczak, E.W. (2009) Handbook of Near-Infrared Analysis. Anal Bioanal Chem, 393:1387–1389.

Cal, K., and Sollohub, K., (2010) Spray drying technique. I. Hardware and process parameters. J. Pharm. Sci. 99, 575–586.

Ceballos, A., Cirri, M., Maestrelli, F., Corti, G. and Mura, P. (2005) Influence of formulation and process variables on in vitro release of theophylline from directly-compressed Eudragit matrix tablets. *Farmaco,* 60 (11-12)**,** 913-8.

Changsheng Liu, Q. W. (2000) Solid-Phase Grafting of Hydroxymethyl Acrylamide onto Polypropylene through Pan Milling. *Pol mat. eng.,* 78**,** 2191-2197.

Chauhan, B., Shimpi, S. and Paradkar, A. (2005) Preparation and evaluation of glibenclamide-polyglycolized glycerides solid dispersions with silicon dioxide by spray drying technique. *Eur J Pharm Sci,* 26 (2)**,** 219-30.

Chiou, W. L., Riegelman, S. (1971) Pharmaceutical applications of solid dispersion systems. *J Pharm Sci,* 60 (9)**,** 1281.

Chiou, W. L. a. R., S (1969) Preparation and dissolution characteristics of several fast-release solid dispersions of griseofulvin. 58 (12).

Christian Leuner, J. D. (2000) Improving drug solubility for oral delivery using solid dispersions. *Eur J Pharm and Biopharm*.

Chokshi RJ, Sandhu HK, Iyer RM, Shah NH, Malick AW, Zia H. (2005) Characterization of physico-mechanical properties of indomethacin and polymers to assess their suitability for hot-melt extrusion processes as a means to manufacture solid dispersion/solution. J Pharm Sci., 94(11), 2463-74.

Corrigan, O. I. (1995) Thermal analysis of spray dried products. *thermochemica acta***,** 245-258.

Crowley, M. M., Zhang, F., Repka, M. A., Thumma, S., Upadhye, S. B., Battu, S. K., McGinity, J. W. and Martin, C. (2007) Pharmaceutical applications of hot-melt extrusion: part I. *Drug Dev Ind Pharm,* 33 (9)**,** 909-26.

Danesh, A., Davies, M.C., Roberts, C.J., Tendler, S.J.B., Williams, P.M. and Wilkins, M.J. (2001) An in situ dissolution study of aspirin crystal planes (100) and (001) by atomic force microscopy. *Pharm. Res.,* 18 (3)**,** 299.

Desiraju, G.R. (1995) Supramolecular Synthons in Crystal Engineering—A New Organic Synthesis. *Angewandte Chemie.*, 34(21), 2311–2327.

Doetsch, W. (2003) Material handling and feeder technology. Pharm Extru Tech, 133, 111–134.

Dhumal, R. S., Kelly, A. L., York, P., Coates, P. D. and Paradkar, A. (2010) Cocrystalization and simultaneous agglomeration using hot melt extrusion. *Pharm Res,* 27 (12)**,** 2725-33.

Dong, Z., Chatterji, A., Sandhu, H., Choi, D. S., Chokshi, H. and Shah, N. (2008) Evaluation of solid state properties of solid dispersions prepared by hot-melt extrusion and solvent co-precipitation. *Int J Pharm,* 355 (1-2)**,** 141-9.

Dwayne T. Friesen, † Ravi Shanker,‡ Marshall Crew,†,§ Daniel T. Smithey,†,W. J. Curatolo,‡ and J. A. S. Nightingale† (2008) Hydroxypropyl Methylcellulose Acetate Succinate-Based Spray-Dried Dispersions: An Overview. *Mol Pharm,* 5 (6)**,** 1003–1019.

Europian Medicines Agency, 2014.

Farzana S. Bandarkar, Ibrahim S. Khattab (2011) Lyophilized Gliclazide-Poloxamer Solid Dispersions For Enhancement Of Invitro Dissolution And In-Vivo Bioavailability. *Int J Pharm Pharm Sci*, 3(2), 122-127.

Feeley, J.C., Sumby, B.S., Dicks, H. (1998) Determination of surface properties and flow characteristics of salbutamol sulphate, before and after micronisation. *Int J Pharm,* 172**,** 89-96.

Festo Damian , N. B., Lieve Naesens , Jan Balzarini , Renaat Kinget , Patrick Augustijnsa, Guy Van den Mootera, (2000) Physicochemical characterization of solid dispersions of the antiviral agent UC-781 with polyethylene glycol 6000 and Gelucire 4414. *Pharma Sci*.

Fichtner, F., Mahlin, D., Welch, K., Gaisford, S. and Alderborn, G. (2008) Effect of surface energy on powder compactibility. *Pharm Res,* 25 (12)**,** 2750-9.

Friscic, T. and Jones, W. (2009) Recent Advances in Understanding the Mechanism of Cocrystal Formation via Grinding. Cryst. Growth Des., 9 (3), 1621–1637.

Ghaderi, R. (1999) Preparation of biodegradable microparticles using solution-enhanced dispersion by supercritical fluids (SEDS).

Ghaste, R. C., (2009) Solid Dispersions : An Overview. Pharm Rev. 7.

Ghosh, I., Snyder, J., Vippagunta, R., Alvine, M., Vakil, R., Tong, W. Q. and Vippagunta, S. (2011) Comparison of HPMC based polymers performance as carriers for manufacture of solid dispersions using the melt extruder. *Int J Pharm,* 419 (1-2)**,** 12-9.

Gibaldi, M. (1977) Biopharmaceutics and Clinical Pharmacokinetics, Lea and Febiger, 2 (4-3), 47.

Goldberg, A.H., Gibaldi. M. and Kanig, J.L. (1965) Increasing dissolution rates and gastrointestinal absorption of drugs via solid solutions and eutectic mixtures. *J Pharm Sci*.

Guyot, M., Bildet, F.F.J, Bonini, F., Lagueny, A.M (1995) Physicochemical Characterization and Dissolution of Norfloxacin Cyclodextrin Inclusion-Compounds and Peg Solid Dispersions. *Int J Pharm,* 10.

Hanpin, L. (2012) Dissolution and Solubility Enhancement of the Poorly Water Soluble Drug by Forming Solid Dispersion with a Novel Polymeric Solubilizer (Soluplus®). PhD Thesis Dissertation, School of the University of maryland, Baltimore.

Hasegawa, S., Ke, P. and Buckton, G. (2009) Determination of the structural relaxation at the surface of amorphous solid dispersion using inverse gas chromatography. *J Pharm Sci,* 98 (6)**,** 2133-9.

Hammer mills: hammer mills. (2013)http://www.feedmachinery.com/glossary/equipment/hammer_mill/ 2013.

Hattori, Y., Haruna, Y., Otsuka, M. (2013) Dissolution process analysis using model-free Noyes–Whitney integral equation. Coll Surf B: Bio, 102, 227–231.

Ho, R., Dilworth, S. E., Williams, D. R. and Heng, J. Y. Y. (2011) Role of Surface Chemistry and Energetics in High Shear Wet Granulation. *Ind Eng Chem Res,* 50 (16)**,** 9642-9649.

Holmes, J.A. (1957) A contribution to the study of comminution: a modified form of Kick's law. Trans Inst Chem Eng (London), 35, 125–138.

Ho, R., Naderi, M., Heng, J. Y., Williams, D. R., Thielmann, F., Bouza, P., Keith, A. R., Thiele, G. and Burnett, D. J. (2012) Effect of milling on particle shape and surface energy heterogeneity of needle-shaped crystals. *Pharm Res,* 29 (10)**,** 2806-16.

Ho, R., Wilson, D. A. and Heng, J. Y. Y. (2009) Crystal Habits and the Variation in Surface Energy Heterogeneity. *Crystal Growth Design,* 9 (11)**,** 4907-4911.

Huang, H. and Dai, W. (2014) Fundamental aspects of solid dispersion technology for poorly soluble drugs. Acta Pharmaceutica Sinica B., 4(1), 18–25.

Hughey, J.R., DiNunzio, J.C., Bennett, R.C., Brough, C., Miller, D.A., Ma, H., WilliamsIII, R.O., and McGinity, J.W. (2010) Dissolution Enhancement of a Drug Exhibiting Thermal and Acidic Decomposition Characteristics by Fusion Processing: A Comparative Study of Hot Melt Extrusion and KinetiSol® Dispersing. AAPS PharmSciTech., 11(2), 760–774.

Ilevbare, G.A., Liu, H., Edgar, K.J., Taylor, L.S. (2012) Understanding polymer properties important for crystal growth inhibition: impact of chemically diverse polymers on solution crystal growth of ritonavir. *Cryst Growth Des.*, 12, 3133–3143.

Jankovic, A. (2010) Proposal for a Solomonic settlement between the theories of von Rittinger, Kick and Bond. 110.

Jones, W., Motherwell, S. and Trask, A.V. (2006) Pharmaceutical Cocrystals: An Emerging Approach to Physical Property Enhancement. MRS Bulletin, 31(11), 875-879.

Juhasz, A. Z. and Opoczky, L. (1990) *Mechanical activation of minerals by grinding pulverizing and morphology of particles.*

Kang, B. K., Lee, J. S., Chon, S. K., Jeong, S. Y., Yuk, S. H., Khang, G., Lee, H. B. and Cho, S. H. (2004) Development of self-microemulsifying drug delivery systems (SMEDDS) for oral bioavailability enhancement of simvastatin in beagle dogs. *Int J Pharm,* 274 (1-2)**,** 65-73.

Kang, H., Liu, W., He, B., Shen, D., Ma, L. and Huang, Y. (2006) Synthesis of amphiphilic ethyl cellulose grafting poly(acrylic acid) copolymers and their self-assembly morphologies in water. *Polymer,* 47 (23)**,** 7927-7934.

Karavas, E., Ktistis, G., Xenakis, A. and Georgarakis, E. (2006) Effect of hydrogen bonding interactions on the release mechanism of felodipine from nanodispersions with polyvinylpyrrolidone. *Eur J Pharm Biopharm,* 63 (2)**,** 103-14.

Kaufman, H.S., Falcetta, J.J. (1977) Introduction to Polymer Science and Technology. John Wiley & Sons, New York.

Kelly, A. L., Gough, T., Dhumal, R. S., Halsey, S. A. and Paradkar, A. (2012) Monitoring ibuprofen-nicotinamide cocrystal formation during solvent free continuous cocrystallization (SFCC) using near infrared spectroscopy as a PAT tool. *Int J Pharm,* 426 (1-2)**,** 15-20.

Khadka, P., Ro, J., Kim, H., Kim, I., Kim, J.T., Kim, H., Cho, J.M., Yun, G., Lee, J. (2014) Pharmaceutical particle technologies: An approach to improve drug solubility, dissolution and bioavailability. Asian J. Pharm Sci. 9 (6), 304–316.

Kim, J. S., Kim, M. S., Park, H. J., Jin, S. J., Lee, S. and Hwang, S. J. (2008) Physicochemical properties and oral bioavailability of amorphous atorvastatin hemi-calcium using spray-drying and SAS process. *Int J Pharm,* 359 (1-2)**,** 211-9.

Kim, K. T. (2011) Solid Dispersions as a Drug Delivery System. J Pharm Invest, 41(3), 125-142.

Knight, J. B., Jaeger, H. M. and Nagel, S. R. (1993) Vibration-induced size separation in granular media: The convection connection. *Physical Review Letters,* 70 (24)**,** 3728-3731.

Kulkarni, C., Kendrick, J., Kelly, A., Gough, T., Dash, R.C. and Paradkar, A. (2013) Polymorphic transformation of artemisinin by high temperature extrusion. CrystEngComm., 15, 6297-6300.

Labultima 222 spray dryer, (2008) http://www.labultima.com/lu228.htm.

Lakshman, J.P., Kowalski, Y.C.J., and Serajuddin, A.T.M (2008) Application of Melt Extrusion in the Development of a Physically and Chemically Stable High-Energy Amorphous Solid Dispersion of a Poorly Water-Soluble Drug. *Mol Pharm,* 5 (6)**,** 994-1002.

Little, D. and Rice, D. (2004) Thermokinetic mixer and method of using. United States Patent 6709146.

Liu, J., Cao, F., Zhang, C. and Ping, Q. (2013) Use of polymer combinations in the preparation of solid dispersions of a thermally unstable drug by hot-melt extrusion. *Acta Pharmaceutica Sinica B,* 3 (4)**,** 263-272.

Liu, Y., Li, J. and Wang, Q. (2008) Solid State Shear Milling to Prepare Magnesium Hydroxide Flame-Retardant Polyamide 6 with High Performance. *Mat Mfg Proc,* 23 (3)**,** 284-288.

Liu, Y. *et al*., (2007) Preparation of High Loading Magnesium Hydroxide Flame Retardant Polypropylene by Solid State Shear Milling. J Com Mat, 41(16).

Li, S., Jones, D.S., Andrews, G.P., Wilson, M. (2013) Process Optimization of Cocrystal Suspensions Manufactured Using Hot-Melt Extrusion. AAPS

Liu, R. (2008) Water-insoluble drug formulation. 669.

Liu, X *et al*., (2011) Improving the chemical stability of amorphous solid dispersion with cocrystal technique by hot melt extrusion. Pharm Res.29(3) 806-17.

Lordi, G. (1984) Thermal-Analysis Studies of Glass Dispersion-Systems. *Drug Dev Ind Pharm,* 10 (3)**,** 425.

Lu, C. and Wang, Q. (2004) Preparation of ultrafine polypropylene/iron composite powders through pan-milling. *J Mat Proc Tech,* 145 (3)**,** 336-344.

Luker, K. (2003) Single-screw extrusion and screw design. Pharmaceutical extrusion technology. Drug Pharm Sci, 133, 39-68.

Mackin, L., Sartnurak, S., Thomas, I., Moore, S. (2001) The impact of low levels of amorphous material (5%) on the blending characteristics of a direct compression formulation. *Inte J Pharm*.

Mahlin, D., Ponnambalam, S., Hockerfelt, M. H. and Bergstrom, C. A. (2011) Toward in silico prediction of glass-forming ability from molecular structure alone: a screening tool in early drug development. *Mol Pharm,* 8 (2)**,** 498-506.

Majerik, V., Charbit, G., Badens, E., Horváth, G., Szokonya, L., Bosc, N. and Teillaud, E. (2007) Bioavailability enhancement of an active substance by supercritical antisolvent precipitation. *J Supercrit Fluids,* 40 (1)**,** 101-110.

Mao, S. (1994) Unit process for solid dosage form. Pharmaceutics, Shenyang Pharmaceutical University.

Miller, D. and Gil, M. (2012) Spray-Drying Technology. In: Williams Iii, R. O., *et al*. (Eds.) *Formulating Poorly Water Soluble Drugs.* (AAPS Advances in the Pharmaceutical Sciences Series) Vol. 3. Springer New York, pp. 363-442.

Mogal, S. A., Gurjar, P. N., Yamgar, D. S. and Kamod, A.C. (2012) Solid dispersion technique for improving solubility of some poorly soluble drugs. Der Pharmacia Lettre, 4 (5), 1574-1586.

Nainar, S., Rajiah, K., Angamuthu, S., Prabakaran, D. and Kasibhatta, R. (2012) Biopharmaceutical Classification System in Invitro/ In-vivo Correlation: Concept and Development Strategies in Drug Delivery. *Tropical Journal of Pharm Res,* 11 (2).

Nokhodchi, A., Valizadeh, H., Jalali, M.B. (2007) An Investigation on the Solid Dispersions of Chlordiazepoxide. *Int J Biomed Sci,* 3 (3).

Norbert Rasenack, B. W. M. (2002) Crystal habit and tableting behavior. *Int J Pharm,* 244**,** 45-57.

Obi, K. (1961) Studies on Absorption of Eutectic Mixture. *Faculty Pharm Sci,* 62 (13)**,** 4125-4130.

Ohara, T., Kitamura, S., Kitagawa, T. and Terada, K. (2005) Dissolution mechanism of poorly water-soluble drug from extended release solid dispersion system with ethylcellulose and hydroxypropylmethylcellulose. *Int J Pharm,* 302 (1-2)**,** 95-102.

Olusanmi, D., Roberts, K. J., Ghadiri, M. and Ding, Y. (2011) The breakage behaviour of Aspirin under quasi-static indentation and single particle impact loading: Effect of crystallographic anisotropy. *Int J Pharm,* 411 (1–2)**,** 49-63.

Owusu-Ababio, G., Ebube, N. K., Reams, R. and Habib, M. (1998) Comparative Dissolution Studies for Mefenamic Acid-Polyethylene Glycol Solid Dispersion Systems and Tablets. *Pharm Dev Tech,* 3 (3)**,** 405-412.

Padrela, L., Rodrigues, M.A., Velaga, S.P., Matos, H.A., de Azevedo, E.G. (2009) Formation of indomethacin–saccharin cocrystals using supercritical fluid technology. Eur. J. Pharm. Sci. 38, 9–17.

Pagire, S., Korde, S., Ambardekar, R., Deshmukh, S., Dash, R.C., Dhumal, R. and Paradkar, A. (2013) Microwave assisted synthesis of caffeine/maleic acid co-crystals: the role of the dielectric and

physicochemical properties of the solvent. CrystEngComm, 15, 3705-3710.

Paradkar, A., Ambike, A. A., Jadhav, B. K. and Mahadik, K. R. (2004) Characterization of curcumin–PVP solid dispersion obtained by spray drying. *Int J Pharm,* 271 (1-2)**,** 281-286.

Patterson, J. E., James, M. B., Forster, A. H., Lancaster, R. W., Butler, J. M. and Rades, T. (2005) The influence of thermal and mechanical preparative techniques on the amorphous state of four poorly soluble compounds. *J Pharm Sci,* 94 (9)**,** 1998-2012.

Patterson, J. E., James, M. B., Forster, A. H. and Rades, T. (2008) Melt extrusion and spray drying of carbamazepine and dipyridamole with polyvinylpyrrolidone/vinyl acetate copolymers. *Drug Dev Ind Pharm,* 34 (1)**,** 95-106.

Paudel, A., Worku, Z. A., Meeus, J., Guns, S. and Van den Mooter, G. (2013) Manufacturing of solid dispersions of poorly water soluble drugs by spray drying: formulation and process considerations. *Int J Pharm,* 453 (1)**,** 253-84.

Porter, W.W., Elie, S.C., Matzger, A.J. (2008) Polymorphism in Carbamazepine Cocrystals. Cryst Growth Des. 8(1), 14-16.

Pouton, C. W. (2006) Formulation of poorly water-soluble drugs for oral administration: physicochemical and physiological issues and the lipid formulation classification system. *Eur J Pharm Sci,* 29 (3-4)**,** 278-87.

Paudel, A. and Mooter, G.V. (2010) Theoretical and exper-imental investigation on the solid solubility and miscibility of naproxen in poly(vinylpyrrolidone). *Mol. Pharma.,* 7 (4)**,** 1133-1148.

Qi, S., Gryczke, A., Belton, P. and Craig, D. Q. (2008) Characterisation of solid dispersions of paracetamol and EUDRAGIT E prepared by hot-melt extrusion using thermal, microthermal and spectroscopic analysis. *Int J Pharm,* 354 (1-2)**,** 158-67.

Qian, F., Huang, J. and Hussain, M. A. (2010) Drug-polymer solubility and miscibility: Stability consideration and practical challenges in amorphous solid dispersion development. *J Pharm Sci,* 99 (7)**,** 2941-7.

Qiao, N., Li, M., Schlindwein, W., Malek, N., Davies, A., Trappitt, G. (2011) Pharmaceutical cocrystals: an overview. Int. J. Pharm. 419, 1–11.

Rahman, Z., Agarabi, C., Zidan, A. S., Khan, S. R. and Khan, M. A. (2011) Physico-mechanical and stability evaluation of carbamazepine cocrystal with nicotinamide. *AAPS PharmSciTech,* 12 (2)**,** 693-704.

Ritthide, P. D. a. G. C. (1997) Development of Diclofenac Sodium Controlled Release Solid Dispersions by Spray Drying Using Optimization Strategy I. Powder Formulation. *Communication,* 23(8)**,** 842-848.

Rhodes, M. (1998) Introduction to Particle Technology. John Wiley and Sons, Chichester.

Rasenack, N. and Muller, B.W. (2004) Micron-size drug particles: common and novel micronization techniques. *Pharm. Dev. Technol*. 9, 1-13.

Rodier, E., Lochard, H., Sauceau, M., Letourneau, J. J., Freiss, B. and Fages, J. (2005) A three step supercritical process to improve the dissolution rate of eflucimibe. *Eur J Pharm Sci,* 26 (2)**,** 184-93.

Roller mill, Feed machinery, http://www.feedmachinery.com/glossary/equipment/roller_mills/ 2013.

Salazar, J., Müller, R.H., Möschwitzer, J.P. (2013) Application of the combinative particle size reduction technology H 42 to produce fast dissolving glibenclamide tablets. Eur J Pharm Sci. 49(4), 565-77.

Sarode, A. L., Sandhu, H., Shah, N., Malick, W. and Zia, H. (2013) Hot melt extrusion (HME) for amorphous solid dispersions: predictive tools for processing and impact of drug-polymer interactions on supersaturation. *Eur J Pharm Sci,* 48 (3)**,** 371-84.

Schultheiss, N., and Newman, A. (2009) Pharmaceutical Cocrystals and Their Physicochemical Properties. *Crystal Growth & Design,* 9 (6)**,** 2950-2967.

Sekiguchi, K. and Obi, N. (1961) Studies on Absorption of Eutectic Mixture. I. A Comparison of the Behavior of Eutectic Mixture of Sulfathiazole and that of Ordinary Sulfathiazole in Man. *Chem Pharm Bulletin,* 9 (11)**,** 866-872.

Serajuddin, A. T. (1998) Solid dispersion of poorly water-soluble drugs early promises, subsequent problems, and recent breakthroughs. *Pharm Res Inst,* 88 (10)**,** 1058.

Sethia, S. and Squillante, E. (2004) Solid dispersion of carbamazepine in PVP K30 by conventional solvent evaporation and supercritical methods. *Int J Pharm,* 272 (1-2)**,** 1-10.

Shah, S., Lin, S., Madan, P.L. (2011) Preparation and characterization of spironolactone solid dispersions using hydrophilic carriers. Asian J Pharm Sci (40).

Shan, N., Toda, F., Jones, W. (2002) Mechanochemistry and co-crystal formation: effect of solvent on reaction kinetics. Chem. Commun., 2372–2373.

Shan, N., Zaworotko, M.J. (2008) The role of cocrystals in pharmaceutical science. Drug Discov Today. 13(9-10), 440-6.

Shao, W. and Wang, Q. (2006) Partial exfoliation and layer expansion of vermiculite layer in solid state by solid state shear milling (S3M) method. *J App Poly Sci,* 101 (3)**,** 1806-1809.

Shao, W., Wang, Q. and Li, K. (2005) Intercalation and exfoliation of talc by solid-state shear compounding (S3C) using pan-mill equipment. *Poly Eng Sci,* 45 (4)**,** 451-457.

Shao, W., Wang, Q., Wang, F. and Chen, Y. (2006a) The cutting of multi-walled carbon nanotubes and their strong interfacial interaction with polyamide 6 in the solid state. *Carbon,* 44 (13)**,** 2708-2714.

Shao, W., Wang, Q., Wang, F. and Chen, Y. (2006b) Polyamide-6/natural clay mineral nanocomposites prepared by solid-state shear milling using pan-mill equipment. *J Polymer Sci Part B: Polymer Phys,* 44 (1)**,** 249-255.

Shao, S., Chen, Y. and Gu, Y. (2006) Preparation and Properties of Polypropylene Vermiculite Nanocomposite ThroughSolid-State Shear Compounding (S3C) Method Using Pan-Mill Equipment. *Mat Mfg Proc,* 21.

Shin, S., Lee, Y., Choi, H., Choi, J.S. (1998) Enhanced dissolution of furosemide by coprecipitating or cogrinding with crospovidone. *Int J Pharm,* 175**,** 17-24.

ShinEtsu, (2009) HPMC technical report.

Sareen, S., Mathew, G. and Joseph, L. (2012) Improvement in solubility of poor water-soluble drugs by solid dispersion. *Int J Pharm Investig*. 2(1), 12–17.

Simonelli, A.P. and Higuchi, W.I. (1969) Dissolution Rates of High Energy Polyvinylpyrrolidone (PVP) Sulfathiazole Coprecipitates. *J Pharm. Sci.*

Singh, S., Baghel, R.S. and Yadav, L. (2011) A review on solid dispersion. *Int. J. of Pharm. & Life Sci.*, 2(9), 1078-1095.

Sibik, J., Sargent, M. J., Franklin, M. and Zeitler, J. A. (2014) Crystallization and Phase Changes in Paracetamol from the Amorphous Solid to the Liquid Phase. *Mol Pharm,* 11 (4)**,** 1326-1334.

Sladkova, V., Cibulkova, J., Eigner, V., Sturc, A., Kratochvil, B. and Rohlicek, J. (2014) Application and Comparison of Cocrystallization Techniques on Trospium Chloride Cocrystals. Cryst. Growth Des., 14 (6), 2931–2936.

Stehr, N. (1983) Residence Time Distributions in a Stirred Ball Mill and their Effect on Comminution. *Chem Eng J,* 18**,** 73-83.

Tanaka, N., Imai, K., Okimoto, K., Ueda, S., Tokunaga, Y., Ibuki, R., Higaki, K. and Kimura, T. (2006) Development of novel sustained-release system, disintegration-controlled matrix tablet (DCMT) with solid dispersion granules of nilvadipine (II): in vivo evaluation. *J Control Release,* 112 (1)**,** 51-6.

Thakuria, R., Delori, A., Jones, W., Lipert, M.P., Roy, L., Rodríguez-Hornedo, N. (2013) Pharmaceutical cocrystals and poorly soluble drugs. International Journal of Pharmaceutics, 453, 101– 125.

Thomasa, P., Varughese, K.T., Dwarakanath, K. and Varma, K.B.R. (2013) High-Dielectric-Constant PP BaTiO_3 Composites Prepared by Solid State Shear Milling.

Traini, D., Rogueda, P., Young, P. and Price, R. (2005) Surface energy and interparticle forces correlations in model pMDI formulations. *Pharm Res,* 22 (5)**,** 816-25.

Trafford, A.D., Moffata, A.C. and Grahamb, P. (1998) A rapid quantitative assay of intact paracetamol tablets by reflectance near-infrared spectroscopy. *The Analyst,* 124**,** 163-167.

Tran, T., Poudel, B., Marasini, N., Woo, J., Choi, H.-G., Yong, C. and Kim, J. (2013) Development of raloxifene-solid dispersion with improved oral bioavailability via spray-drying technique. *Archives Pharm Res,* 36 (1)**,** 86-93.

Trask, A.V., Motherwell, W.D.S., Jones, W. (2004) Solvent-drop grinding: green polymorph control of cocrystallisation. Chem. Commun., 890–891.

Van den Mooter, G., Weuts, I., De Ridder, T. and Blaton, N. (2006) Evaluation of Inutec SP1 as a new carrier in the formulation of solid dispersions for poorly soluble drugs. *Int J Pharm,* 316 (1-2)**,** 1-6.

van Drooge, D. J., Braeckmans, K., Hinrichs, W. L. J., Remaut, K., De Smedt, S. C. and Frijlink, H. W. (2006) Characterization of the Mode of Incorporation of Lipophilic Compounds in Solid Dispersions at the Nanoscale Using Fluorescence Resonance Energy Transfer (FRET). *Macromolecular Rapid Communications,* 27 (14)**,** 1149-1155.

Van Eerdenbrugh, B. and Taylor, L. S. (2011) An ab initio polymer selection methodology to prevent crystallization in amorphous solid dispersions by application of crystal engineering principles. *CrystEngComm,* 13 (20)**,** 6171.

Vasconcelos, T., Sarmento, B. and Costa, P. (2007) Solid dispersions as strategy to improve oral bioavailability of poor water soluble drugs. *Drug Discov Today,* 12 (23-24)**,** 1068-75.

Vehring, R. (2008) Pharmaceutical particle engineering via spray drying. *Pharm Res,* 25 (5)**,** 999-1022.

Venkitachalam, T. S. (1992) Studies on Solid Dispersions of Nifedipine. *Drug Dev Ind Pharm,* 18 (15)**,** 1663.

Vilhelmsen, T., Eliasen, H. and Schaefer, T. (2005) Effect of a melt agglomeration process on agglomerates containing solid dispersions. *Int J Pharm,* 303 (1-2)**,** 132-42.

Wang, Q., Chen, H. and Liu, Y. (2002) LDPE-g-MAH prepared through solid-phase mechanochemistry and its compatibilizing effects on HDPE/CaCO3. *Polymer-Plastics Tech Eng,* 41 (2)**,** 215-228.

Wang, Q., Jingui Huang, J.C., and Xu, X. (1997) A Study on the Pan-Milling Process and the Pulverizing Efficiency of Pan-Mill Type Equipment. 37 (6).

Wang, G. (2008) Structure and Properties of Poly(ethylene terephthalate)/Na1-Montmorillonite Nanocomposites Prepared by Solid State Shear Milling (S3M) Method. Journal of Polymer Science: Part B: Polymer Physics, 46, 807–817.

Weyna, D.R., Shattock, T., Vishweshwar, P., Zaworotko, M.J. (2009) Synthesis and structural characterization of cocrystals and pharmaceutical cocrystals:mechanochemistry vs slow evaporation from solution. Cryst. Growth Des. 9, 1106–1123.

Wu, K., Li, J., Wang, W. and Winstead, D. A. (2009) Formation and characterization of solid dispersions of piroxicam and polyvinylpyrrolidone using spray drying and precipitation with compressed antisolvent. *J Pharm Sci,* 98 (7)**,** 2422-31.

Xia, H., Wang, Q., Li, K. and Hu, G.H. (2004) Preparation of polypropylene/carbon nanotube composite powder with a solid-state mechanochemical pulverization process. *J App Pol Sci,* 93 (1)**,** 378-386.

Xu, X., Wang, Q., Kong, X., Zhang, X. and Huang, J. (1996) Pan Mill type Equipment Designed for Polymer Stress Reactions Theoretical Analysis of Structure and Milling Process of Equipment. 25**,** 152-158.

Yao, W.W., Bai, T.C., Sun, J.P., Zhu, C.W., Hu, J. and Zhang, H.L. (2005) Thermodynamic properties for the system of silybin and poly(ethylene glycol) 6000. *Thermochimica Acta,* 437 (1-2)**,** 17-20.

Yang, Z., Nollenberger, K., Albers, J., Qi, S. (2014) Molecular implications of drug-polymer solubility in understanding the destabilization of solid dispersions by milling. *Mol Pharm.* 11(7), 2453-65.

Zhang, F. and McGinity, J. W. (1999) Properties of Sustained-Release Tablets Prepared by Hot-Melt Extrusion. *Pharm Dev Tech,* 4 (2)**,** 241-250.

Zhang, W., Liang, M. and Lu, C. (2007) Morphological and structural development of hardwood cellulose during mechanochemical pretreatment in solid state through pan-milling. *Cellulose,* 14 (5)**,** 447-456.

Zhao, X., Liu, X., Gan, L., Zhou, C. and Mo, J. (2011) Preparation and physicochemical characterizations of tanshinone IIA solid dispersion. *Archives of Pharm Res,* 34 (6)**,** 949-959.

Zhu, J., Zhang, X., Liang, M. and Lu, C. (2010) Enhancement of processability and foamability of ground tire rubber powder and LDPE blends through solid state shear milling. *J Pol Res,* 18 (4)**,** 533-539.

Zilinskas, G. J., Soleimani, A. and Gillies, E. R. (2012) Poly(ester amide)-Poly(ethylene oxide) Graft Copolymers: Towards Micellar Drug Delivery Vehicles. *Int J Pol Sci,* 2012**,** 1-11.

Appendix 1

Presentation of research work in conferences

1. Presented poster entitled “Melt casted transdermal tadalafil films” in the UK PharmSci 2012, held in Nottingham University, UK.

2. Presented poster entitled “Self emulsifying formulation of curcumin for transdermal drug delivery” in the UK PharmSci 2013, held in Edinburgh, Scotland.

3. Presented poster entitled “Pharmaceutical amorphous composite by S3M technology” in the RCUK Science Bridges China/EPSRC Global Engagements Research Workshop, co-hosted with Sichuan University and the Chengdu Science & Technology Bureau, 2013 held in Sichuan University, Chengdu, China.